

**NASA  
Technical  
Memorandum**

NASA TM-103521

**PREDICTING THUNDERSTORM EVOLUTION USING  
GROUND-BASED LIGHTNING DETECTION NETWORKS**

By Steven J. Goodman

Space Science Laboratory  
Science and Engineering Directorate

November 1990

(NASA-TM-103521) PREDICTING THUNDERSTORM  
EVOLUTION USING GROUND-BASED LIGHTNING  
DETECTION NETWORKS (NASA) 210 p CSCL 04K

N91-15660

Unclass

63/47 0326307



National Aeronautics and  
Space Administration

George C. Marshall Space Flight Center





## Report Documentation Page

1. Report No. <b>NASA TM-103521</b>		2. Government Accession No.		3. Recipient's Catalog No.	
4. Title and Subtitle <b>Predicting Thunderstorm Evolution Using Ground-Based Lightning Detection Networks</b>				5. Report Date <b>November 1990</b>	
				6. Performing Organization Code <b>ES44</b>	
7. Author(s) <b>Steven J. Goodman</b>				8. Performing Organization Report No.	
				10. Work Unit No.	
9. Performing Organization Name and Address <b>George C. Marshall Space Flight Center Marshall Space Flight Center, AL 35812</b>				11. Contract or Grant No.	
				13. Type of Report and Period Covered <b>Technical Memorandum</b>	
12. Sponsoring Agency Name and Address <b>National Aeronautics and Space Administration Washington, DC 20546</b>				14. Sponsoring Agency Code	
15. Supplementary Notes <b>Prepared by Space Science Laboratory, Science and Engineering Directorate.</b>					
16. Abstract  <b>Lightning measurements acquired principally by a ground-based network of magnetic direction finders are used to diagnose and predict the existence, temporal evolution, and decay of thunderstorms over a wide range of space and time scales extending over four orders of magnitude. The non-linear growth and decay of thunderstorms and their accompanying cloud-to-ground lightning activity is described by the three parameter logistic growth model. The growth rate is shown to be a function of the storm size and duration, and the limiting value of the total lightning activity is related to the available energy in the environment. A new technique is described for removing systematic bearing errors from direction finder data where radar echoes are used to constrain site error correction and optimization (best point estimate) algorithms. A nearest neighbor pattern recognition algorithm is employed to cluster the discrete lightning discharges into storm cells and the advantages and limitations of different clustering strategies for storm identification and tracking are examined.</b>					
17. Key Words (Suggested by Author(s)) <b>Thunderstorms, Lightning, Radar, Nowcasting, Mesoscale Meteorology</b>				18. Distribution Statement <b>Unclassified — Unlimited</b>	
19. Security Classif. (of this report) <b>Unclassified</b>		20. Security Classif. (of this page) <b>Unclassified</b>		21. No. of pages <b>210</b>	22. Price <b>NTIS</b>

## ACKNOWLEDGMENTS

I wish to thank the many individuals who allowed me to have engaging discussions with them. Dr. Robert Brown of the University of Alabama in Huntsville introduced me to the time series analysis and forecasting literature, and helped me down a path of enlightenment to discover a broad range of approaches to modeling the behavior of non-linear dynamical systems. Drs. Hugh Christian of Marshall Space Flight Center, Marx Brook of the New Mexico Institute of Mining and Technology and Bernard Vonnegut of the State University of New York at Albany helped me to appreciate the complexity of natural phenomena and gain a greater understanding of thunderstorm electrification and cloud physics. Dr. Richard Johnson of SouthWest Research Institute not only taught me a great deal about radio direction finding and provided assistance in obtaining the FFIIX eigenvector optimization source code and documentation, but also supplied me with the AZRN subroutine for computing the distance between two points on a sphere.

Mr. Dennis Buechler and Mr. Patrick Wright assisted in the daily operation of the lightning location network and also provided some of the radar and precipitation data sets. Mr. Steven Williams assisted in the installation of the magnetic direction finder sites. This research was supported by the Physical Climate and Hydrologic Systems research program (formerly the Mesoscale Processes research program) at NASA Headquarters.

## TABLE OF CONTENTS

	<u>Page</u>
LIST OF TABLES .....	vi
LIST OF FIGURES .....	vii
LIST OF SYMBOLS .....	xiii
 Chapter	
I. INTRODUCTION .....	1
The Need for Real-Time Lightning Observations .....	6
Review of Nowcasting and Extrapolation Forecasting Algorithms ..	7
Quantifying the Valid Extrapolation Range .....	10
Study Objectives .....	12
II. A CONCEPTUAL MODEL OF THE THUNDERSTORM LIFE-CYCLE .....	15
Air Mass Thunderstorms .....	15
A Multi-cellular Thunderstorm.....	20
Convective Storm Complexes .....	20
Positive Polarity Cloud-to-Ground Flashes .....	25
A Conceptual Model of Cloud Electrical Development and Lightning Activity .....	26
The Logistic Growth Model .....	28
III. OPTIMIZATION METHODS FOR LOCATING LIGHTNING FLASHES USING MAGNETIC DIRECTION FINDING NETWORKS .....	32
Introduction .....	32
Overview of the FFIX Algorithm .....	34

Proof of Concept .....	37
BPE Calculation for a 4-DF Network .....	37
BPE Calculation for a 6-DF Network .....	40
Systematic Error Corrections .....	48
Defining the Sample Subset .....	49
Computing the Bearing Deviations .....	49
Computing New Solutions With the Corrected Bearings .....	52
Site Error Polynomials .....	54
IV. CLUSTERING METHODOLOGY .....	60
Storm Identification .....	60
Selecting a Clustering Algorithm .....	63
The K-Means Algorithm .....	64
Demonstration of Method .....	65
Define the Region of Interest .....	66
Identify the Cluster Seeds .....	73
Determine the Cluster Memberships .....	79
Tracking Seeds and Clusters .....	85
Synergism With Radar .....	93
V. THUNDERSTORM LIFE-CYCLES AND EXTRAPOLATION FORECASTING .....	100
Testing and Evaluation of the Logistic Growth Model .....	100
Isolated and Multicellular Storms .....	100
Total Lightning Activity for Airmass Storms .....	103
Long-lived Storm Complexes .....	110
Interpretation of Results .....	114
Role of the Environment in Limiting $\alpha$ .....	117
An Examination of the Residual Errors .....	121

Applications to Extrapolation Forecasting .....	122
Thunderstorm Duration .....	122
Thunderstorm Existence .....	123
VI. SUMMARY AND CONCLUSIONS .....	130
VII. RECOMMENDATIONS .....	133
APPENDICES	
A. The FFIX Algorithm .....	139
Mathematical Formulation of the Best Point Estimate (BPE) .....	139
Simplifying the Problem .....	142
The Confidence Region .....	144
B. Lightning Analysis Software .....	147
C. Cluster Analysis Software .....	181
BIBLIOGRAPHY .....	187

## LIST OF TABLES

Table	<u>Page</u>
1. Typical Linear Extrapolation Time Scales for Various Weather Events.....	2
2. Real-Time Users of the MSFC Lightning Network .....	8
3. Lightning Discharge Data Base .....	39
4. Error Ellipse Characteristics for 6-DF Network .....	47
5. DF Bearings and Site Error Corrections .....	51
6. Cluster Characteristics at 2215-2220 UTC .....	84
7. Hybrid Clustering Algorithm at 2220-2225 UTC .....	91
8. Parameters of the Logistic Growth Model .....	101
9. Objective Forecast Scoring Criteria .....	127

## LIST OF FIGURES

Figure	<u>Page</u>
1. Efficacy of different approaches to short-term forecasting over a range of time and space scales (after Doswell, 1986) .....	3
2. Demonstration national lightning network direction finder (DF) sites. Three sites are part of the MSFC network at Tullahoma, TN (DF 2 = TI), Centerville, TN (DF 3 = Ce), and Barton, AL (DF 4 = MS). DF 1 (at MSFC) is not part of the national network .....	5
3. Possible extrapolation model fits to a non-linear process based on two prior observations (OB1, OB2) and the current observation: <u>a</u> , linear extrapolation model; <u>b</u> , valid extrapolation range defined by acceptable error bounds; <u>c</u> , non-linear model fit that is worse than linear fit; <u>d</u> , good non-linear model fit (after Doswell, 1986) .....	11
4. Composite chart of thunderstorm development observed by radar, radiosonde and electrical sensors (after Workman and Reynolds 1949) ...	16
5. Lightning and precipitation history of an airmass thunderstorm that produced a microburst on 20 July 1986 at Huntsville, AL: <u>above left</u> , total flash rate time series where $N_{IC}$ and $N_{CG}$ represent the number of intracloud and cloud-to-ground flashes produced by the parent storm; <u>right</u> , time-height cross-section of cloud top infrared temperature ( $^{\circ}C$ ), 0 dBZ and 30 dBZ echo contours and maximum reflectivity; <u>lower left</u> , vertically integrated liquid water content (VIL), storm mass, rain flux and echo volume; <u>right</u> , peak reflectivity (Z) and storm average rain rates (R) as indicated (after Goodman et al., 1988) .....	18
6. Lightning-rainfall relationships for a small multi-cellular storm on 25 July 1986 .....	21
7. Lightning-rainfall relationships for a mesoscale convective system on 13 July 1986 .....	22
8. Hourly cloud-to-ground lightning rates and rainfall as a function of Mesoscale Convective Complex (MCC) life-cycle (adapted from Goodman and MacGorman, 1986; McAnelly and Cotton, 1986) .....	23

9.	NSSL lightning network shown in satellite projection with the infrared cloud top image of a MCC during its mature phase (maximum cloud shield extent). The 4-DF deployment during 1983 and the 350 km range ring are denoted by crosses (after Goodman and MacGorman, 1986) .....	24
10.	Conceptual model of the temporal evolution of cloud electrical, kinematic, and microphysical development .....	27
11.	Logistic model with limiting value $\alpha$ plotted as a function of time $t$ .....	29
12.	FFIX algorithm flowchart .....	35
13.	Deployment of the lightning, radar and rawinsonde network for the Cooperative Huntsville Meteorological Experiment conducted near Huntsville, AL in 1986 .....	38
14.	Lightning during the period 2315–2325 UTC on 13 July 1986 superimposed onto the CP-2 radar echo prior to ground truth corrections: $\cdot$ = negative polarity discharges; $+$ = positive polarity discharges. Radar reflectivity contoured at 18 dBZ and 40 dBZ .....	41
15.	The location and 50% error ellipses ( $2^\circ$ bearing standard deviation) for each discharge after radar ground truth corrections .....	42
16.	Overlay of corrected lightning location estimates with the radar echo. Same as in Figure 15 but with $1.5^\circ$ bearing standard deviation .....	43
17.	FFIX solutions for cloud-to-ground flash detected in Kansas by the NSSL DF network .....	44
18.	Distribution of radar echoes and lightning activity corresponding to the time of the FFIX solution in Kansas. Large cross indicates solution #1. Radar contours at 18, 30, 40, 45, 50 and 55 dBZ .....	46
19.	Bearing lines from each of the DFs to the reflectivity core of the subject storm .....	50
20.	Location estimates and 50% error ellipses for each flash before radar ground truth corrections .....	53
21a.	Site error polynomial and residual for DF 1 .....	55
21b.	Site error polynomial and residual for DF 2 .....	56
21c.	Site error polynomial and residual for DF 3 .....	57
21d.	Site error polynomial and residual for DF 4 .....	58
22.	Lightning plots during the period 2300–2330 UTC with semimajor ellipse axis thresholds: <u>a</u> , infinity; <u>b</u> , 2 km; <u>c</u> , 10 km; <u>d</u> , 20 km .....	59

23.	Map of ground discharges in the Tampa Bay, FL area on 8 August 1979 from 1700-2000 UTC (1300-1600 EDT) by a 2 DF network. Map scale is in thousands of feet (adapted from Peckham et al., 1984) .....	61
24.	Cloud-to-ground lightning contour maps (number of discharges per cell per 5 min) of storms embedded within a mesoscale convective system in North Alabama on 11 June 1986. Time in UTC. (after Goodman et al., 1988) .....	62
25.	Composite precipitation pattern at 2000 UTC (1400 CST) on 15 November 1989 observed by the regional network of NWS radars. The radar reflectivity is contoured at 18,30,40,45,50,55 dBZ (VIP levels 1-6). <u>Small solid circle</u> = Reflectivity cores > 45 DBZ; <u>large solid circle</u> = track of the tornadic supercell storm every 15 min. The motion vector of cells within the squall line indicated by the wind barb is $25 \text{ m s}^{-1}$ from $235^\circ$ .....	67
26.	Composite precipitation pattern at 2100 UTC on 15 November 1989 .....	68
27.	Composite precipitation pattern at 2200 UTC on 15 November 1989 .....	69
28.	Composite precipitation pattern at 2230 UTC on 15 November 1989 .....	70
29.	Cloud-to-ground lightning activity from 2105-2236 UTC on 15 November 1989. $\cdot$ = negative polarity discharges; $+$ = positive polarity discharges .....	71
30.	County and state outlines in the lightning analysis region. Range rings are every 50 km. The site of the MIT/Lincoln Laboratory FL2 Doppler radar is at the center of the rings .....	72
31.	Centroid of all lightning within the analysis region in 5-min intervals (labeled 1-9-A-D) during the period 2130-2235 UTC. <u>I</u> = track of the tornadic storm echo every 15 min beginning at 2130 UTC; <u>t</u> = location of tornado touchdown and tree damage on Redstone Arsenal. The FL2 radar is at the geographic center of the map at the point (0,0) .....	74
32.	Lightning analysis region with 10 km gridpoints .....	75
33.	Evolution of cloud-to-ground lightning activity in 5-min intervals between 2135-2235 UTC. Contours are approximately 0.01 discharges $\text{km}^{-2}$ and 0.02 discharges $\text{km}^{-2}$ (shaded) .....	76
34.	Contoured lightning density map during the period 2215-2220 UTC. Contour interval is every 0.01 discharges $\text{km}^{-2}$ beginning with the value 0.02 discharges $\text{km}^{-2}$ .....	77
35.	Diagram of the 3 x 3 point search window moving through the m-row x n-column data matrix D. Lightning shown for the period 2215-2220 UTC at each 10 km gridpoint .....	78
36.	Diagram of the seed matrix S after one pass through the data matrix. The search window is centered at the point $S(i,j) = (17,20)$ .....	80

37.	Diagram of the final seed matrix S .....	80
38.	Cluster assignments for each flash during the period 2215-2220 UTC. <u>Circled lower case letters (a-e)</u> = cluster seeds with values greater than 0.02 discharges $\text{km}^{-2}$ ; T = location of tornadic storm echo at 2215 UTC .....	81
39.	Cluster assignments for each flash during the period 2215-2220 UTC. <u>Circled lower case letters (a-e)</u> = cluster seeds with values greater than 0.02 discharges $\text{km}^{-2}$ ; <u>Circled lower case letters (f-i)</u> = cluster seeds each represented by a single negative polarity discharge .....	83
40.	Cluster assignments for each flash during the period 2220-2225 UTC. <u>Circled lower case letters (a-i)</u> = cluster seeds with values greater than 0.02 discharges $\text{km}^{-2}$ .....	86
41.	Cluster assignments for each flash during the period 2225-2230 UTC. <u>Circled lower case letters (a-e)</u> = cluster seeds with values greater than 0.02 discharges $\text{km}^{-2}$ .....	87
42.	Cluster assignments for each flash during the period 2230-2235 UTC. <u>Circled lower case letters (a-f)</u> = cluster seeds with values greater than 0.02 discharges $\text{km}^{-2}$ .....	88
43.	Hybrid clustering algorithm assignments during the period 2220-2225 UTC. <u>Circled lower case letters (a-e)</u> = cluster seeds with values greater than 0.02 discharges $\text{km}^{-2}$ .....	90
44.	Seed tracks during the period 2200-2230 UTC. <u>Lower case letters (a-e)</u> = seed position for each 5-min interval that the seed value exceeds a threshold of 0.02 discharges $\text{km}^{-2}$ . <u>Upper case letters (A-E)</u> = seed seed location at 2215 UTC; <u>T</u> = Position of tornadic storm echo at 2200, 2215 and 2230 UTC .....	92
45.	Cluster assignments during the period 2135-2140 UTC. A seed threshold of 0.01 discharges $\text{km}^{-2}$ produces 21 clusters (A-T). <u>T</u> = tornadic storm discharges .....	94
46.	Plan-view of a small multicellular storm complex observed by the CP2 radar on 13 July 1986 at 2328 UTC. <u>Circled upper case letters (A,B)</u> = two storm centroids identified by the NEXRAD storm identification and tracking algorithm; <u>solid contour</u> = reflectivity > 40 dBZ; <u>shaded region</u> = reflectivity > 55 dBZ. Distance units in kilometers from CP2 .....	96
47.	Three-dimensional structure of the storm complex in Figure 46 .....	97
48.	Cluster assignments using two centroids identified by NEXRAD algorithm. <u>Circled lower case letters (a,b)</u> = radar echo cluster seeds; <u>Upper case letters (A,B)</u> = cluster assignments .....	98

49.	Cluster assignments using four centroids identified from peak reflectivity ( $Z > 55$ dBZ) maxima. <u>Circled lower case letters (a,b,c,e)</u> = radar echo cluster seeds; <u>Upper case letters (A,B,C,E)</u> = cluster assignments .....	99
50.	Cloud-to-ground lightning clusters during 5-min intervals on 17 July 1986. Distance units in kilometers from FL2 radar. (Time in UTC.) .....	102
51.	Base scan radar echoes observed by the Nashville radar: <u>upper left</u> , 1600 UTC; <u>upper right</u> , 1630 UTC; <u>lower left</u> , 1700 UTC; <u>lower right</u> , 1730 UTC. Contour interval every 10 dBZ beginning at 10 dBZ .....	104
52.	Lightning and rainflux time series for storms A and C: <u>Upper case letters</u> , number of ground discharges in 10 min; <u>lower case letters</u> , radar estimated rainflux .....	105
53.	Logistic model regression and residual error for 17 July 1986 Storm A. <u>Top</u> : For each 10 min observation period, <u>A</u> = the observed flash rate; <u>P</u> = model prediction. <u>Bottom</u> : Residual error = $(A - P)$ .....	106
54.	Logistic model regression and residual error for 17 July 1986 Storm C. <u>Top</u> : For each 10 min observation period, <u>A</u> = the observed flash rate; <u>P</u> = model prediction. <u>Bottom</u> : Residual error = $(A - P)$ .....	107
55.	Logistic model regression and residual error for 20 July 1986 airmass storm. <u>Top</u> : For each 10 min observation period, <u>A</u> = the observed flash rate; <u>P</u> = model prediction. <u>Bottom</u> : Residual error = $(A - P)$ .....	108
56.	Total lightning time series (discharges per 5 min) for two thunderstorms observed near Cape Canaveral, Florida .....	109
57.	Cloud-to-ground lightning time series (discharges per 10 min) during the period 1600 UTC 15 November to 0100 UTC 16 November 1989 for a mesoscale convective system observed in the Tennessee Valley .....	111
58.	Logistic model regression and residual error for 15 November 1989 mesoscale weather system. <u>Top</u> : For each 10 min observation period, <u>A</u> = the observed flash rate; <u>P</u> = model prediction. <u>Bottom</u> : Residual error = $(A - P)$ .....	112
59.	Cloud-to-ground lightning discharge histograms and composite lighting life-cycle for mesoscale convective complexes (MCCs). The four life-cycle phases are identified as first storms (F), initiation (I), cold cloud shield maximum extent (M), and termination (T). The composite is plotted with respect to the time and magnitude ( $\pm$ one standard deviation) of the average peak flash rate. (After Goodman and MacGorman, 1986) .....	113

60.	Average hourly cloud-to-ground discharge rates are normalized to the average peak flash rate of MCCs and are shown relative to the time of occurrence of the peak. $N$ is the percentage of the peak rate at a given hour and $R^2$ is the correlation coefficient for each of the exponential curves. <u>Open circles</u> , denote the time and magnitude of the lightning rates for each of the MCC life-cycle phases F, I, M, T (After Goodman and MacGorman, 1986) .....	115
61.	Logistic model regression and residual error for MCC composite life-cycle. <u>Top</u> : For each hourly observation period, $A$ = the observed flash rate; $P$ = model prediction. <u>Bottom</u> : Residual error = $(A - P)$ .....	116
62.	Regression plot of maximum hourly flash rate ( $Y$ ) as a function of the lifted index ( $X$ ) computed from the Redstone Arsenal 1200 UTC soundings taken during June 1986. The 95 percent confidence limits are indicated by the dotted lines .....	118
63.	Regression plot of total cloud-to-ground flashes observed each day ( $y$ ) as a function of Convective Available Potential Energy (CAPE) ( $x$ ) computed from the Redstone Arsenal 1200 UTC soundings taken during June and July 1986. The 95 percent confidence limits are indicated by the dotted lines .....	119
64.	Maximum rain rate as a function of maximum parcel energy for 67 storm days near Ottawa, Canada during the summer of 1969-1970. (After Zawadzki et al., 1981) .....	120
65.	Cloud-to-ground lightning time series (per 5 min) of the 15 November 1989 storm system during the period 2130-2235 UTC .....	124
66.	Eleven-period ahead extrapolation (valid 2225-2230 UTC) of lightning activity observed during the period 2130-2135 UTC .....	126
67.	Observed lightning activity during the period 2225-2230 UTC .....	126
68.	One-period ahead extrapolation (valid 2230-2235 UTC) of lightning activity observed during the period 2225-2230 UTC .....	129
69.	Observed lightning activity during the period 2230-2235 UTC .....	129
70.	NEXRAD network sites .....	134
71.	NEXRAD sites in the Southeastern United States with 125 km range circles. The track of the 15 November 1989 tornado at Huntsville, Alabama is indicated by the cross and solid line .....	135
72.	Proposed $10.5^\circ$ field of view centered at $2^\circ\text{N}$ latitude and $75^\circ$ longitude for the lightning mapper sensor on GOES-Next .....	136
73.	Spherical triangle relationships used in the FFI algorithm .....	140

## LIST OF SYMBOLS

Symbol	<u>Page</u>
a	145
b	145
$d_L$	121
$d_U$	121
D	121
<b>D</b>	73
$D_i$	141
$e_t$	121
$e_{t-1}$	121
$e_2$	145
$H_0$	121
$H_1$	121
k	31
M	19
$N_i$	138
P	144
P	142
r	20
R	17

$s_k$	sum of squared bearing errors for a set of $k$ bearings .....	138
$S$	lightning seed matrix for cluster analysis .....	74
$S_i$	direction finder station $i$ .....	138
$t$	time .....	13
$t_i$	time of inflection of the logistic growth curve .....	31
$T$	environmental temperature .....	117
$T_v$	virtual temperature of air parcel .....	117
$T$	target vector .....	138
$w$	vertical velocity .....	117
$w_i$	weighting factor for the $i$ th bearing .....	138
$W_i$	matrix of weights for $i$ th station .....	141
$Z$	radar reflectivity .....	17
$Z_e$	equivalent radar reflectivity .....	18
$Z_{DR}$	differential reflectivity .....	18
$Z_H$	radar reflectivity at horizontal polarization .....	18
$\alpha$	limiting value parameter of the logistic growth curve .....	29
$\alpha_i$	angle defining the dot product of the target and $i$ th normal vector .....	143
$\alpha_o$	significance level in hypothesis test .....	122
$\beta$	time scale parameter of the logistic growth curve .....	31
$\epsilon_i$	bearing error at the $i$ th station .....	138
$\lambda_i$	eigenvalues of the matrix of rotation $P$ .....	142
$\Lambda$	diagonal $(\lambda_1, \lambda_2, \lambda_3)$ .....	142
$\Theta$	bearing angle .....	54
$\rho$	autocorrelation parameter .....	121
$\rho_i$	angle defining the dot product of the target and $i$ th station vector .....	138
$\sigma_i$	standard deviation of the bearing errors at the $i$ th station .....	138
$\sigma_i^*$	range weighted bearing standard deviation at the $i$ th station .....	138

$\Delta t$	time increment .....	13
$\chi^2$	chi-square test statistic .....	36



## CHAPTER I.

### INTRODUCTION

Weather radars and imaging sensors on geostationary weather satellites are currently the most widely used remote sensing tools for the short-term forecasting or nowcasting of warm season convective storms and for warning of severe thunderstorm hazards. Zipser (1983) defines nowcasting as "the description of the state of the current weather and forecasts within the valid extrapolation range for each phenomenon which are based on intensive observations". The valid extrapolation range is further defined "as the period within which weather forecasts based upon observations and extrapolation are useful". The valid extrapolation period as well as the amount of lightning activity depend on the phenomena being described, geography, season of occurrence, instability of the atmosphere, and structure of the storm environment (Table 1). Dynamical forecast models with explicit physics are presently more applicable to greater time and space scales (Figure 1).

In a discussion of the stages of nowcasting, Wilson and Carbone (1984) state "the first element of forecasting is simple extrapolation of event position and intensity. Prediction of completely new development or onset of dissipation of the existing event is a distinctly more ambitious nowcast objective". Forecasts of the future location and intensity of clouds, precipitation, lightning, or storm severity can be assessed by asking yes/no or how much. Did it rain at all? Was there any lightning with that storm? Was there severe weather (flooding, hail, tornadoes, microbursts)? How much rain was forecast? How much lightning? Extrapolation forecasting is akin to conditional expectation. What is the probability of rain at point  $P_1$  in the next hour or two, given that it is

**Table 1. Typical Linear Extrapolation Time Scales for Various Weather Events**

Weather Event	Time Scale for Linear Extrapolation Validity (Nowcast)	Nonlinear Predictive Capability (Beyond Nowcast)	Accompanying Lightning Activity
Downburst/Microburst	~1 to a Few Minutes	Very Limited	Often Many Intracloud Flashes, Few Ground Flashes
Tornado	~1 to a Few Minutes	Very Limited	Often Many Intracloud Flashes, Ground Flash Rates Variable
Thunderstorm, Individual	5–20 Minutes	Very Limited	Variable Ratio of Intracloud to Ground Flashes
Severe Thunderstorm	10 Minutes to 1 Hour	Very Limited	Typically Many Intracloud Flashes, Ground Flashes Variable
Thunderstorm Organized on Mesoscale	~1–2 Hours	Some	Typically Many Intracloud and Ground Flashes
Flash-Flood Rainfall	~1 to a Few Hours	Very Limited	Varies From Many Ground Flashes to None
High Wind, Orographic	~1 to a Few Hours	Some	–
Lake-Effect Snowstorms	A Few Hours	Very Limited	Some
Heavy Snow/Winter Storm/Blizzard	A Few Hours	Some	Not Usually
Frost/Freeze	Hours	Some	–
Low Visibility	A Few Hours	Some	–
Air-Pollution Episode	Hours	Some	–
Wind	Hours	Some	–
Precipitation	Hours	Some	Variable
Hurricane	Many Hours	Fair	Variable
Frontal Passage	Many Hours	Fair to Good	Variable
*Adapted From Zipser (1983); Doswell (1986)			

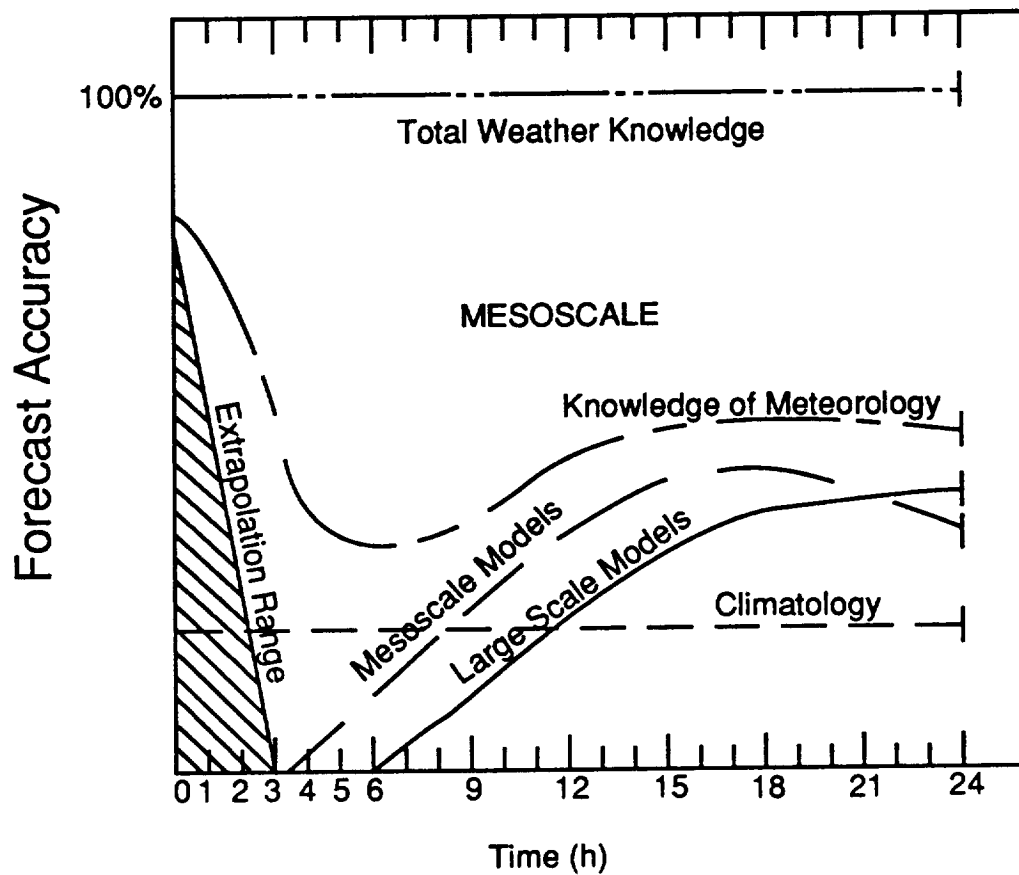


Figure 1. Efficacy of different approaches to short-term forecasting over a range of time and space scales (after Doswell, 1986).

raining at point  $P_0$  now? Any ability to determine the presence, increase, or decrease of lightning activity as a storm approaches a given location or facility will provide valuable information to the user of these data.

With the recent advent of lightning detection and location technology, it is now possible to directly measure the existence and frequency of lightning activity in storms over large areas. The deployment of regional and national networks (Figure 2) using magnetic direction finding (Krider et al., 1976) and time-of-arrival (Bent and Lyons, 1984) techniques to detect and locate cloud-to-ground lightning offers a new and decidedly different nowcasting data source for real-time multisensor data fusion. In the future total lightning rates (intracloud and cloud-to-ground) will also be observed in real-time by a lightning sensor in geostationary orbit (Christian et al., 1989).

The observed lightning activity may be used in determining the existence, initiation, movement, dissipation, configuration, areal extent, intensity, and redevelopment of convective storms (Goodman et al., 1988a; Lewis, 1989). A recent evaluation of the operational use of lightning data by forecasters at the National Severe Storms Forecast Center (NSSFC) demonstrated great value in monitoring lightning activity for assessing the threat of existing storms and in issuing weather advisories; most frequently when storms were classified as strong (5-min update interval) and less frequently when storms were weak (15-min update interval). Furthermore, when forecasters were asked if lightning activity added knowledge about the general convective activity that could not be obtained from either satellite or radar data, a positive response was acknowledged for 78% of 153 storm episodes considered strong and for 64% of 301 cases of storms considered weak (as subjectively characterized by the forecasters).

These preliminary results suggest that lightning activity and its association with a storm or complex of storms should be quantified and used as a source of nowcasting information in knowledge-based and expert system/artificial intelligence/neural network algorithms being developed and tested (Browning and Collier, 1989; Roberts et al., 1990).

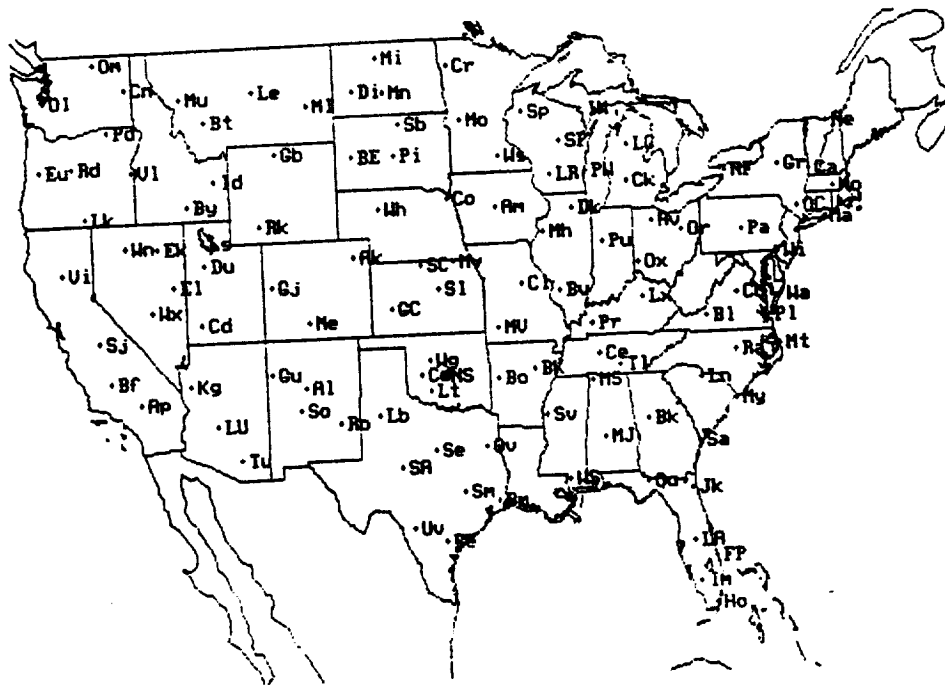


Figure 2. Demonstration national lightning network direction finder (DF) sites. Three sites are part of the MSFC network at Tullahoma, TN (DF 2 = TI), Centerville, TN (DF 3 = Ce), and Barton, AL (DF 4 = MS). DF 1 (at MSFC) is not part of the national network.

The quantitative assessment of lightning activity offers a wide range of opportunities to develop algorithms to evaluate the synergism of these data as an adjunct to the weather radar, satellite, and conventional meteorological data (Watson et al., 1987; Goodman et al., 1988). The Advanced Weather Interactive Processing System (AWIPS) currently under development by the National Weather Service will be the first opportunity for all local forecast offices to integrate, process, and transmit high volume radar, satellite, upper air, and surface data.

### The Need for Real-Time Lightning Observations

A recent survey of federal agency requirements provides a clear impetus for developing real-time techniques to monitor lightning hazards (MSI Services, 1986). Examples include: 1) data requirements by the National Weather Service (NWS) during active thunderstorm periods to issue severe weather warnings; 2) timely information needed by the Federal Aviation Administration for flight safety, dispatch, and air traffic control/operations; 3) reliable tracking of lightning to support the safe and efficient operation of a variety of naval activities including operational and training flights, weapons and munitions handling, and aircraft and in-port ship refueling ; real-time display of the location and direction of movement of cloud-to-ground lightning strikes within 300 km to support Air Force strategic and defensive activities including refueling operations, munitions handling, radar operations, computer operations, safety, and field exercises.

Facility applications of lightning data include various test range activities such as those conducted by the Air Force and National Aeronautics and Space Administration (NASA) in support of the Space Shuttle and unmanned space vehicles, and by the Department of Energy in support of the Nevada test site where underground nuclear tests are conducted. Presently, NASA operates lightning detection systems at Marshall

Space Flight Center (MSFC), AL; Wallops Island, VA; and Kennedy Space Center, FL. Lightning data from a Navy operated network are also distributed to the Stennis Space Center, MS. The operational requirements for lightning data at test facilities are driven primarily by the concern over personal safety. However, improved lightning warnings at Kennedy Space Center also permit safe fueling operations during stormy weather periods at an estimated annual savings of one million dollars. Real-time users of the MSFC lightning network are shown in Table 2.

Utilities presently use lightning data to design protection for power lines and distribution systems, and to deploy repair crews during severe storms (Fischer and Krider, 1982). In general, lightning warnings tend to be very conservative, with many operational and training opportunities cancelled unnecessarily resulting in lost productivity. This brief summary of applications strongly suggests that any lightning sensitive tasks concerned with optimizing the safety and use of material and human resources can benefit from the currently available lightning detection and location technology.

#### Review of Nowcasting and Extrapolation Forecasting Algorithms

A nowcasting system consists of two main parts: 1) some type of characterization of the present weather situation and 2) a means (i.e., a model) to project the situation forward in time and space. Forecast methods using weather radar to extrapolate rainfall (an appropriate analog for lightning patterns), storm position, and intensity typically use some reflectivity (intensity) threshold to define the convective storms as either cells (clusters) or rain areas, correlate two or more successive observations to get a storm motion vector, and extrapolate the intensity pattern some time into the future.

The existing operational radar nowcasting systems extrapolate the characteristics and full intensity of the precipitation pattern without consideration for growth/decay of the rain intensity or its spatial distribution. The primary source of forecast error in a

**Table 2. Real-Time Users of the MSFC Lightning Network**

---

---

U.S. Air Force, Arnold Engineering and Development Center, TN  
U.S. Army, Redstone Arsenal, AL Test and Engineering Directorate  
NASA, Marshall Space Flight Center, AL  
Earth Science and Applications Division  
Rocket Motor Test Areas  
Information Systems Office  
Safety, Reliability, Maintainability, and Quality Assurance Office  
Neutral Buoyancy Simulation Facility  
\*Redstone Airfield Flight Operations  
WAFF 48, Huntsville, AL Television Station  
\*National Weather Service Office, Huntsville, AL  
†State University of New York at Albany, National Lightning Network

---

\*Future Users

†Raw Bearing Information Provided by Three MSFC Antennas

study of rain patterns associated with weather fronts in Great Britain was attributed to the development or decay of rain areas in 16 of 29 (55%) events (Browning et al., 1982). Storm growth/decay, mergers, splitting, and fragmentation also compromise the performance of peak reflectivity trackers (Crane, 1979; Rosenfeld, 1987), centroid trackers (Barclay and Wilk, 1970; Duda and Blackmer, 1972; Zittel, 1976; Bjerkaas and Forsyth, 1980), and (pattern) correlation trackers (Austin and Bellon, 1974; Rinehart and Garvey, 1978; Browning et al., 1982).

Peak reflectivity trackers isolate and track local maxima in the reflectivity or precipitation field. Such techniques tend to overestimate the number of physically realistic storm cells, but do not miss the small, potentially severe storms that may not be identified by the other methods which depend on intensity thresholds to delineate storms. The centroid trackers use the 3-dimensional reflectivity weighted centroids (storm mass) to delineate, characterize, and follow storm movement. Correlation trackers compare a field of reflectivity values at two successive times to get a motion vector for the entire system (more applicable to widespread light rain situations) or in localized sub-areas (applicable to individual thunderstorms).

The Bjerkaas and Forsyth (1980) mass weighted centroid tracker has been implemented as a Next Generation Weather Radar (NEXRAD) system algorithm (NEXRAD, 1985). NEXRAD is the Doppler radar system being jointly deployed across the United States and overseas by the National Weather Service, Federal Aviation Administration, and Air Weather Service to replace the aging WSR-57 and WSR-74 network radars now in service (Leone et al., 1989). These new radars offer numerous advantages over present weather radars in severe thunderstorm warning, rainfall estimation, and the detection of wind shears.

In a study comparing the performance of different types of storm trackers, Elvander (1976) found the cross-correlation tracker performed best when presented only base-scan (lowest elevation level) reflectivity data and the centroid tracker superior for

volume-scan data (the data acquisition mode for NEXRAD). A comparison between the Crane (1979) peak reflectivity tracker and centroid trackers showed general agreement of the storm motion vectors. Brasunas (1984) recommended using the correlation tracker on slowly moving widespread rain areas and the centroid tracker on the more convective storms. For large areas with multiple storm motion vectors, Browning and Collier (1989) suggested applying the correlation tracker to subareas within the confines of the larger system.

Other sources of forecast error can be attributed to incorrect specification and delineation of the initial pattern (measurement errors), errors in estimating the initial pattern trajectory, and errors due to changes in the trajectory during the forecast period. Examples of this latter effect are storms that upon becoming severe tend to move to the right of the mean lower tropospheric wind (Newton and Fankhauser, 1964; 1975), and rainbands associated with tropical hurricanes and extra-tropical cyclones where the ambient wind field imparts both a translational and rotational component to produce a curvilinear trajectory.

#### Quantifying the Valid Extrapolation Range

Linear extrapolation of the present trend is perhaps the easiest and most widely used method for nowcasting. However, the motion of the atmosphere and growth/decay of convective phenomena are examples of complex non-linear dynamical systems. The limitations of linear extrapolation with increasing time scale are readily apparent as the forecast error becomes large and then exceeds the threshold value for an acceptable or "useful" forecast (Figure 3). As noted earlier, the valid extrapolation period will depend on the process under study, which itself will have some mean lifetime. A non-linear

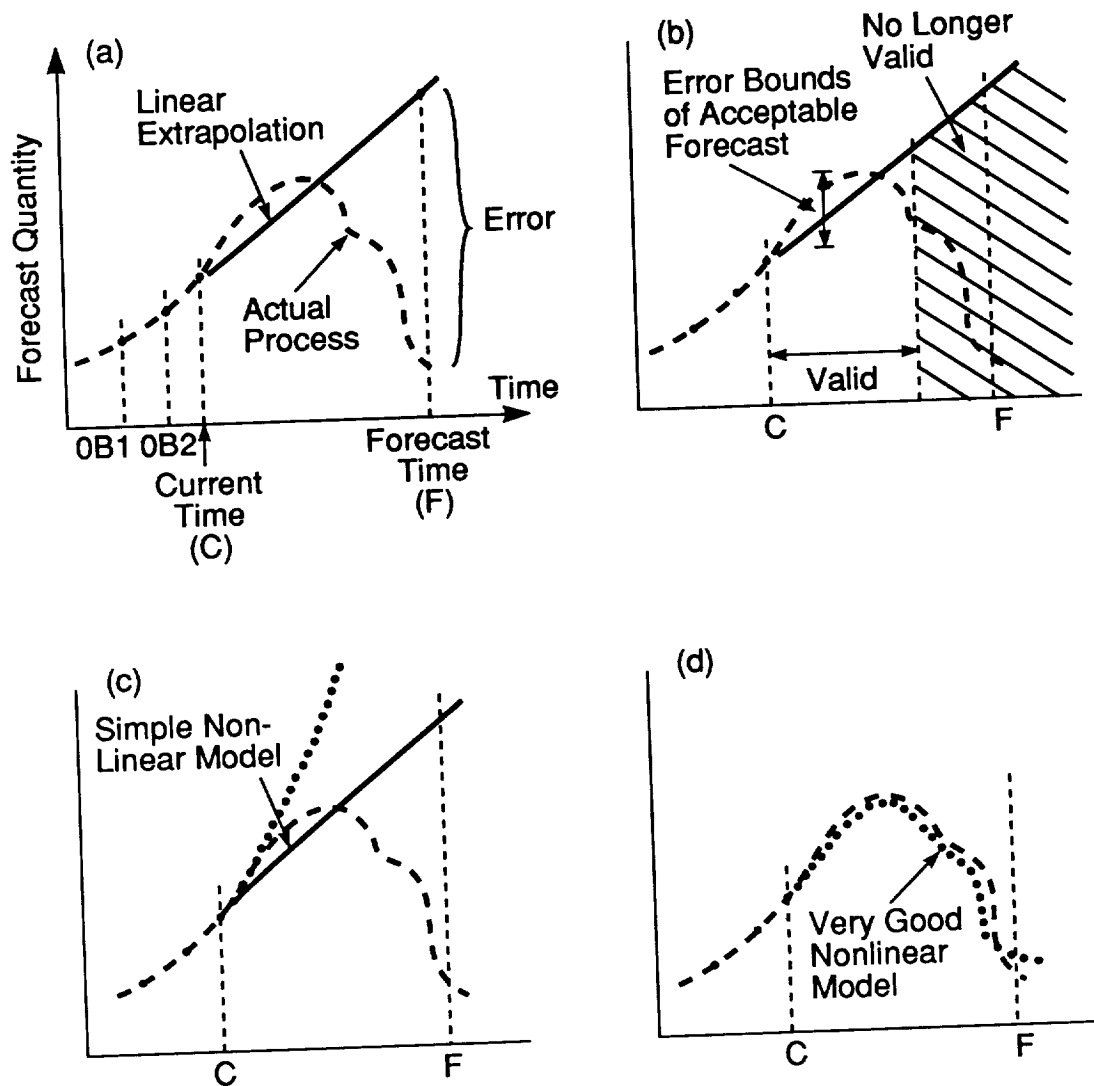


Figure 3. Possible extrapolation model fits to a non-linear process based on two prior observations (OB1, OB2) and the current observation: **a**, linear extrapolation model; **b**, valid extrapolation range defined by acceptable error bounds; **c**, non-linear model fit that is worse than linear fit; **d**, good non-linear model fit (after Doswell, 1986).

model may be inferior to a linear one if the nonlinear model is applied beyond the valid extrapolation range. In general, a non-linear model should provide the best forecast of a non-linear process such as the growth/decay of a thunderstorm.

For large, approximately steady state weather systems containing widespread light to moderate rain showers, extrapolation forecasts can be very accurate for up to 6 h (Browning et al., 1982). Projecting the motion of intense thunderstorms that persist for several hours (supercells) is not too difficult, but predicting if, when, and where it might spawn a tornado is beyond present capabilities. The tornadic storm that struck Huntsville, AL on 15 November 1989 is one example of an isolated supercell storm that could be identified on radar in Mississippi 5 h before it reached the city and produced an F4 intensity tornado that killed 22 people. Yet, the tornado struck with almost no warning. Forecasts of convective weather phenomena at smaller space and time scales can be much more difficult since they change size, shape, and intensity more readily.

### Study Objectives

The objectives of this study are twofold. First, the applicability and limitations of extrapolation techniques are explored relative to the problem of forecasting lightning (i.e., thunderstorm) activity at a future location and time using data acquired primarily from the NASA/MSFC ground strike lightning network installed, operated, and maintained by the author since 1985. Radar echoes and the spatial distribution of the lightning itself will be used to analyze, characterize, track, and examine extrapolative forecasts of storm position and the accompanying lightning activity. Second, the usefulness of physically-based non-linear models will also be examined for their applicability to the lightning forecast problem and to determine the valid extrapolation range for different weather scenarios.

In Chapter 2 the lightning and precipitation time series for storm systems over a wide range of space and time scales are examined. These results are used to develop a conceptual understanding of the thunderstorm life-cycle. The three parameter logistic model is offered as a candidate model of the thunderstorm life-cycle. Its properties and their relevance to the extrapolation nowcasting problem are examined. The success of an extrapolation forecast at time  $t+\Delta t$  is influenced by the quality of the data source (analyzed in Chapter 3), an accurate description of the present situation at time  $t$  (examined in Chapter 4), and correctly accounting for changes during the forecast period (investigated in Chapter 5).

Chapter 3 discusses the process of finding the most accurate locations of the cloud-to-ground lightning discharges. This process involves removing systematic errors from the data and the application of an optimization technique to locate the most probable position of each lightning discharge. A novel approach using isolated radar echoes to constrain the error correction and optimization procedures to remove systematic errors is described.

Chapter 4 presents a pattern recognition scheme that is used to generate initial seeds or "first guess" fields for clustering the discrete lightning discharges into storm cells. The clustering process is critically dependent on the prior accuracy of the lightning location estimates (Chapter 3) and the generation of subsequent storm life-cycle time series (Chapter 5) relies on the cluster analysis procedure assigning the correct number of lightning discharges (objects) to the proper storms (groups). The advantages and limitations of different clustering strategies for storm identification and tracking are examined. Storm identification with lightning data alone is compared to storm identification with radar alone, and some synergies for sensor fusion are explored.

In Chapter 5 the logistic growth model is utilized to examine the storm life-cycle over a wide range of space and time scales and address the potential of non-linear regression models to improve upon short-term extrapolation forecasts. A physical interpretation of the logistic model parameters and the resulting implications for determining the valid extrapolation range is considered.

Chapter 6 summarizes the chief results of this research and discusses how these results move the state of knowledge forward. Chapter 7 concludes the discussion and offers future areas for additional research.

Appendix A provides the mathematical formulation for the optimization algorithm (not currently available in the open literature) employed in Chapter 3 to find the most probable flash locations. Appendix B contains the FORTRAN-77 source code used to convert the raw data into geophysical quantities, correct the systematic errors in the data, and compute the optimal flash location. Lastly, Appendix C contains the FORTRAN-77 source code for the cluster analysis.

## CHAPTER II.

### A CONCEPTUAL MODEL OF THE THUNDERSTORM LIFE-CYCLE

A conceptual understanding or model of the thunderstorm life-cycle is needed for addressing the utility and limitations of extrapolation forecasts of non-steady-state weather phenomena such as thunderstorms and their accompanying lightning activity. The following discussion examines the lightning and precipitation time series for storm systems ranging in size from an isolated airmass storm to a large mesoscale storm complex encompassing an area of nearly 12,000 km<sup>2</sup>.

#### Air Mass Thunderstorms

The relationships between the early electrical development of a thunderstorm cell and the vertical development of the radar echo, precipitation, and cloud top are depicted in Figure 4. A significant fraction of the total lightning (50-95%) occurs between regions of opposite charge within the cloud (intracloud lightning) without ever reaching the earth (cloud-to-ground lightning). The initial discharge will almost always be intracloud. Typically this discharge occurs 5-10 min after initial electrification, which itself begins 5-10 min after the detection of a 35-40 dBZ radar echo aloft. Based on lightning and radar data collected in three different climatic environments (New Mexico, Alabama, and Florida), Buechler and Goodman (1990) find that the time lag from the reflectivity exceeding 40 dBZ at the -10°C level (the height of the main negative charge region in the thunderstorm central dipole) to the first intracloud discharge ranges from 4-33 min. The time lag is related to the rate of vertical development of the cloud. On

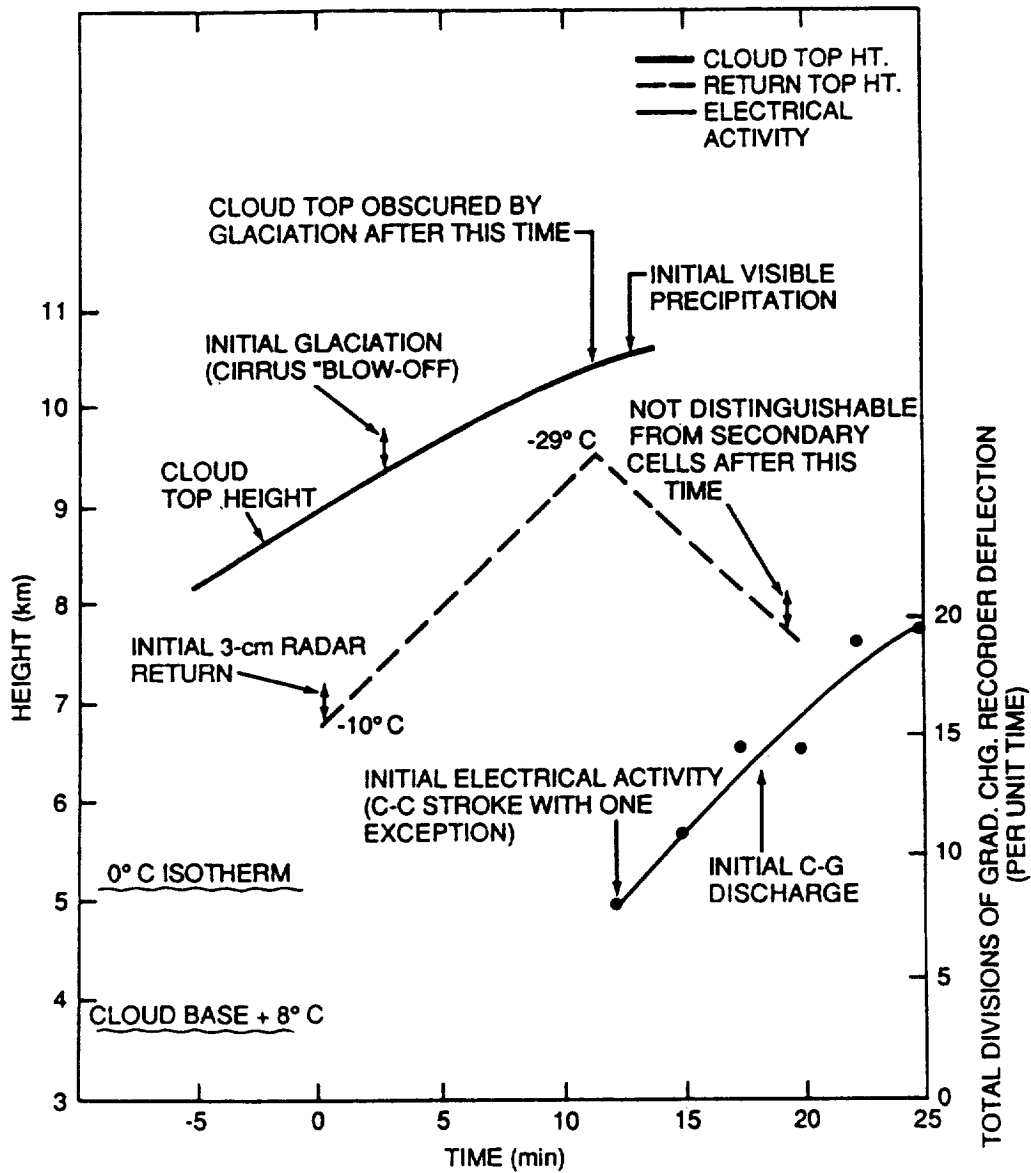


Figure 4. Composite chart of thunderstorm development observed by radar, radiosonde and electrical sensors (after Workman and Reynolds 1949).

average, the first cloud-to-ground discharge will be of negative polarity (it lowers negative charge to ground) and will occur 15-20 min after the initial radar echo is observed in a vertically growing cloud. The stage is now set for the active lightning phase of the thunderstorm life-cycle.

As the cell continues to develop, the active electrical phase may have a duration lasting from a few minutes to many hours. The total amount of lightning and peak flash rates of a storm are a non-linear function of its height, size, mass, duration, and environment (Shackford, 1960; Livingston and Krider, 1978; Williams, 1985; Cherna and Stansbury, 1986; Goodman and MacGorman, 1986; Goodman et al., 1988b).

Figure 5 shows the relationship between lightning occurrence and precipitation in a small airmass thunderstorm 26 km<sup>2</sup> in area (>18 dBZ) observed near Huntsville, AL by the NCAR CP2 radar on 20 July 1986. The storm produced a strong microburst with a velocity differential of 30 m s<sup>-1</sup>. Total lightning (intracloud and cloud-to-ground) activity was measured by an instrumented mobile laboratory operated by the National Severe Storms Laboratory (Rust, 1989). The mobile laboratory was also used for ground truthing the lightning strike network, discussed in greater detail in Chapter 3.

The 20 July case represents a Byers and Braham (1949) type airmass thunderstorm. The mobile laboratory was situated under the storm throughout its 45 min life-cycle and recorded 110 intracloud flashes and 6 cloud-to-ground flashes, all 6 of which were detected by the ground strike network. The first intracloud discharge was observed about 4 min after hail was initially indicated by radar, during a period of rapid vertical development as the cloud top neared its maximum height of 14 km. The first ground discharge occurred 5 min later when the maximum reflectivity core descended to 5.5 km and a weak outflow was detected by the radar.

Storm rain rates are computed from empirical Z-R relations developed by Marshall and Palmer (1948), Jones (1956), and Seliga et al. (1986). The storm rainflux (kg s<sup>-1</sup>), mass (kg), and vertically integrated liquid water content or VIL (kg m<sup>-2</sup>) (Greene

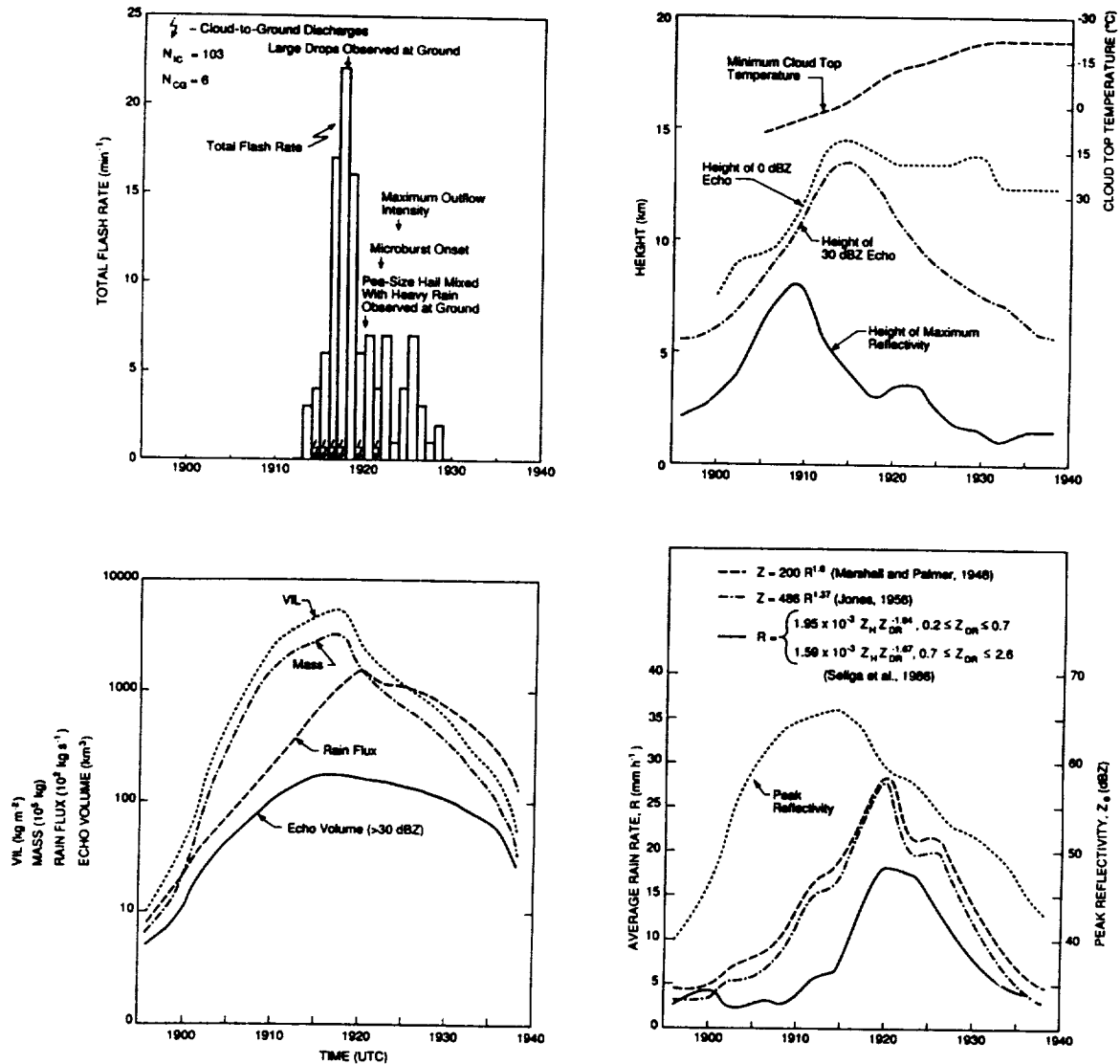


Figure 5. Lightning and precipitation history of an airmass thunderstorm that produced a microburst on 20 July 1986 at Huntsville, AL: above left, total flash rate time series where  $N_{ic}$  and  $N_{cg}$  represent the number of intracloud and cloud-to-ground flashes produced by the parent storm; right, time-height cross-section of cloud top infrared temperature ( $^{\circ}\text{C}$ ), 0 dBZ and 30 dBZ echo contours and maximum reflectivity; lower left, vertically integrated liquid water content (VIL), storm mass, rain flux and echo volume; right, peak reflectivity (Z) and storm average rain rates (R) as indicated (after Goodman et al., 1988).

and Clark, 1972) are calculated using a 30 dBZ threshold and the Jones (1956) relations  $Z=486R^{1.37}$  and  $M=0.052R^{0.97}$ , where  $Z$  ( $\text{mm}^6 \text{ m}^{-3}$ ), or  $Z_H$ , is the CP2 reflectivity at horizontal polarization,  $R$  ( $\text{mm h}^{-1}$ ) is the rain rate and  $M$  ( $\text{g m}^{-3}$ ) is the liquid water content.

The peak total flash rate of  $23 \text{ min}^{-1}$  was reached another 3–4 min after the initial lightning, 6 min prior to the maximum microburst outflows, and in conjunction with the peak in vertically integrated liquid water content ( $5.3 \times 10^3 \text{ kg m}^{-2}$ ), echo volume ( $1.9 \times 10^{11} \text{ m}^3$ ), and storm mass ( $3.3 \times 10^8 \text{ km}$ ). The rainflux ( $1.5 \times 10^5 \text{ kg s}^{-1}$ ) and storm averaged rain rates ( $18.2\text{--}28.2 \text{ mm h}^{-1}$ ) reached their maximum values in association with a visual confirmation of pea-sized hail mixed with heavy rain about 2 min after the peak flash rate.

Rapid-scan (5-min interval) satellite imagery from the GOES-E geostationary weather satellite were collected during the storm life-cycle. The infrared temperature of the cloud continued to show cooling (which could be misinterpreted as continued vertical development) even as the radar echo top and lightning rates decrease (indicating storm collapse). The misleading satellite signature is due to the small size of the storm and the (effectively  $4 \text{ km} \times 8 \text{ km}$ ) field of view of the infrared radiometer (which also "sees" the earth's surface). The radiometer field of view is underfilled at 1900 UTC. The field of view becomes more fully filled as the anvil expands, thereby sensing a decreasing cloud top temperature. However, the abrupt decrease in the total flash rate indicates storm collapse and thus serves as a microburst precursor. Yet, no such signature exists in the cloud-to-ground lightning evolution due to the small number of events (samples).

### A Multi-cellular Thunderstorm

Figure 6 shows the cloud-to-ground lightning and convective rainflux calculated every 10 min from the WSR-57 radar at Nashville, TN for a multi-cellular storm observed on 25 July 1986 over a period of 90 min. The convective rain area is simply defined here as the precipitating area within the 30 dBZ reflectivity contour. The lightning and rainflux are in-phase and are fairly well correlated ( $r=0.77$ ). However, as the storm decays the lighter rainfall area contributes more to the total precipitation such that there is more rainfall per flash during storm decay than during storm growth.

### Convective Storm Complexes

Figure 7 shows cloud-to-ground lightning and rainflux during a 7 h period of observation on 13 July 1986 of a mesoscale convective system in the Tennessee Valley that develops an extensive trailing stratiform rain region in the latter part of its life-cycle. The lightning data recording was briefly interrupted for a tape change at 2240 UTC and continued at 2248 UTC, but the latter period is not shown here. Not long after 2300 UTC the entire storm system could not be sampled adequately from the Nashville radar as the storm moved out of range to the south. This case again shows excellent agreement ( $r=0.96$ ) between the lightning and convective rainflux time histories.

Figure 8 presents a summary of the cloud-to-ground lightning and rainfall time histories of mesoscale convective complexes (MCCs) in the Central United States studied by Goodman and MacGorman (1986) and McAnelly and Cotton (1986). Such storm systems are readily identified by their persistence and extensive cold cloud shields in infrared satellite imagery (Figure 9). The typical precipitating lifetimes of MCCs are on the order of 12 h with spatial extents of a few hundred kilometers. Much of the warm season rainfall in the Northern Hemisphere (up to 70% in the major crop growing

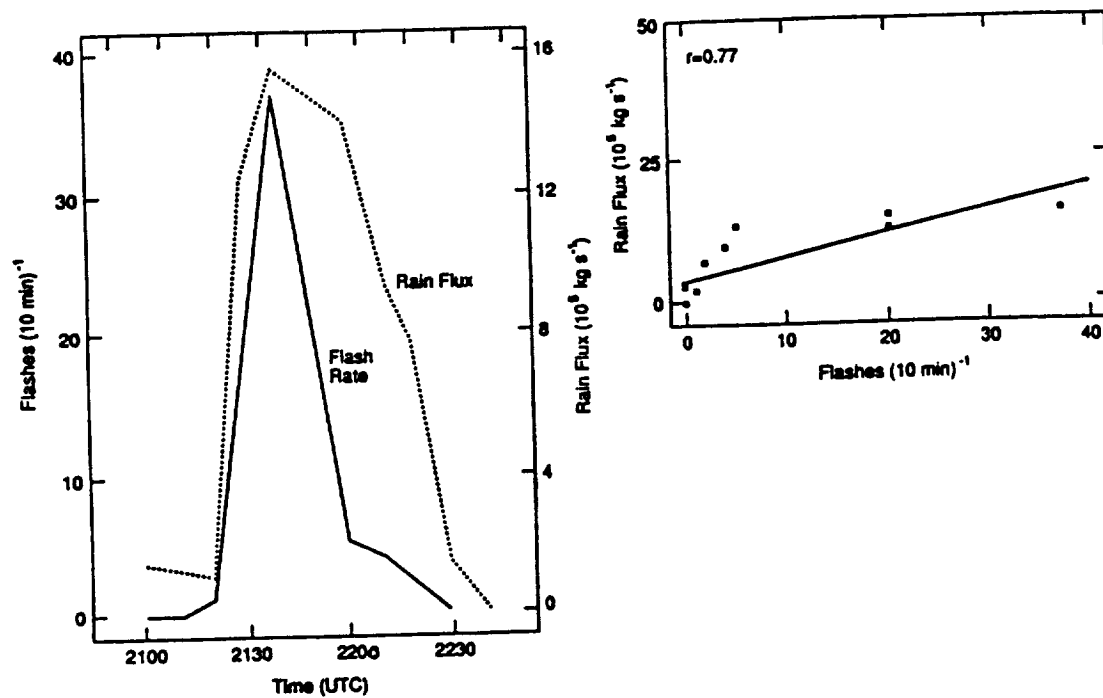


Figure 6. Lightning-rainfall relationships for a small multi-cellular storm on 25 July 1986.

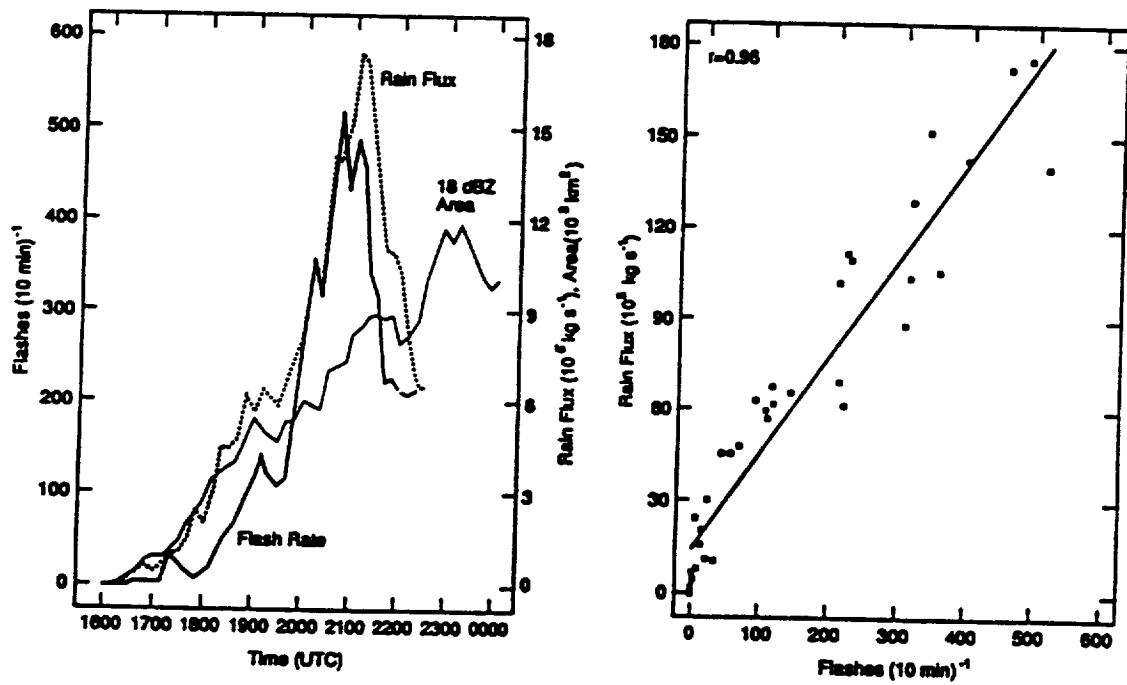


Figure 7. Lightning-rainfall relationships for a mesoscale convective system on 13 July 1986.

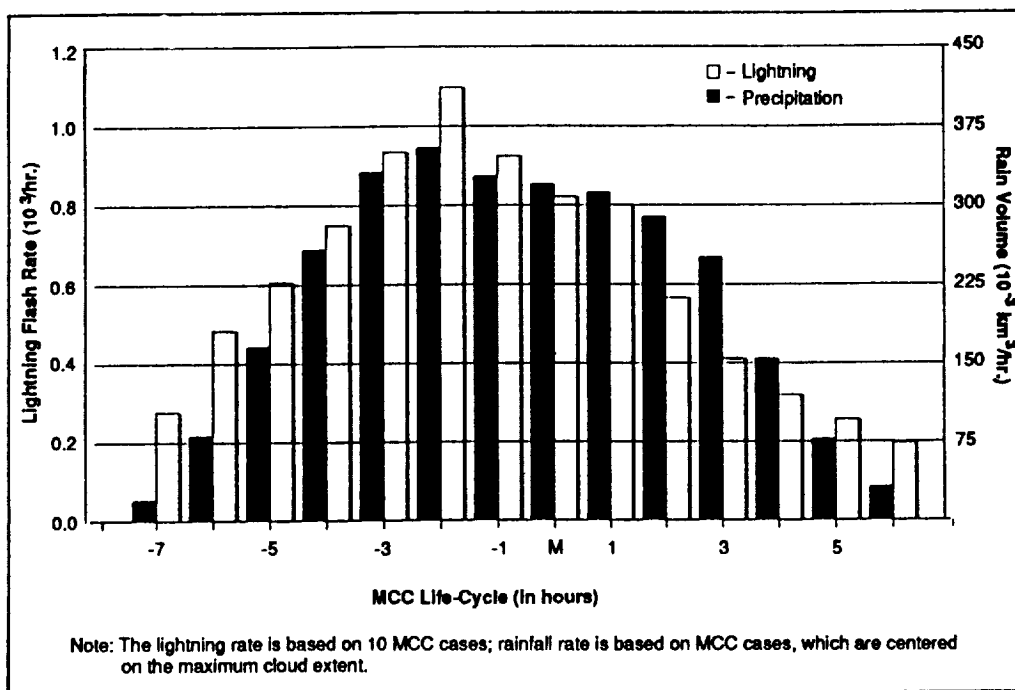


Figure 8. Hourly cloud-to-ground lightning rates and rainfall as a function of Mesoscale Convective Complex (MCC) life-cycle (adapted from Goodman and MacGorman, 1986; McAnelly and Cotton, 1986).

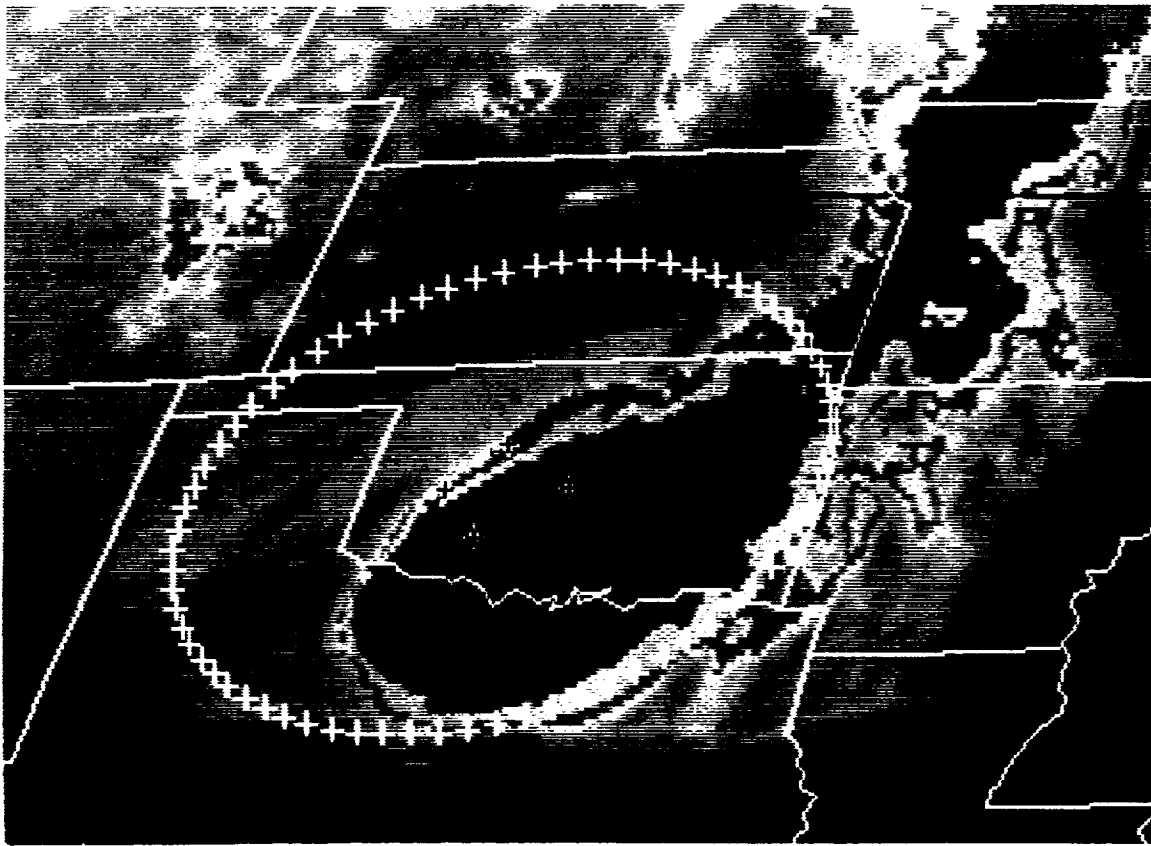


Figure 9. NSSL lightning network shown in satellite projection with the infrared cloud top image of a MCC during its mature phase (maximum cloud shield extent). The 4-DF deployment during 1983 and the 350 km range ring are denoted by crosses (after Goodman and MacGorman, 1986).

regions of the U.S.), extensive flooding, and severe weather is a result of these organized mesoscale circulations (Fritsch et al., 1986). Up to 25% of the entire annual lightning strikes at a given site can be accounted for by the passage of just one MCC (Goodman and MacGorman, 1986). Due to their meteorological and economic significance, any nowcast/forecast skill that can be demonstrated for mesoscale storm systems is a worthwhile endeavor.

The cloud-to-ground lightning activity increases and decreases exponentially over the life-cycle of MCCs. Based on earlier studies and the preceding analysis, this relationship appears to be generally valid for isolated storms, multi-cellular storms, and the ensemble convection embedded in organized mesoscale convective weather systems. The high correlations ( $>0.9$ ) between lightning and rainflux extends over three orders of magnitude from  $10^1$ - $10^4$  km<sup>2</sup>. Earlier scaling studies indicate that precipitating cloud dimensions are self-similar over 5 orders of magnitude (Lovejoy, 1982). Clearly, the non-linear physical interactions that produce the microphysical and dynamical properties of clouds are also relevant to their electrification.

#### Positive Polarity Cloud-to-Ground Discharges

Positive polarity cloud-to-ground discharges are often observed during the dissipation phase of the storm (Krehbiel, 1986). In addition, positive polarity flashes frequently occur 1) from thunderstorm anvils and storms which become severe and produce mesocyclones, large hail, or tornadoes (Rust, 1986); 2) in association with long-lived wet microbursts in low shear environments (Buechler et al., 1988); 3) in the trailing stratiform rain region of mesoscale weather systems (Rutledge and MacGorman, 1988); and 4) in the northern section of mesoscale systems, aligned with the geostrophic wind and downwind from the most vigorous convection, which is dominated by negative

polarity ground discharges (Orville et al., 1988; Engholm et al., 1990). The mesoscale system that led to the Huntsville tornado produced positive polarity discharges in each category listed above during some portion of its life-cycle.

#### A Conceptual Model of Cloud Electrical Development and Lightning Activity

Figure 10 summarizes these lightning observations into a conceptual model of the growth and decay of a typical thunderstorm and its associated total lightning activity. The temporal evolution of the lightning activity is in-phase with the development of the storm updraft and is strongly coupled to the life-cycle of the thunderstorm described above and in earlier studies by Byers and Braham (1949), Workman and Reynolds (1949), and others. These results show the electrical development of the cloud is intimately connected to its dynamical and microphysical development. Laboratory measurements by Jayaratne et al. (1983) suggest that the charge transferred per collision is a complicated function of particle size and type, cloud liquid water content, temperature, and even chemical composition. A possible inference from these observations is that the greater the production rate of precipitation and ice particles in a cloud, the greater the charging rate of the storm. This is partially supported by the growing success of numerical models in simulating the initial electrification of small thunderstorms (e.g., Ziegler et al., 1986; Helsdon and Farley, 1987). Multi-cellular storms will exhibit impulsive updraft, downdraft, precipitation, and flash rate growth and decay. Thus, the time rate-of-change of flash rates also provides a signature of the growth and decay of the thunderstorm.

CONCEPTUAL EVOLUTION OF THE  
ELECTRICAL, DYNAMICAL, AND MICROPHYSICAL PROCESSES INSIDE THUNDERSTORMS

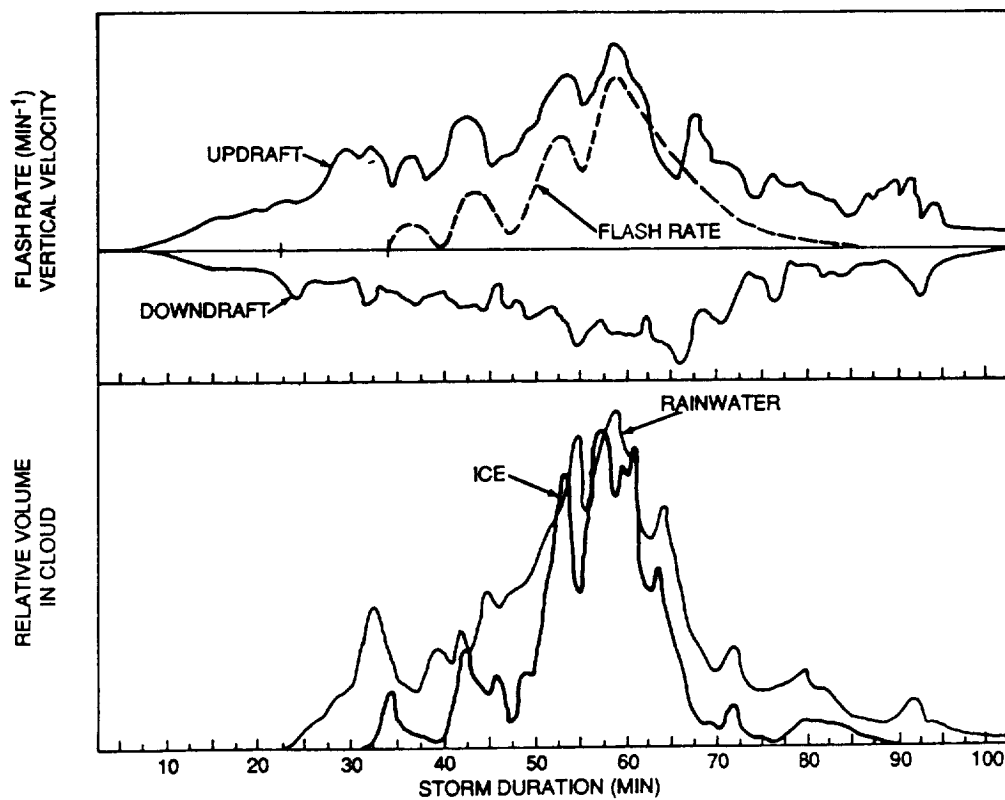


Figure 10. Conceptual model of the temporal evolution of cloud electrical, kinematic, and microphysical development.

### The Logistic Growth Model

Hald (1952) states that "the function used to represent the relationship between variables should as far as possible be chosen on the basis of professional knowledge about the problem under discussion and the reasons advanced for this choice are of fundamental importance as regards confidence in extrapolations". The storm system size and precipitation particle population have been shown to be important factors in maintaining the charging/discharging process. One can attempt to characterize this process by simple first order differential equations which have been applied to population dynamics to describe the phenomena of growth and decay (Hald, 1952; Bard, 1974; Boyce and DiPrima, 1977; Haberman, 1977).

The type of model needed depends on the the type of growth that occurs. These types of models are mechanistic in nature, rather than empirical. Mechanistic models are derived from assumptions on the type of growth, and these assumptions can be represented by differential or difference equations (Draper and Smith, 1981). Empirical models are chosen to approximate the unknown mechanistic models. One likely candidate mechanistic growth equation is the "logistic" or sigmoid curve (Figure 11). The logistic curve has frequently been used to describe the growth rates of populations (cells, human and animal populations, chemical kinetics, telephone subscribers, and business transactions).

Let  $t$  denote time or the magnitude of a growth factor which influences the size  $y$  of the phenomenon observed, then  $dy/dt$  denotes the rate of growth per unit time. Let the process be characterized by the general equation

$$\frac{dy}{dt} = f(t,y) \quad (2.1)$$

where the growth rate depends on both time and the size of the population.

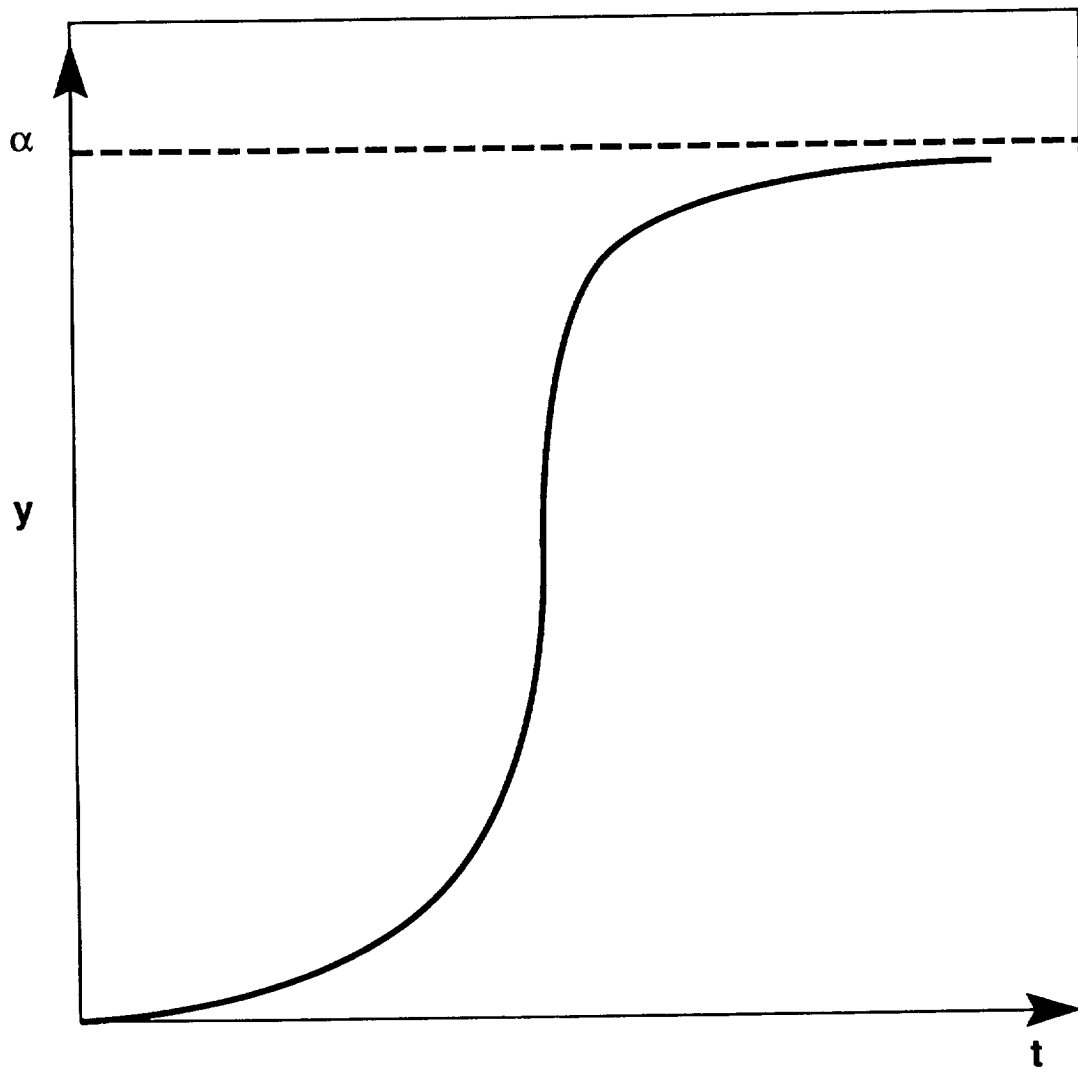


Figure 11. Logistic model with limiting value  $\alpha$  plotted as a function of time  $t$ .

Consider the following three special cases where

$$\frac{dy}{dt} = f(y)g(t). \quad (2.2)$$

Letting  $f(y)=1$ ,  $y$ , and  $y(\alpha-y)$  gives

$$\frac{dy}{dt} = g(t) \quad (2.3)$$

$$\frac{dy}{dt} = yg(t) \quad (2.4)$$

$$\frac{dy}{dt} = y(\alpha-y)g(t), \quad (0 < y < \alpha). \quad (2.5)$$

In (2.3) the growth rate  $y$  depends on time, but not on the size reached. In (2.4) the growth rate is proportional to the size reached and to a function of time. In (2.5) the growth rate is proportional to both the size reached and the remaining size, as well as a function of time. The latter case is the one of most interest. Now, write (2.2) as

$$\frac{dy}{f(y)} = g(t)dt. \quad (2.6)$$

Introducing the "logarithmic differential coefficient" (Hald, 1952, p.659)

$$\frac{d\ln(y)}{dt} = \frac{1}{y} \frac{dy}{dt} \quad (2.7)$$

and letting  $f(y) = y(\alpha-y)$  and  $g(t)=\beta$  gives a relation where the growth rate is proportional to the size of the population and remaining size (where  $\alpha$  denotes the growth is limited to some maximum amount, i.e., the value that  $y$  approaches as  $t$  increases) as well as a function of time. The growth rate relative to its present size,  $1/y$  ( $dy/dt$ ), decreases linearly as  $y$  increases. The resulting solution of the differential equation is the logistic function

$$y = \frac{\alpha}{(1+\beta e^{-kt})}. \quad (2.8)$$

This model is but one of many possible exponential growth models having similar forms (Hald, 1952; Williams, 1959; Richards, 1959; Draper and Smith, 1981; Bard, 1974; Haberman, 1977; and Myers, 1986). At  $t=0$ , the starting growth rate is  $\alpha/(1+\beta)$ . Also, as  $t \rightarrow \infty$ ,  $y \rightarrow \alpha$ .

The slope of the logistic curve is positive and the second derivative (Draper and Smith, 1981; Prof. Don Ryan, personal communication)

$$\frac{d^2y}{dt^2} = \left(\frac{k^2}{\alpha^2}\right)y(\alpha-y)(\alpha-2y) \quad (2.9)$$

has inflection points at  $y=0$ ,  $\alpha$ , and  $\alpha/2$ . At the point of inflection  $y = \alpha/2$ , substitution in Eq. (2.8) gives the time of inflection as  $t_i=(\ln\beta)/k$ . We note that the curve is symmetric about this point, i.e., the system decays or diminishes at the same rate at which it grows. Thus, for nowcasting purposes one might first compute the rate at which the lightning activity increases (i.e., a growth rate) and the time required for a storm to reach its peak discharge rate (the point of inflection). Based on symmetry, one would then predict the storm to decay at this same rate and reach the end of its life-cycle in the same number of time steps needed to produce the initial 50% of the total lightning.

In order to test and evaluate this model, one must develop a methodology for associating the discrete lightning events with their parent thunderstorms. This process is addressed in Chapter 4. Next, generate a time series at uniform sampling intervals. During each successive sampling period the parent storm must be tracked with time and correlated with its past position. The extrapolation forecast results are presented in Chapter 5. However, the pattern recognition process is strongly dependent on the quality and limitations of the lightning strike data which is described next in Chapter 3.

CHAPTER III.  
OPTIMIZATION METHODS FOR LOCATING LIGHTNING FLASHES USING  
MAGNETIC DIRECTION FINDING NETWORKS

Introduction

Magnetic direction finding (DF) networks for locating lightning strikes to ground require that two or more receivers detect the characteristic radio signal produced by return strokes (Krider et al., 1976). Once the signal is detected, an estimate of the most probable flash position, sometimes referred to as the best point estimate (BPE), and a confidence region can be constructed. The spatial distribution (or clustering) of the lightning flashes, however, is a function of the dimension and vigor of the storm, the orientation of the lightning channel and hence its radiation field, and the errors (both random and systematic) associated with the technique.

The systematic errors due to DF site effects are a major source of network degradation (Ross and Horner, 1952; Horner, 1954; Gething, 1978). When one or more of the network DFs do not detect the flash, the location estimate must be determined from a less favorable geometry (e.g., a flash along the baseline of two DFs, or a flash more distant from one site than another site in a more optimal geometry). The reliability of a fix (i.e., position estimate) can generally be maximized by using only the two closest stations to the target (Stansfield, 1947). However, near the baseline of the two DFs it is better to use a more distant receiver in a more favorable geometry (which will usually produce a smaller confidence ellipse). This is the basis for the real-time algorithm implemented in the earlier versions of the lightning DF networks manufactured

by Lightning, Location, and Protection (LLP), Inc. (Krider et al., 1980). This algorithm chooses the DF pair having the greatest signal strengths (presumably the two closest DFs to the flash). If the flash is near the baseline of the DF pair, a solution can be computed with the DF having the next strongest signal strength. An algorithm called "multiple correlation optimization" now replaces the simple 2 DF technique described above when three or more DFs detect a flash (LLP, Inc., 1988). This algorithm basically performs a least squares minimization between the most probable flash position and the sum of the bearing errors.

This latter algorithm, first introduced by Hiscox et al. (1984) and a more recent eigen-vector algorithm introduced by Orville (1987) are very similar to a technique first proposed more than ten years earlier by Wangsness (1973). All three algorithms attempt to minimize the same objective function although different methods are used to reject or flag "wild" bearings. Hiscox et al. (1984) also proposed the use of properly normalized signal amplitudes as an additional weighting factor (or constraint) to determine the optimal location. The improvement in solution accuracy by this latter method is a function of network geometry and the lightning location relative to that geometry. More recently, stochastic optimization techniques known as simulated annealing (Kirkpatrick et al., 1983; Szu and Harley, 1987a; 1987b) have been successfully applied to the general multiple DF/multiple bearing problem.

This chapter describes the application of an eigen-vector algorithm (called FFIX) which is based on the technique described by Wangsness (1973). FFIX was developed on or before January, 1973 (but apparently never published) for finding radio transmitter locations anywhere on earth from multiple DF bearings. The technique characterizes the measured bearings by bearing planes that pass through the center of the earth and by their unit normal vectors. The BPE is determined from the vector from the center of

the earth that minimizes the weighted sum of squares of its inner products with the normal vectors. A BPE and confidence ellipse are computed from the bearing data in terms of the eigenvalues and eigenvectors of a  $3 \times 3$  matrix.

This paper offers the first ever adaptation of the FFIX algorithm to the lightning location problem. The author is indebted to Dr. R. Johnson of the Southwest Research Institute and his sponsors at the Department of Defense for providing some documentation and the source code in 1985. The mathematical formulation for FFIX is provided in Appendix A. Appendix B contains the FORTRAN-77 source code for the FFIX subroutine.

### Overview of the FFIX Algorithm

Individual DF bearings are corrected for systematic errors and correlated in time for each lightning discharge before being submitted to FFIX to determine the most probable lightning ground strike point (Figure 12). The input data consist of  $n$  station bearings and their respective standard deviations (random plus any remaining systematic errors). The root mean square (RMS) bearing error for each LLP DF is about  $1^\circ$ . Previous attempts to iteratively remove the systematic error have not wholly eliminated them (Mach et al., 1986; Schutte et al., 1987). These techniques reduce the total bearing error (i.e., the standard deviation) to a value approaching  $2^\circ$  at best. It will be shown below that the standard deviation impacts both the BPE calculation and the confidence ellipse.

Sines of the bearing errors are assumed to be independent normally distributed random variables with zero means, but some bearings may be "wild". "Wild" bearings are rejected by a process where all combinations of bearings are exhaustively evaluated until

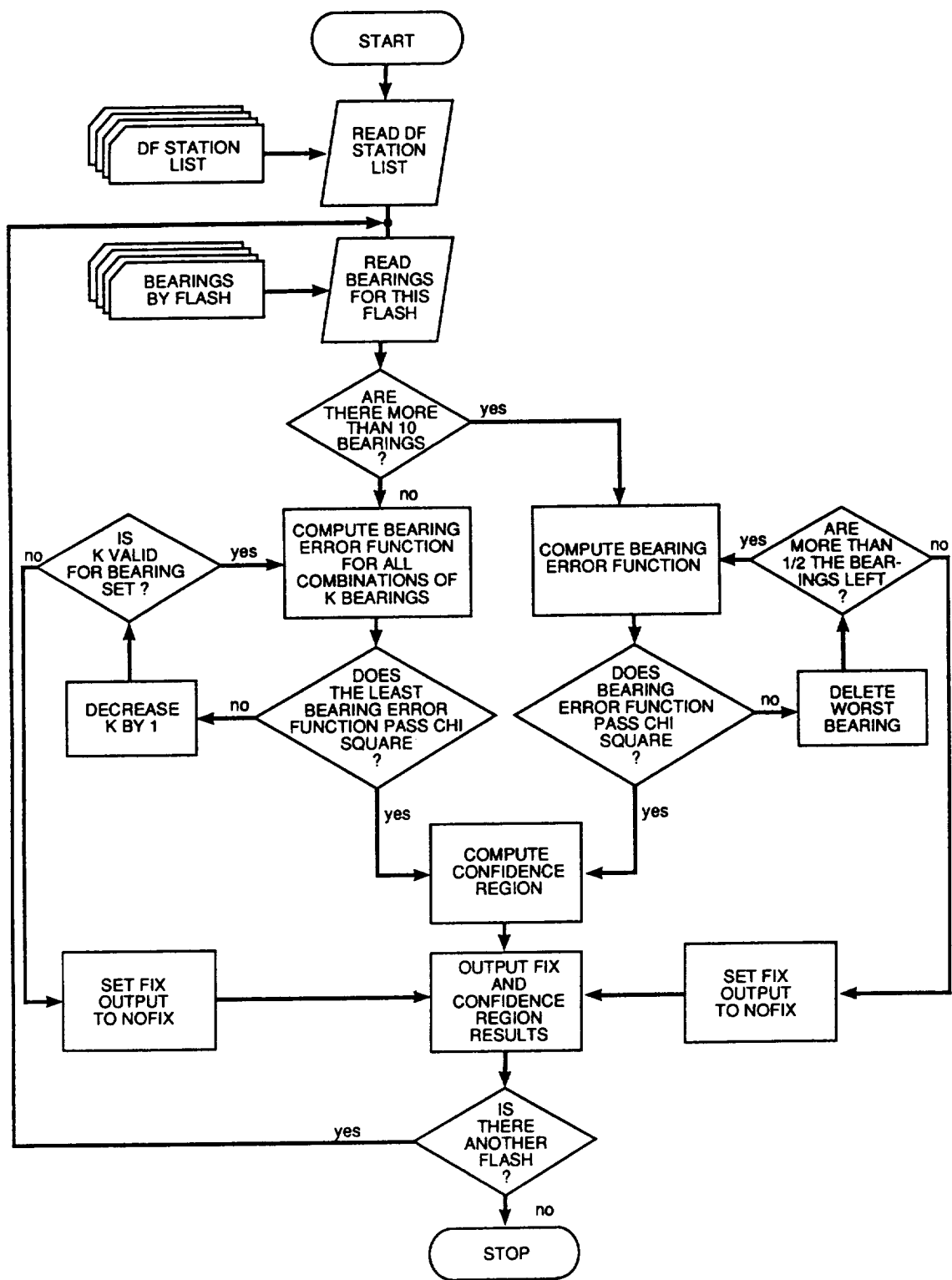


Figure 12. FFIX algorithm flowchart.

a consistent subset of bearings is obtained. A set of  $n$  bearings is "consistent" if the associated sum of squared bearing errors from the best point estimate is less than the 80% value of  $\chi^2_{n-2}$ .

The BPE and confidence ellipse are computed from the largest "consistent" subset of bearings. The algorithm employs two approaches for rejecting the "wild" bearings. The first approach, called the "exhaustive method", is invoked when ten or fewer bearings are submitted for a BPE. If the submitted bearings lack sufficient consistency to form a BPE, then all subsets of  $n$  bearings are taken  $(n-j)$  at a time, where  $j = 1, 2, 3, \dots$ , until an acceptable solution is identified or a lower limit on the number of bearings is reached, in which case there is no solution. The lower limit is the greater of  $n/2$  or 3. Thus, the largest subset of consistent bearings forms the BPE. A "sequential method" is employed when more than ten bearings are submitted for a BPE. If all  $n$  bearings fail the consistency test, then the bearing that is more "inconsistent" with the bearing set is rejected (i.e., the wild bearing). The remaining set of  $(n-j)$  bearings is examined as before. In this way the most "wild" bearings are rejected sequentially.

In the event that the chi-square consistency test fails, the "best solution" is chosen as the intersection of the bearing pair having the minimum semimajor axis in its confidence ellipse. This argument assumes the best network geometry also gives the best solution, all other factors being equal. This approach is supported by the earlier work of Stansfield (1947). This final iteration is necessary in a small direction finder network such as that run by MSFC (4 DFs) because nearly 50% of all flashes are seen by only 2 DFs. The probability of detection for the network as a whole would be significantly poorer without this last iteration process.

## Proof of Concept

### BPE Calculation for a 4-DF Network

The Marshall Space Flight Center (MSFC) 4-DF network has been in operation in the Tennessee Valley (southern TN and northern AL) since 1984. Figure 13 shows the deployment of the DF stations and other ground-based remote sensing systems such as radars and rawinsondes. The additional systems were operational during June and July 1986 in support of the Cooperative Huntsville Meteorological Experiment (COHMEX) multi-agency field program (Dodge, et al., 1986). The radar and rawinsonde data are used in this study to determine the location and characteristics of thunderstorms as well as the structure (vertical profiles of temperature, humidity, and winds) of the storm environment.

At the present time FFIIX is used only in post analysis and follows the exhaustive rejection path shown in Figure 12. An example of the information computed for each flash is given in Table 3. The flashes are stored in rows and columns which indicate the hour of occurrence and flash sequence number. The file also contains the Julian day (DAY); hour (UTC) of occurrence (TIME); number of flashes in the selected interval (CMAX); flash time in hours, minutes, and seconds (HMS); latitude (LAT) and longitude (LON) of the flash; an estimate of the first stroke peak current in kAmps (KA); the maximum normalized signal strength (NSTR); the number of return strokes (RS); the semimajor axis (SMA) in km; semiminor axis (SMI) in km; orientation (ORI) in degrees; and area (AREA) of the error ellipse in  $\text{km}^2$ ; flash polarity (FLAG= '-' for negative and '+' for positive); and time of the flash in hundredths after the last second (MS). The flash polarity is also indicated by the sign of the KA and NSTR fields.

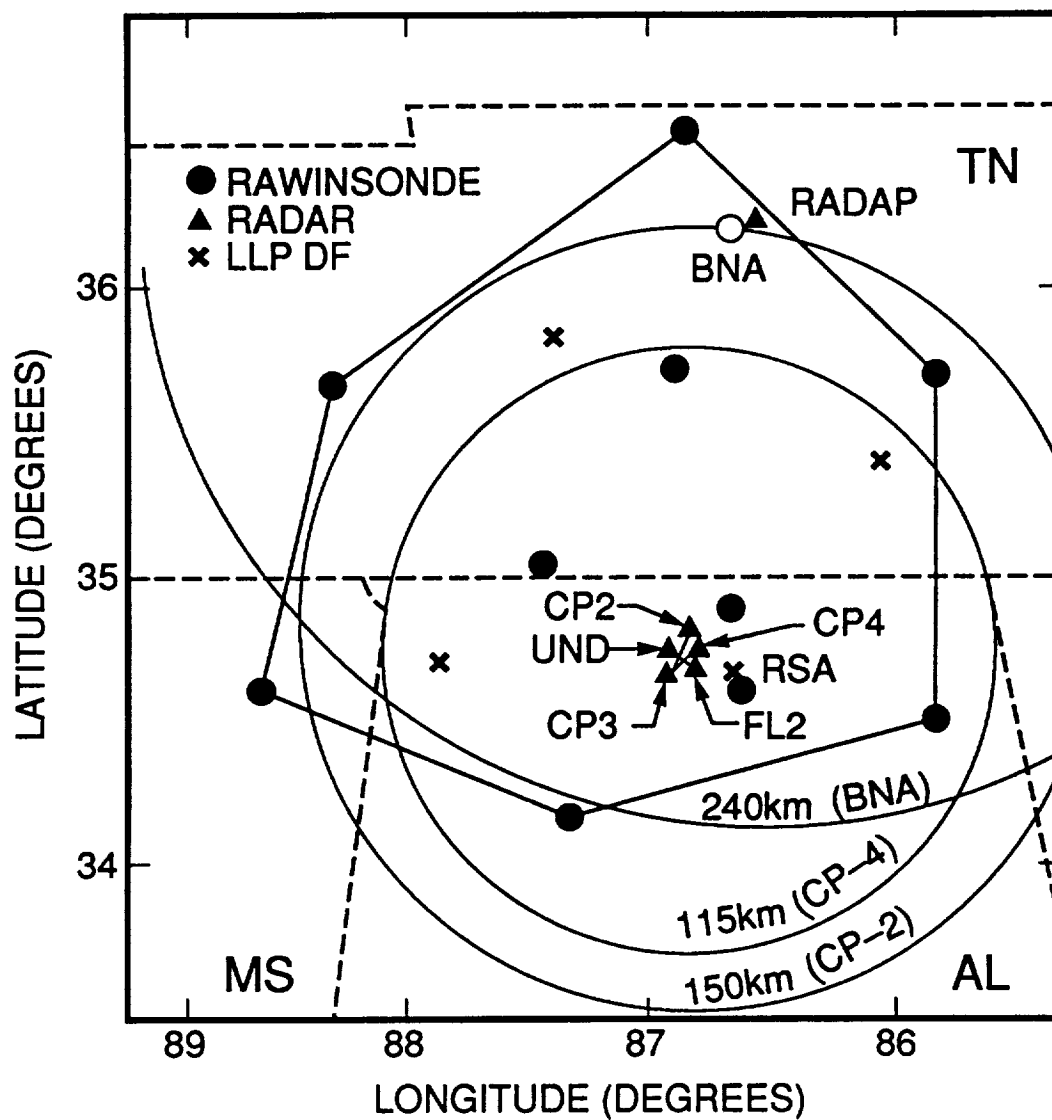


Figure 13. Deployment of the lightning, radar and rawinsonde network for the Cooperative Huntsville Meteorological Experiment (COHMEX) conducted near Huntsville, AL in 1986.

Table 3. Lightning Discharge Data Base

```
--RECORD AT (ROW,COL) = ( 24, 6)
[DAY =      86194 SYD [ TIME =      230000 HMS [ CMAX =          11
[HMS =      232021 HMS [ LAT  =      35.8841 DEG [ LON  =      86.0345 DEG
[KA  =       -87.6   [ NSTR =      -483.1   [ RS   =          2
[SMA =        6.3 KM [ SMI  =        1.1 KM [ ORI  =        5.9 DEG
[AREA =       23.6 KM2 [ FLAG =          .   [ MS   =        0.00 HMS

--RECORD AT (ROW,COL) = ( 24, 7)
[DAY =      86194 SYD [ TIME =      230000 HMS [ CMAX =          11
[HMS =      232145 HMS [ LAT  =      35.8995 DEG [ LON  =      86.0451 DEG
[KA  =     -110.5   [ NSTR =     -260.8   [ RS   =          3
[SMA =        9.2 KM [ SMI  =        2.5 KM [ ORI  =       79.0 DEG
[AREA =       72.3 KM2 [ FLAG =          .   [ MS   =        0.62 HMS

--RECORD AT (ROW,COL) = ( 24, 8)
[DAY =      86194 SYD [ TIME =      230000 HMS [ CMAX =          11
[HMS =      232218 HMS [ LAT  =      35.8602 DEG [ LON  =      86.1261 DEG
[KA  =       -57.6   [ NSTR =     -144.6   [ RS   =          3
[SMA =        3.6 KM [ SMI  =        2.1 KM [ ORI  =       62.3 DEG
[AREA =       24.6 KM2 [ FLAG =          .   [ MS   =        0.81 HMS

--RECORD AT (ROW,COL) = ( 24, 9)
[DAY =      86194 SYD [ TIME =      230000 HMS [ CMAX =          11
[HMS =      232301 HMS [ LAT  =      35.8586 DEG [ LON  =      86.1433 DEG
[KA  =       -70.2   [ NSTR =     -178.6   [ RS   =          1
[SMA =        3.5 KM [ SMI  =        2.1 KM [ ORI  =       62.7 DEG
[AREA =       24.1 KM2 [ FLAG =          .   [ MS   =        0.75 HMS
```

Figures 14 and 15 show an expanded view of a radar echo (as seen from the CP-2 radar) and the accompanying lightning strikes (shown as dots enclosed by the 50% error ellipse) for a small storm in Tennessee on 13 July 1986. The ellipse is generated from the type of information contained in Table 3. The lightning centroid is less than 5 km from the main echo. Figure 15 is produced using a bearing standard deviation of  $2^\circ$ . Figure 16 shows the corrected locations, but with a  $1.5^\circ$  bearing standard deviation, superimposed on the radar reflectivity. The spatial dispersion of strikes is on the order of 10 km and is well correlated with the radar echo. By reducing the bearing standard deviation from  $2^\circ$  to  $1.5^\circ$ , the semimajor axes of the 50% ellipse for flashes 6 and 7 (Table 3) are reduced (i.e., improved by) 40% and 24%, respectively.

Earlier studies of the natural distribution of lightning strikes produced by isolated storms show that the lightning clusters are approximately 10 km in diameter (Feteris, 1952; Hatakeyama, 1958; Krider, 1988; Goodman et al., 1988). In contrast, however, the spatial distribution of the lightning in the trailing stratiform rain region behind summertime squall lines and in wintertime regimes can be very sparse and widespread (Rutledge and MacGorman, 1988; Engholm et al., 1990).

#### BPE Calculation for a 6-DF Network

Figure 17 shows an example of a flash detected by the 6 (now 7) DF lightning network operated by the National Severe Storms Laboratory (NSSL) in Norman, OK (Rutledge and MacGorman, 1988). This example shows how the consistency criterion is used to reject "wild" bearings. The BPE labeled FIX #1 (SMA=9.2 km) uses all six DFs as input, but the BPE uses only five bearings (DF 6 is rejected). The BPE labeled FIX #2 (SMA=32.1 km) uses only the four DFs in Oklahoma as input, using all four. FIX #2 using only the Oklahoma DFs is located 28 km northwest of FIX #1. The other

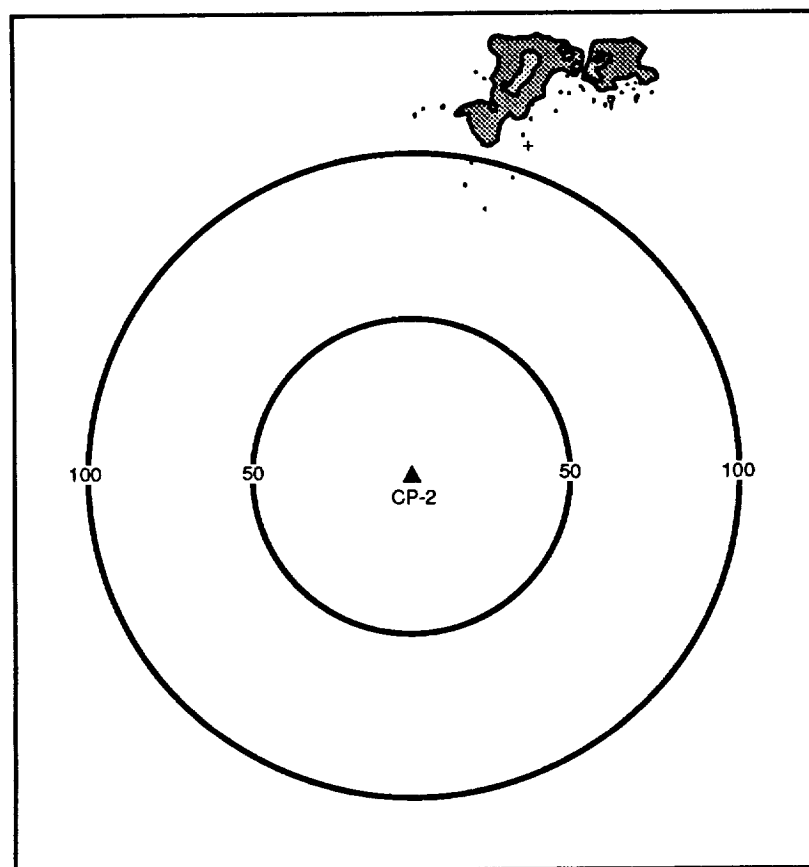


Figure 14. Lightning during the period 2315-2325 UTC on 13 July 1986 superimposed onto the CP-2 radar echo prior to ground truth corrections:  $\cdot$  = negative polarity discharges;  $+$  = positive polarity discharges. Radar reflectivity contoured at 18 dBZ and 40 dBZ.

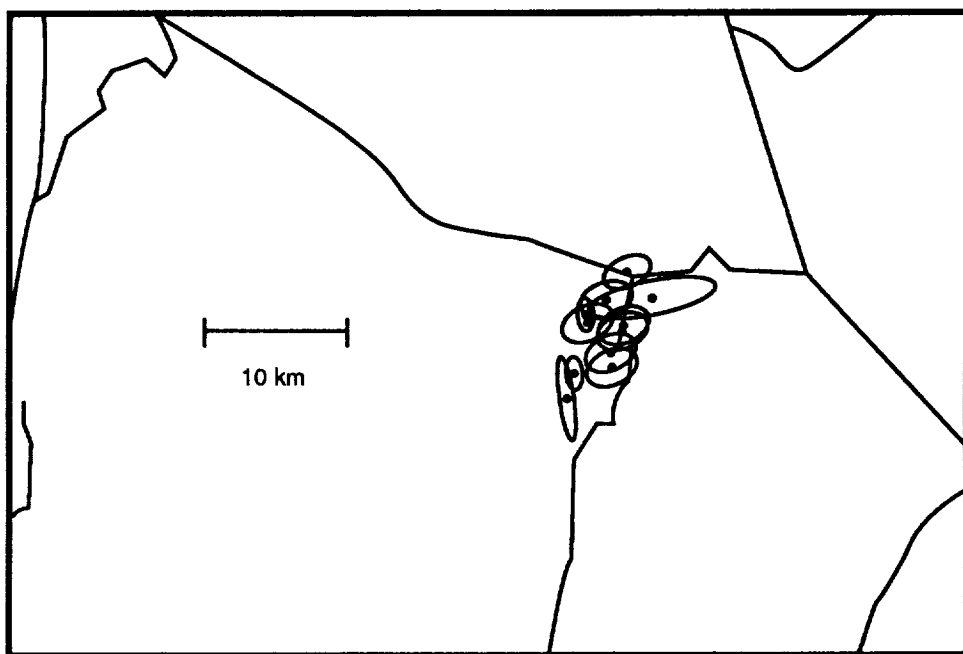


Figure 15. The location and 50% error ellipses ( $2^\circ$  bearing standard deviation) for each discharge after radar ground truth corrections.

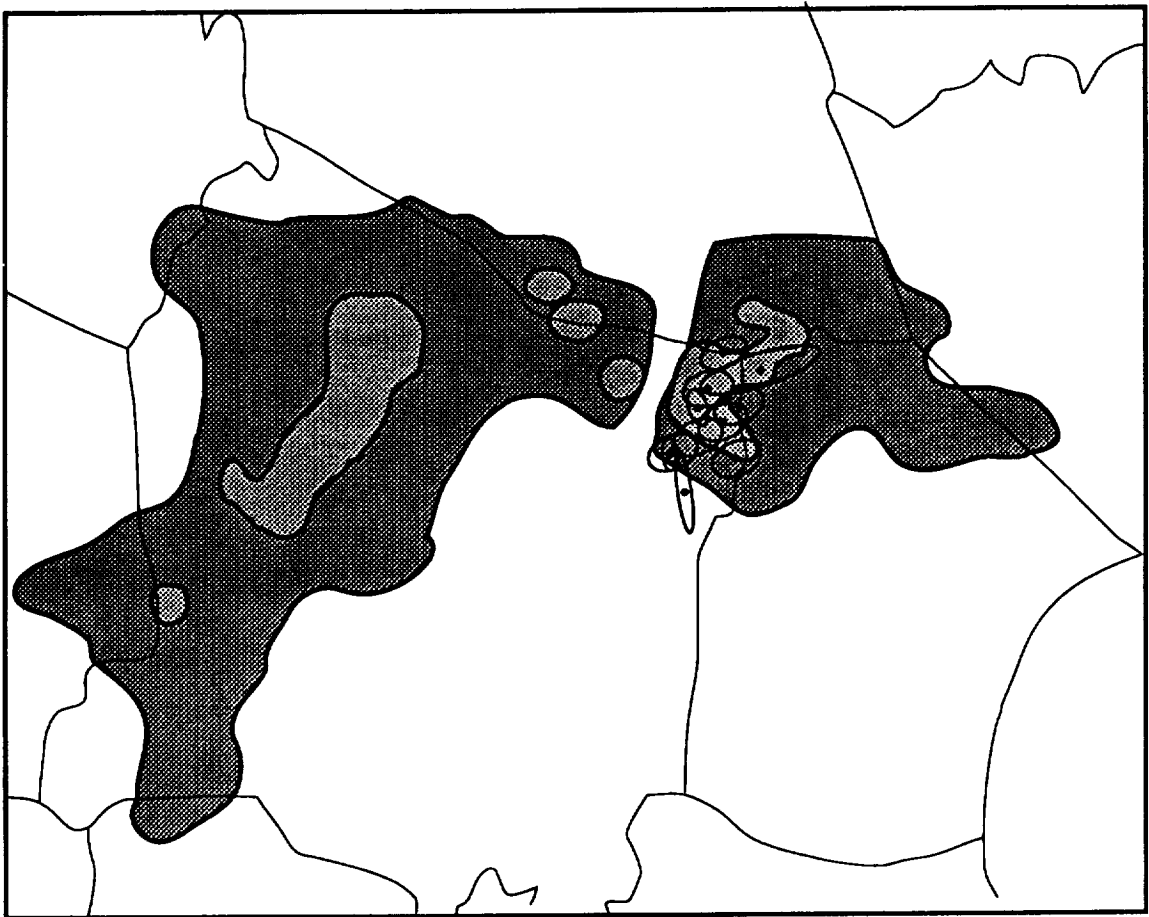


Figure 16. Overlay of corrected lightning location estimates with the radar echo. Same as in Figure 15 but with  $1.5^\circ$  bearing standard deviation.

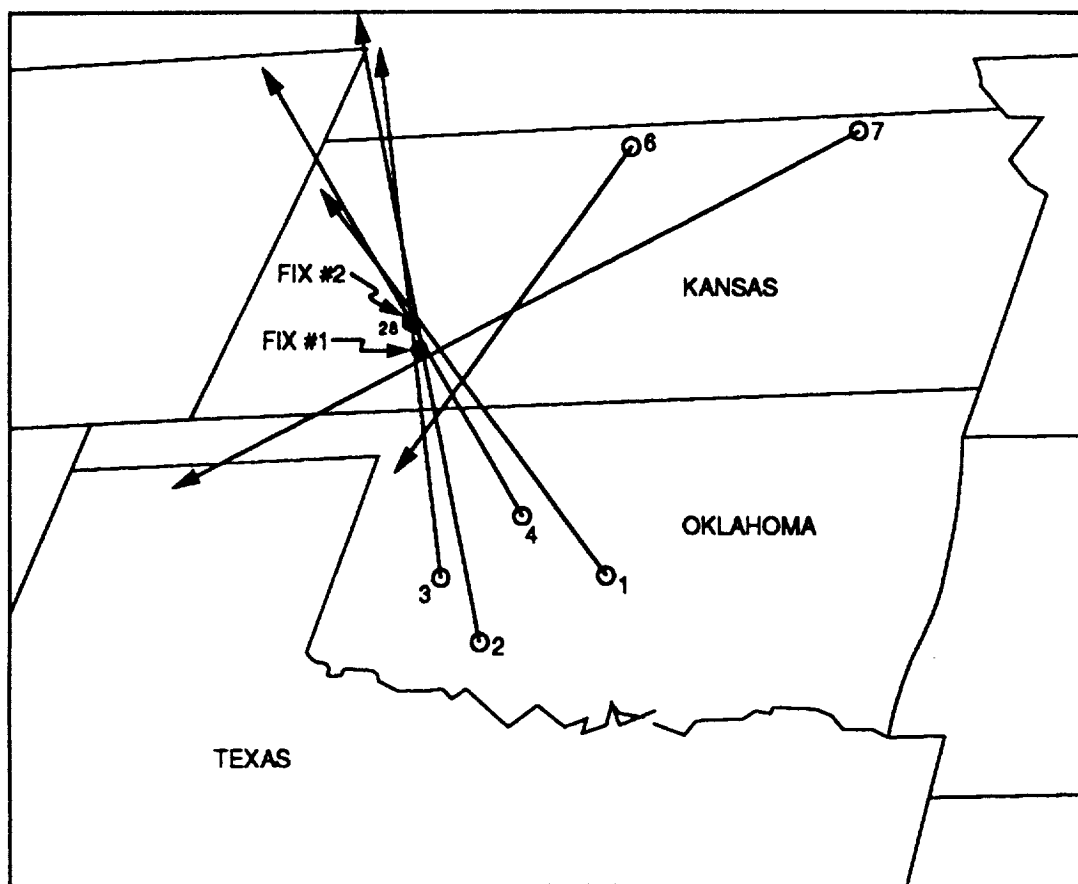


Figure 17. FFIX solutions for cloud-to-ground flash detected in Kansas by the NSSL DF network.

intersection points where bearing pairs intersect represent false or ghost targets. Figure 18 also shows the corresponding radar echo distribution and the location of FIX #1 (indicated by the large cross in southwestern Kansas).

Table 4 gives the error ellipse characteristics for FIXs #1 and #2, and for each bearing pair. When a BPE cannot be computed for  $\sigma_i = 1.5^\circ$ , one can increase  $\sigma_i$  by  $0.5^\circ$  increments until a solution is acquired. In this way, the standard deviation is treated more as a tolerance factor, rather than as an absolute.

The results of this test show that FIX #1 has the smallest error ellipse of all submitted DF combinations. For all paired-bearing combinations the DF (1,7) BPE has the smallest semi-major axis, but the DF (4,7) BPE has the smallest ellipse area. Although a solution is possible near the baseline of DFs (2,3), the error ellipse is quite substantial because of the poor geometry, reflected in the large value of  $\sigma_i$ . The three greatest signal strengths are reported at DFs 4, 3 and 6, in that order. An algorithm that uses the bearing pair having the greatest signal strengths would form a solution using the DF (3,4) combination, but the resulting semi-major axis for the ellipse is 201.9 km and the solution is displaced 14 km from the FIX #1 BPE. A solution could not be obtained until  $\sigma_i$  was increased to  $5^\circ$ , again indicating a poor geometry. However, a solution formed with the DF (4,6) combination reduces the semi-major axis to 23.3 km. Yet, any solution with DF 6 must be treated with caution, since it is inconsistent with the other bearings. One should ask whether the DF 6 bearing deviation is due to site errors or if it is just a "wild" bearing. If this particular DF 6 bearing angle is inconsistent with other flash BPEs in the same direction, then the deviation is due to systematic or site errors. However, if it is just a chance occurrence, say 9 of 10 bearings at this angle are consistent with the other DFs, then it was most likely a "wild" bearing. Following the completion of the aforementioned analysis a large systematic error at DF 6 was independently confirmed and the station moved to a new location in northern Kansas.

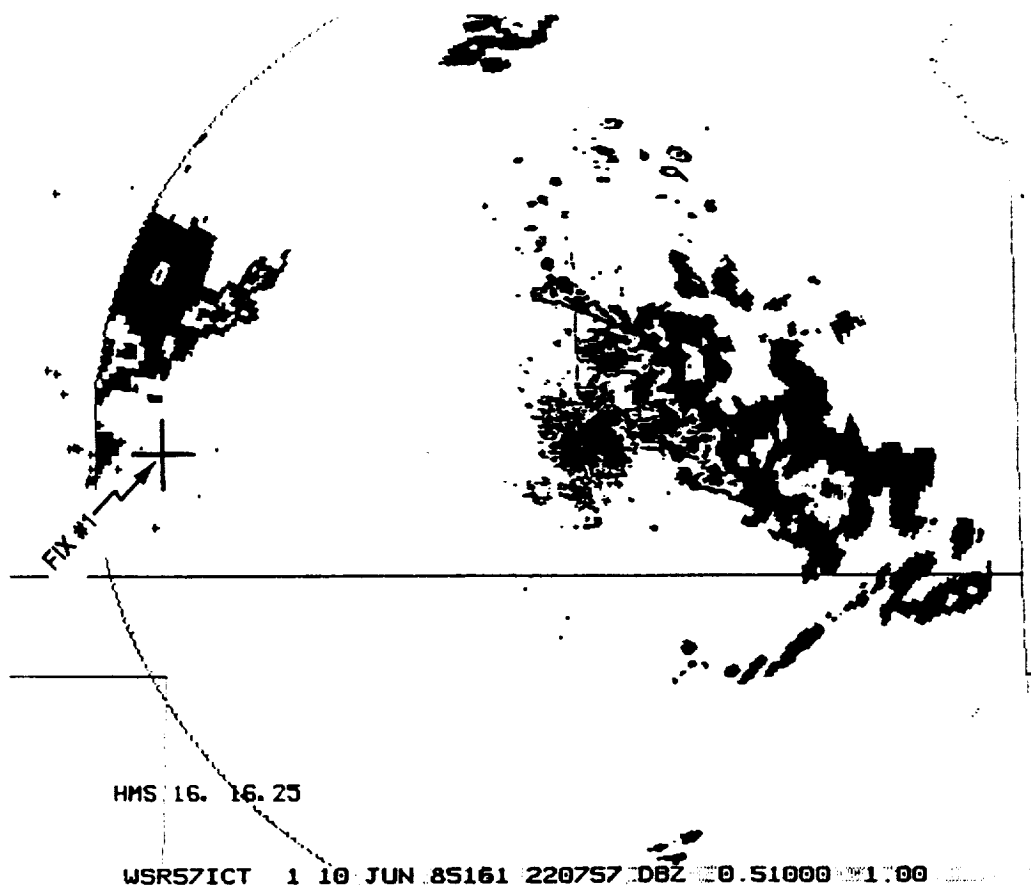


Figure 18. Distribution of radar echoes and lightning activity corresponding to the time of the FFIX solution in Kansas. Large cross indicates solution #1. Radar contours at 18, 30, 40, 45, 50 and 55 dBZ.

Table 4. Error Ellipse Characteristics for 6-DF Network

DFs Submitted	$\sigma$ (deg)	LAT (deg)	LONG (deg)	SMA (km)	SMI (km)	ORI (deg)	AREA (km <sup>2</sup> )	RADIUS (km)
1,2,3,4,6,7	1.5	37.659	100.058	9.2	4.0	151.3	116.9	7.4
1,2,3,4	1.5	37.874	100.220	32.1	4.3	149.1	437.4	24.6
1,2	5.0	37.976	100.230	258.2	35.2	147.7	28,508.9	198.0
1,3	5.0	38.086	100.347	213.0	33.2	150.3	22,201.9	163.4
1,4	1.5	39.592	101.995	550.1	13.1	140.5	22,600.1	422.8
1,6	1.5	37.298	99.521	18.7	9.1	168.0	535.9	15.1
1,7	1.5	37.704	99.943	14.2	13.5	152.7	601.6	13.8
2,3	6.5	38.940	100.791	2,455.9	50.9	156.6	392,398.0	1,888.1
2,4	1.5	37.557	99.991	75.5	8.0	147.4	1904.0	57.9
2,6	1.5	36.915	99.630	27.0	8.9	171.6	751.7	21.1
2,7	1.5	37.639	100.038	16.8	12.4	8.6	655.2	14.8
3,4	5.0	37.751	100.175	201.9	26.8	149.8	16,968.5	154.8
3,6	1.5	36.754	99.675	26.3	6.9	166.1	566.5	20.3
3,7	1.5	37.598	100.098	16.3	10.6	175.2	544.4	13.9
4,6	2.0	37.114	99.573	23.3	9.3	154.7	676.1	18.4
4,7	1.5	37.626	100.057	14.5	10.2	146.7	465.1	12.6
6,7	1.5	38.158	99.272	23.0	6.9	23.5	500.3	17.9

### Systematic Error Corrections

The FFIIX algorithm has also been used in this study to correct for the systematic errors arising from site effects (Horner, 1954; Gething, 1978). Site errors cause bearing errors that are themselves a function of direction. The 12° bearing deviation from the BPE at DF 6 in the previous example was due to unresolved site errors. Site errors are one of the chief limitations to achieving the optimal location accuracy, and perhaps the most difficult problem degrading network performance.

Previous attempts to correct for the systematic errors associated with lightning direction finding systems employed some type of optimization procedure that minimized the difference between the observed bearings and the "true" target location. The "true" target location can be determined by visual ground-truth (Mach et al., 1986) or by assuming that one or more of the direction finder bearings is correct (Hiscox, 1984; Orville, 1987). This latter method will give self-consistent solutions (as applied to the DF 6 bearing deviation described above), but spatial bias effects may still be present (e.g., lightning clusters offset from radar echoes). Rocket triggered lightning strikes at Kennedy Space Center, FL have also been used to provide ground-truth, but this is only applicable to a single bearing line from any direction finder station. In practice, it is very difficult to obtain visual ground-truth at a large number of discrete bearings. Schutte et al. (1987) reversed the role of transmitter and receiver by radiating a 1 MHz signal successively through each loop of the direction finder antenna whose amplitude could then be measured by a radio receiver at a number of bearings from the site.

The ultimate litmus test of any of these methods (and the practical usefulness of these data over a large domain) should be determined by the degree of spatial correlation between clusters of lightning strikes and their associated radar echoes. Most lightning strike networks have either partial or full weather radar coverage, thus making this

validation technique practical for all but a few users. A new technique is presented below that uses isolated radar echoes to constrain the error correction and optimization procedures to remove the systematic errors.

### Defining the Sample Subset

A sample subset of lightning strikes is constructed for a short time interval corresponding to low-level radar scans of isolated storms distributed about each DF (refer to Figure 14). The interval should account for the propagation of the echo. If the echo moves slowly, then the time increment can be increased to enlarge the lightning sample size.

### Computing the Bearing Deviations

Next, the lightning strikes are superimposed on the radar image and the position of the reflectivity core is marked. The bearings from each DF to the storm core are computed and these are referred to as the "true" bearings. The lightning flashes are replotted (Figure 19) and the deviations between the observed and "true" bearings are computed. There are 11 flashes associated with this storm in the 10 min interval between 2315 and 2325 UTC.

Flashes 6 and 7 (refer to Table 3) have the two largest semimajor axes of 6.3 km and 9.2 km, respectively. Table 5 shows that these are two of the three flashes only detected by just two DFs. The low number of flashes seen by DF 2 indicates another source of network performance degradation. Poor detection efficiencies and even "blind spots" due to site effects (e.g., poor ground conductivity) have been noted by other users of such systems. Because one or more sites may not detect a flash, the location must be determined from a less favorable geometry (e.g., a flash along the baseline of two DFs or

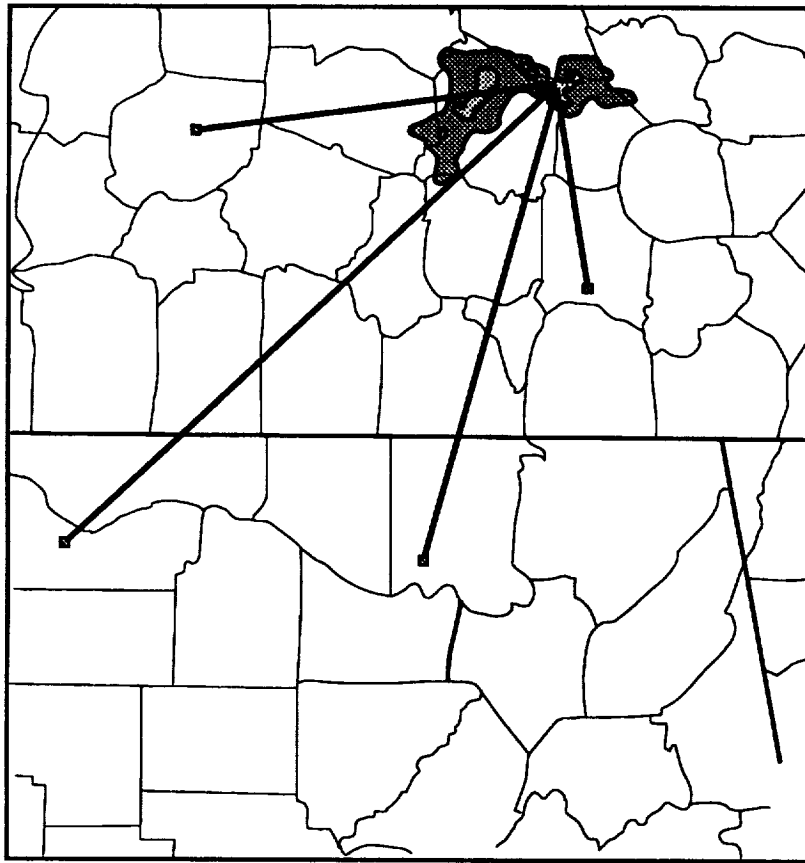


**Figure 19.** Bearing lines from each of the DFs to the reflectivity core of the subject storm.

Table 5. DF Bearings and Site Error Corrections

Flash	DF 1	DF 2	DF 3	DF 4
1	19.9	5.6	86.3	51.4
2	18.2	-	84.6	48.9
3	19.8	-	87.3	51.3
4	18.7	-	85.5	50.7
5	19.8	-	87.6	-
6	-	4.1	-	51.7
7	-	-	86.5	51.2
8	19.6	-	88.2	51.1
9	18.8	-	88.0	51.9
10	19.6	9.5	87.2	51.6
11	19.4	4.6	88.4	52.1
Median	18.7	5.1	87.5	51.5
True	17.1	350.4	84.8	49.0
Deviation	-1.6	-14.7	-2.7	-2.5

a flash more distant from one site than another in a more optimal geometry). Over a large area, say 300 km from the center of the network, we find that nearly 50% of all flashes are only detected by two DFs.

Because of the small sample sizes, choose the median bearing as the measure of central tendency. The median is a more robust estimator in that it is less sensitive to outliers or "wild" bearings than is the sample mean. Others have chosen median estimation for dealing with bearing information for just this reason (e.g., Lenth, 1981). In practice, one would try to find a number of storms close to the bearing angles in use here (we try to get samples in  $6^\circ$  azimuth bins) to further increase the sample size. The median observed bearing and "true" bearing to the storm are also presented in Table 5. The nearly  $15^\circ$  deviation at DF 2 is further evidence that the site is poor. Large site errors such as this in certain directions, however, are not that uncommon (e.g., Schutte et al., 1987).

#### Computing New Solutions With the Corrected Bearings

Figure 20 shows a close-up view of the lightning locations before any site error corrections are used (shown as dots) and after the initial bearing corrections are implemented (again described by the 50% error ellipse). The lightning centroid is displaced 10 km to the southeast of the main echo. Figures 15 and 16 show the lightning locations described by the 50% error ellipse after the bearing corrections from Table 5 are implemented. The lightning centroid is now less than 5 km from the main echo. The impact of uncorrected bearing errors on the clustering process and storm identification is discussed further in Chapter 4.

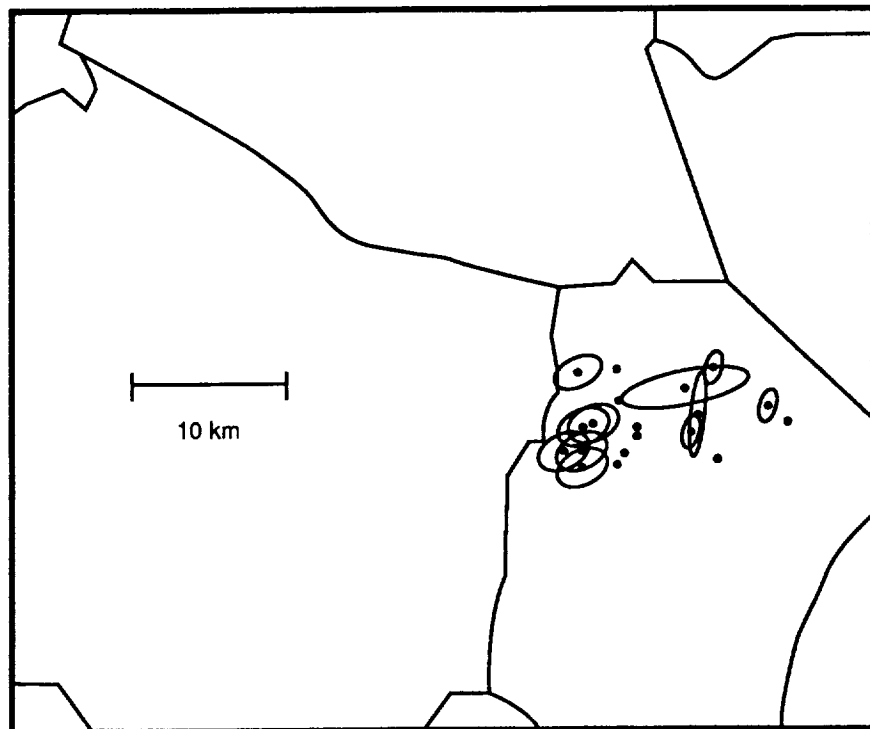


Figure 20. Location estimates and 50% error ellipses for each flash before radar ground truth corrections.

### Site Error Polynomials

Once the data base on site error corrections is generated, one would fit a polynomial to the data having the form

$$y = a_0 + \sum_k (s_k \sin k\theta + c_k \cos k\theta), k=1,2,3,\dots,6 \quad (3.1)$$

where  $y$  is the site error correction to the observed bearing  $\theta$ . One of the motivations for choosing a polynomial fit of this form is that the real-time hardware can implement the polynomial (but only to 4th-order) in real-time. Figure 21 shows the site error correction curves for the four DFs. The curves were produced by computing site error corrections in  $6^\circ$  bins using the technique described by Mach et al. (1986) and Orville (1987). A nonlinear regression was performed using the method of Marquardt (1963) to compute the polynomial fit to Eqn. (3.1).

Another way to examine the network performance using the error ellipse is to make plots such as Figure 22 where 30 min of lightning data are shown from 2300–2330 UTC with increasing thresholds of the semimajor axis (SMA). The locations compare reasonably well with the radar data even with a semimajor axis of 20 km.

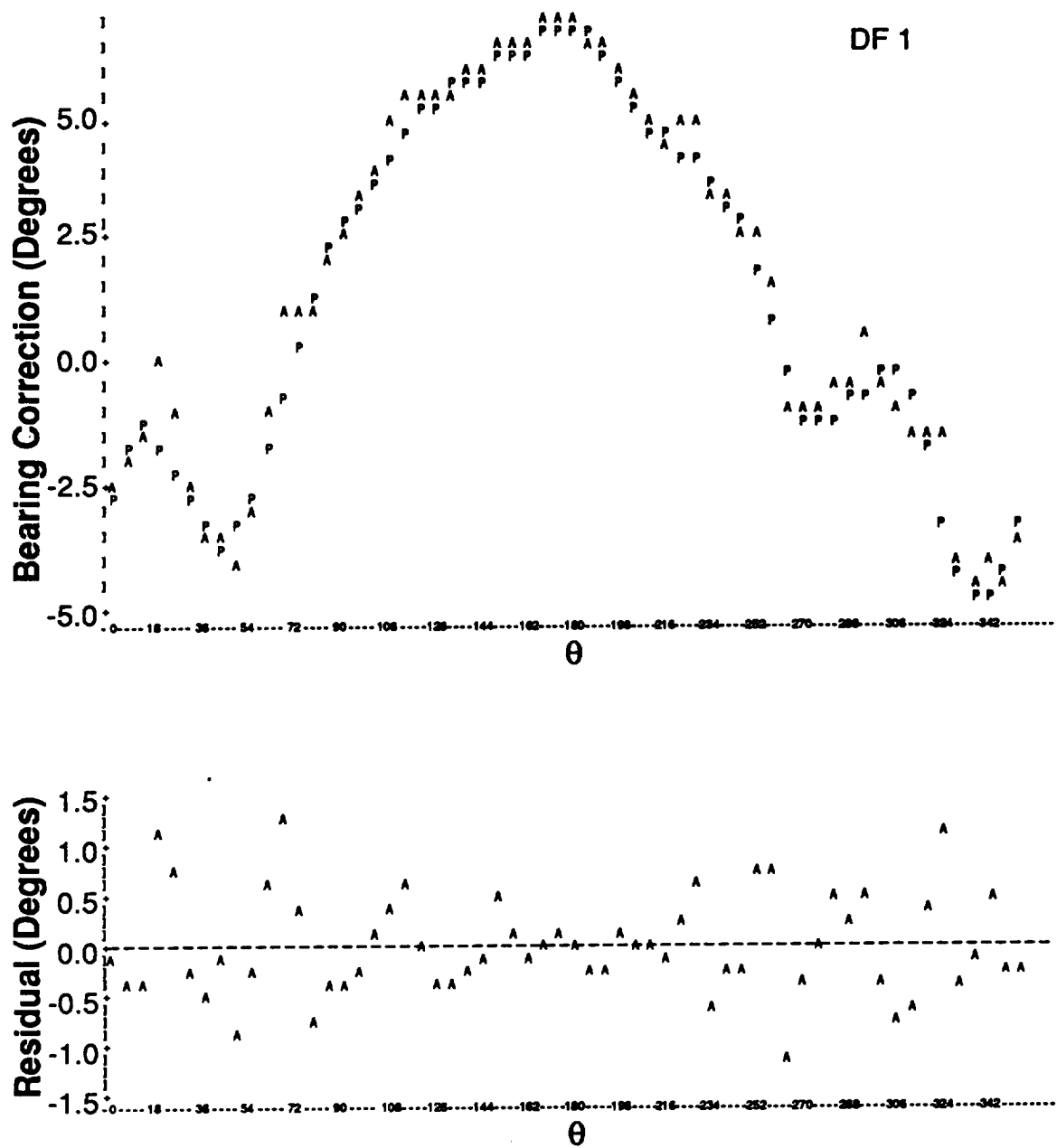


Figure 21a. Site error polynomial and residual for DF 1.

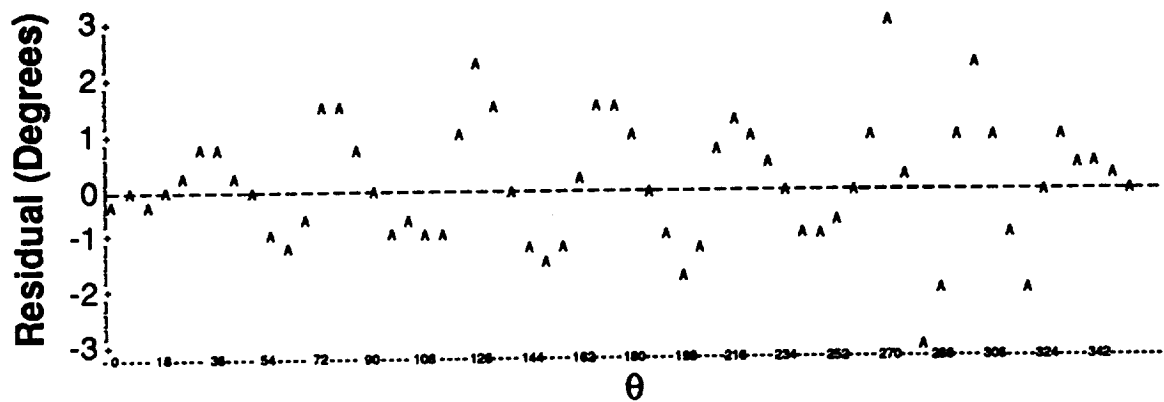
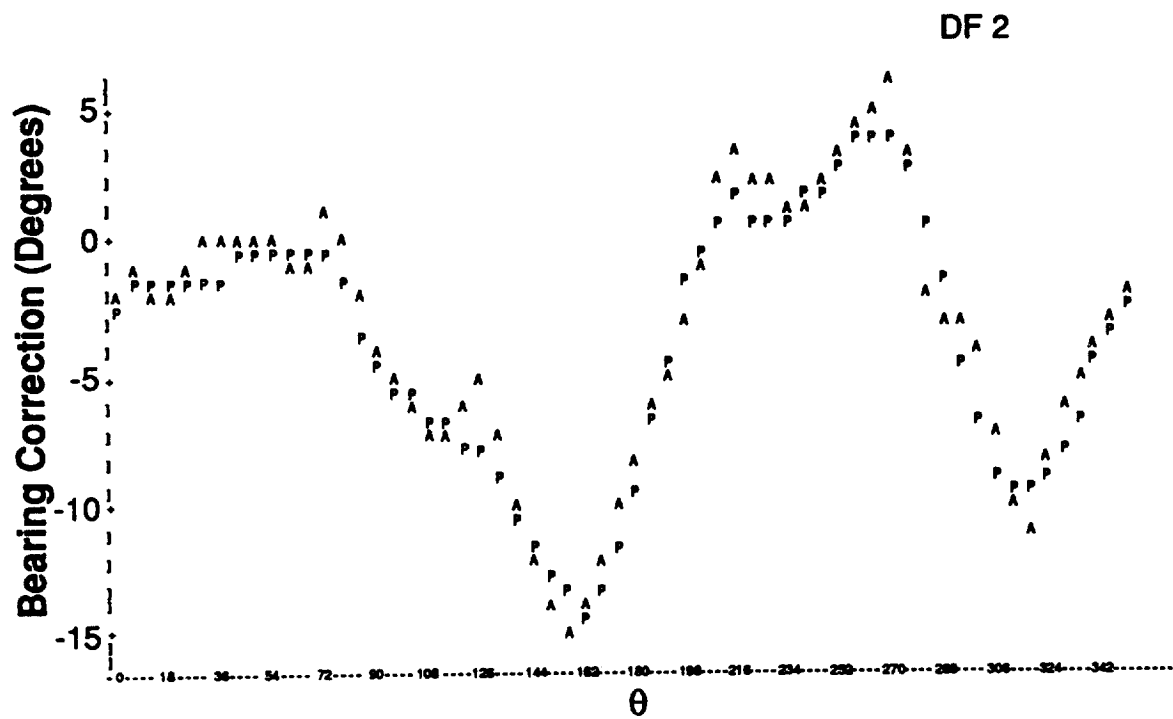


Figure 21b. Site error polynomial and residual for DF 2.

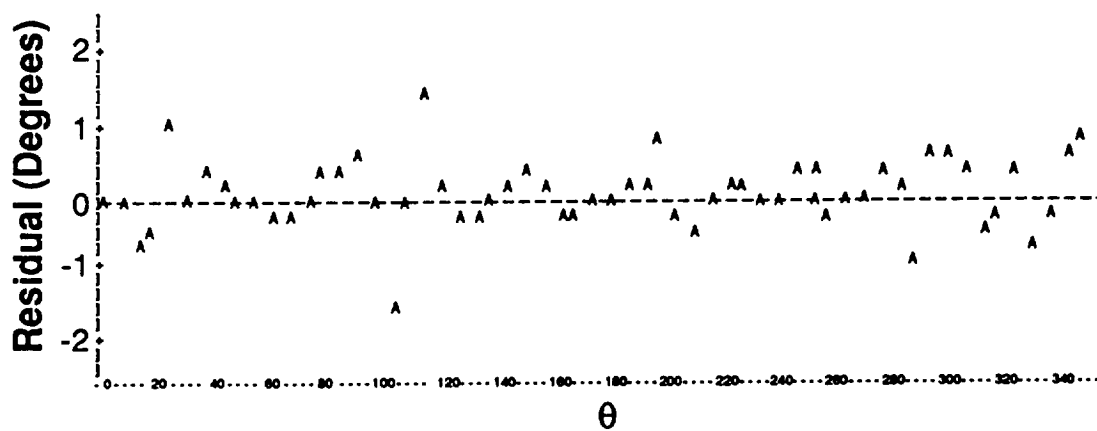
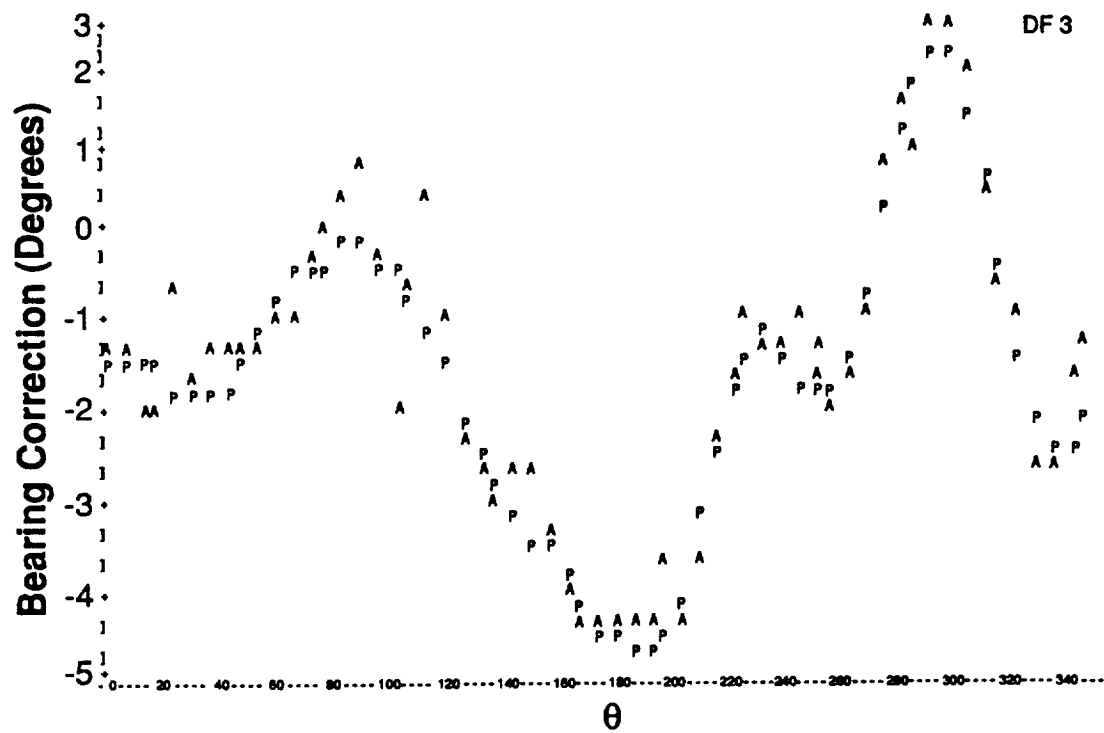


Figure 21c. Site error polynomial and residual for DF 3.

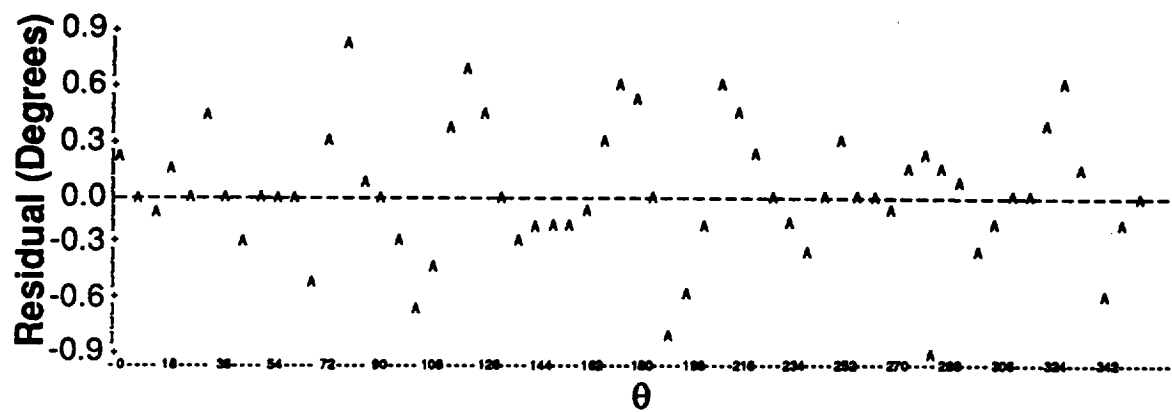
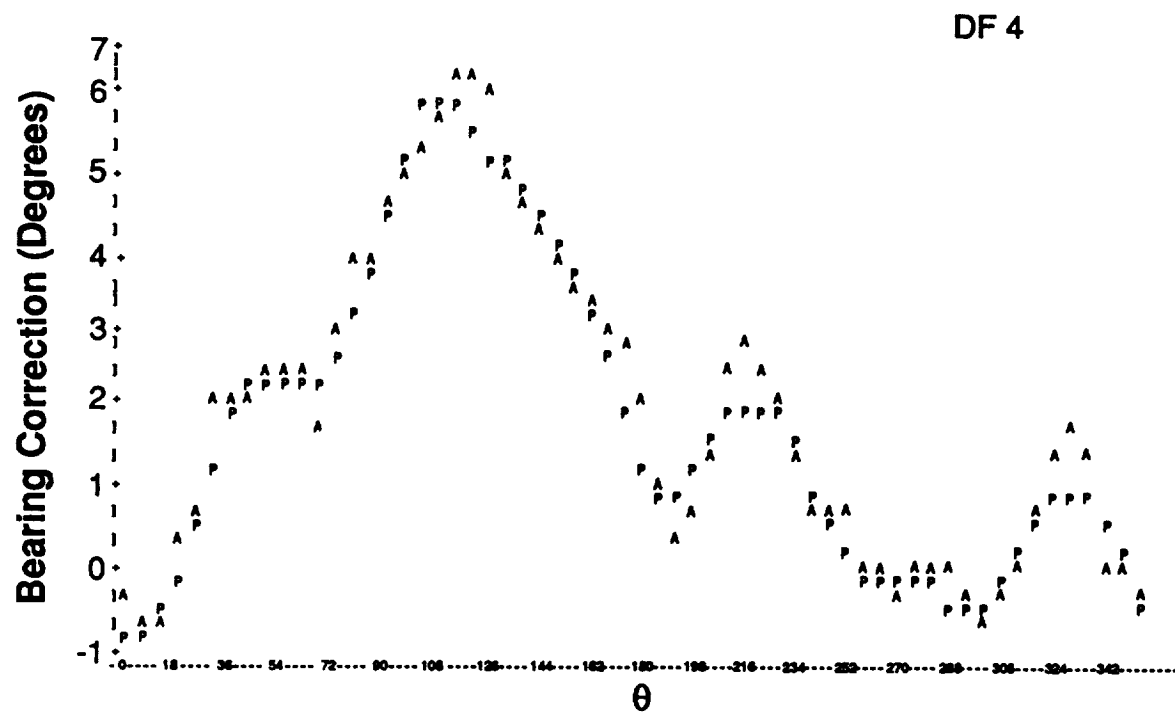


Figure 21d. Site error polynomial and residual for DF 4.

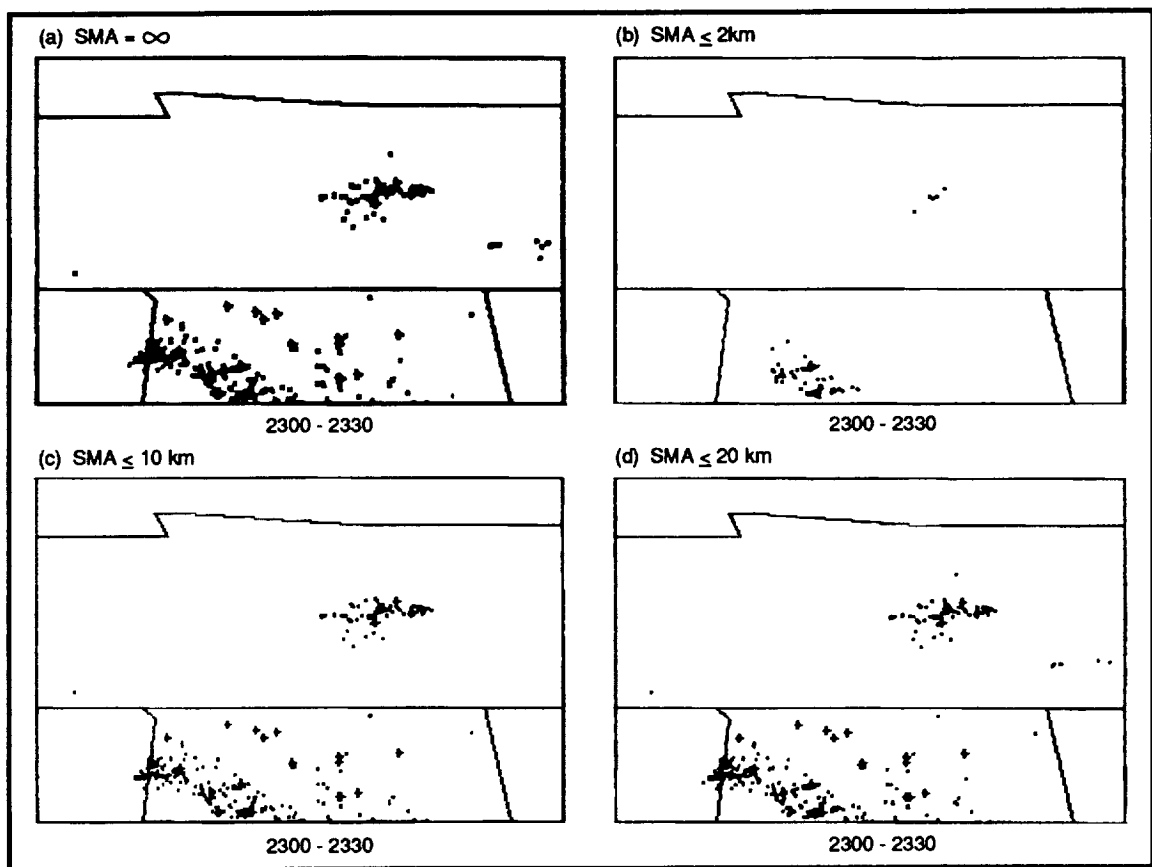


Figure 22. Lightning plots during the period 2300-2330 UTC with semimajor ellipse axis thresholds: a, infinity; b, 2 km; c, 10 km; d, 20 km.

## CHAPTER IV.

### CLUSTERING METHODOLOGY

#### Storm Identification

Before generating a lightning time series, a pattern recognition scheme is needed to identify the collection of flashes belonging to an individual storm or storm complex. For example, Peckham et al. (1984) manually identified storms and storm systems during a 3-h sample period using a 2-station lightning network in Florida (Figure 23). Closer inspection of Figure 23 shows subareas of greater flash density within the closed contours representing the boundaries of the 13 storm cells labeled A-M. Given that the average thunderstorm lifetime is less than 1 h, these subareas are highly suggestive of smaller thunderstorms that existed during a portion of the 3 h observation period.

In a recent investigation examining the fusion of lightning ground strike information with satellite imagery, Goodman et al. (1988a) subdivided the lightning flashes contained within a  $4 \times 10^5 \text{ km}^2$  area into grid cells having a dimension of  $0.1^\circ$  latitude by  $0.1^\circ$  longitude. The selected grid cell dimension of approximately 10 km is much greater than the random position errors, yet also represents the typical diameter of an individual thunderstorm cell. This process was applied during a 1 h period to successive 5-min sample intervals to permit the manual (human judgment) identification of individual and multi-cellular storms using an interactive workstation (Figure 24). The closed contours outline the lightning density maxima and can be used to track the movement, merger, and splitting of clusters. The 5-min sample period is commensurate with the NEXRAD radar and geostationary weather satellite sampling intervals. In the section below this process is taken a step further and investigate the use of a clustering

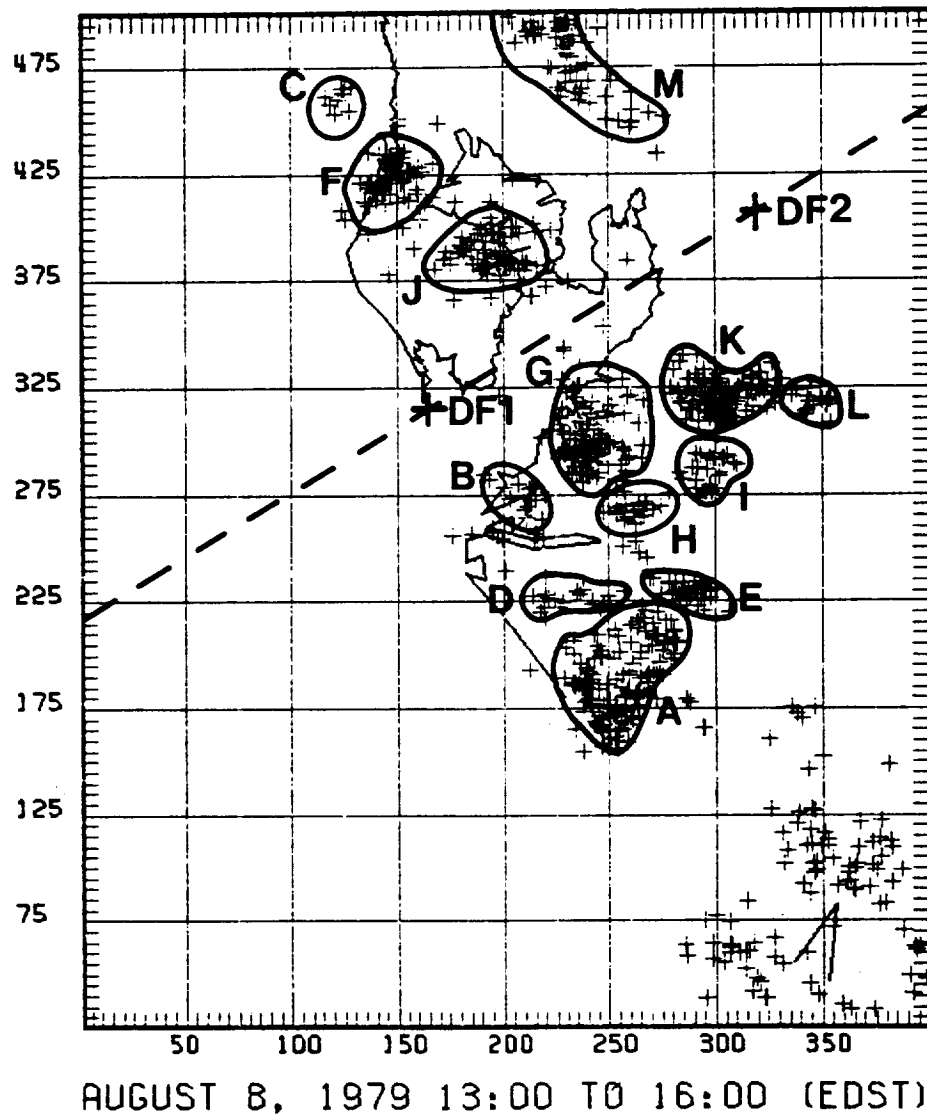


Figure 23. Map of ground discharges in the Tampa Bay, FL area on 8 August 1979 from 1700-2000 UTC (1300-1600 EDT) by a 2 DF network. Map scale is in thousands of feet (adapted from Peckham et al., 1984).

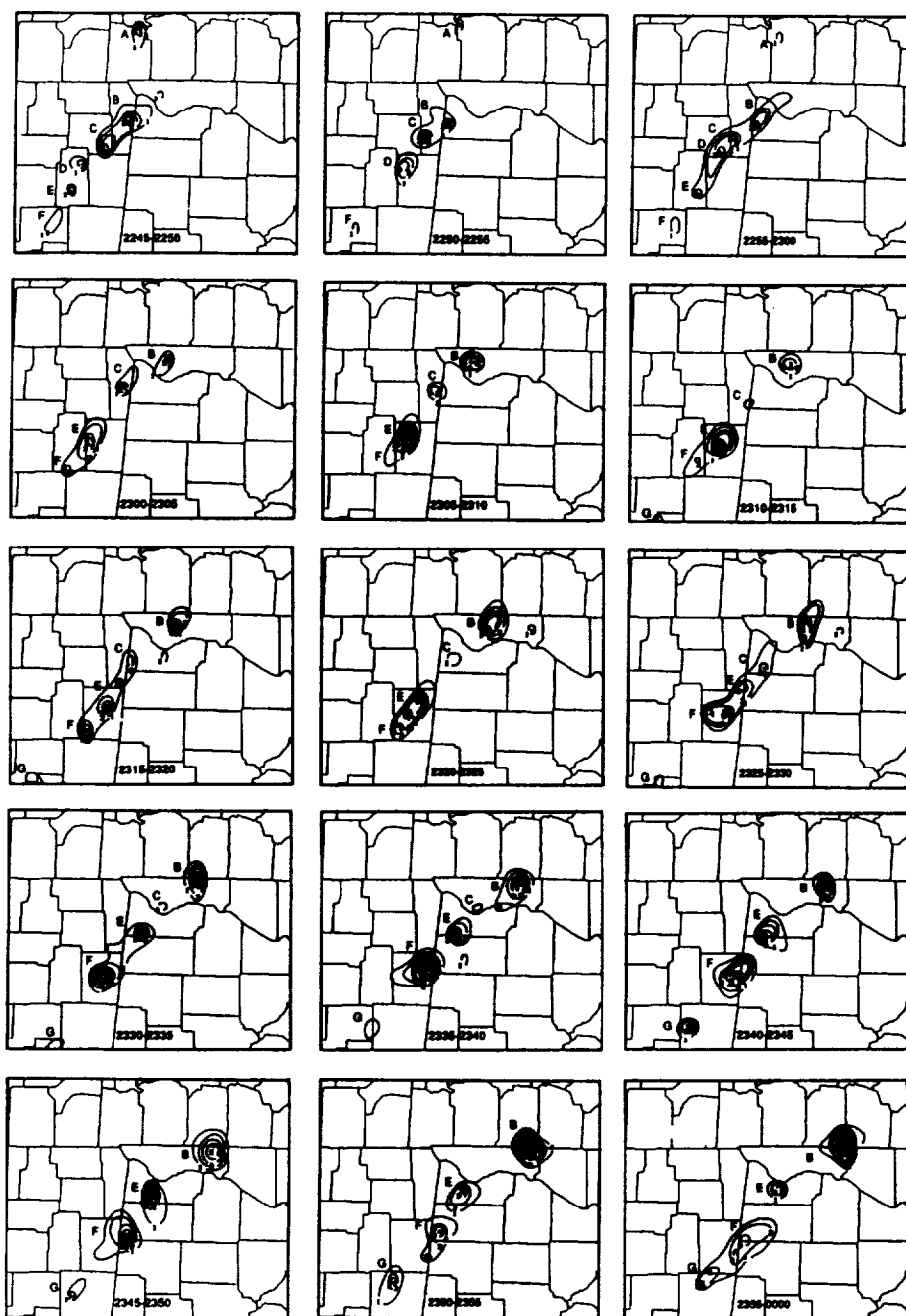


Figure 24. Cloud-to-ground lightning contour maps (number of discharges per cell per 5 min) of storms embedded within a mesoscale convective system in North Alabama on 11 June 1986. Time in UTC. (after Goodman et al., 1988).

algorithm to assign the individual lightning flashes (the objects) to their respective storms (the groups). New members can be assigned iteratively to a new or existing storm during each sampling interval and tracked with time.

### Selecting a Clustering Algorithm

Various clustering methods can be used for such object classifications. Sokal and Sneath (1963), Anderberg (1973), Hartigan (1975), and Romesburg (1984), for example, have written entire books on the subject of cluster analysis. At its most basic level, clustering is the grouping of similar objects. All clustering algorithms are procedures for searching through the set of all possible clusterings to find the one that fits the data reasonably well (Hartigan, 1975).

The clustering procedure begins with the choice of some initial partition of the data which is then modified so as to obtain a better partition. The basic concept of these methods is similar to that of the steepest descent algorithms used for unconstrained optimization in non-linear programming (Anderberg, 1973). These algorithms begin with an initial point and generate a sequence of moves to find an improved value of the objective function until a local optimum is found. The search may involve sorting by variables, switching objects between clusters, joining objects together, splitting objects apart, adding objects to pre-existing clusters, or specialized searching of a subset of clusters (Hartigan, 1975).

Joining algorithms have been used previously to identify storms from radar base-scan reflectivity patterns for the purpose of extrapolating storm motion (Blackmer and Duda, 1976; Browning et al., 1982). The basic method follows:

Step 1. Identify all gridpoints with local reflectivity maxima above some threshold value.

Step 2. Compute the spatial separation between each pair of maxima.

**Step 3.** Combine the nearest pair together to form a new cluster.

**Step 4.** Repeat steps 1-3 until only one cluster remains or a stopping condition has been reached (e.g., a threshold on the minimum separation distance needed to define a cluster as a storm or storm complex). The result can be visualized as a linkage tree or dendrogram describing the level (distance) where individual clusters join together.

**Step 5.** Repeat steps 1-4 for successive radar images. Compute motion vectors from the individual cluster displacements between sampling intervals.

### **The K-Means Algorithm**

The joining algorithms produce a large number of clusters which are then reduced to a manageable number more for the sake of convenience rather than for quantitative reasons related to the physical process itself. Chiefly for this reason, and because of computational expense (as many as 8000 discharges per hour have been detected by the MSFC network), a switching (or transfer) algorithm called the K-means or K-nearest neighbor algorithm was selected for grouping the lightning discharges into storm clusters. The algorithm begins with an initial partition of the data (referred to as seed points) and obtains new partitions until no additional switches in the neighborhood of the initial partition improve the classification. Thus, a local rather than a global optimum is sought. The stopping criterion is reached when no movement of an object from one cluster to another will reduce the within-cluster total sum of squares. The IMSL implementation of algorithm AS 136 developed by Hartigan and Wong (1979) was used for this purpose. Appendix C contains the FORTRAN-77 programs developed by the author for generating the seeds and calling the IMSL subroutine KMEANS. The clustering of the lightning data is implemented as follows:

**Step 1.** Define an area of interest and subdivide the lightning flashes occurring during a sample interval into grid cells having a dimension of 10 km x 10 km. Sample intervals of 5-min and 10-min are used with the choice a function of either the corresponding radar sampling interval (when used for intercomparison or validation experiments) or storm lifetime.

**Step 2.** Search the data matrix for isolated lightning density maxima and label these as possible seeds. A default threshold of 0.02 discharges  $\text{km}^{-2}$  (2 ground discharges per 100  $\text{km}^2$ ) is used almost exclusively (see Step 5 below).

**Step 3.** Use the K-means algorithm to obtain optimal partitioning of the lightning into storm clusters.

**Step 4.** (For storm tracking purposes). Repeat steps 1-3 for successive sample intervals. A storm motion vector can be computed from the successive cluster centroid displacements and a time series can be constructed from the successive cluster memberships.

**Step 5.** (Hybrid Scheme). Step 2 may generate more seeds than desired (or physically realistic) in which case the clusters are not sufficiently coherent to track during successive time intervals in Step 4. Occasionally too few seeds are generated and Step 3 fails to converge to a solution. In the former case with a richness of seeds, the initial clusters are joined until the number of remaining lightning clusters can be correlated (i.e., tracked) over successive sampling intervals. The clusters can be joined further until only a single cluster representing an entire complex of storms remains. This final cluster can be used to generate and analyze a time series for the entire storm system. In the latter case having a deficit of seeds, the seed threshold value is lowered to 0.01 discharges  $\text{km}^{-2}$  or a 5 km x 5 km grid subarea is searched for additional seeds.

**Step 6.** (Sensor Fusion Scheme). Steps 1-5 address thunderstorm identification with the ground discharges alone. An alternative seeding method employing radar data has been evaluated. In this case, the peak reflectivity tracker or NEXRAD tracker schemes can be used to identify the storm cells. These cell centroids then serve as the seed points for clustering the ground discharges with the K-Means algorithm.

### Demonstration of Method

Storm systems ranging from individual thunderstorms to large complexes of storms are used to evaluate the performance of the clustering procedures. The basic algorithm is first described for a case of thunderstorm cells embedded within a fast

moving pre-frontal squall line that produced widespread severe weather as it crossed the Tennessee Valley during a 9 h period in the afternoon of 15 November 1989. The widespread precipitation pattern (rain/no rain) and reflectivity peaks (above a threshold of 40 dBZ) are depicted at 2000 UTC (1400 CST) in Figure 25. The most active hour of cloud-to-ground lightning activity takes place from 2000-2100 UTC. The image is a composite constructed from several NWS network (e.g., Nashville, TN; Centerville, AL; Jackson, MS) and local warning (e.g., Huntsville, AL; Tupelo, MS) radars in the region. An isolated supercell storm ahead of the line (labeled T) was overtaken as the line moved northeastward more rapidly than the cell (Figures 26-28). The average system motion vector was  $25 \text{ m s}^{-1}$  from  $235^\circ$  (due north is defined as  $0^\circ$ ). The merger and subsequent interaction of the gust front from the squall line with the supercell led to an F4 intensity tornado (estimated wind speeds of  $92\text{--}116 \text{ m s}^{-1}$ ) at 2230 UTC that killed 22 people in Huntsville, AL. The ambient wind in the lower troposphere derived from atmospheric soundings at 1200 UTC ( $235^\circ$  at  $6.7 \text{ m s}^{-1}$  at Centerville, AL (CKL) and  $230^\circ$  at  $8.5 \text{ m s}^{-1}$  at Nashville, TN (BNA)) is much less than the storm motion vector. In addition, the supercell storm had an average storm motion vector (indicated by the large dots) of  $243^\circ$  at  $18.3 \text{ m s}^{-1}$ ,  $8^\circ$  to the right of the mean wind.

#### Define the Region of Interest

Isolated lightning discharges of both positive and negative polarity occurred both ahead of the line from thunderstorm anvils and from the trailing stratiform rain region behind the main line of storms. Lightning activity during a 1.5 h period prior to the Huntsville, AL tornado is shown in Figure 29. The analysis region of interest is shown in Figure 30. The lightning flashes are converted from earth coordinates (latitude, longitude) to rectangular coordinates (x,y). For convenience, the geographic coordinate (0,0) at the center of the map represents the location of the MIT/Lincoln Laboratory

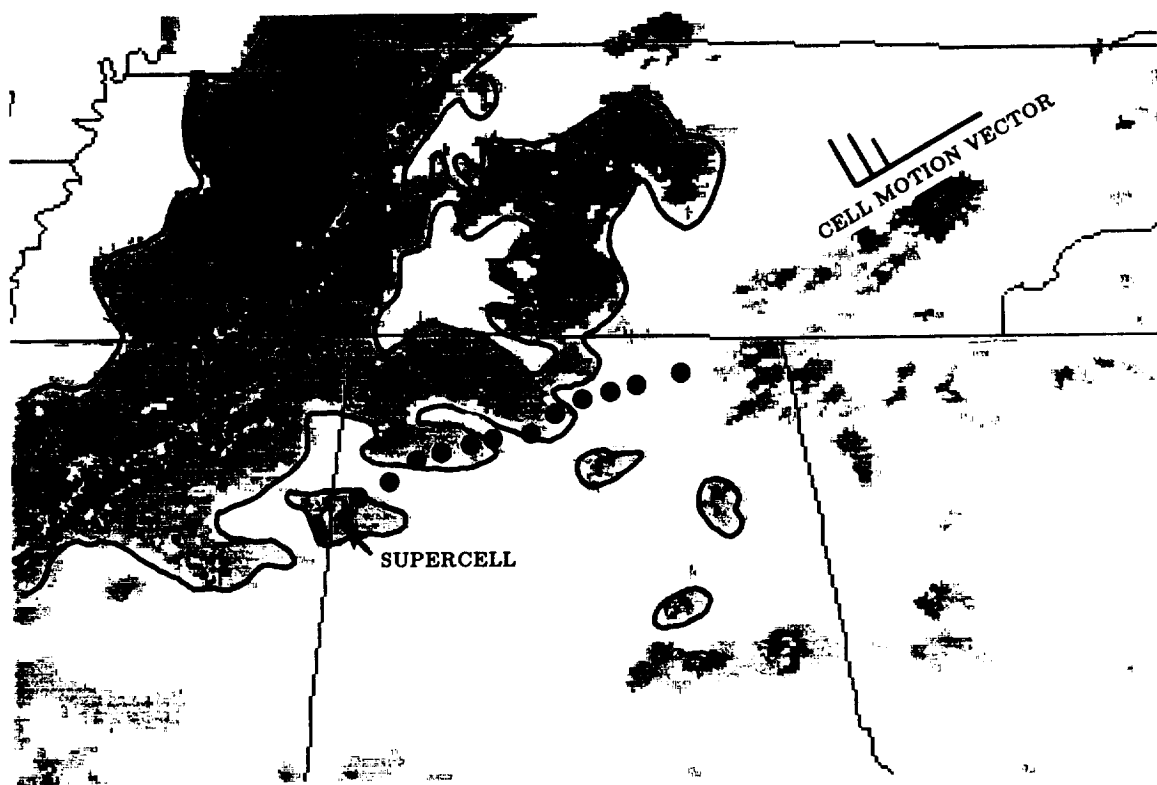


Figure 25. Composite precipitation pattern at 2000 UTC (1400 CST) on 15 November 1989 observed by the regional network of NWS radars. The radar reflectivity is contoured at 18,30,40,45,50,55 dBZ (VIP levels 1-6). Small solid circle = Reflectivity cores > 45 DBZ; large solid circle = track of the tornadic supercell storm every 15 min. The motion vector of cells within the squall line indicated by the wind barb is  $25 \text{ m s}^{-1}$  from  $235^\circ$ .

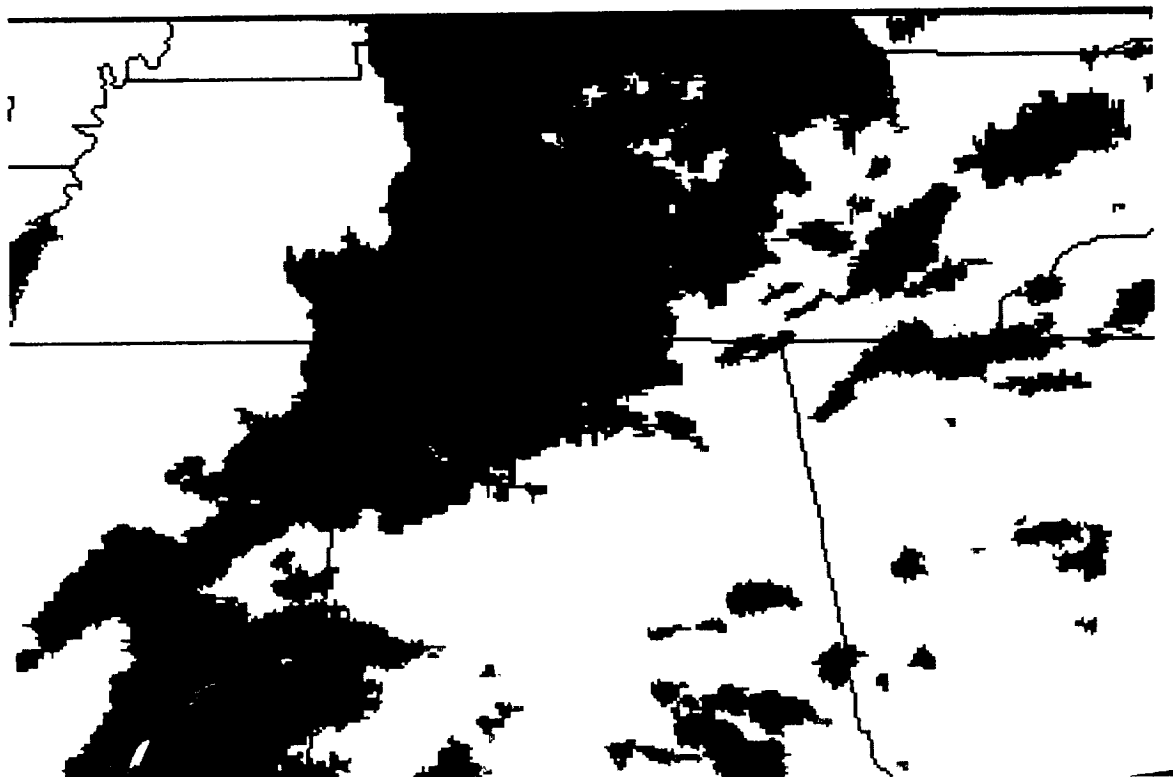


Figure 26. Composite precipitation pattern at 2100 UTC on 15 November 1989.

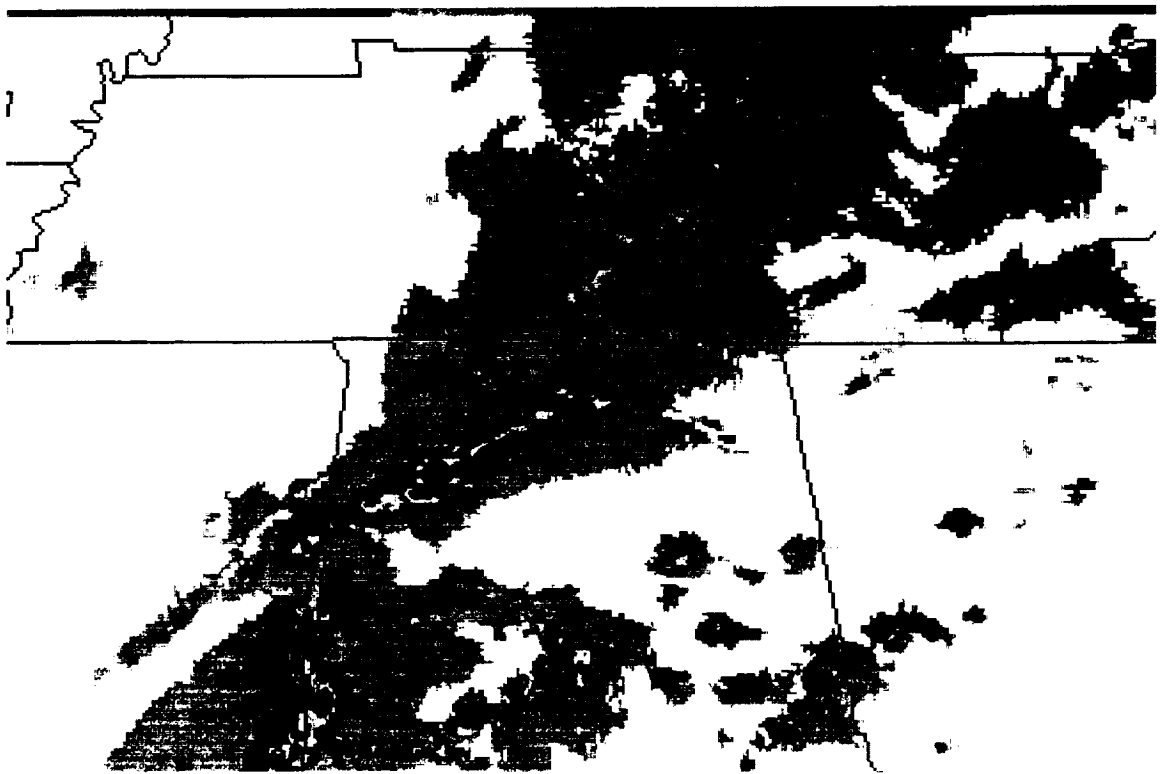


Figure 27. Composite precipitation pattern at 2200 UTC on 15 November 1989.

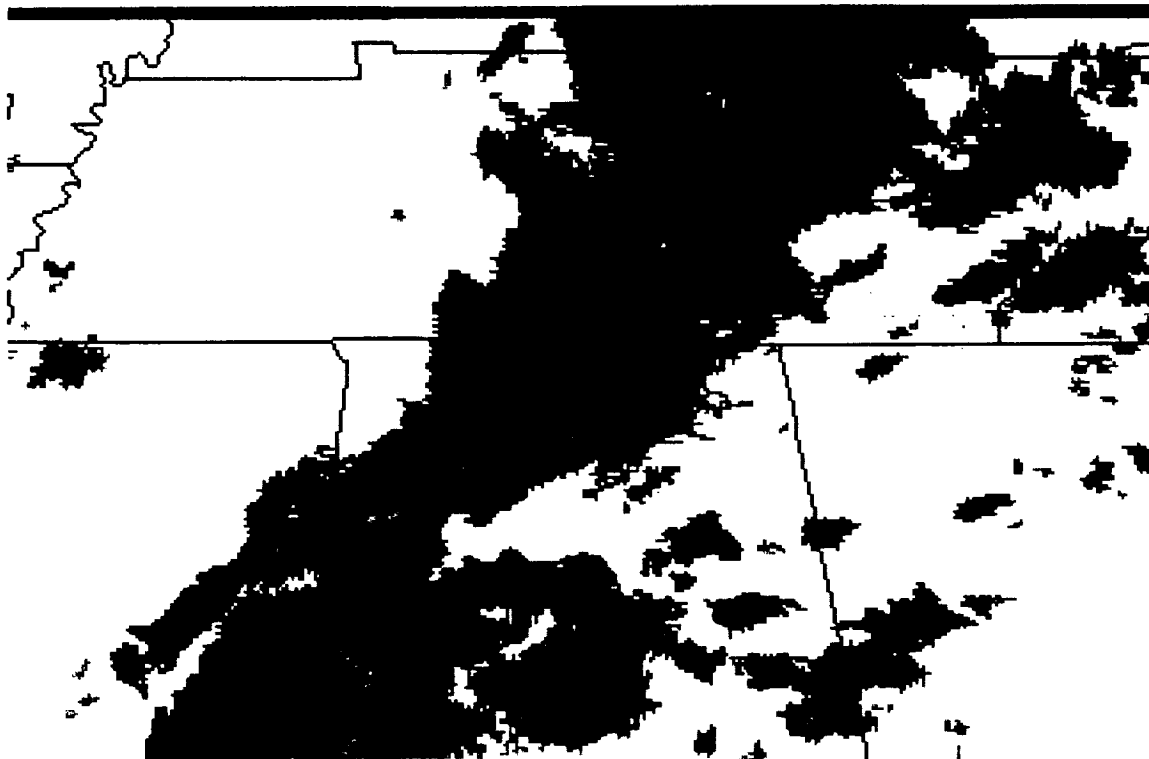


Figure 28. Composite precipitation pattern at 2230 UTC on 15 November 1989.

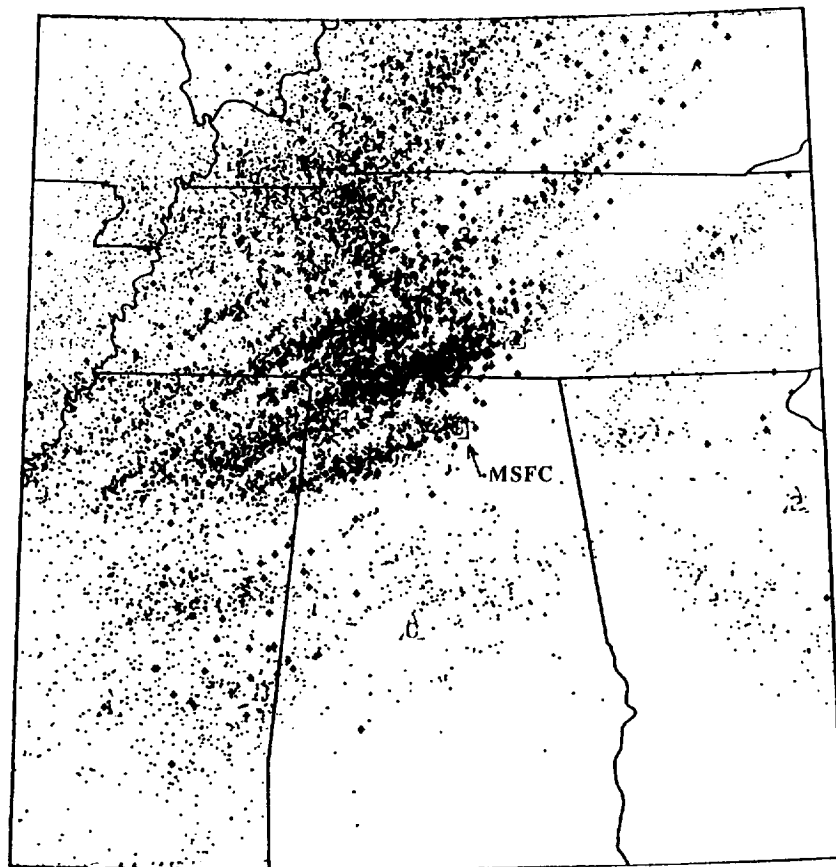
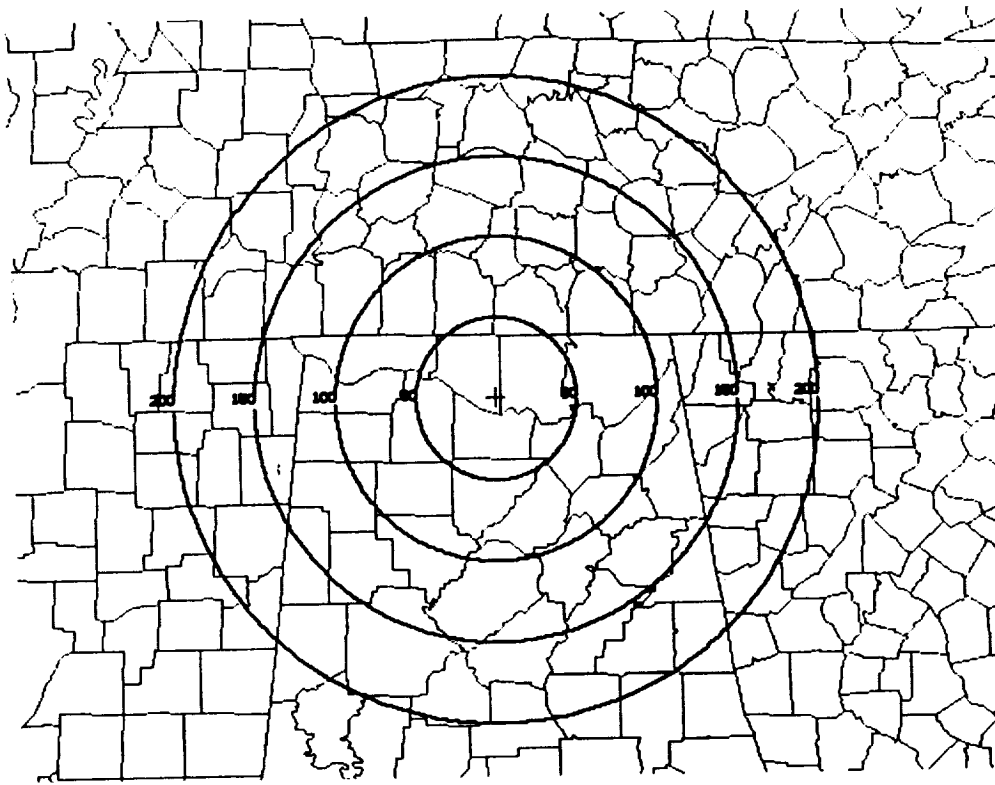


Figure 29. Cloud-to-ground lightning activity from 2105-2236 UTC on 15 November 1989. • = negative polarity discharges; + = positive polarity discharges.



**Figure 30.** County and state outlines in the lightning analysis region. Range rings are every 50 km. The site of the MIT/Lincoln Laboratory FL2 Doppler radar is at the center of the rings.

FL2 Doppler radar (refer also to Figure 24). The radar was situated just north of the Huntsville airport (HSV) during the COHMEX field campaign to study thunderstorm downdrafts, outflows, and gust fronts hazardous to aviation. This transformation is for the convenience of some lightning-radar intercomparisons discussed later. Figure 31 depicts the centroid of all lightning activity in successive 5-min intervals from 2130-2235 UTC. The plotted track of the tornadic supercell storm, T, was computed every 15-min during the interval 2130-2230 UTC from the National Climatic Data Center 16 mm film-archive of the Nashville, TN (BNA) radar scope. The initial damage from the tornado (labeled t) occurred on Redstone Arsenal at 2230 UTC.

The clustering procedure begins by summing the lightning discharges into 10 km grids within an m-row by n-column matrix such as that pictured in Figure 32. The evolution of the lightning activity associated with the main line of storms can be followed from the series of contour maps ( $> 0.02$  flashes  $\text{km}^{-2}$  shaded) in Figure 33. A contoured lightning map during the 5-min interval 2215-2220 UTC indicates the locations of greatest lightning density that might serve as candidate seed points (Figure 34). In the following discussion, the gridpoint (20,20) is at the center of the data matrix and corresponds to the aforementioned geographic reference point at (0,0).

### Identify the Cluster Seeds

Step 1. A copy of the m x n data matrix **D** is generated and designated as the seed matrix **S**.

Step 2. A 3 x 3 point window searches directionally by rows through **S** from the upper left-hand corner (1,1) to the lower right-hand corner (m,n) to identify isolated lightning density maxima (Figure 35). Any non-zero grid point  $S(i,j)$  at the center of the 3 x 3 window having a neighbor greater or equal to itself is also set equal to zero. Otherwise, the point is left undisturbed in **S** as a candidate seed. For example, the gridpoint  $S(15,20)=8$  is greater than its neighbors and is designated as a seed. When the center of the window reaches the gridpoint  $S(16,20)=6$ , the value of 6 is less than the neighbor above it and is set equal to zero. A single pass through **S** would produce the seeds indicated in Figure 36. However, note that the points

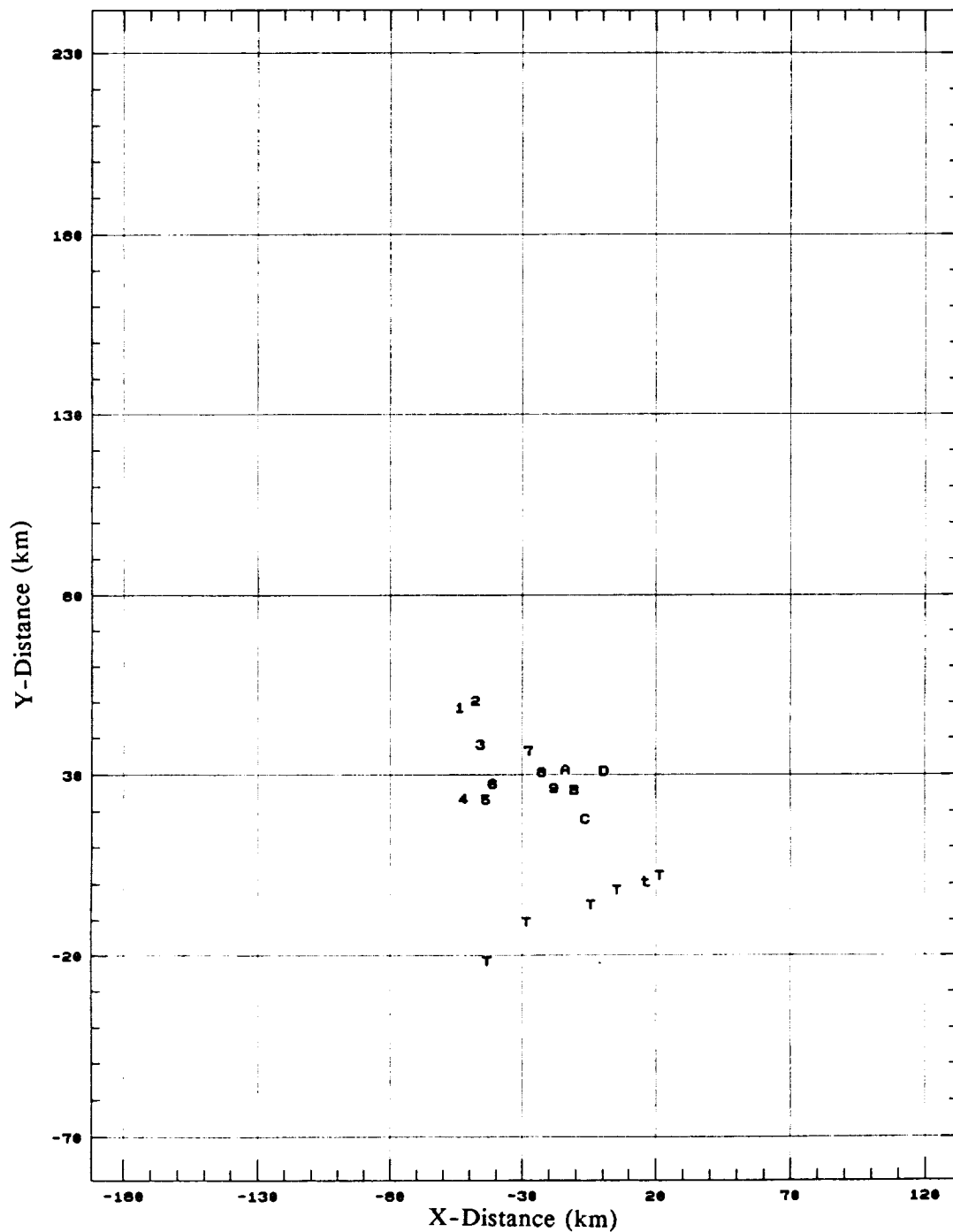


Figure 31. Centroid of all lightning within the analysis region in 5-min intervals (labeled 1-9-A-D) during the period 2130-2235 UTC.  $\overline{T}$  = track of the tornadic storm echo every 15 min beginning at 2130 UTC;  $\underline{t}$  = location of tornado touchdown and tree damage on Redstone Arsenal. The FL2 radar is at the geographic center of the map at the point (0,0).

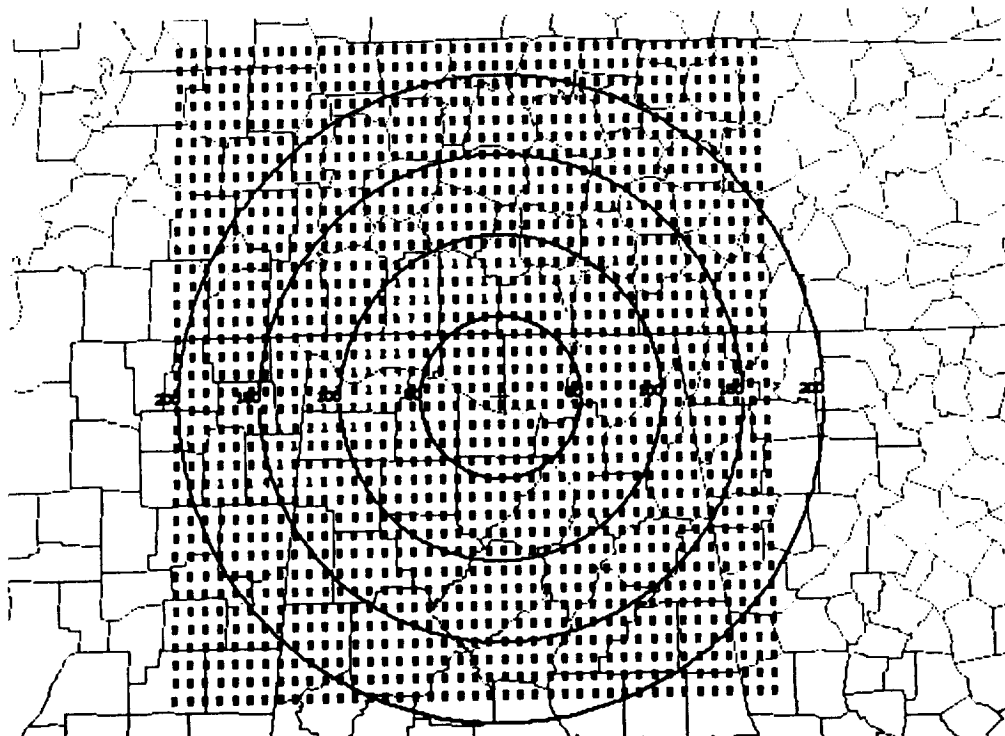


Figure 32. Lightning analysis region with 10 km gridpoints.

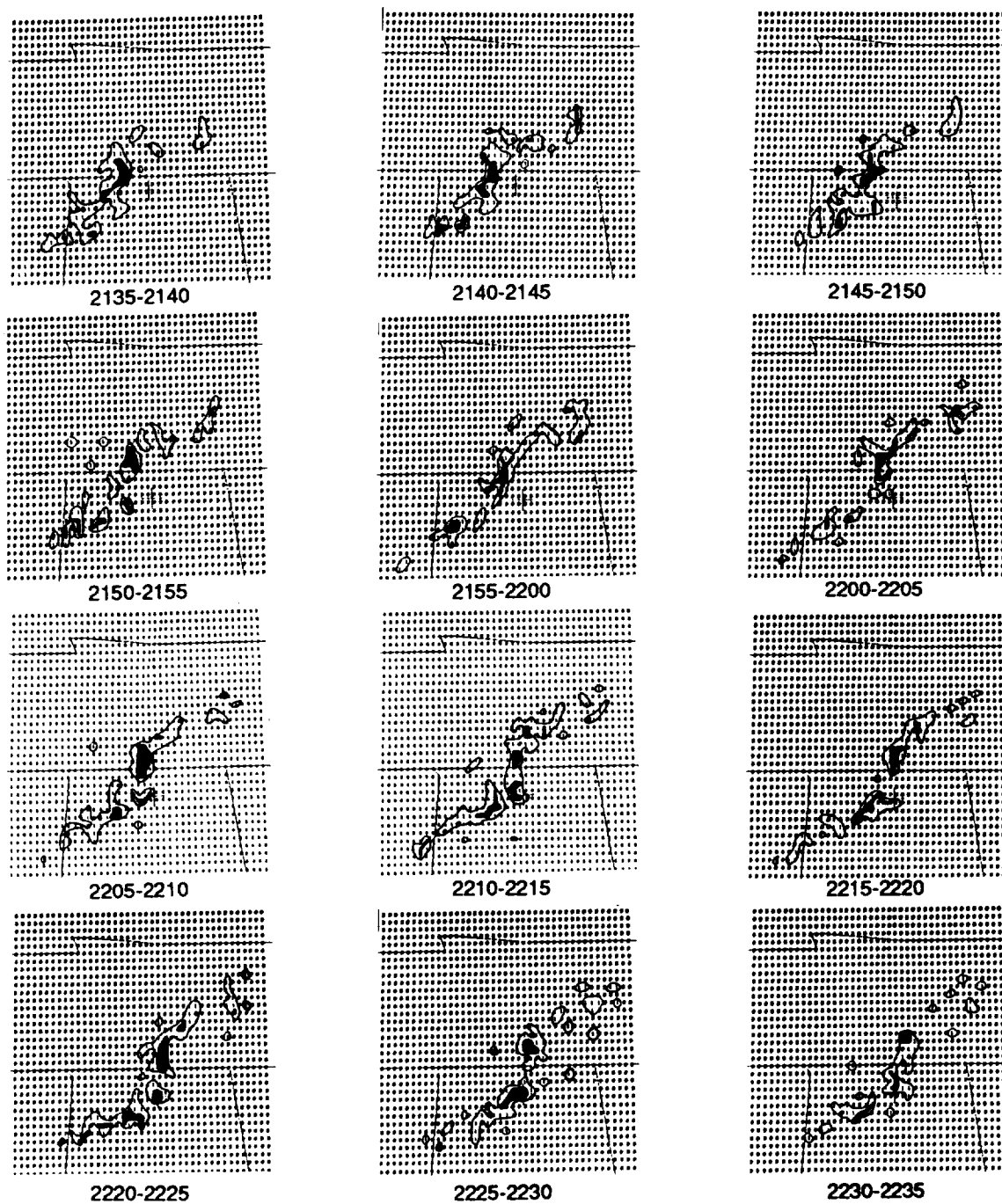


Figure 33. Evolution of cloud-to-ground lightning activity in 5-min intervals between 2135-2235 UTC. Contours are approximately 0.01 discharges  $\text{km}^{-2}$  and 0.02 discharges  $\text{km}^{-2}$  (shaded).

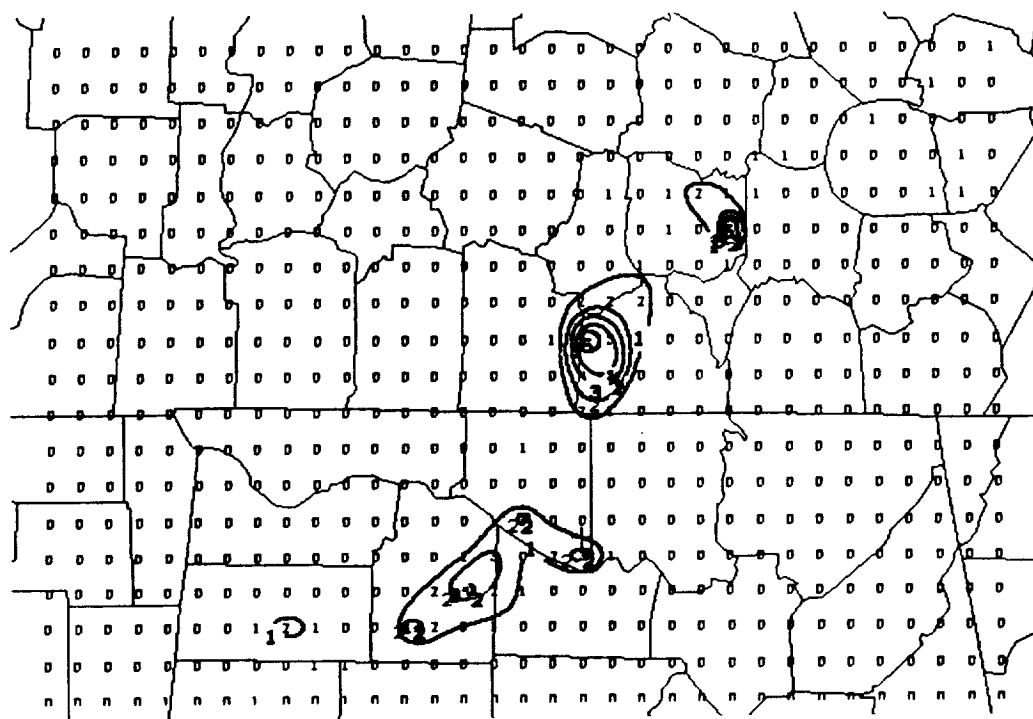


Figure 34. Contoured lightning density map during the period 2215-2220 UTC. Contour interval is every 0.01 discharges  $\text{km}^{-2}$  beginning with the value 0.02 discharges  $\text{km}^{-2}$ .

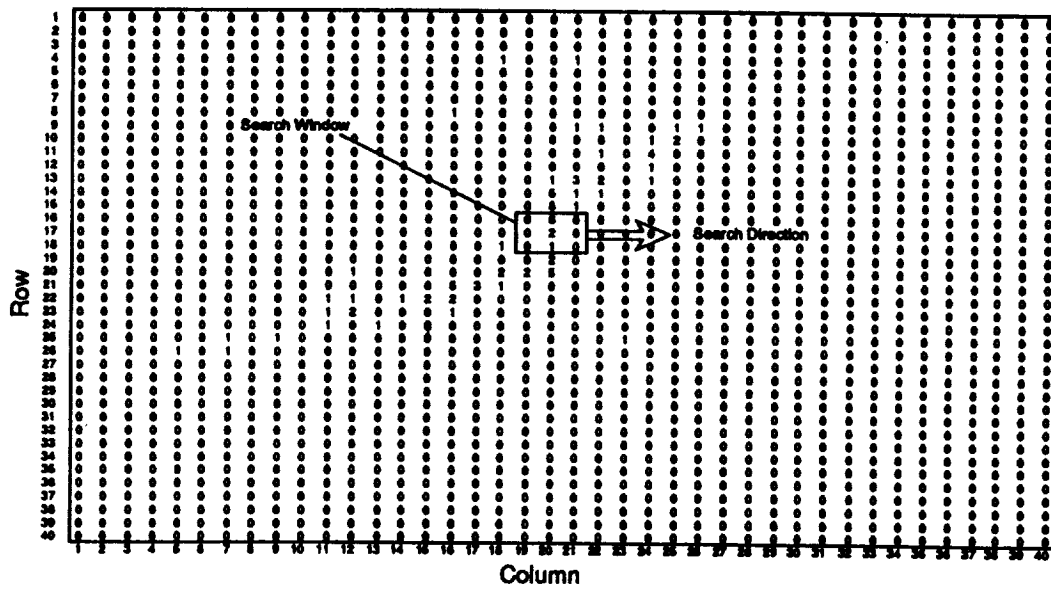


Figure 35. Diagram of the 3 x 3 point search window moving through the m-row x n-column data matrix  $D$ . Lightning shown for the period 2215-2220 UTC at each 10 km gridpoint.

$S(13,22)=2$  and  $S(17,20)=2$  are not isolated maxima in  $D$ , but result from the left to right search direction of the  $3 \times 3$  window. Such spurious seeds are removed by step 3.

**Step 3.** The original data matrix  $D$  is scanned locally for a neighbor that might be larger than the candidate seed itself, but had been set to zero in  $S$  in the prior step. If a neighbor is not a seed, but is still greater than the candidate point in question, then the candidate point is not an isolated maxima and is set to zero. For example, let the window continue moving through  $S$  until the center of the window is at  $S(17,20)=2$ .  $S(17,20)$  is now a candidate because  $S(16,20)=0$  resulted from step 2. However,  $S(17,20) < D(16,20)$  so  $S(17,20)$  should also be set to zero. Thus, one pass produces the final  $S$  matrix of exactly  $K$  seeds (Figure 37).

**Step 4.** Define a set of criteria for establishing the number of valid seeds. In this example, there are 17 seed points having at least 0.01 flashes  $\text{km}^{-2}$  (or 1 flash within a  $10 \text{ km} \times 10 \text{ km}$  grid). The possible seeds consist of 7 seeds produced by single lightning discharges of positive polarity, 5 produced by single discharges of negative polarity, and 5 seeds with a density greater than 0.02 flashes  $\text{km}^{-2}$ . A sensitivity study of possible criteria and their justification are discussed below.

#### Determine the Cluster Memberships

The initial partition of  $K$  seeds is critical since the  $K$ -means algorithm must optimally assign the lightning flashes to one of exactly  $K$  clusters. A different initial partition (determined by the number and location of the seeds) might produce a different final partition and storm motion vector based on the tracking of the seeds. Furthermore, any change in cluster membership also alters its time series.

Figure 38 shows the the cluster assignment for each flash occurring between 2215-2220 UTC and the location of the 5 seeds (labeled a-e) identified in step 4 above with a density of 0.02 flashes  $\text{km}^{-2}$  or greater. Seed densities of 0.01 flashes  $\text{km}^{-2}$  are excepted and the location of the tornadic supercell storm (labeled T) as observed by the BNA radar is indicated. The Tennessee-Alabama border is approximately 45 km north of the reference point.

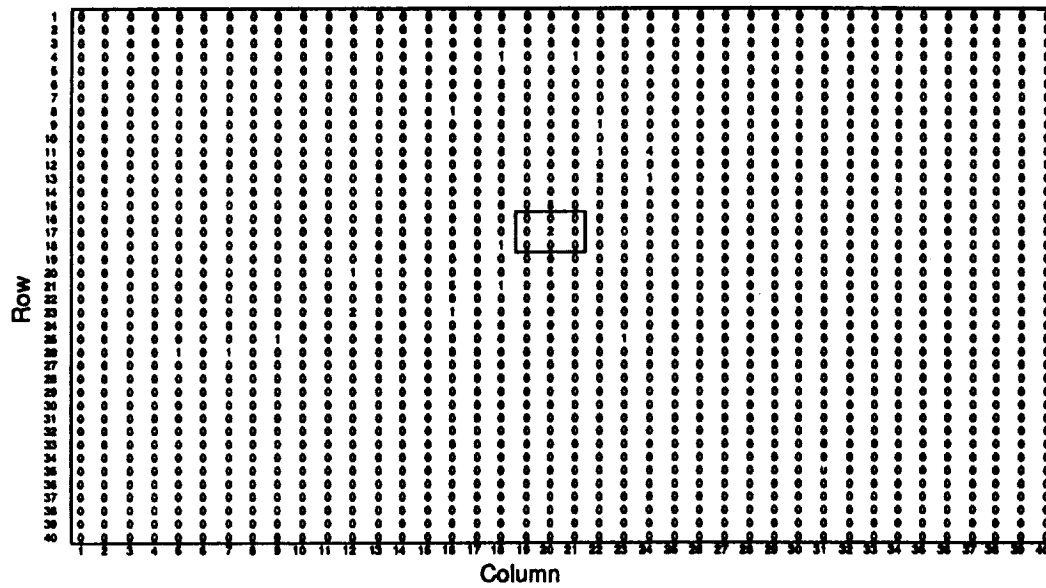


Figure 36. Diagram of the seed matrix S after one pass through the data matrix. The search window is centered at the point  $S(i,j) = (17,20)$ .

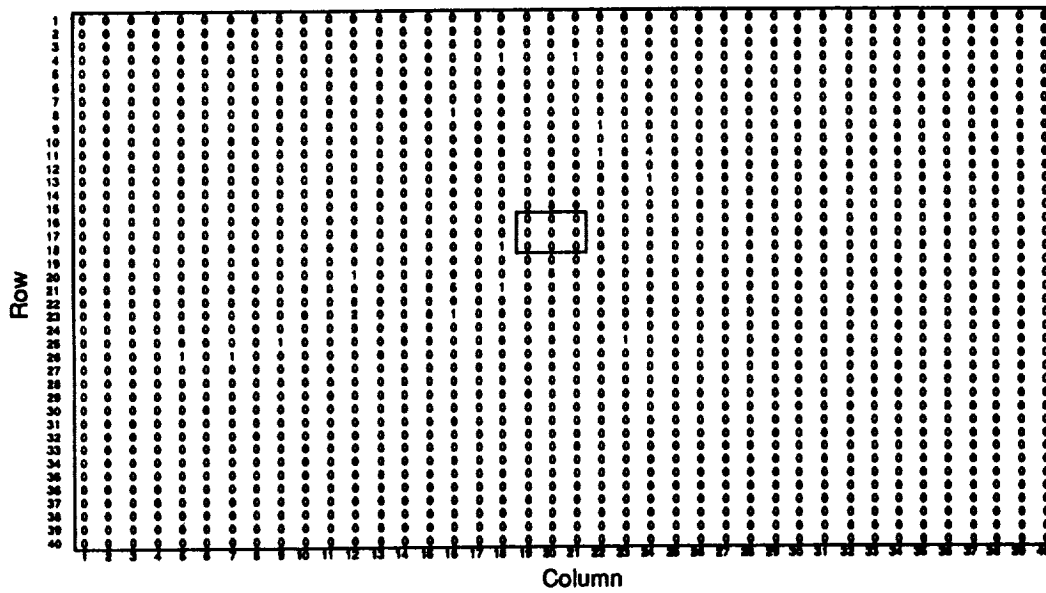


Figure 37. Diagram of the final seed matrix S.

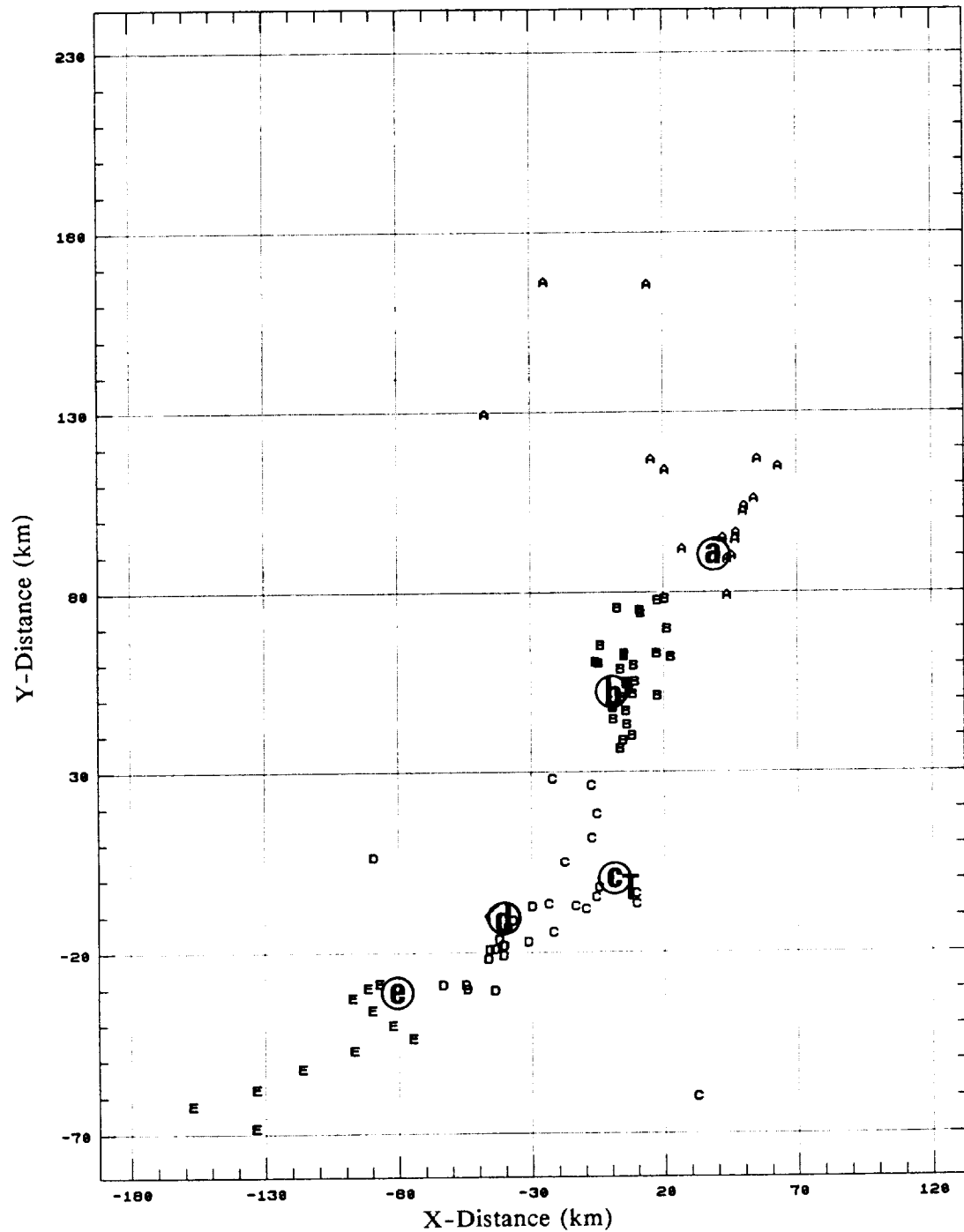


Figure 38. Cluster assignments for each flash during the period 2215-2220 UTC.  
Circled lower case letters (a-e) = cluster seeds with values greater than 0.02  
discharges  $\text{km}^{-2}$ ; T = location of tornadic storm echo at 2215 UTC.

Clusters B,C, and D have the smallest displacements between their seed (first guess) and final centroid. Clusters A and E are more spread out with the four northwesternmost flashes assigned to cluster A being of positive polarity. A comparison with the lightning density contour maps (Figures 33; 34) and the regional radar image at 2215 UTC (Figure 27) indicates good agreement between the 5 lightning centroids and the largest thunderstorm echoes. The positive polarity flashes in the northwest quadrant of cluster A are seen to be located in the trailing stratiform rain behind the main line of thunderstorms.

Next, let the 5 single discharges of negative polarity serve as additional seeds (f-j) and consider the impact on the preceding example (Figure 39). The distribution of the 10 seeds splits apart cluster E into E, I, and J. Cluster A is split into clusters A and F, where F is comprised entirely of the scattered positive polarity flashes in the trailing stratiform rain. Cluster B is subdivided into clusters B and G and lastly, cluster H is split off from cluster C. Comparison with the 2215 UTC radar image indicates that cluster H is probably best represented by the solitary echo southeast of the main line of thunderstorms. However, the remaining subdivisions appear less realistic.

The effect of changing cluster memberships is presented in Table 6. The original cluster membership changes (and decreases) when the number of seeds increases from 5 to 10 seeds. Cluster D maintains the same total membership, but exchanges members with clusters C and E. In addition, the within group sum of squares (WSS) decreases as the number of seeds is increased.

Due to the natural spatial variability of the lightning strikes, a single flash within a  $100 \text{ km}^2$  grid is just as likely to have occurred in any of the bordering grids. Indeed, ground-based radar and high altitude airplane lightning measurements of large weather systems such as this have shown lightning flashes occasionally propagating over 100 km horizontally before striking the earth (Ligda, 1956; Goodman et al., 1988c).

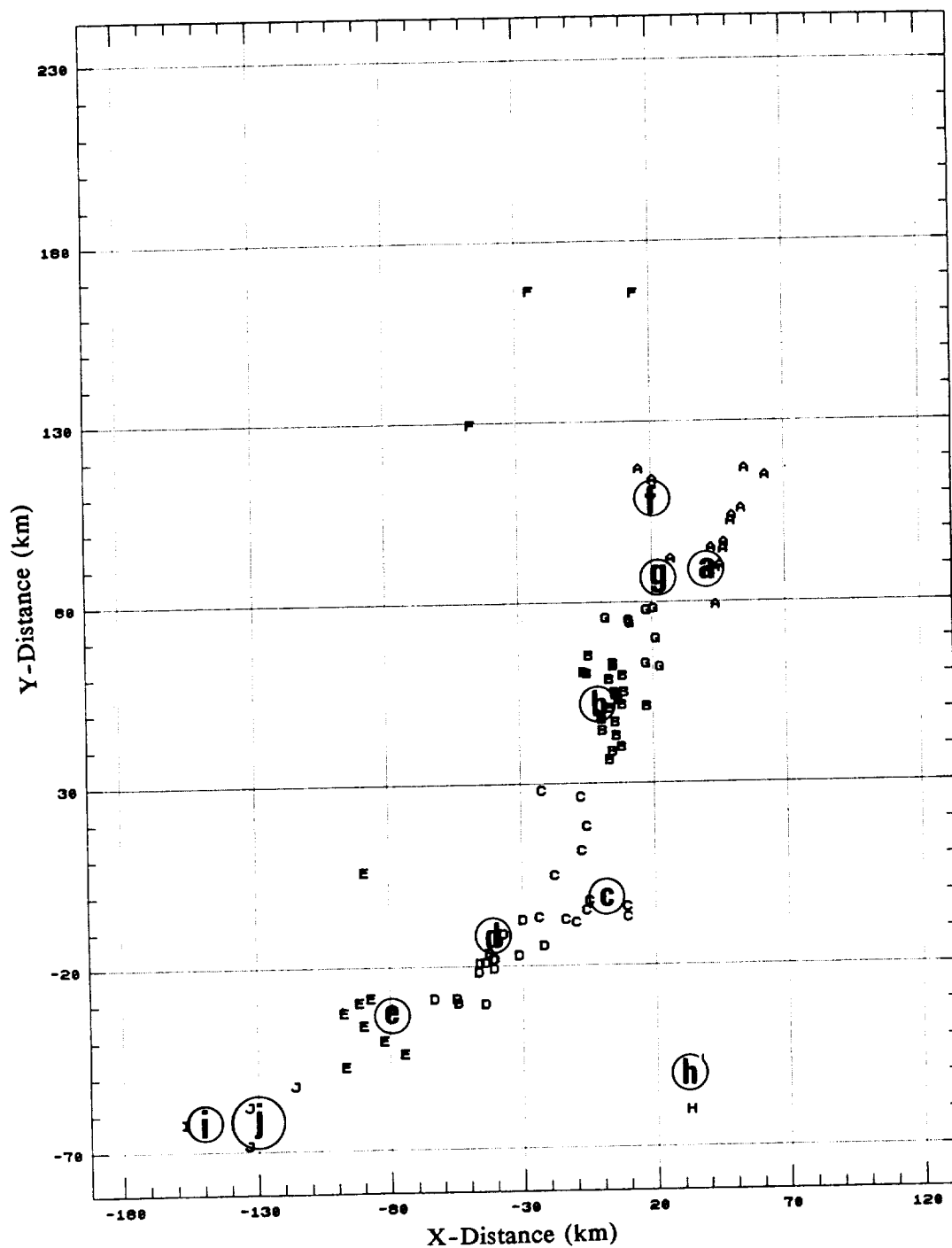


Figure 39. Cluster assignments for each flash during the period 2215-2220 UTC. Circled lower case letters (a-e) = cluster seeds with values greater than 0.02 discharges km<sup>-2</sup>; Circled lower case letters (f-i) = cluster seeds each represented by a single negative polarity discharge.

Table 6. Cluster Characteristics at 2215-2220 UTC

Cluster	Seed (x, y) (km)	Seed Density (x 10 <sup>-2</sup> km <sup>-2</sup> )	Cluster $(\bar{x}, \bar{y})$ (km)		Members		WSS (km <sup>2</sup> )	
			(5)	(10)	(5)	(10)	(5)	(10)
A	(40,90)	6	(32.2, 110.3)	(43.3, 101.0)	17	14	23543	4137
B	(0, 50)	8	(7.4, 57.5)	(4.4, 52.2)	30	22	5662	1984
C	(0, 0)	5	(-6.2, -1.5)	(-8.2, 4.4)	14	12	9000	3225
D	(-40, 10)	5	(-46.4, -13.2)	(42.2, -19.5)	16	16	4374	2226
E	(-80, -30)	2	(-105.3, -45.1)	(-88.6, -31.2)	11	8	8580	2335
F	(20, 110)	1	-	(-19.2, 154.0)	-	3	-	2811
G	(20, 90)	1	-	(15.6, 72.1)	-	8	-	610
H	(30, -50)	1	-	(32.6, -59.8)	-	1	-	0
I	(-150, -60)	1	-	(-157.1, -62.2)	-	1	-	0
J	(-130, -60)	1	-	(-127.5, -59.3)	-	3	-	0

### Tracking Seeds and Clusters

The eastward propagation of the lightning activity can be followed over the three subsequent 5-min periods 2220-2225 UTC (Figure 40), 2225-2230 UTC (Figure 41), and 2230-2235 UTC (Figure 42). In each case a threshold seed density of  $0.02 \text{ flashes km}^{-2}$  is employed to identify the clusters. The seed and cluster letter identifiers are newly assigned each 5-min sample period in the order the seeds are identified. Thus, the assignment follows the search direction from upper left to lower right within the seed matrix S.

Cluster A beginning at 2215 UTC can be tracked from the continuity between 5-min observation periods from 2215-2230 UTC as A-A-A-A. Since no local seed is identified at 2230 UTC, the singular A event near the coordinate (70,120) in Figure 42 is misclassified as a member of the cluster to its south, rather than to the decaying northern storm. Cluster B beginning at 2215 UTC can be tracked as B-(B+C)-B-A. The tornadic storm cluster can be tracked as C-(D+E)-C-C. The two clusters initially identified at 2215 UTC as B and C are each split apart into two distinct groups at 2220 UTC before merging again. The additional lightning clusters at 2220 UTC makes subsequent tracking of all but the largest storms difficult. However, such storms also produce a greater number of discharges and hence pose the greatest threat. Isolated storms, large or small, tend to maintain their identity. Storms that merge and split apart cause identification problems for the radar echo tracking techniques as well.

An approach that might be considered for reducing the number of clusters to only those that are coherent (i.e., trackable) from sample to sample is to make use of a hybrid scheme using multiple methods. One possible hybrid approach has been applied to this problem. The K-means algorithm is run initially as before, but then a variation of the joining algorithm is used to reduce the number of clusters to the same number identified in the prior sampling interval. The final number of clusters desired can be

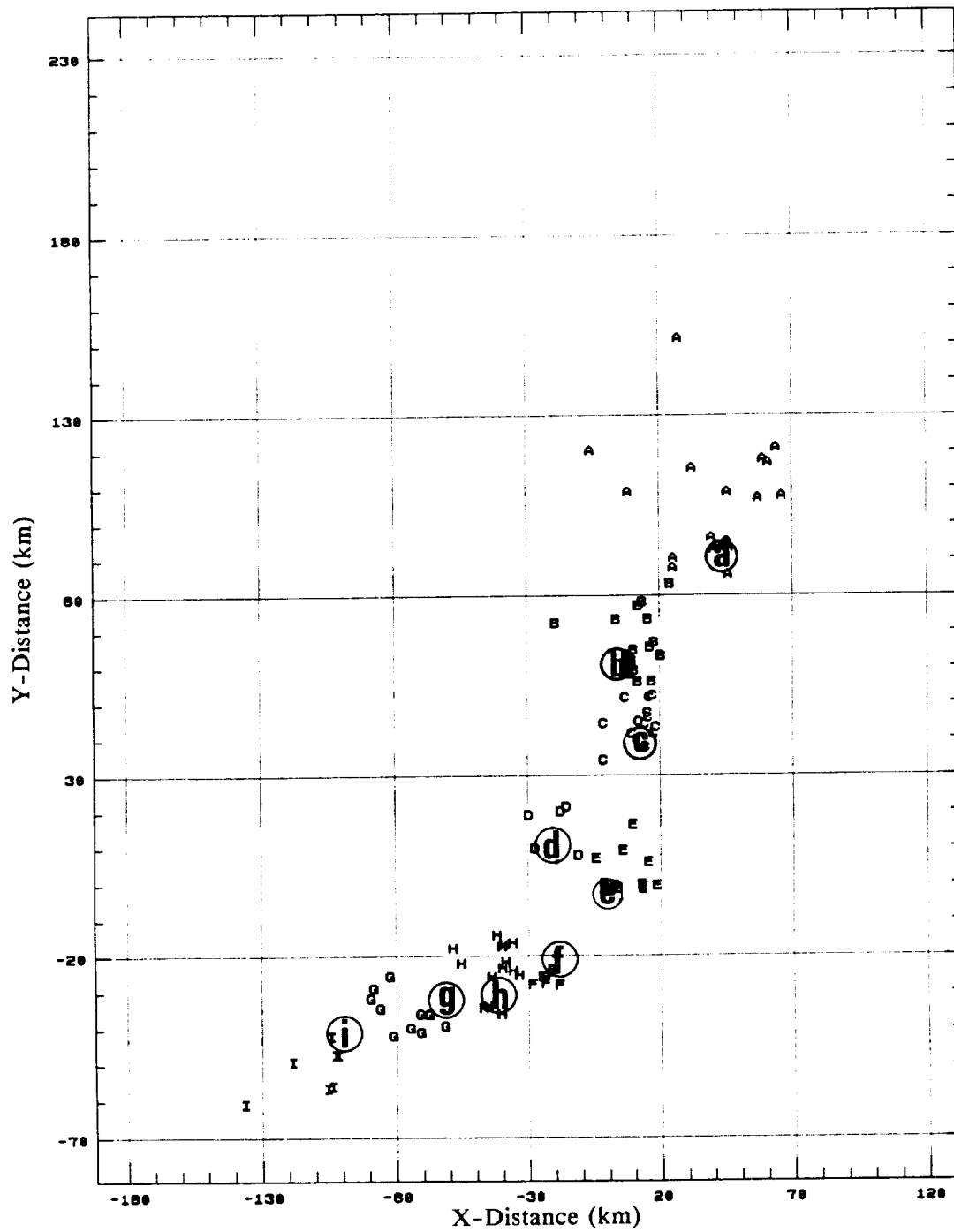


Figure 40. Cluster assignments for each flash during the period 2220-2225 UTC. Circled lower case letters (a-i) = cluster seeds with values greater than 0.02 discharges  $\text{km}^{-2}$ .

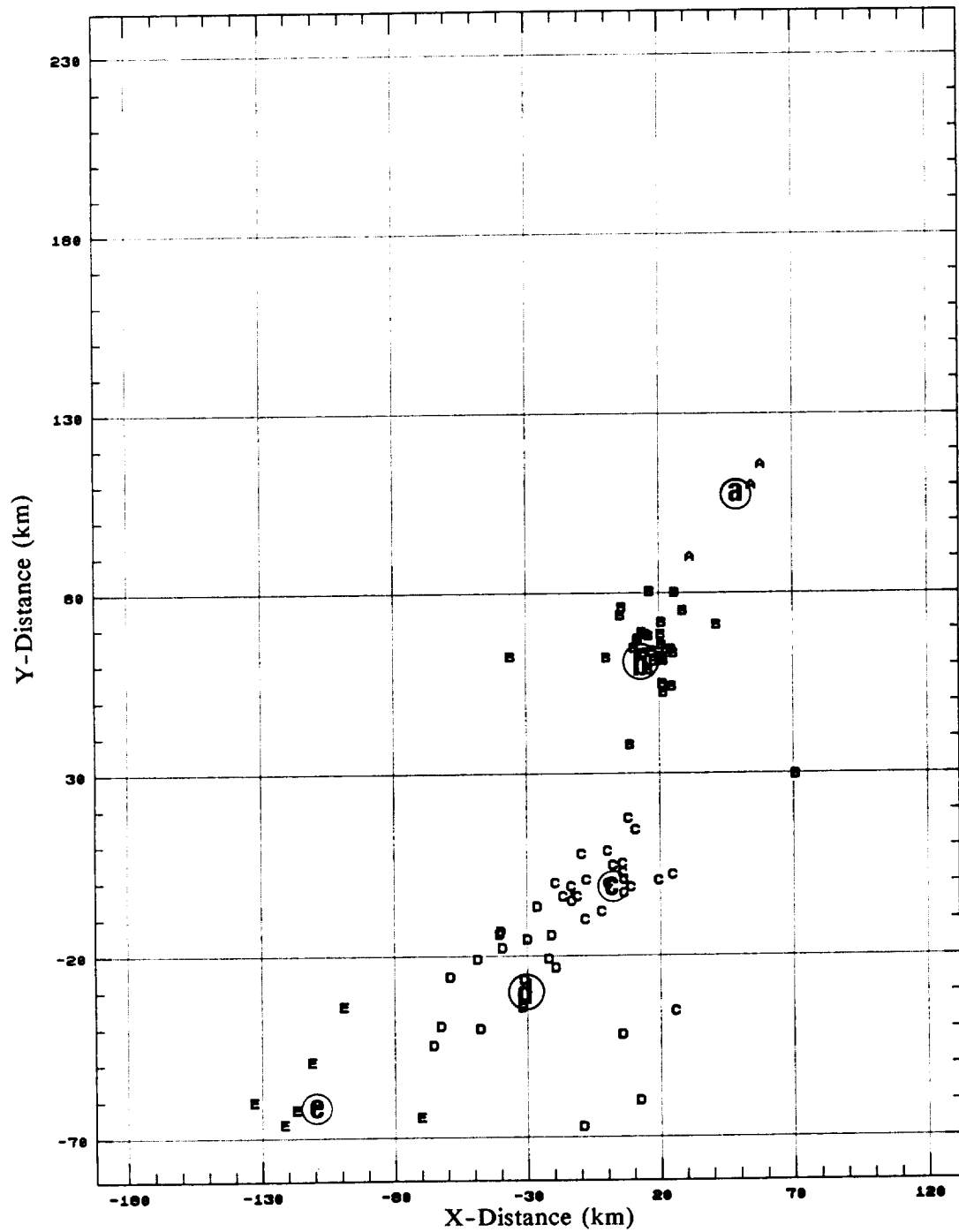


Figure 41. Cluster assignments for each flash during the period 2225-2230 UTC.  
Circled lower case letters (a-e) = cluster seeds with values greater than 0.02  
discharges  $\text{km}^{-2}$

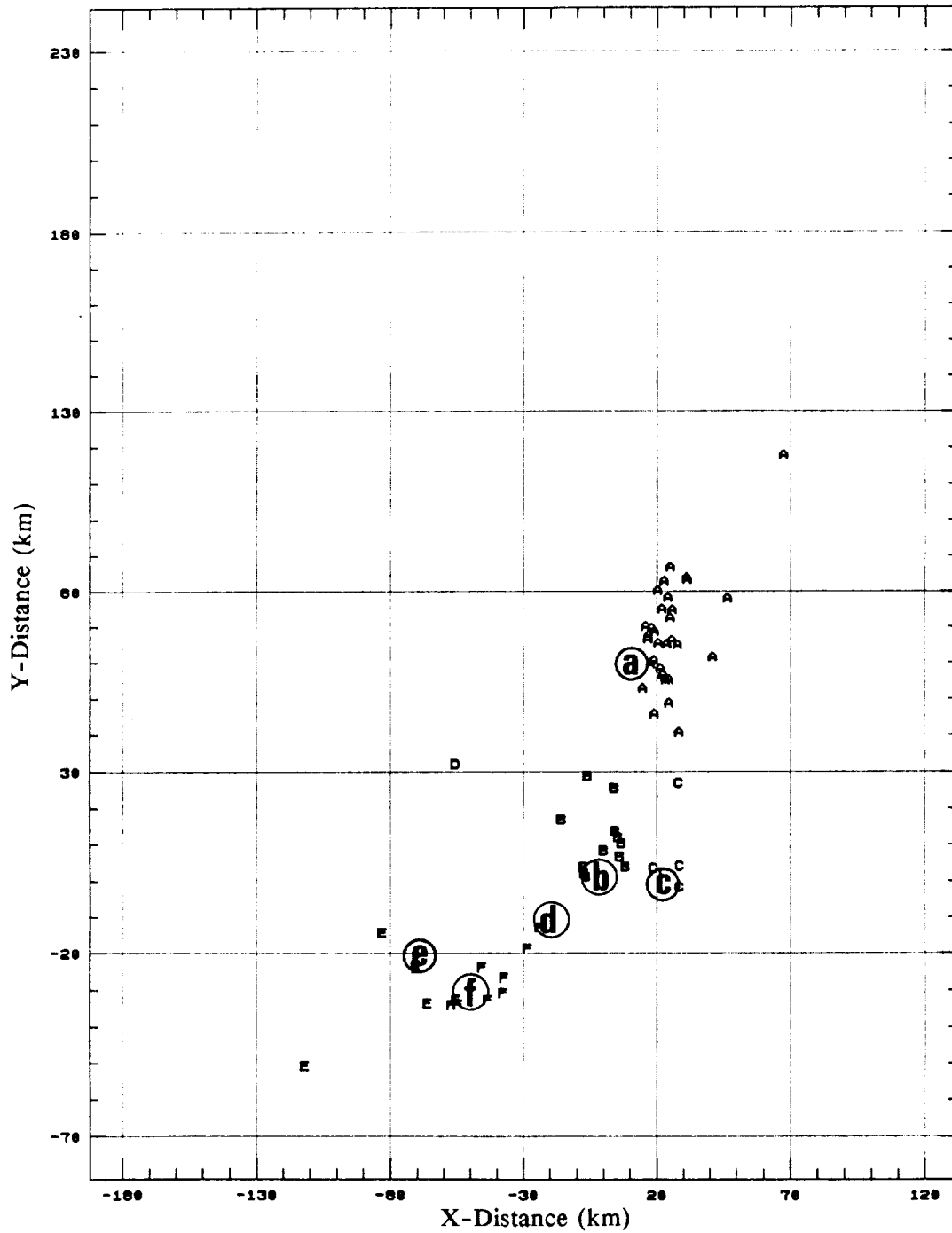


Figure 42. Cluster assignments for each flash during the period 2230-2235 UTC.  
Circled lower case letters (a-f) = cluster seeds with values greater than 0.02  
discharges  $\text{km}^{-2}$ .

based on having a manageable number of entities to track, correspondence with radar measurements, or perhaps based on some criteria such as desired storm size (by setting a minimum areal extent threshold). The result is shown in Figure 43 for the period 2220–2225 UTC. The hybrid implementation involves finding the mean (x,y) coordinate of the two nearest clusters to be paired until the total number of seeds is reduced from the original set of 9 seeds (refer to Figure 40) to a revised set of 5 seeds. Table 7 lists the results of changing the the number of seeds. When clusters D and E are joined, the seed location of cluster E is used instead of a mean location for the pair because of the greater seed density and greater number of members assigned to E in the first application of the K-means algorithm.

Alternatively, the grid cell dimension could be increased to 20 km x 20 km or greater to allow greater seed densities and fewer seeds, but this approach will reduce the accuracy of the seed locations and the ability to resolve small storms as individual entities. We have found that it is better to generate more seeds and iteratively join the clusters than to generate too few seeds and be unable to resolve new cells that may produce low flash rates or identify decaying storms which produce scattered discharges. The Huntsville, AL tornadic storm, for example, produces a flash density of 1 discharge per 100 km<sup>2</sup> earlier in its life-cycle. Other alternative approaches using only lightning data, considered to be beyond the scope of this study, would be 1) to set a threshold on the seed density or total cluster membership at some level greater than 0.02 flashes km<sup>-2</sup> that might be considered to be physically meaningful, or 2) define a maximum search radius, say 20 km, which would be the maximum distance a flash could be from a seed point for consideration as a cluster member.

Figure 44 shows 30-min seed tracks (representing the gridpoint with the largest local flash density) from 2200–2230 UTC for the clusters identified at 2215 UTC as A–E. The lower case letters identify only the 5-min periods when the seed value is greater than the 0.02 flashes km<sup>-2</sup> threshold. The upper case letters indicate the location

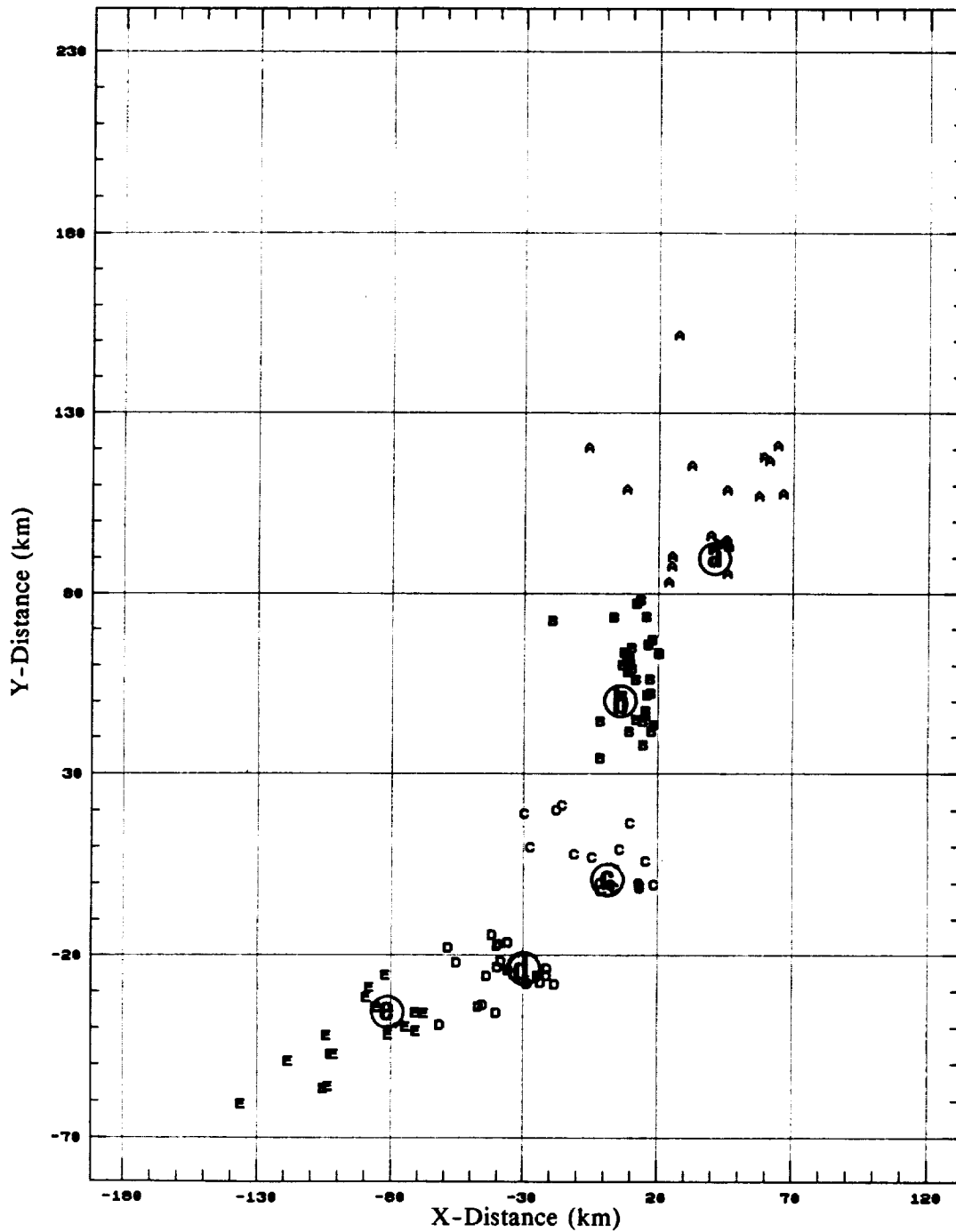


Figure 43. Hybrid clustering algorithm assignments during the period 2220-2225 UTC. Circled lower case letters (a-e) = cluster seeds with values greater than 0.02 discharges  $\text{km}^{-2}$ .

Table 7. Hybrid Clustering Algorithm at 2220-2225 UTC

Cluster	Seed (x, y) (km)		Seed Density ( $\times 10^{-2} \text{ km}^{-2}$ )	Cluster $(\bar{x}, \bar{y})$ (km)		Members		WSS ( $\text{km}^2$ )	
	(9)	(5)	(9)	(9)	(5)	(9)	(5)	(9)	(5)
A	(40, 90)	(40, 90)	5	(40.5, 105.7)	(39.7, 104.6)	19	20	11031	11768
B	(0, 60)	(5, 50)	6	(11.1, 66.0)	(11.0, 57.2)	21	(33)	2664	(6330)
C	(10, 40)		6	(11.8, 44.8)		13		891	
D	(-20, 10)	(0, 0)	2	(-20.4, 15.8)	(-0.8, 6.2)	5	(18)	410	(4772)
E	(0, 0)		7	(6.7, 2.5)		13		1073	
F	(-20, -20)	(-30, -25)	5	(-22.6, -32.8)	(-37.1, -27.1)	7	(22)	1924	(6303)
H	(-40, -30)		3	(-42.6, -23.3)		14		1302	
G	(-60, -30)	(-80, -35)	2	(-77.2, -35.2)	(-92.6, -42.0)	10	(16)	1066	(6917)
I	(-100, -40)		3	(-110.2, -51.1)		7		1240	

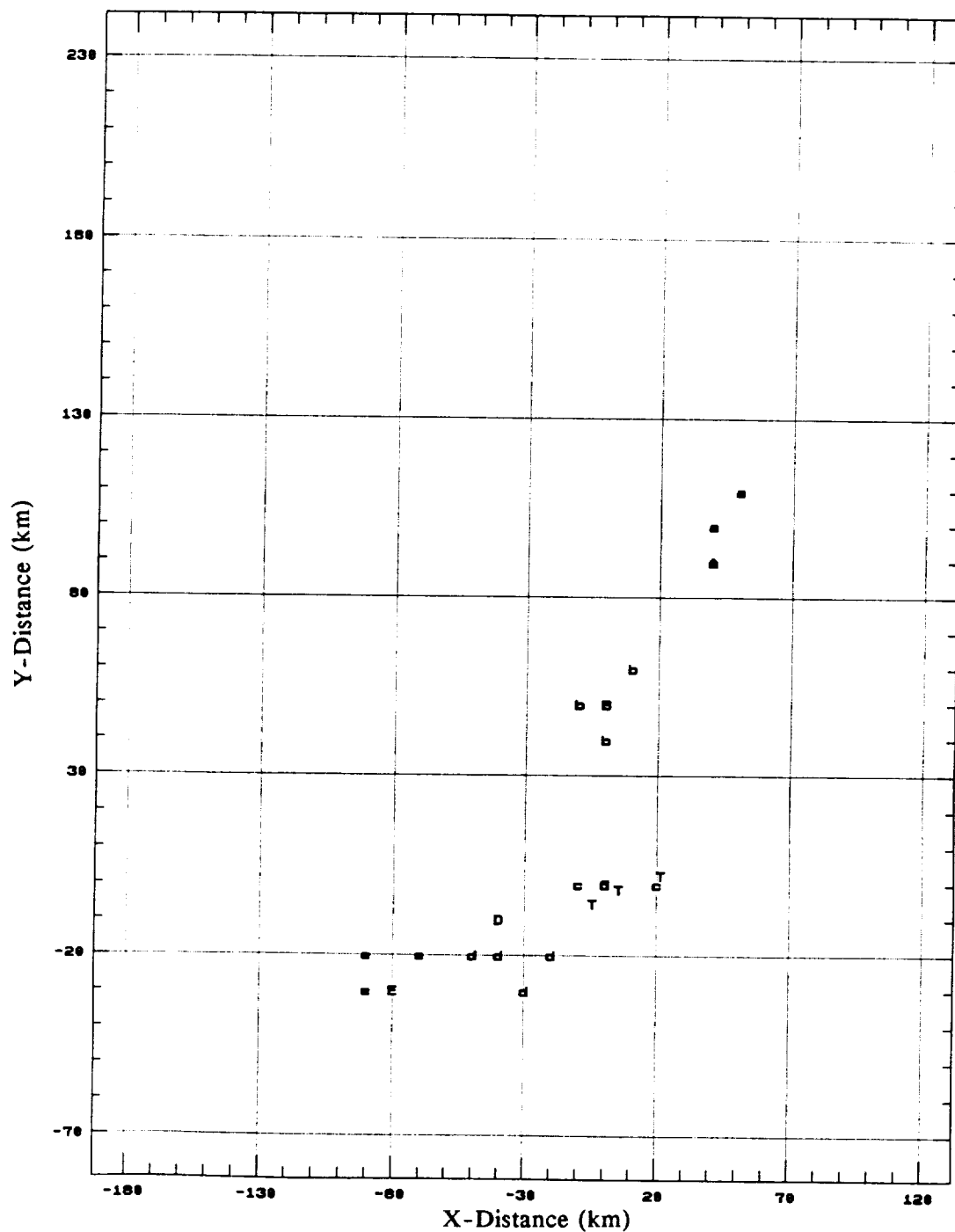


Figure 44. Seed tracks during the period 2200-2230 UTC. Lower case letters (a-e) = seed position for each 5-min interval that the seed value exceeds a threshold of 0.02 discharges km<sup>-2</sup>. Upper case letters (A-E) = seed seed location at 2215 UTC; **I** = Position of tornadic storm echo at 2200, 2215 and 2230 UTC.

of the seeds at 2215 UTC and the location of the tornadic storm echo at 2200 UTC, 2215 UTC, and 2230 UTC. All clusters are generally moving from west to east, with lightning cluster C within 1-gridpoint of the storm echo. However, only seeds B and D are greater than the threshold value during each 5-min interval. The track variations suggest a moving or weighted average of past tracks be used instead of updating the track with each observation. Such techniques are also employed in the radar echo trackers described earlier.

### Synergism With Radar

A primary objective of using a clustering algorithm for pattern recognition is to allow the identification and tracking of storms and their changing membership using the lightning data alone. However, the previous intercomparisons between the lightning clusters and the radar echoes suggest that a fusion of the data sources would be useful. For example, the radar echo trackers could provide seeds for clustering the lightning. Consider the tornadic storm at 2135 UTC when the maximum flash density is only 1 flash per gridpoint. Using a seed threshold of  $0.01 \text{ flashes km}^{-2}$  produces 21 total clusters and permits a separate cluster of two flashes, labeled T, for the tornadic storm (Figure 45). Using a seed threshold of  $0.02 \text{ flashes km}^{-2}$  causes the two lightning flashes to be assigned to cluster C.

On the other hand, the size and intensity criteria used in radar echo tracking could be given adaptive thresholds to capture small, electrically active storms that do not meet the default threshold criteria. In a study of the effect of radar echo size and asymmetry on the identification of small, electrically active microbursts occurring in Alabama and Florida, Buechler and Goodman (1990) find that the operational NEXRAD storm identification algorithms have a probability of detection less than 0.5. The algorithms are designed to detect large severe storms. Small storms (less than 5 km in

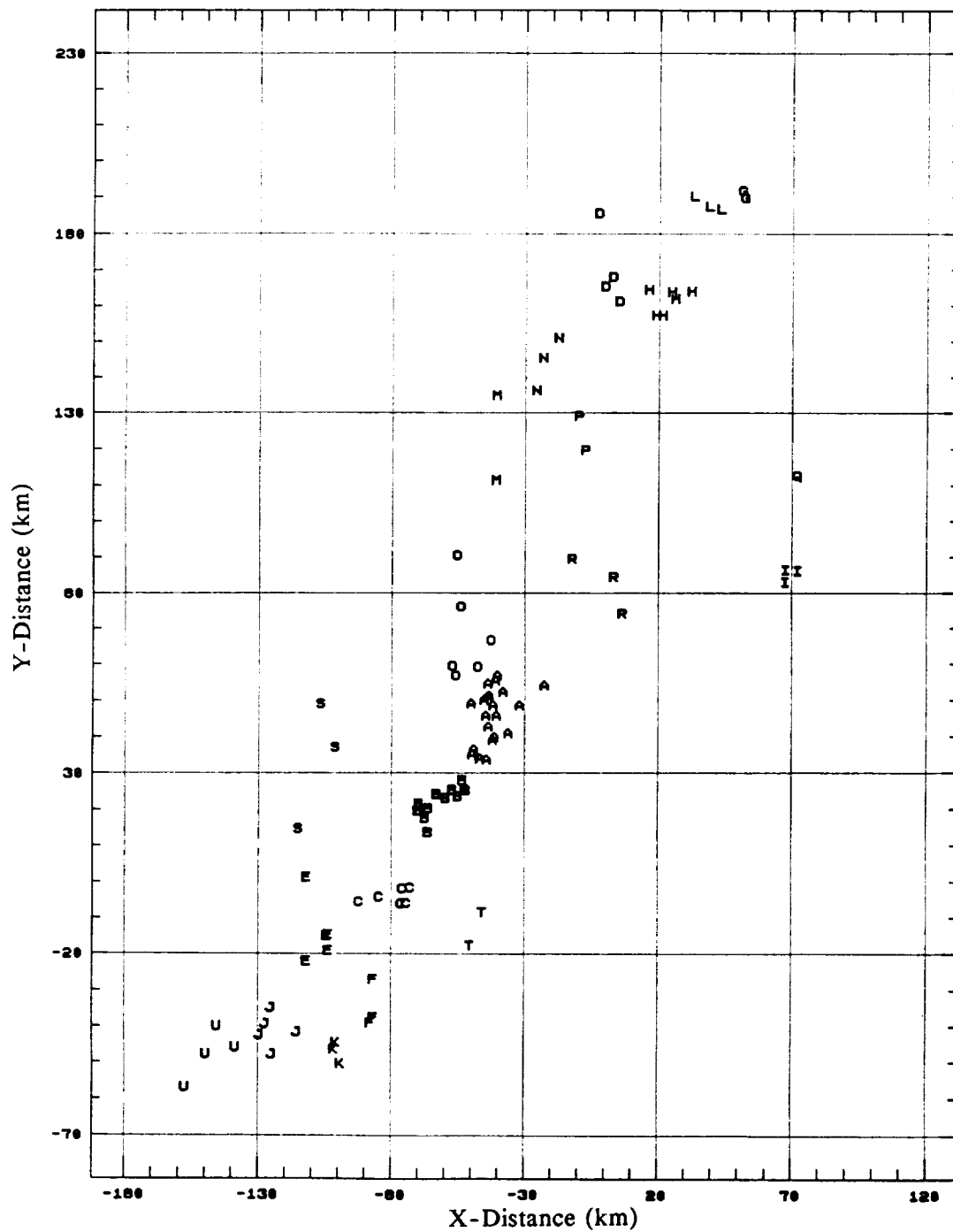


Figure 45. Cluster assignments during the period 2135-2140 UTC. A seed threshold of  $0.01 \text{ discharges km}^{-2}$  produces 21 clusters (A-T).  $\text{I}$  = tornadic storm discharges.

diameter), changing echo shapes, and mergers sometimes cause the radar echo trackers to lose (fail to identify) a storm from one 5-min scan period to the next. The continued occurrence of lightning could thus be used to alert the echo tracker to adjust threshold.

A comparison of the different lightning clusters produced from radar echo seeds follows. The NEXRAD storm identification and tracking algorithm (Bjerkaas and Forsyth, 1980) is implemented with S-band radar data collected on 13 July 1986 at 2328 UTC by the CP2 radar. The tracking algorithm yields two echo centroids, labeled A and B, for this multi-cellular complex of storms (Figure 46). A smaller length threshold (5 km) and intensity threshold (30 dBZ) could produce more than two distinct storms. A peak reflectivity tracker (e.g., Crane, 1979; Rosenfeld, 1987) would produce at least four echo centroids, indicated by the shaded area representing reflectivity values in excess of 55 dBZ. The 3-dimensional structure of these storms is portrayed in Figure 47. The lightning seeding algorithm (with its 10 km grid) would produce only a single seed located between the points (36,115) and (46,125) depending on the placement of the grid. In this isolated storm example, a joining-type clustering algorithm could be used instead to assign the 28 lightning flashes to possibly four distinct lightning clusters. The lightning locations in Figures 48 and 49 suggest four storm clusters offset ahead of the peak reflectivity maxima. The offset is partially physical in that the lightning strikes generally occur outside of the storm reflectivity core, but there also appears to be a directional bias to the southeast of the echo centroids, likely due to unrecovered systematic errors at one or more of the antennas. This initial examination of the performance and limitations of lightning clustering algorithms demonstrates their usefulness in identifying and tracking thunderstorms. In addition, it appears that more than one method and stopping criteria is best suited to the various space and time scales examined here.

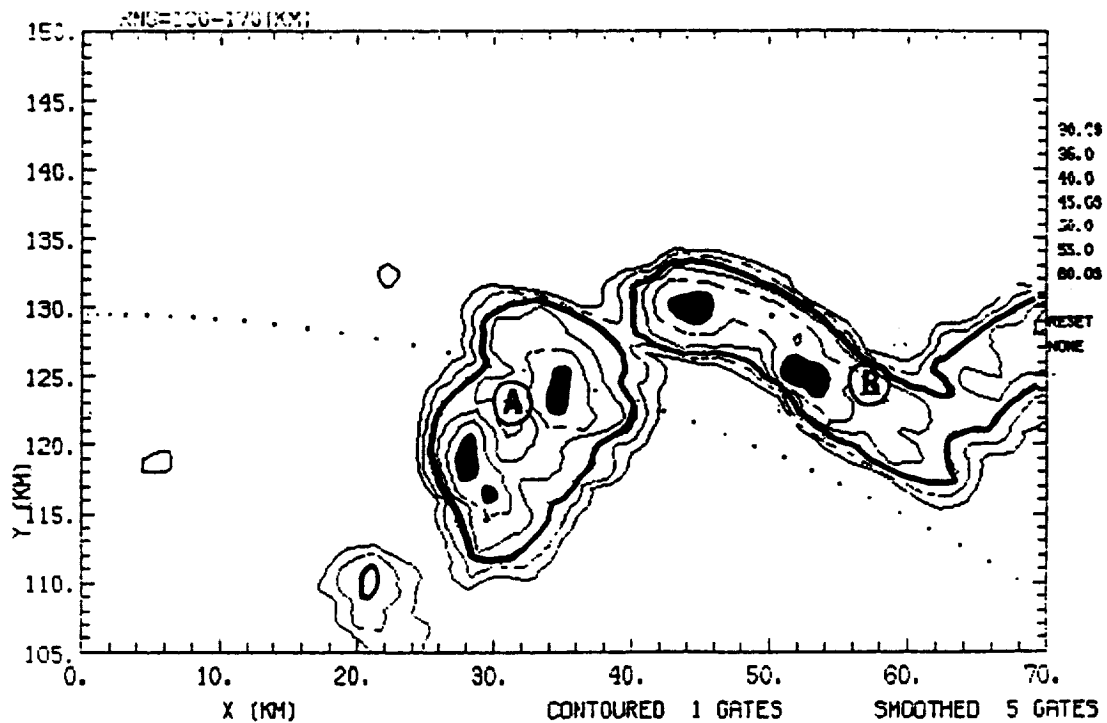


Figure 46. Plan-view of a small multicellular storm complex observed by the CP2 radar on 13 July 1986 at 2328 UTC. Circled upper case letters (A,B) = two storm centroids identified by the NEXRAD storm identification and tracking algorithm; solid contour = reflectivity > 40 dBZ; shaded region = reflectivity > 55 dBZ. Distance units in kilometers from CP2.

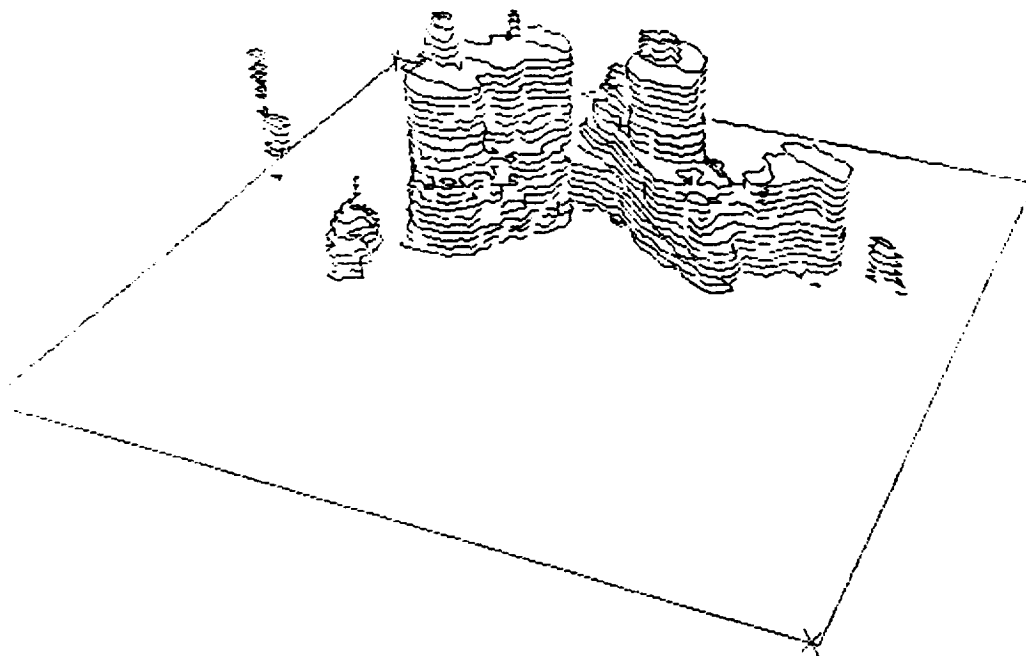


Figure 47. Three-dimensional structure of the storm complex in Figure 46.

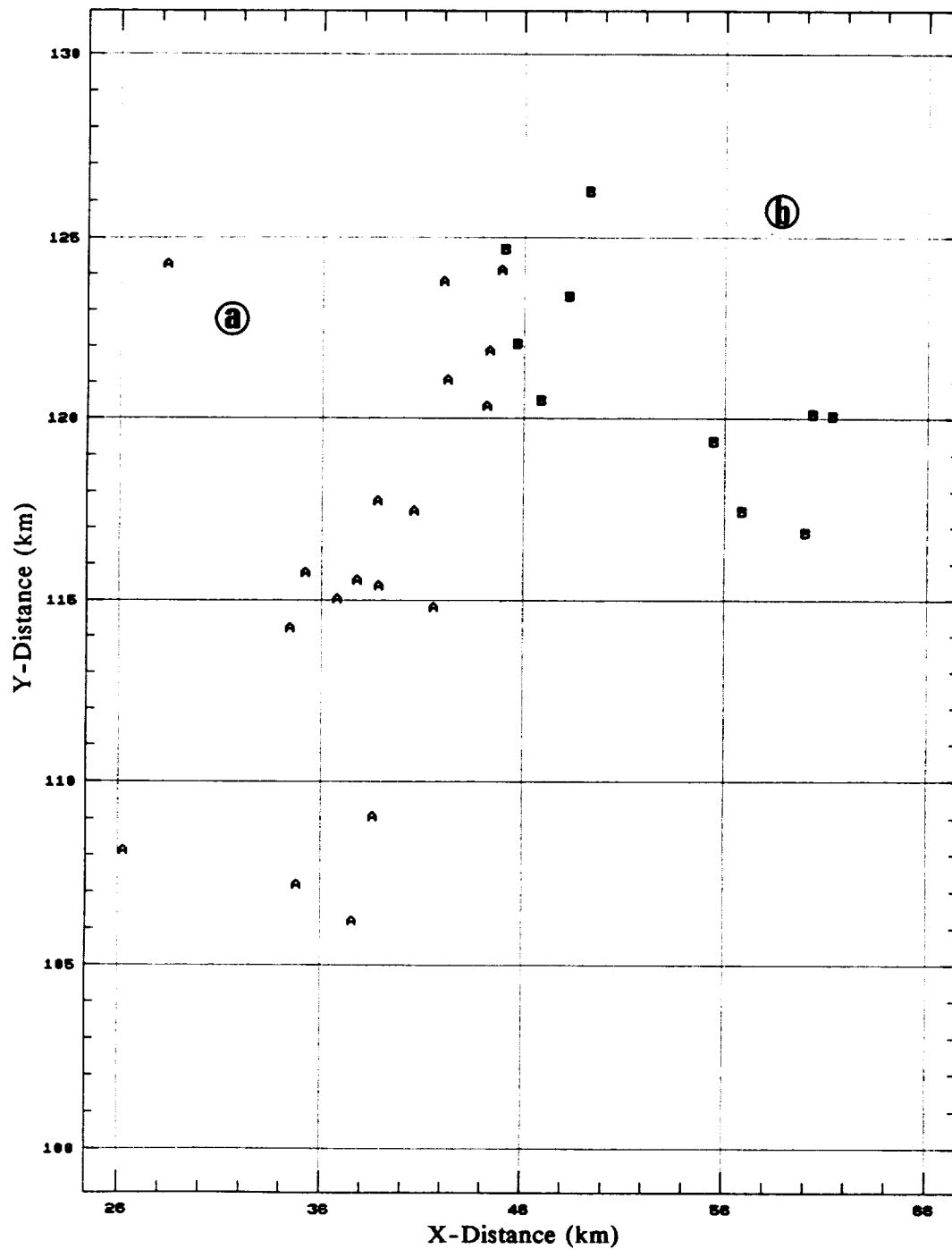


Figure 48. Cluster assignments using two centroids identified by NEXRAD algorithm. Circled lower case letters (a,b) = radar echo cluster seeds; Upper case letters (A,B) = cluster assignments.

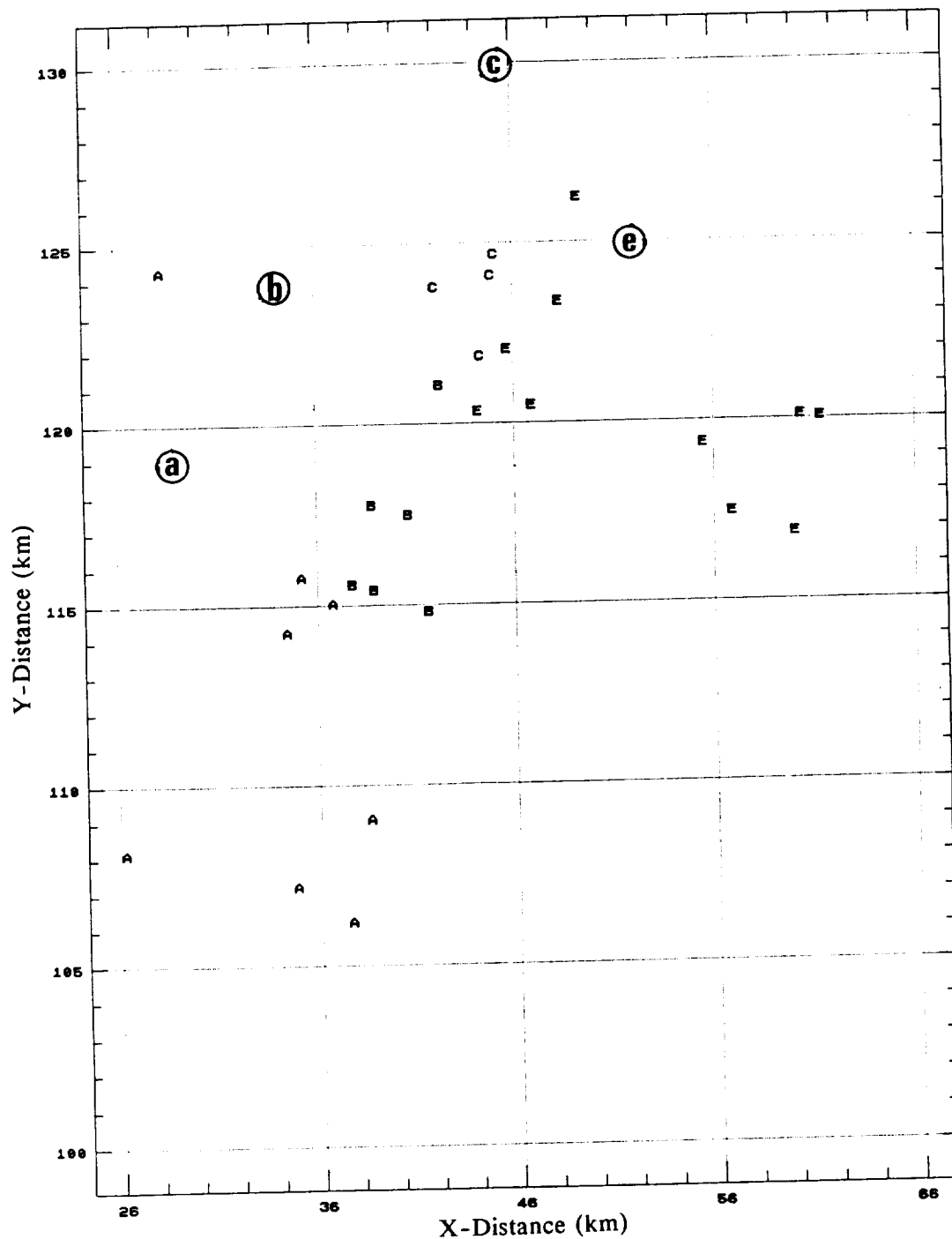


Figure 49. Cluster assignments using four centroids identified from peak reflectivity ( $Z > 55$  dBZ) maxima. Circled lower case letters (a,b,c,e) = radar echo cluster seeds; Upper case letters (A,B,C,E) = cluster assignments.

## CHAPTER V.

### THUNDERSTORM LIFE-CYCLES AND EXTRAPOLATION FORECASTING

#### Testing and Evaluation of the Logistic Growth Model

The storm identification and tracking process using clustering methods sets the stage for assessing the validity of the logistic growth model and predictability of lightning activity during the storm life-cycle. Table 8 gives the model parameters for a selected number of cases. A total of 14 storm systems have been examined ranging in size from small, short-lived air mass storms (< 1 h duration) to large, long-lived mesoscale convective systems. The total (intracloud and cloud-to-ground) lightning life-cycle has been computed for 3 of the short-lived storms. These latter cases are included to demonstrate the applicability of the logistic model to storms for which the total lightning rates portray the growth and decay process, yet the storm may produce too few discrete cloud-to-ground flashes to establish a trend (e.g., the 20 July case). The cloud-to-ground lightning data were summed over 1, 5, 10, 30 and 60 min sampling intervals depending on the availability of data or the duration of the storm life-cycle. The SAS (1985) non-linear regression procedure NLIN using the Gauss-Newton method was used to estimate the parameters  $\beta$  and  $k$  from each set of observations and limiting values of  $\alpha$  corresponding to the total number of lightning flashes produced by each storm event.

#### Isolated and Multicellular Storms

Figure 50 shows the evolution of the cloud-to-ground lightning activity associated with 3 distinct storms observed in Southern Tennessee on 17 July 1986. The storms were identified from the cluster analysis during the interval 1605-1845 UTC

Table 8. Parameters of the Logistic Growth Model

Case	Geographic Location	$\alpha$	$\beta$	k	Observation Periods	$\Delta t$ (min)	Duration of Lightning Activity (min)
17 July 1986 (A)	TN	102	54.9	0.89	8	10	80
17 July 1986 (C)	TN	453	33.0	0.76	11	10	110
3 June 1986	AL/TN	3089	136.1	0.32	40	10	400
25 June 1986	TN	1626	128.7	0.41	21	10	210
13 July 1986	AL/TN	6094	419.9	0.23	37	10	370
14 July 1986 (1)	TN	72	106.7	0.87	10	5	50
14 July 1986 (2)	TN	61	41.5	0.94	9	5	45
15 November 1989	AL/TN	9442	52.4	0.15	53	10	530
20 July 1986*	AL	91	156.6	0.86	13	1	13
8 August 1977*	FL	12.5	36.4	0.52	15	5	75
11 July 1978*	FL	155	24.7	0.94	8	5	40
9 June 1985	OK/KS	122	121.3	0.77	12	10	120
3 June 1985	OK/KS	6070	24.2	0.40	18	30	540
MCC Composite	OK/KS	1.0	32.7	0.42	18	60	1080
* Total Lightning Activity							

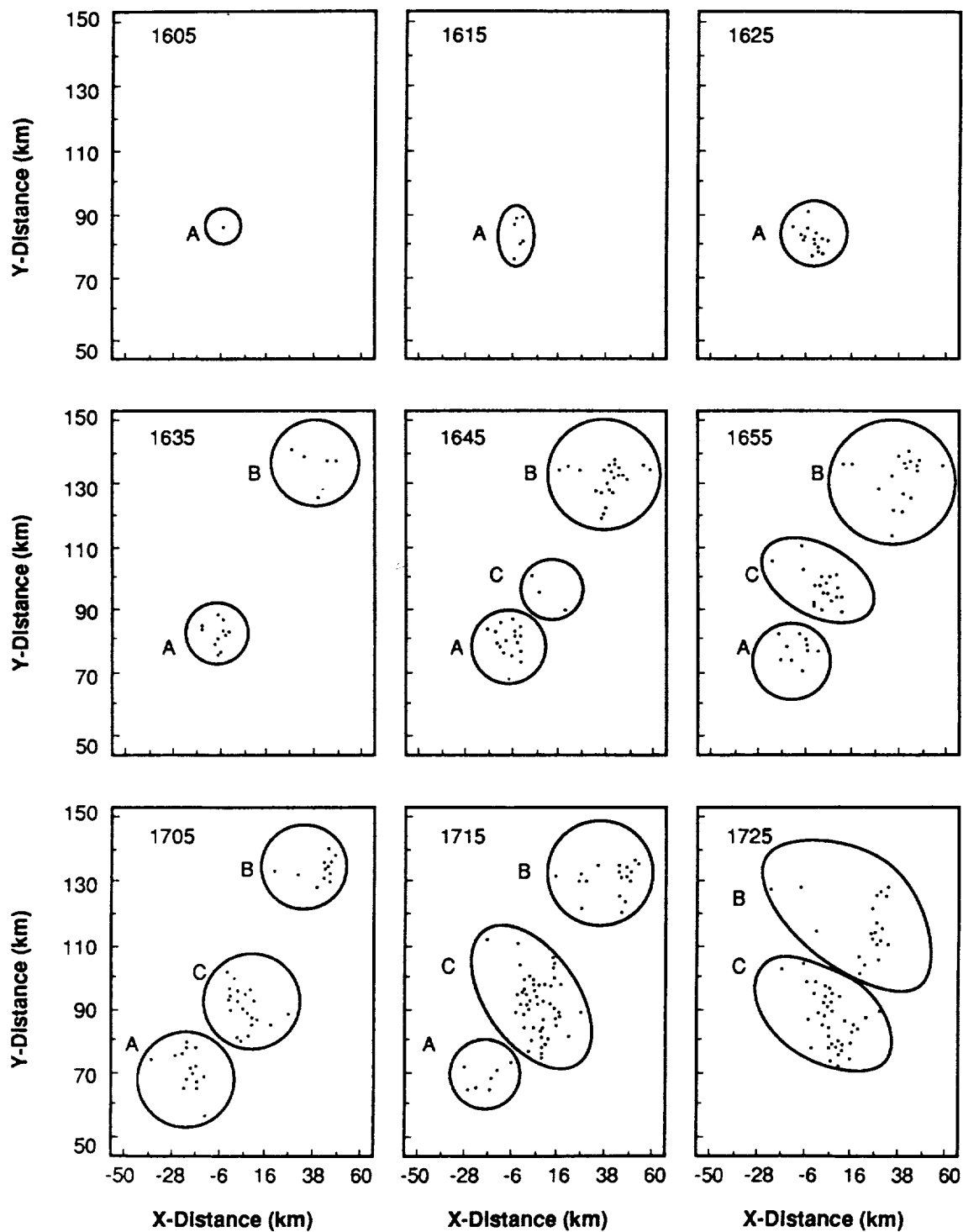


Figure 50. Cloud-to-ground lightning clusters during 5-min intervals on 17 July 1986. Distance units in kilometers from FL2 radar. (Time in UTC.)

(1105-1345 CDT). The maps were produced every 10 min from 1605-1735 UTC, a period which encompasses the entire 90 min life-cycle of cell A. The corresponding radar echo time history is summarized in Figure 51 from 30 min observations made with the Nashville, TN radar. The center coordinate of each radar map is approximately 6 km east and 9 km north of the FL2 radar (used as the center of the lightning maps).

The lightning and rainflux time series for storms A and C are shown in Figure 52. Cell A undergoes a secondary surge in lightning activity after an initial peak. The rainflux time history also shows two peaks, each lagging the lightning maxima by 10 min. Cell C shows a single maxima in both lightning activity and rainflux.

The logistic model regression (P), observed flash rate (A), and residual error (A-P), for storms A and C are plotted in Figures 53 and 54. The model fit is excellent in both cases with correlation coefficient  $r > 0.998$ . Cell A produced 102 ground discharges (the observed  $\alpha$ ) and Cell C produced 453 ground discharges during its 120 min life-cycle. The steepness of the curves along the time axis are described by the parameter  $k$ . For storm lifetimes of 1-2 h (sampled at 10 min intervals), the median value of  $k$  (Table 8) is approximately 0.8.

#### Total Lightning Activity for Airmass Storms

The value of  $k$  increases to 0.9 for storms with lifetimes less than about 1 h. Figure 55 shows the logistic model results for the total lightning produced by the 20 July airmass storm described in Chapter 2. Due to the short-lived 13 min duration of the lightning activity a more frequent sampling period of 1 min was chosen. Again, the residual error is only a few percent. The other two storms occurred in Florida in 1977 and 1978 (Figure 56), and have been studied previously by Piepgrass et al. (1982) and Krehbiel (1986). The 11 July 1978 single peak storm is similar to the 20 July storm, but the secondary peak of the 8 August storm is likened more to Storm A on 17 July 1986.

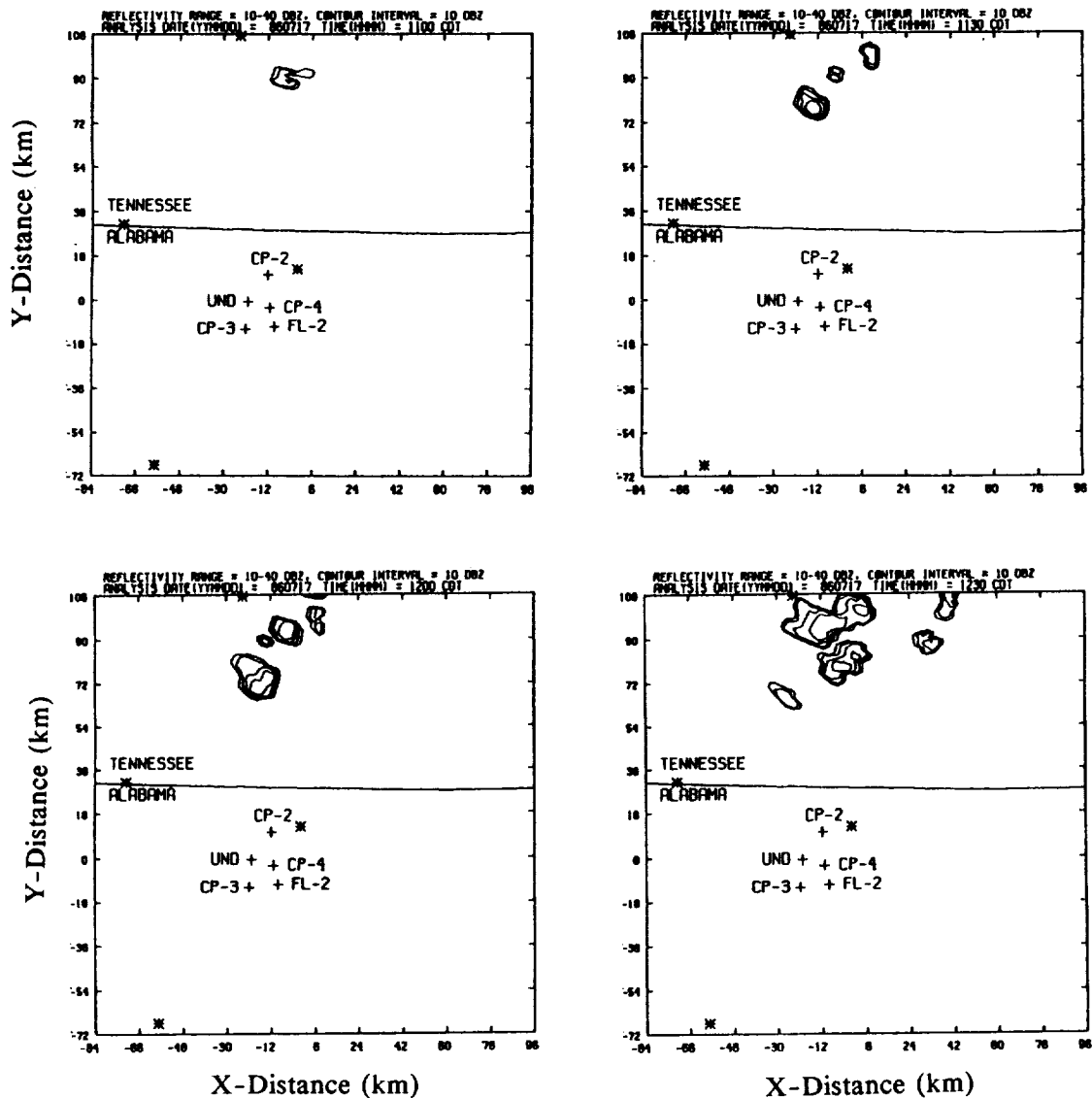


Figure 51. Base scan radar echoes observed by the Nashville radar: upper left, 1600 UTC; upper right, 1630 UTC; lower left, 1700 UTC; lower right, 1730 UTC. Contour interval every 10 dBZ beginning at 10 dBZ.

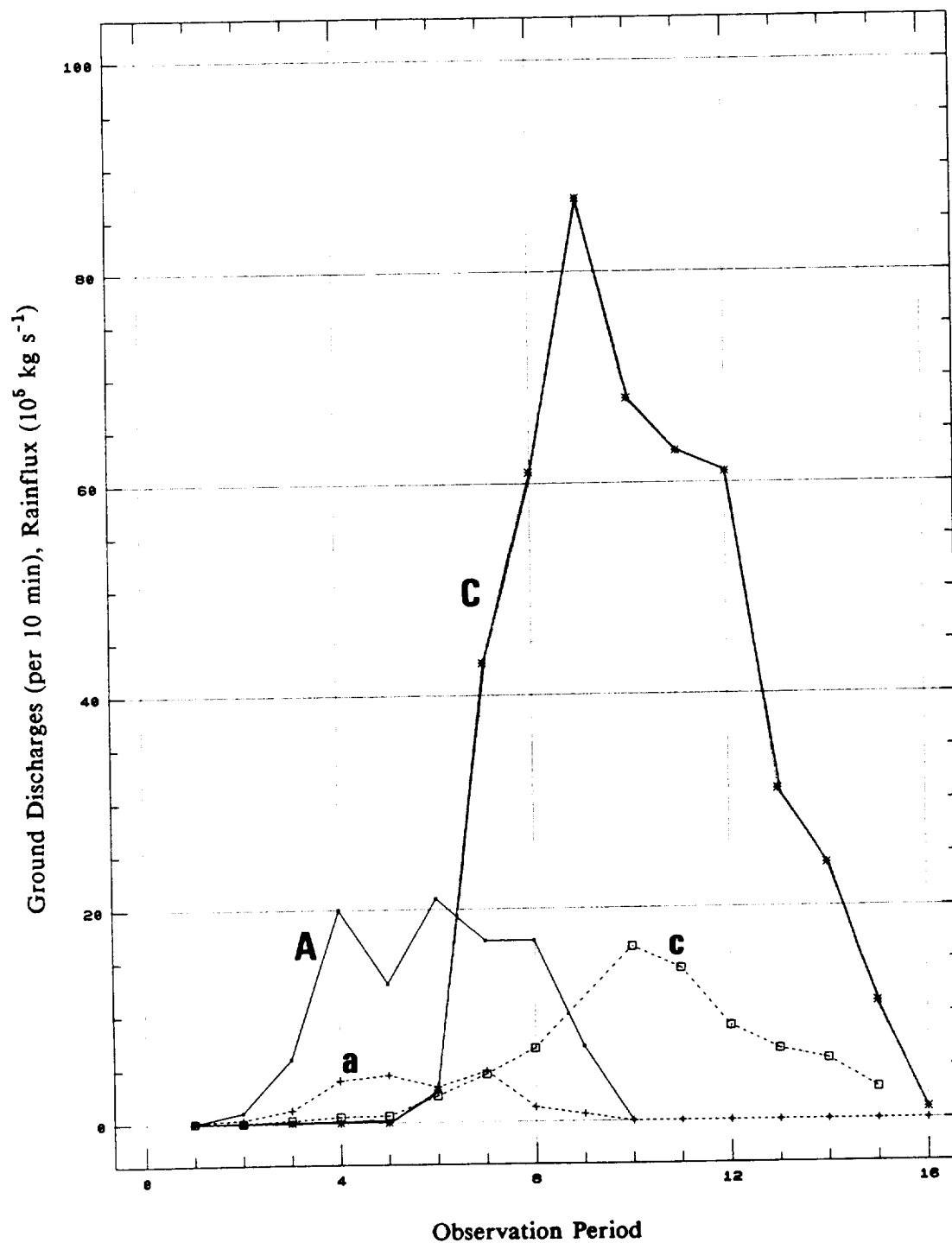


Figure 52. Lightning and rainflux time series for storms A and C: Upper case letters, number of ground discharges in 10 min; lower case letters, radar estimated rainflux.

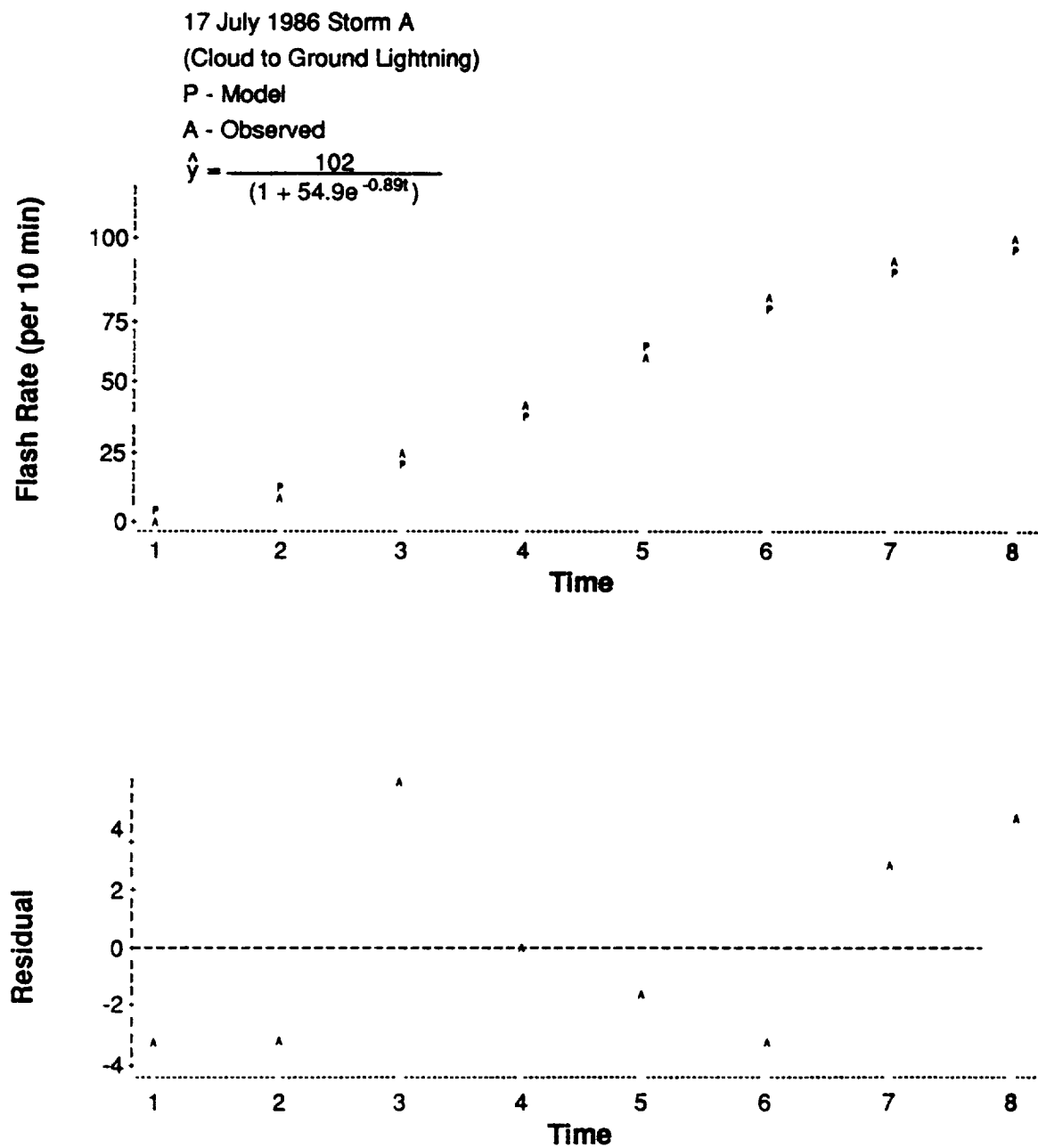


Figure 53. Logistic model regression and residual error for 17 July 1986 Storm A.  
Top: For each 10 min observation period,  $\Delta$  = the observed flash rate;  
 $P$  = model prediction. Bottom: Residual error =  $(A - P)$ .

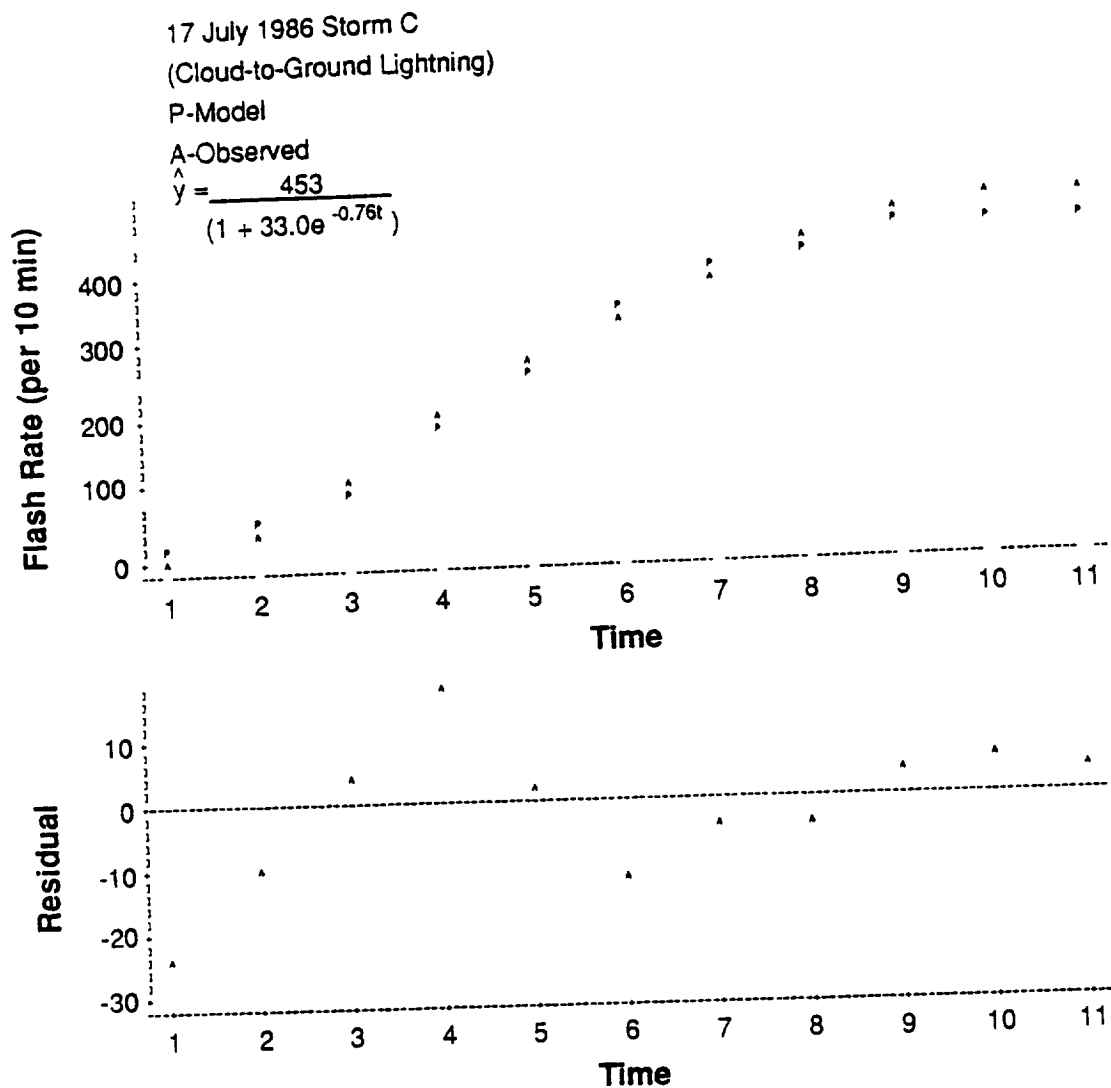


Figure 54. Logistic model regression and residual error for 17 July 1986 Storm C.  
Top: For each 10 min observation period,  $\hat{A}$  = the observed flash rate;  
 $\hat{P}$  = model prediction. Bottom: Residual error = (A - P).

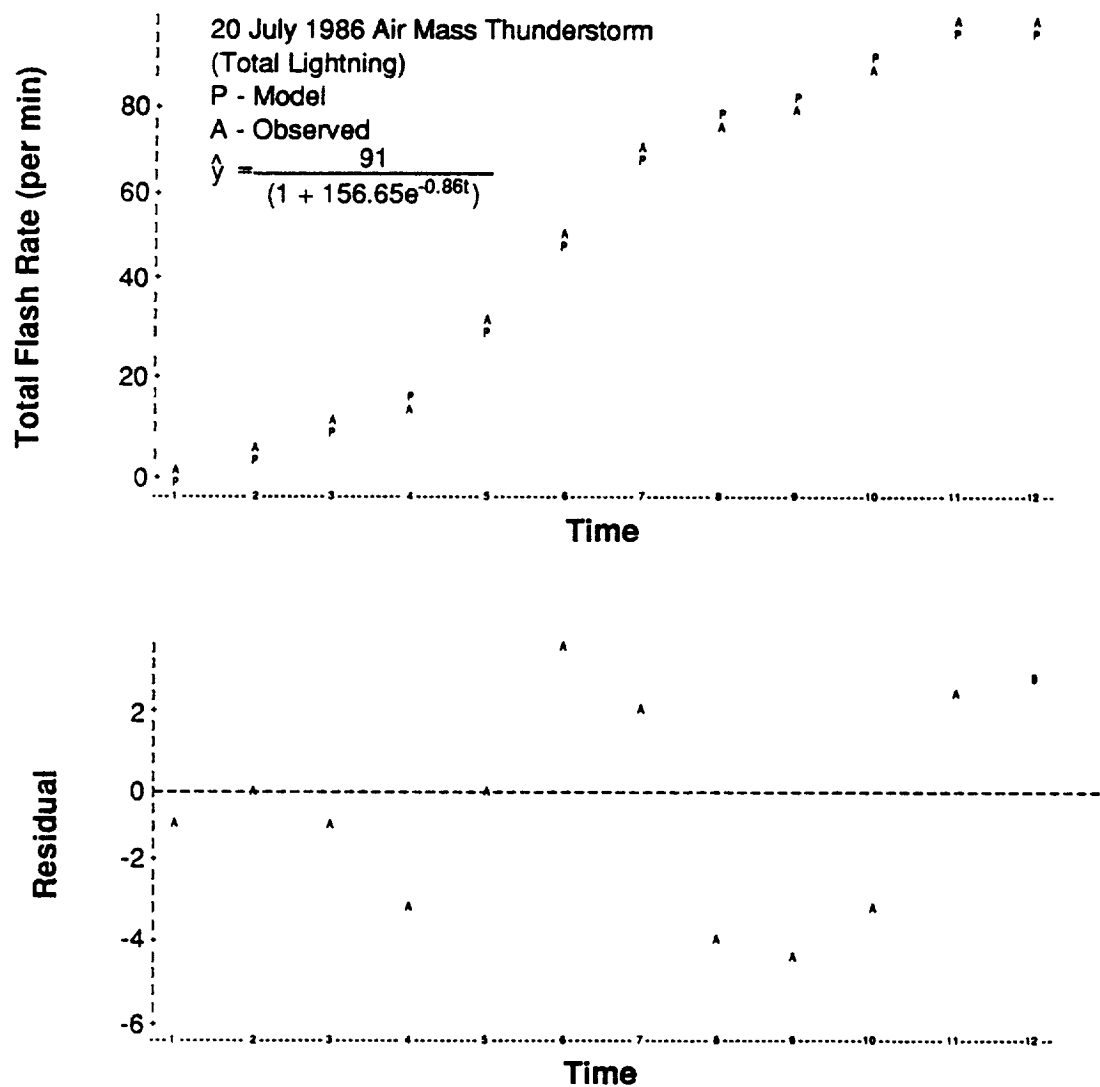


Figure 55. Logistic model regression and residual error for 20 July 1986 airmass storm. Top: For each 10 min observation period, A = the observed flash rate; P = model prediction. Bottom: Residual error = (A - P).

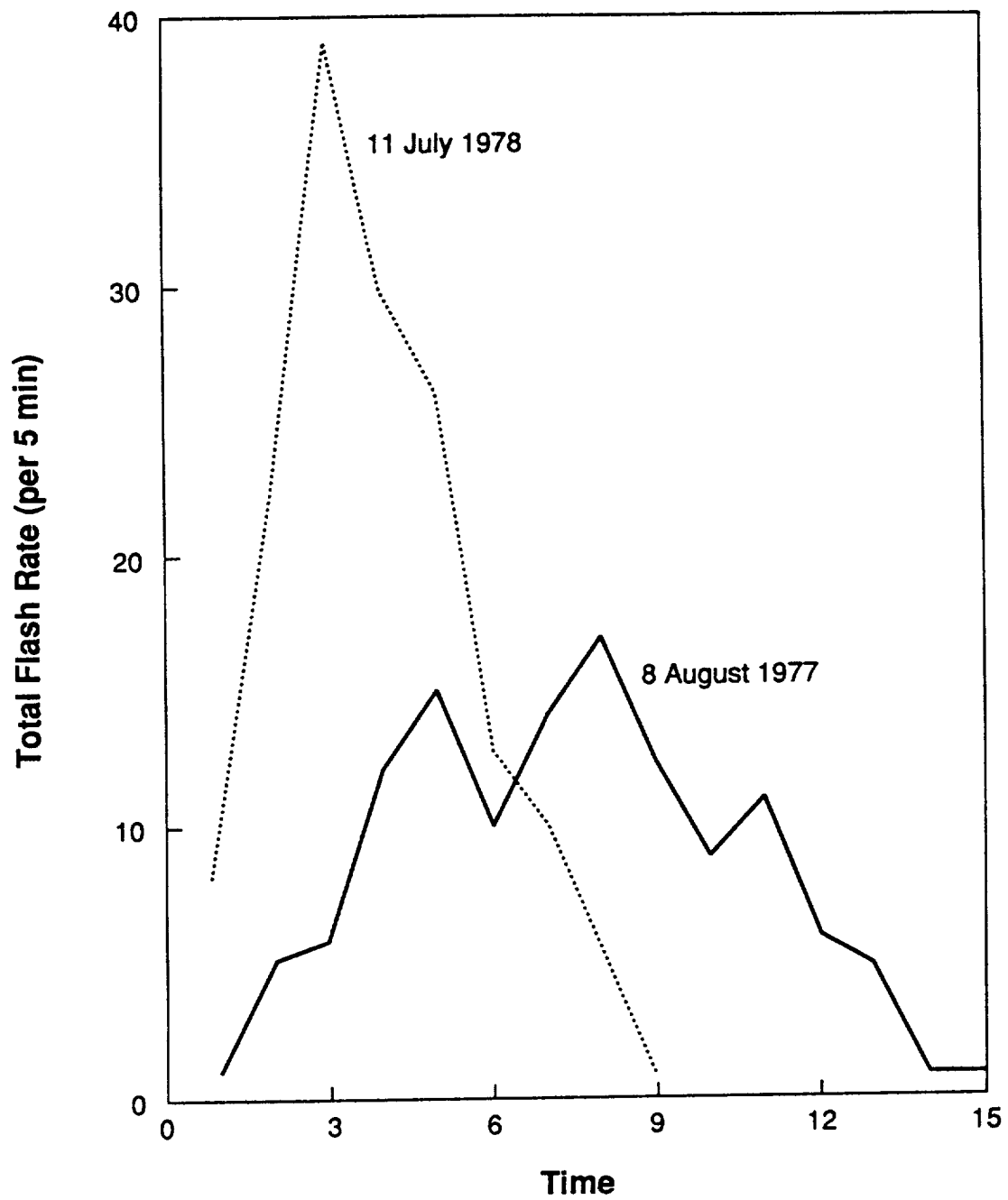


Figure 56. Total lightning time series (discharges per 5 min) for two thunderstorms observed near Cape Canaveral, Florida.

In the latter case the total system life-cycle is nearly symmetric within the envelope encompassing the storm, but the large individual peaks indicate 2 or 3 embedded cells or resurgent growth and decay. Few ground discharges were observed in all three cases.

### Long-lived Storm Complexes

Figure 57 depicts the life-cycle of the 15 November 1989 mesoscale weather system through much of its life-cycle. The time series covers the period 1600 UTC 15 November to 0100 UTC 16 November in 10 min increments. Despite the multiple peaks superimposed upon the curve (due primarily to cell mergers), the envelope of the lightning activity exhibits symmetry about the maxima of 360 flashes which occurs at time period 27 (2030-2040 UTC). There are 19 time steps between 100 flashes and the maximum during the growth phase and 17 time steps from the maximum to 100 flashes during the decay phase. This 2 time step difference is just 20 min over a 6 h period.

The logistic growth curve in Figure 58 again fits the data well, thus reinforcing the concept of symmetric growth and decay at yet larger space and time scales. The long-lived ( $>2$  h) storm systems have  $k$  values less than about 0.4, with  $k$  inversely proportional to storm lifetime (Table 8). Using the symmetry that characterizes logistic growth, we can estimate that the duration of the decay phase will approximately equal the duration of the growth phase. This estimate also defines the valid extrapolation period for yes/no (presence/absence of lightning activity) forecasts. Forecasts of the duration of these large storms are valuable because their long lifetimes and severe weather production makes them the most disruptive and hazardous weather systems during the Spring and Summer.

Figure 59 shows ten individual lightning ground strike time histories and a composite life-cycle for convective storm complexes observed in the Oklahoma/Kansas region of the Southern Great Plains with the NSSL ground strike network (Goodman and

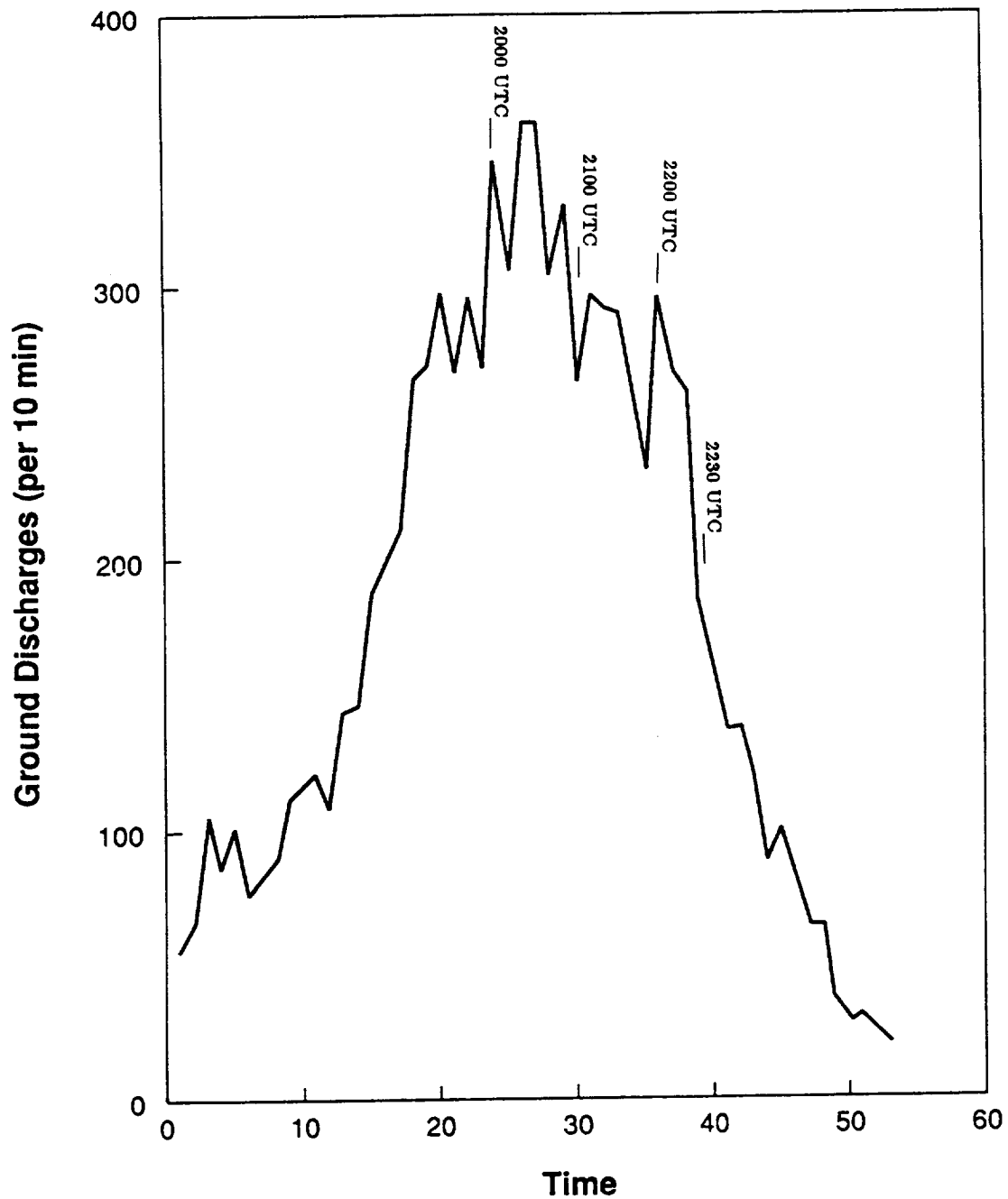


Figure 57. Cloud-to-ground lightning time series (discharges per 10 min) during the period 1600 UTC 15 November to 0100 UTC 16 November 1989 for a mesoscale convective system observed in the Tennessee Valley.

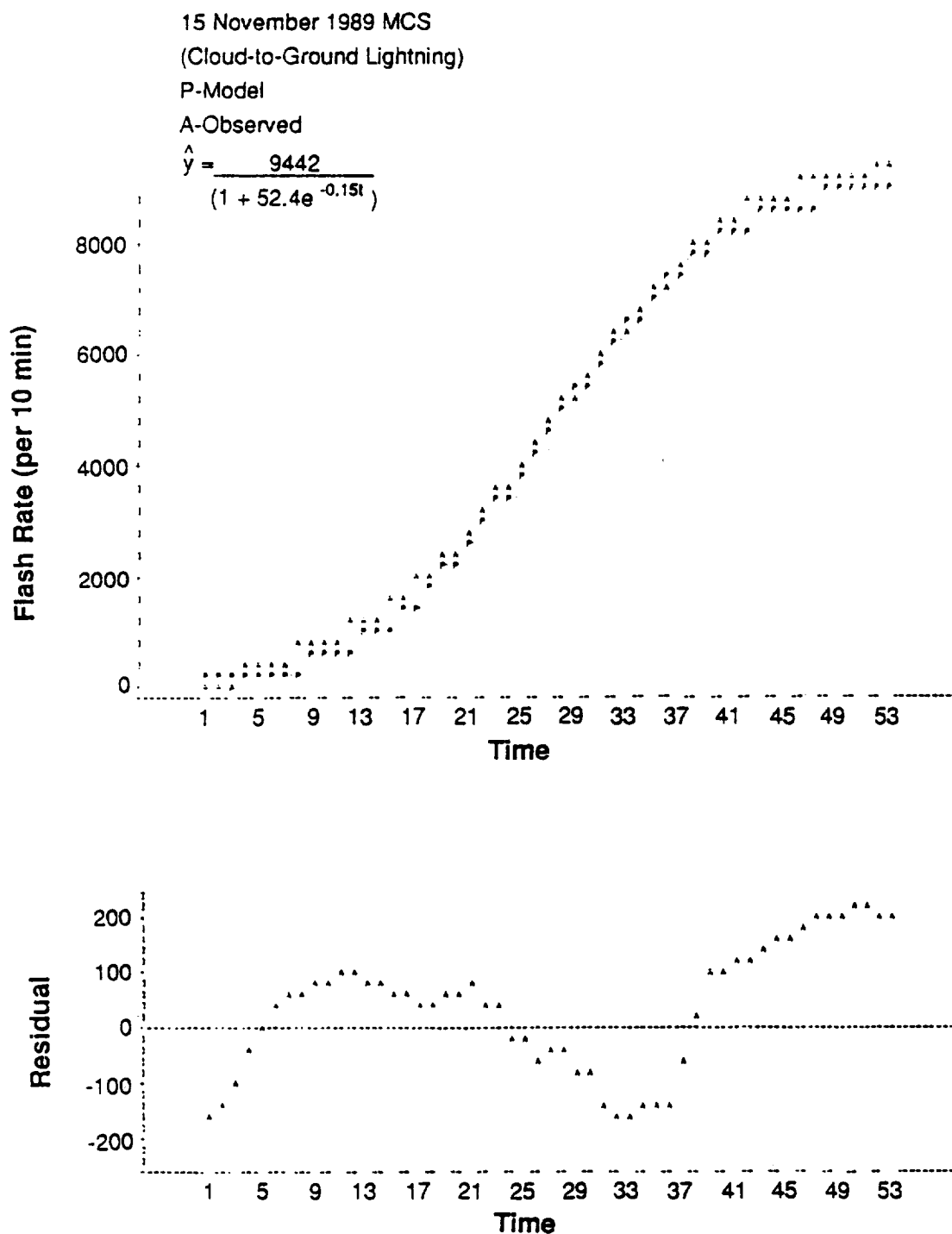


Figure 58. Logistic model regression and residual error for 15 November 1989 mesoscale weather system. **Top:** For each 10 min observation period, A = the observed flash rate; P = model prediction. **Bottom:** Residual error = (A - P).

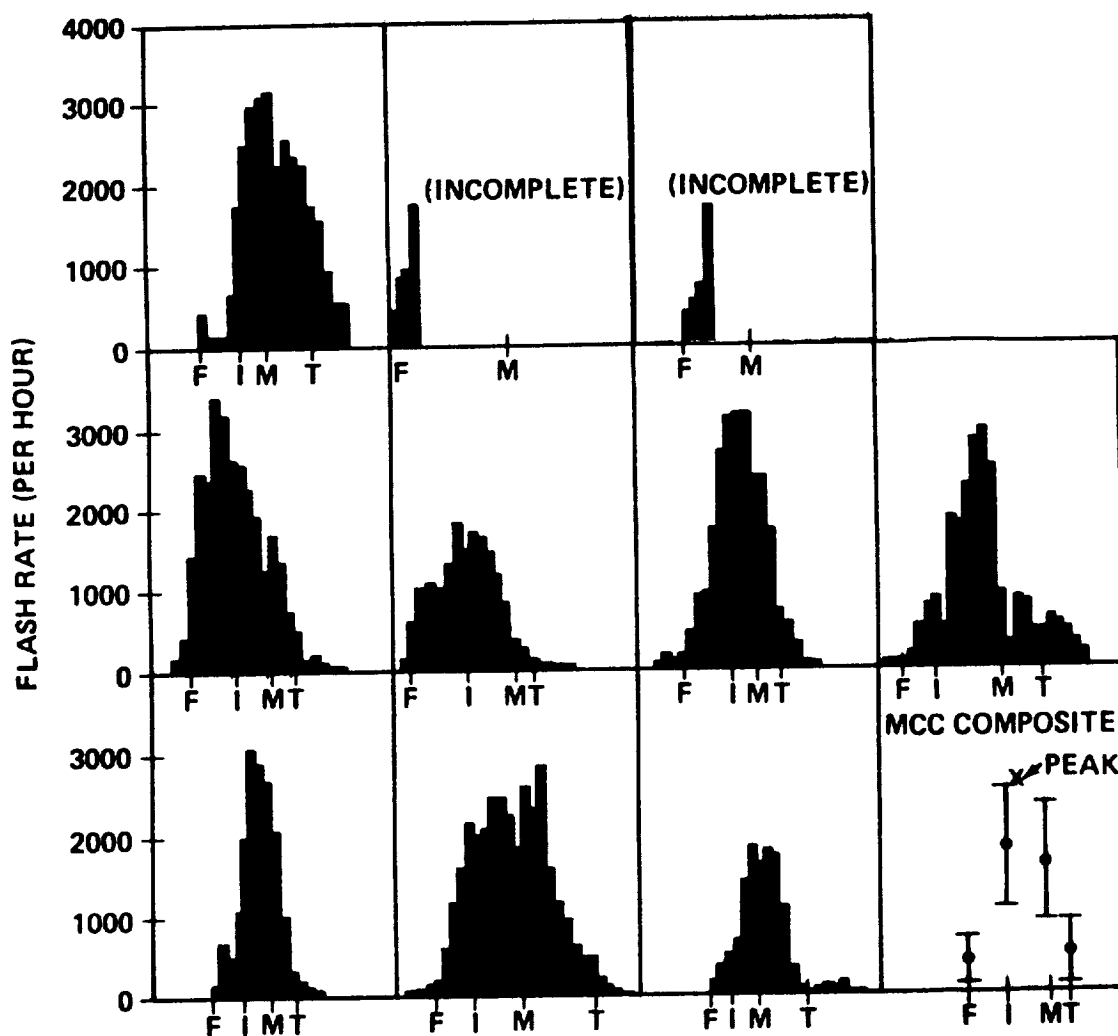


Figure 59. Cloud-to-ground lightning discharge histograms and composite lighting life-cycle for mesoscale convective complexes (MCCs). The four life-cycle phases are identified as first storms (F), initiation (I), cold cloud shield maximum extent (M), and termination (T). The composite is plotted with respect to the time and magnitude ( $\pm$  one standard deviation) of the average peak flash rate. (After Goodman and MacGorman, 1986).

MacGorman, 1986). The life-cycle is identified from the infrared cloud temperature criteria developed by Maddox (1980). The dimension of the cold cloud top observed by satellite is used to define four phases of the storm system life-cycle. These phases identify the formation of the first storms (F), the initial time at which the size criteria threshold is reached (I), maximum extent of the cloud shield (M), and the final time at which the size threshold is exceeded (T).

In Figure 60 the composite life-cycle has been normalized to the maximum hourly flash rate and to the time at which it occurred. The flash rates increase and decrease exponentially with time. The exponential relations best fitting the data are also shown where  $N$  is the fraction of discharges in a given hour occurring at a time,  $t$ , relative to the magnitude and occurrence of the peak. The logistic model fit to the composite is given in Figure 61.

### Interpretation of Results

In general, the longer a convective storm takes to reach its maximum intensity, the longer it takes to decay. A storm cell that grows rapidly often decays rapidly. The logistic model provides a good fit to the observed data. In each case the model residual error is only a few percent for individual time series of cloud-to-ground lightning and total lightning activity. The rate constant  $k$  is greatest for the shorter-lived storms (refer to Table 8). The limiting value,  $\alpha$ , is a function of storm duration and the environmental factors that serve to sustain strong convection (e.g., atmospheric instability, a moisture source, and a triggering mechanism such as an upper level jet streak, front, storm merger, or outflow boundary). The limiting value  $\alpha$  and residual error will now be considered in greater detail.

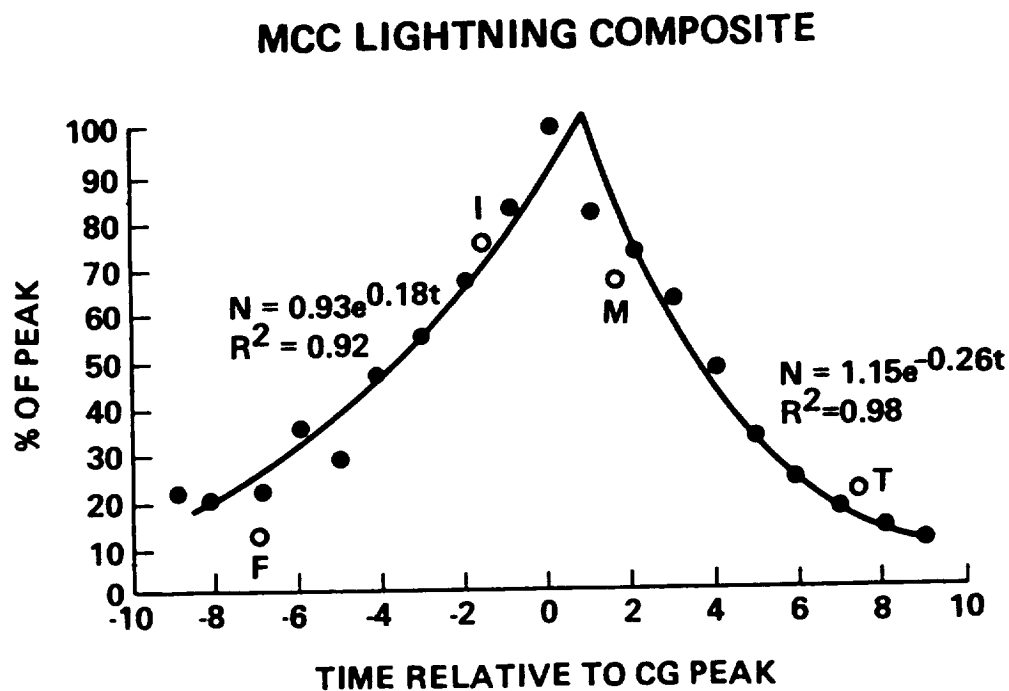


Figure 60. Average hourly cloud-to-ground discharge rates are normalized to the average peak flash rate of MCCs and are shown relative to the time of occurrence of the peak.  $N$  is the percentage of the peak rate at a given hour and  $R^2$  is the correlation coefficient for each of the exponential curves. Open circles, denote the time and magnitude of the lightning rates for each of the MCC life-cycle phases F, I, M, T (After Goodman and MacGorman, 1986).

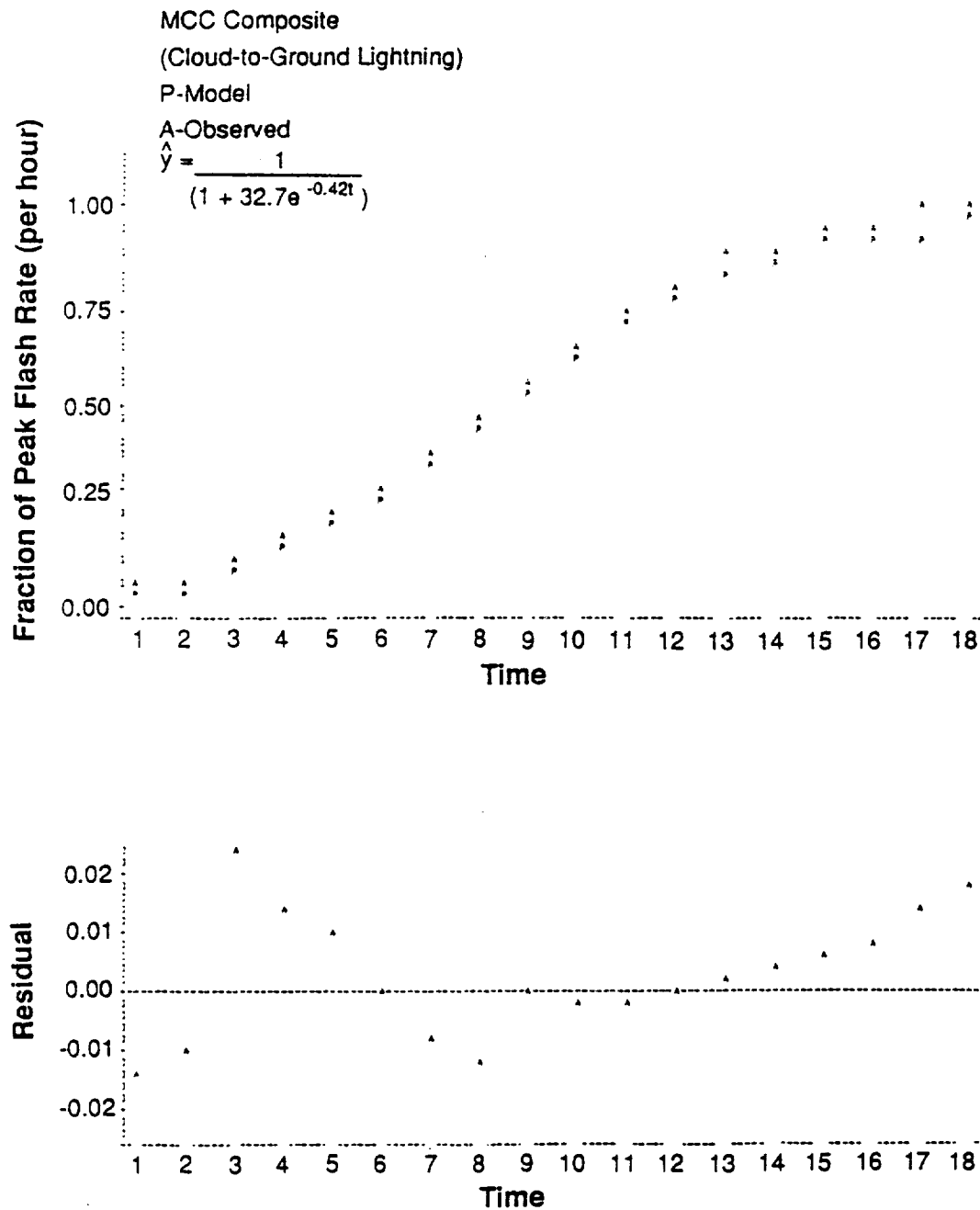


Figure 61. Logistic model regression and residual error for MCC composite life-cycle. Top: For each hourly observation period, A = the observed flash rate; P = model prediction. Bottom: Residual error = (A - P).

## Role of the Environment in Limiting $\alpha$

One frequently used index to describe the instability of the storm environment is the lifted index. The lifted index ( $^{\circ}\text{C}$ ) is found by lifting a positively buoyant saturated parcel of air, having the thermodynamic characteristics of the lowest 100 mb layer of the atmosphere, from its level of free convection (where the buoyancy is first positive) to 500 mb. The temperature excess of the parcel,  $T_p$ , to that of the environment,  $T$ , at 500 mb is the lifted index in  $^{\circ}\text{C}$ . Figure 62 shows the relationship between maximum hourly flash rate during June 1986 within the 8 state area shown in Figure 29 and the 1200 UTC lifted index computed from soundings made at Redstone Arsenal, AL. Total flash rates are seen to increase non-linearly with decreasing atmospheric stability.

A related parameter that describes the environment and offers additional physical insight is the convective available potential energy (CAPE). CAPE is proportional to the square of the maximum parcel updraft speed,  $w^2$ , and thus represents the increase in kinetic energy of a parcel associated with its vertical acceleration (Weisman and Klemp, 1982). CAPE is also commonly referred to as the available buoyant energy, i.e., the kinetic energy due to buoyancy. Figures 63 and 64 show, respectively, the relationship between 1) total cloud-to-ground lightning and CAPE; and 2) maximum rain rate and maximum parcel energy (CAPE as defined by Zawadzki et al., 1981). Both cloud-to-ground lightning ( $r=0.62$ ) and rainfall ( $r=0.79$ ) are positively correlated with the buoyant energy in the environment. It should be noted that the predicted value of  $w$  ignores the effects of precipitation (or mass) loading, vertical pressure gradient perturbations, and mixing which would lower  $w$  estimates by as much as 50%. Yet, it is suspected that the total lightning rates would produce an even greater correlation. Such measurements will not be possible for large storm systems until total lightning observations are available from space in the late 1990s with NASA's lightning mapping sensors (see Chapter 7).

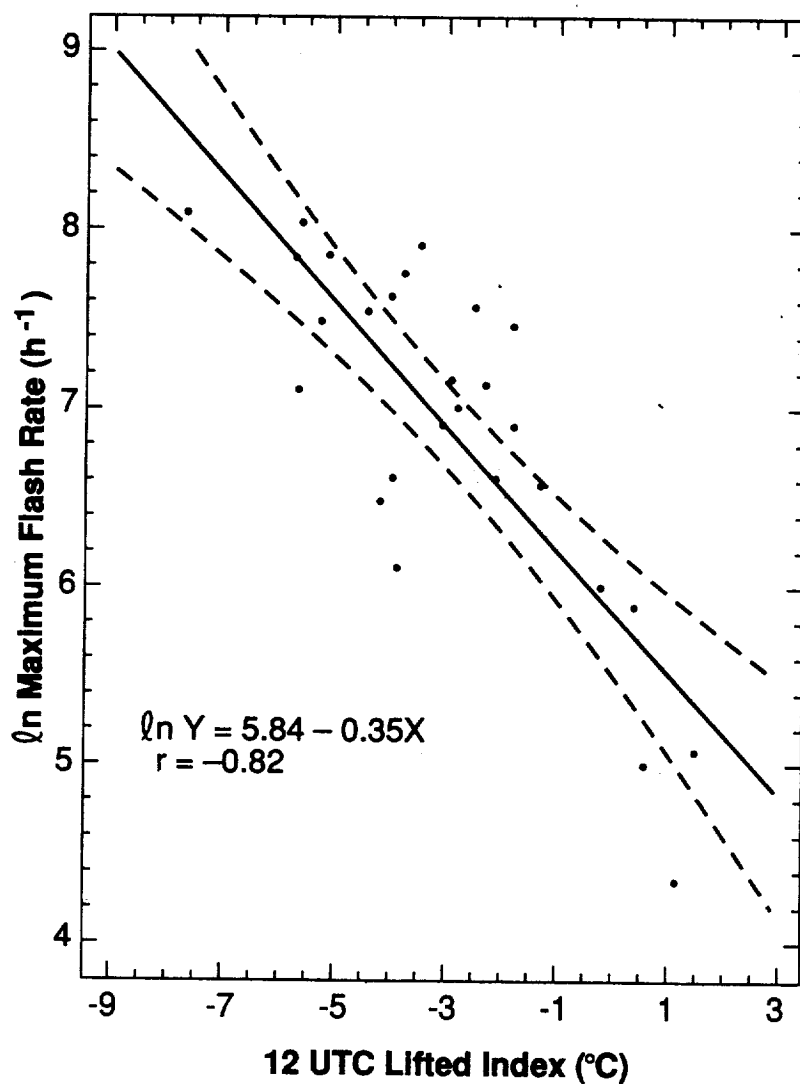


Figure 62. Regression plot of maximum hourly flash rate (Y) as a function of the lifted index (X) computed from the Redstone Arsenal 1200 UTC soundings taken during June 1986. The 95 percent confidence limits are indicated by the dotted lines.

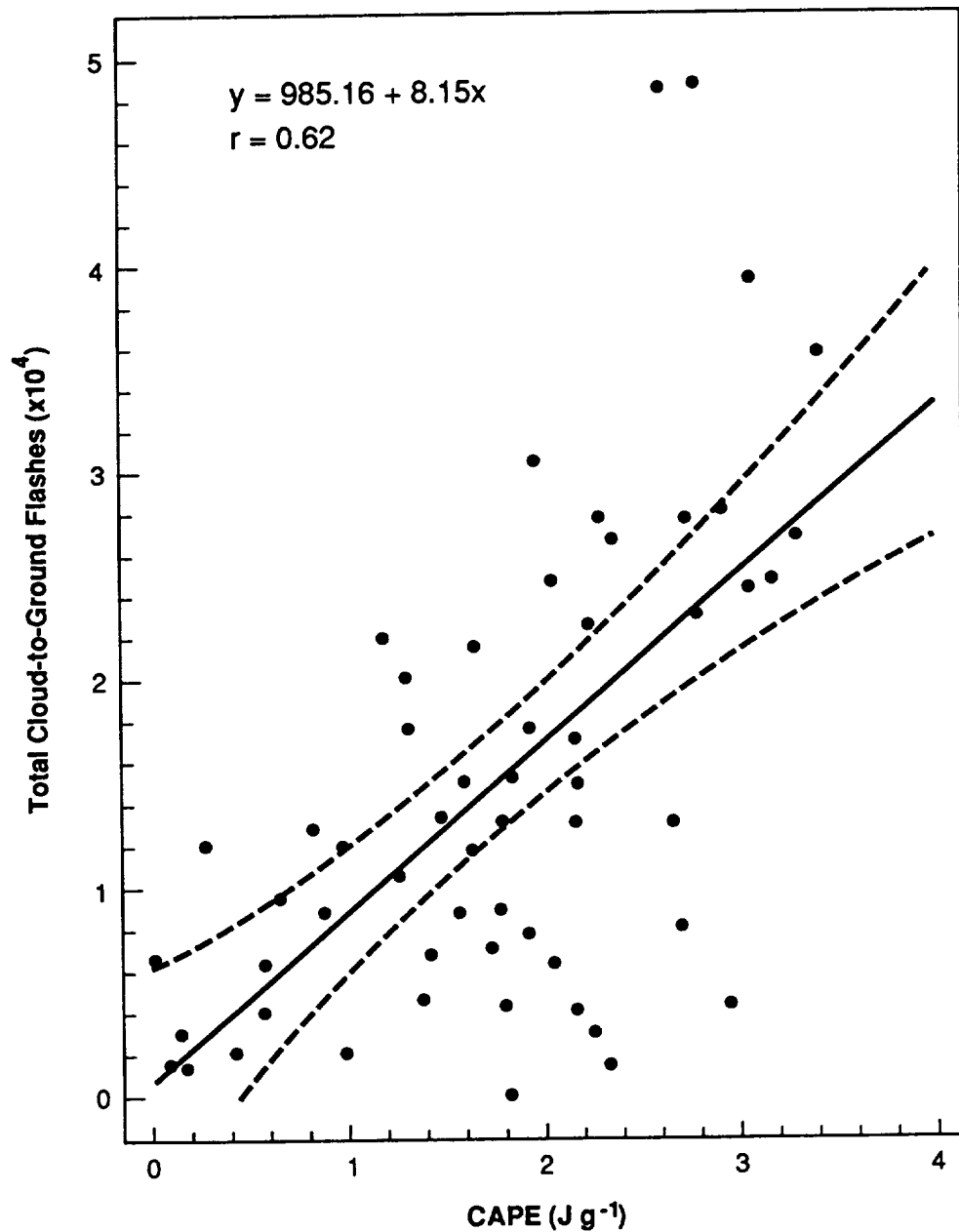


Figure 63. Regression plot of total cloud-to-ground flashes observed each day (y) as a function of Convective Available Potential Energy (CAPE) (x) computed from the Redstone Arsenal 1200 UTC soundings taken during June and July 1986. The 95 percent confidence limits are indicated by the dotted lines.

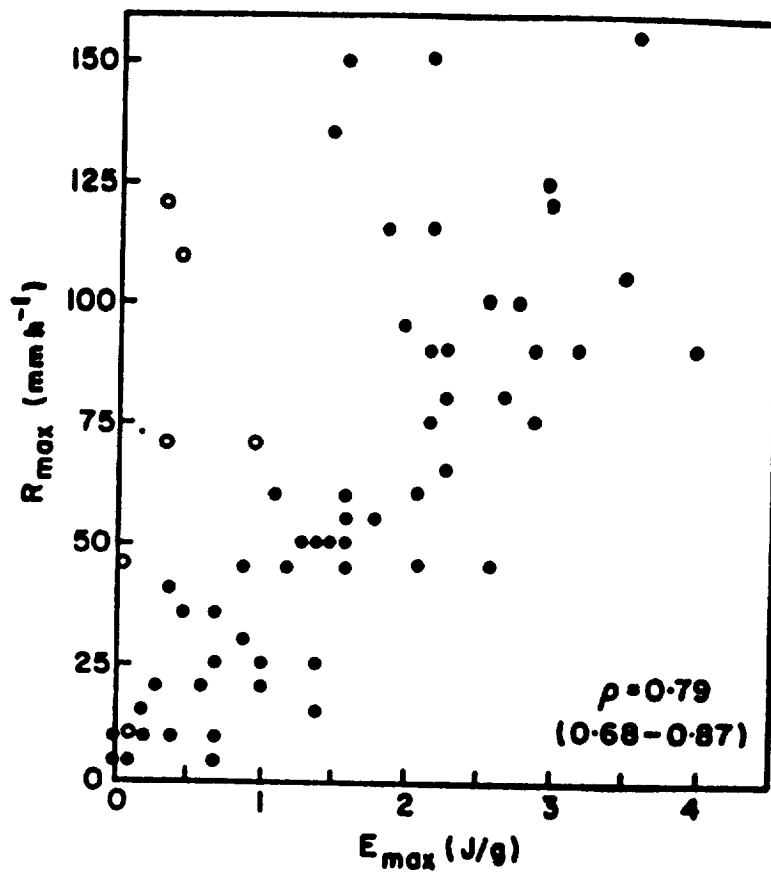


Figure 64. Maximum rain rate as a function of maximum parcel energy for 67 storm days near Ottawa, Canada during the summer of 1969-1970. (After Zawadzki et al., 1981).

### An Examination of the Residual Errors

Although we claim the logistic model describes the thunderstorm life-cycle reasonably well, there may be other non-linear models that describe the life-cycle just as well, if not better. The logistic model offers a high degree of correlation with the observed data and errors are small, but we note that the residuals are consistently above or below the fitted values for short periods. Such patterns suggest positive autocorrelation in the error terms. Such correlation patterns further suggest improved models can be constructed by adding one or more independent variables to the present model. We can evaluate the error terms quantitatively with the Durbin-Watson test statistic (Neter et al., 1983). The test statistic,  $D$ , is defined as

$$D = \frac{\sum_{t=2}^n (e_t - e_{t-1})^2}{\sum_{t=1}^n e_t^2}, \quad (5.1)$$

where  $n$  is the number of sample periods,  $e_t$  is the residual error from the least squares regression,  $\sum e_t^2$  is the residual sum of squares, and the term  $(e_t - e_{t-1})$  is the difference in the residuals at two successive times. The usual hypothesis test alternatives are

$$\begin{aligned} H_0 : \rho &= 0 \\ H_1 : \rho &> 0, \end{aligned} \quad (5.2)$$

where  $\rho$  is the autocorrelation parameter. The decision rule is as follows:

$$\begin{aligned} \text{If } D &> d_U, \text{ conclude } H_0, \\ \text{If } D &< d_L, \text{ conclude } H_1, \end{aligned} \quad (5.3)$$

where  $d_U$  and  $d_L$  are the upper and lower bounds obtained by Watson and Durbin, such that a value of  $D$  outside these bounds leads to a decision and any  $d_L < D < d_U$  gives an inconclusive result.

Estimating the two parameters  $\beta$  and  $k$  ( $\alpha$  is proscribed), results in  $d_L=1.34$  and  $d_U=1.42$  at a level of significance  $\alpha_0=0.01$  (Table A-6 in Neter et al., 1983). For example, the 15 November 1989 storm system has  $n=53$  and a value of  $D=0.06 \ll d_L$ . Thus, one concludes the error terms are positively correlated. For the MCC composite  $n=18$ ,  $d_L=0.90$ , and  $d_U=1.12$ ,  $D=0.84 < d_L$ , and again conclude  $H_1$ . Small values of  $D$  usually lead to the conclusion that  $\rho > 0$  because successive error terms tend to be of the same magnitude. The residual errors tend to be largest when cells merge or cells redevelop/intensify, both factors which lead to a short term increase in the observed flash rates. The 15 November 1989 case shows a number of such peaks associated with cell mergers. Much of this variation is reduced in the MCC composite by averaging the ten cases. These smaller scale interactions can be included in the basic logistic model by the inclusion of additional (e.g., exponential) terms.

### Applications to Extrapolation Forecasting

#### Thunderstorm Duration

The relationship between the environmental instability and energy can be used as a "first guess" of  $\alpha$ . The storm system duration will increase and the system growth rate will decrease as  $\alpha$  increases. Thus,  $\alpha$  can serve as an index to provide some insight into the potential life-cycle of the storms to the forecaster. Since the logistic curve is symmetric about its inflection point, knowledge of when a storm or storm complex has begun the decay phase of its life-cycle (as indicated by decreasing lightning discharge rates) can be used to estimate the valid extrapolation range. One might also predict that

lightning activity will decrease exponentially in the same time it took to reach its peak. This type of information can be used in the context of yes/no (lightning/no lightning) forecasts. The existing extrapolation forecasting procedures use an arbitrary forecast period determined by some ad-hoc method. Using an appropriate storm or system motion vector, one now has a physical basis and empirical evidence upon which to make the determination of longer or shorter extrapolations.

### Thunderstorm Existence

Consider the yes/no forecast of lightning activity for the 15 November 1989 storm system using the lightning grids. A total of 1269 cloud-to-ground flashes occurred in association with the line of storms that came through the Tennessee Valley during the 1 h interval 2130-2235 UTC within the analysis sub-region shown in Figure 33. The time series (in 5-min intervals) over this 1 h period is shown in Figure 65.

A full intensity extrapolation forecast would simply move the lightning in one map with the storm motion vector  $\Delta t$  (5-min) steps forward. If the storm motion vector placed the system and individual embedded storms in the correct location  $t+\Delta t$  step ahead, the existence question would be answered correctly.

Since the total cloud-to-ground lightning for the system is changing (growth and decay), the forecast error will depend on the number of steps ahead to forecast. For example, the system motion vector of the lightning from 2130-2135 UTC to the next 5-min interval is 4.8 km from the southwest at  $246^\circ$  (due north is  $0^\circ$ ). An extrapolation of the pattern  $t+\Delta t$  steps ahead is simply

$$\hat{x} = x_o + n\Delta t(\Delta x) \quad (5.4)$$

$$\hat{y} = y_o + n\Delta t(\Delta y) \quad (5.5)$$

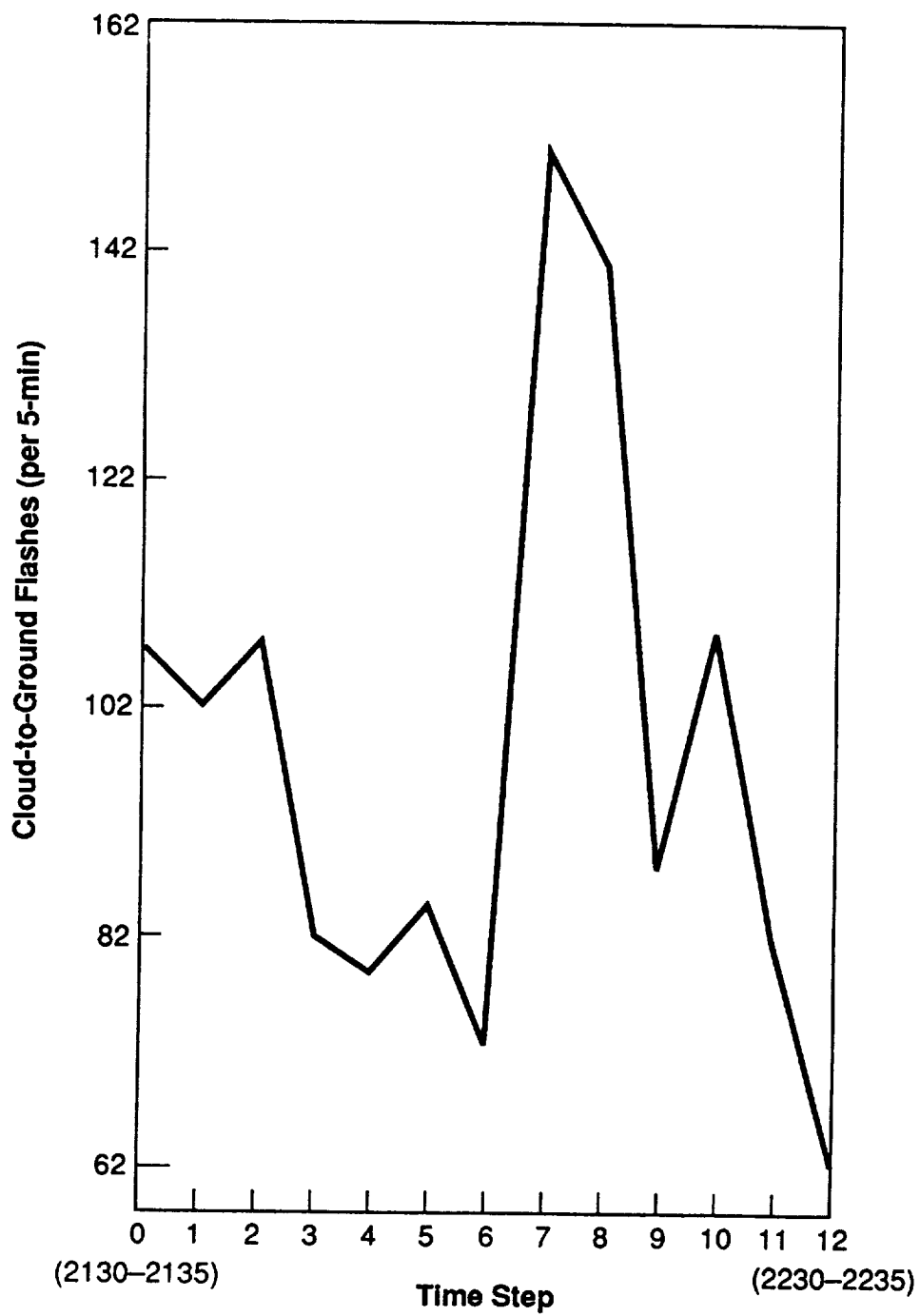


Figure 65. Cloud-to-ground lightning time series (per 5 min) of the 15 November 1989 storm system during the period 2130-2235 UTC.

where  $n$  is the number of sample periods ahead, and  $\Delta x$  and  $\Delta y$  are the  $x$  and  $y$  components of the storm motion vector. The displacement of each lightning discharge is computed first and then a grid is generated at the desired time. Consider the lightning activity at 2130-2135 UTC which is extrapolated in space 11 periods ahead (Figure 66). Compare this forecast grid against the observed grid at 2225-2230 UTC (Figure 67). A qualitative evaluation of the forecast can be made using the evaluation criteria developed by Donaldson et al. (1975) and successfully used by Browning et al. (1982) and many others for evaluating radar echo extrapolations. The scoring criteria for lightning are given in Table 9. The evaluation criteria of interest are the Threat Score or Critical Success Index (CSI), probability of detection (POD), and false alarm rate (FAR) defined as

$$CSI = \frac{A}{(A+B+C)} \quad (5.6)$$

$$POD = \frac{A}{(A+B)} \quad (5.7)$$

$$FAR = \frac{C}{(A+C)} \quad (5.8)$$

$A$  is defined as the number of gridpoints predicted to have a flash density  $\geq 0.02 \text{ km}^{-2}$  at the valid forecast time ( $t+\Delta t$ ) and an observed density of  $0.01 \text{ km}^{-2}$  or greater within a local neighborhood of the gridpoint. A  $3 \times 3$  point verification grid centered at the gridpoint of interest is used for this purpose.  $B$  is defined as the number of gridpoints where there is no flash density  $\geq 0.02 \text{ km}^{-2}$  predicted at the valid forecast time, yet there is a gridpoint observed in its neighborhood with a density  $\geq 0.02 \text{ km}^{-2}$ . Lastly,  $C$  is defined as the number of gridpoints predicted to have a flash density  $\geq 0.02 \text{ km}^{-2}$ , yet no lightning is observed in the local neighborhood. The validation focuses on hitting

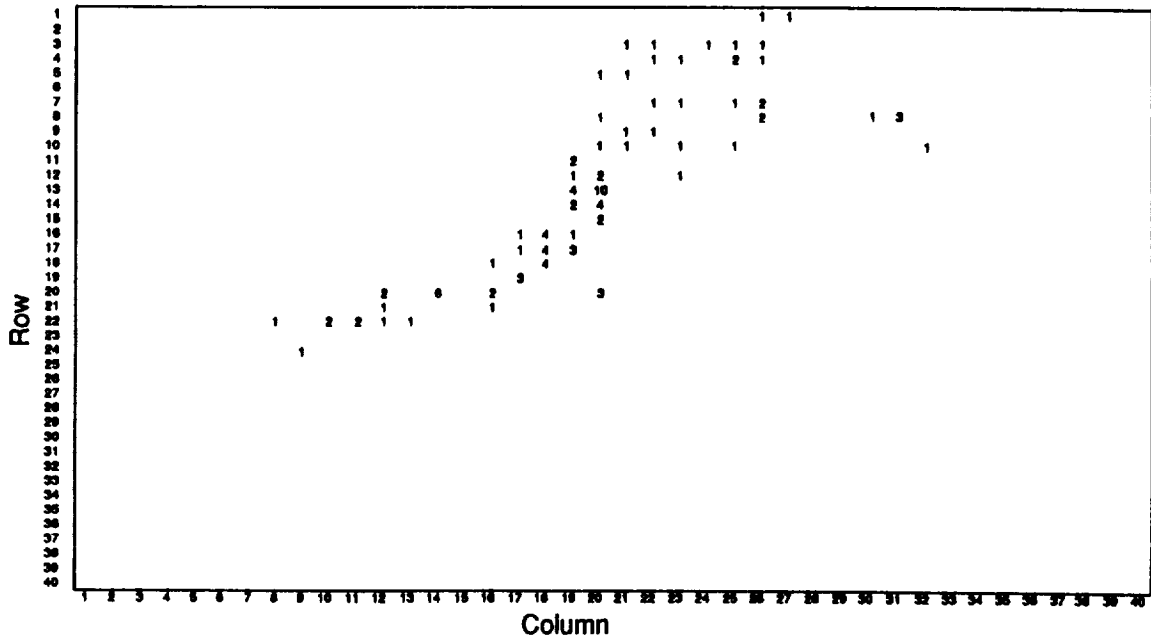


Figure 66. Eleven-period ahead extrapolation (valid 2225-2230 UTC) of lightning activity observed during the period 2130-2135 UTC.

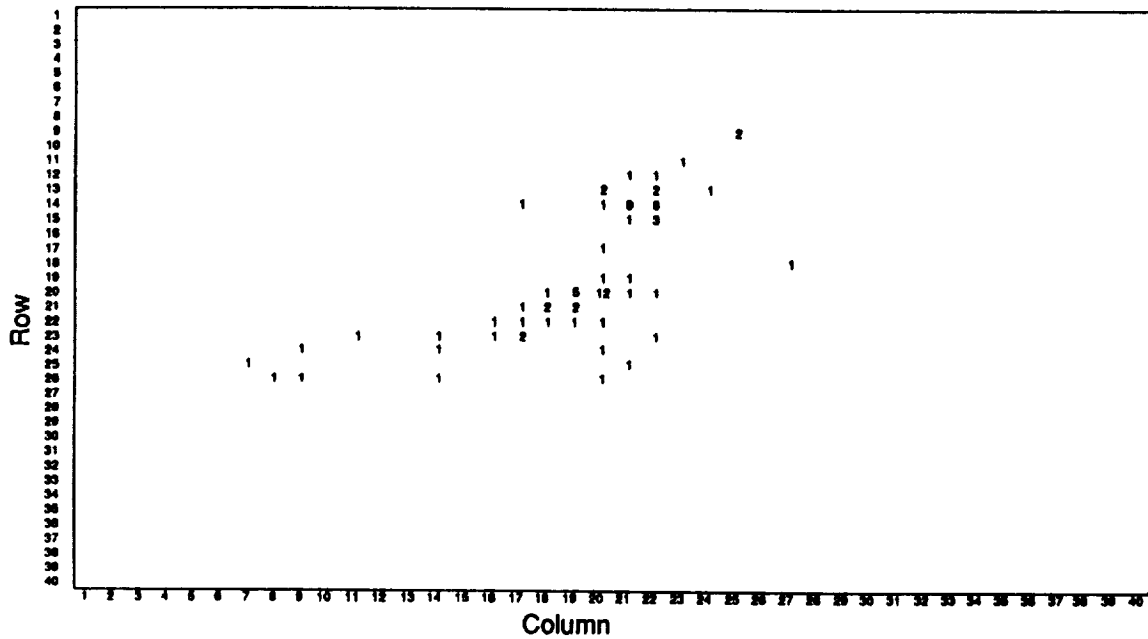


Figure 67. Observed lightning activity during the period 2225-2230 UTC.

Table 9. Objective Forecast Scoring Criteria

Observed	Forecast	
Lightning No Lightning	Lightning	No Lightning
	A	B
	C	D

or missing the major storm centers and the validation area is similar to that of Browning et al. (1982) who used 20 km x 20 km grids to validate their rain/no rain extrapolation forecasts.

The 11 period ahead forecast produced a CSI=0.46, POD=0.71, and FAR=0.43. The residual error  $e_t=3$  for forecasting the number of seeds or clusters. A total of 8 seeds were identified at 2130-2135 UTC (forecast to still be extant at 2225-2230 UTC since the full system was moved forward in time) and only 5 seeds are observed (refer to Chapter 4). The loss of storms most severely reduces the CSI and FAR since we assume the storm clusters will still be present nearly an hour later. Due to the birth and death process, the CSI and FAR tend to improve with decreasing lag. We note that the lightning cluster identified as I (Figure 45) has long since dissipated (2140 UTC), yet it is the forecast valid at 2225-2230 UTC.

Lastly, consider the 1-period ahead extrapolation of the lightning activity from (2225-2230 UTC) to (2230-2235 UTC) (Figure 68) and compare this grid with the observed lightning grid at (2230-2235 UTC) (Figure 69). We find the CSI=0.67, POD=0.71, the FAR=0.08, and the number of clusters increases from 5 to 6. In this example the FAR is greatly reduced with a lesser improvement in the CSI. Although we generally expect better forecasts at shorter lags, a number of varied weather scenarios need to be studied to understand ways to improve the forecast scores.



## CHAPTER VI.

### SUMMARY AND CONCLUSIONS

The goal of this research was to develop a mechanistic model that can be used for extrapolative forecasting of lightning and thunderstorm activity. The original research reported herein has resulted in the development of a 3-parameter logistic growth model to explain the exponential growth and decay of lightning activity accompanying thunderstorms, at different space and time scales extending over four orders of magnitude. The logistic model depicts a process where the growth rate is proportional to the size reached, the remaining size of the population, and is a function of time. The growth rate constant depends on the size of the storm while the limiting value of the total lightning activity and lifetime is related to the available energy in the environment.

Short-lived storms may not produce sufficient cloud-to-ground lightning discharges to exhibit a continuous growth and decay life-cycle. Instead, the total (intracloud and ground) discharge rate best describes the thunderstorm life-cycle. In two severe weather cases, a short-lived microburst-producing storm and a long-lived tornadic supercell storm, peak total lightning rates were greater than 22 flashes  $\text{min}^{-1}$  and 40 flashes  $\text{min}^{-1}$ , respectively. Yet cloud-to-ground flashes occurred at rates of only 1-5  $\text{min}^{-1}$ . The logistic growth model using cloud-to-ground lightning data is more appropriate for describing the evolution of storm complexes, where the longer sampling period is less affected by sudden surges in growth. The short-lived cells produce too few samples (ground discharges) to adequately describe the system and detect significant trends.

The model residual errors, though small, have been shown to exhibit positive serial correlation. This is a result of the merger and reinvigoration of storms giving rise to multiple local maxima in the lightning time series during the growth and decay of the storm system. Suggested techniques for resolving or deconvolving these multiple peaks to gain further insight into their behavior (and implications for nowcasting) might include other non-linear models with additional parameters, stochastic time series models (Box and Jenkins, 1976; Abraham and Ledolter, 1983), and simple first-order difference equation formulations of the logistic model that are used to describe the chaotic behavior of non-linear dynamical systems. The predator-prey relationships in animal and biological populations have been modeled in this way (May, 1974; May 1976).

Many of the physical (non-instrumental) sources of forecast error examined have the same root causes that affect the radar echo extrapolation systems, i.e., incorrect extrapolation vectors, new storms (births), renewed growth (due to cell mergers or a change in the storm environment, storm decay or total dissipation (deaths). The most promising improvements to extrapolation forecasts should come from the use of appropriate non-linear models to understand the birth and death process. It appears appropriate to maintain a history on the life-cycle of the system when two or more storms merge, and not, as current methods do, begin a new description from the time of the merger. This will lead to incomplete life-cycle descriptions and delete the information needed to predict the decay of storm complexes.

A novel constrained optimization approach was developed to remove systematic errors from the cloud-to-ground lightning data base. An optimization algorithm constrained by the observed position of isolated radar echoes produces the best estimate of the lightning locations for subsequent analysis. These lightning locations are next clustered into groups that define single thunderstorm cells and storm complexes. This is accomplished by creating grids of lightning activity in 5-10 min intervals and finding isolated lightning density maxima within the grids. These maxima, typically 2 flashes per

100 km<sup>2</sup>, are then used to determine the total number of storms and as seed (initial guess) points for a K-Means nearest neighbor clustering algorithm that optimally assigns the flashes to the proper storm. Subsequent groupings of the individual storms permitted the identification of entire storm complexes. Uncorrected location errors will degrade the process of objectively identifying and assigning the individual lightning strikes to their parent thunderstorms. These misclassifications, in turn, could alter the true nature of the lightning life-cycle time series.

Lightning data offers synergistic information to the radar tracking and cell identification algorithms in operational use. The NEXRAD radar storm identification techniques rely on a base scan reflectivity threshold to identify storm cells. It has been demonstrated that lightning strikes can be clustered into discrete cells, thus offering an opportunity for augmenting the decision criteria that are based on the radar algorithms alone.

## CHAPTER VII.

### RECOMMENDATIONS

During the 1990s, the NEXRAD radars will provide storm coverage over the conterminous United States (Figure 70). Figure 71 shows the radar coverage at a range of 125 km with the track of the 15 November 1989 Huntsville, AL tornado superimposed. At 125 km, for example, the 1° NEXRAD radar beam is about 1 km in diameter and the base-scan height (minimum elevation) is 1 km above the surface of the earth. Note that the distance from the Nashville, TN and Birmingham, AL NEXRAD radars to the tornado is 190 km. At this distance the beam width is 3.4 km. Such a broad sampling volume will degrade the performance of the storm identification and tracking algorithms, and the Doppler wind velocity estimates will be compromised. Yet, the ground-based lightning network will provide overlapping coverage with the radar for improved storm identification.

Finally, a lightning mapping sensor using CCD-focal plane technology will allow total lightning activity to be monitored continuously from space (Christian et al., 1989). This instrument is planned for the next generation of operational weather satellites (called GOES-Next) and will provide coverage from Canada to Brazil (Figure 72). These data will have a spatial resolution of 10 km, sufficient for the identification of individual thunderstorms. The satellite lightning data will not require the sensitive site error corrections required by the cloud-to-ground lightning networks. The clustering and extrapolation forecasting methodologies are equally applicable to the data collected by



## NEXRAD COVERAGE AT 125 KM

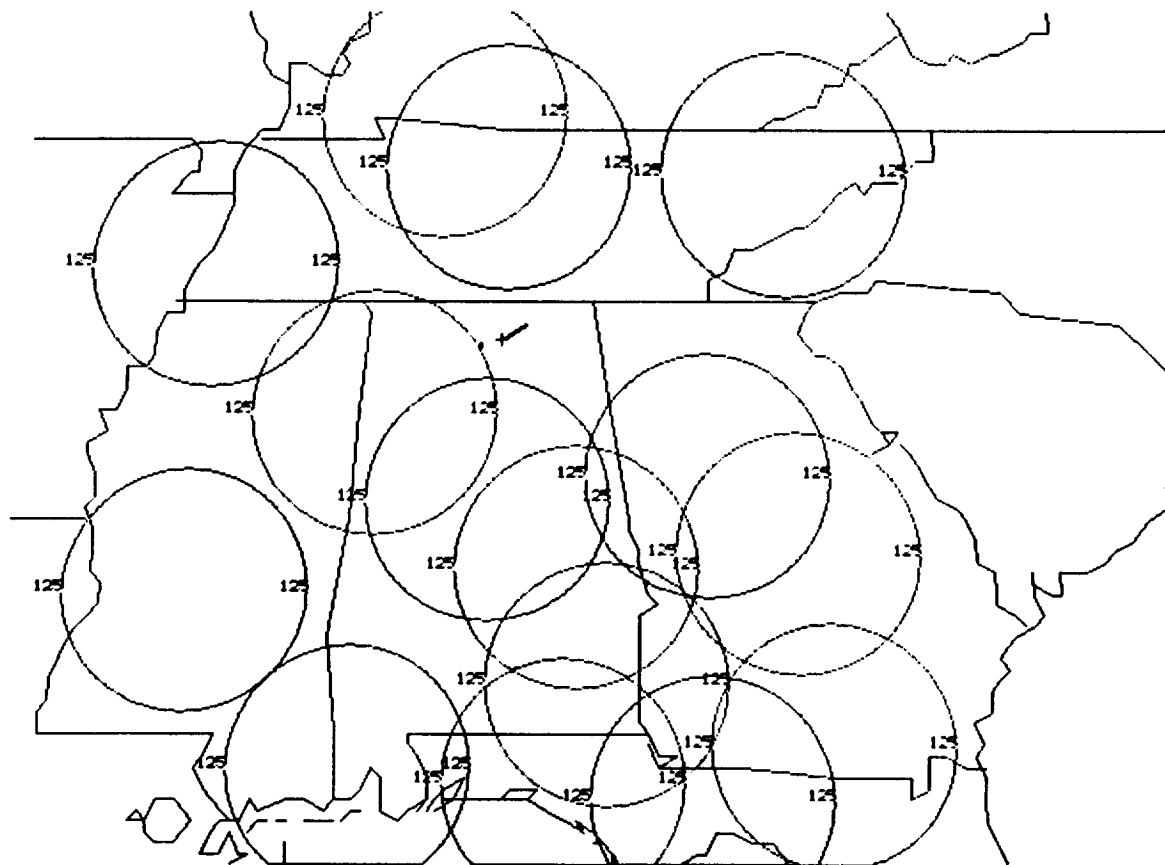


Figure 71. NEXRAD sites in the Southeastern United States with 125 km range circles. The track of the 15 November 1989 tornado at Huntsville, Alabama is indicated by the cross and solid line.



Figure 72. Proposed 10.5° field of view centered at 2°N latitude and 75° longitude for the lightning mapper sensor on GOES-Next.

the lightning mapper. Sensor fusion with lightning data should provide more capability for diagnosing the present and future weather situation than any one of these sensors can possibly offer by itself.



## APPENDIX A: THE FFIX ALGORITHM

### Mathematical Formulation of the Best Point Estimate (BPE)

FFIX is based on the result that if there are no bearing errors, then the target vector  $T$  lies in each of the individual bearing planes and, therefore, is normal to the normal vectors,  $N_i$ , to each of the bearing planes, i.e.,  $T \cdot N_i = 0$  (Figure 73). The observed bearing planes are defined by their respective bearing and station vectors as measured from the center of the earth. The bearing vector,  $\beta_i$ , gives the direction from which the signal from the lightning strike is sensed at station  $S_i$ . Due to the random and systematic errors, the observed bearing planes do not generally contain a common target vector,  $T$ . The true bearing to the target is represented by  $\rho_i$ . Thus, we choose  $T$  such that the dot products,  $T \cdot N_i$ , are a minimum. FFIX applies the method of weighted least squares that minimizes the objective function

$$f(T) = \sum w_i (T \cdot N_i)^2, \quad (A.1)$$

subject to the constraint  $|T| = 1$ . The choice of the weights,  $w_i$ , is based on the principle of maximum likelihood first examined by Stansfield (1947). This is equivalent to minimizing

$$s_k = \sum (\epsilon_i / q_i^*)^2, \quad (A.2)$$

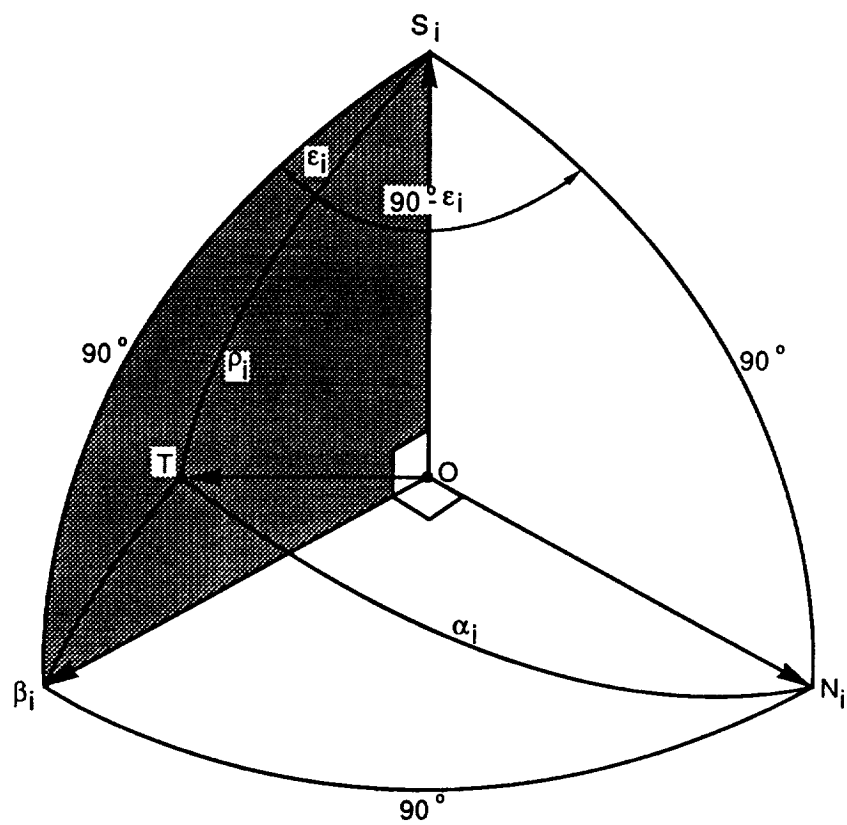


Figure 73. Spherical triangle relationships used in the FFIX algorithm.

where  $s_k$  is the sum of squared bearing errors for a set of  $k$  bearings,  $\epsilon_i$  is the difference between the observed bearing and the bearing from station  $S_i$  to the BPE and  $\sigma_i^*$  is the range weighted bearing standard deviation for the  $i$ th station. That is,

$$\sigma_i^* = \sigma_i D_i, \quad (A.3)$$

where  $\sigma_i$  is the standard deviation of the bearing errors and  $D_i$  is the distance from DF station  $S_i$  to the BPE. For the first iteration when there is no BPE the weight for DF station  $S_i$  is simply

$$w_i = (1/\sigma_i)^2. \quad (A.4)$$

Each successive iteration uses the previous BPE for its initial location estimate, which in turn determines each of the  $D_i$ s. Thus, DF stations having larger bearing errors and at a further distance from the BPE will be given lesser weight. Define

$T$  as a  $3 \times 1$  column vector,  
 $N$  as a  $n \times 3$  matrix of normals  
 $W$  as a  $n \times n$  diagonal matrix of weights.

If  $C$  is defined as  $C = N^T W N$ , then the objective function (Eqn. A.1) can be expressed as

$$f(T) = T^T C T. \quad (A.5)$$

For real data  $C$  will be positive definite, i.e.,  $f(T) > 0$  if  $T \neq 0$ .

### Simplifying the Problem

First,  $T^T C T = k$  is the equation of an ellipsoid for any  $k > 0$ . The problem is simplified if we rotate the axes of the ellipsoid to get the equation in standard form (see also Gething, 1978). Note that

$$T = P y \quad (A.6)$$

is a rotation if

$$P^T P = I, \quad (A.7)$$

where  $P$  is the matrix of rotation and  $I$  is the identity matrix. The required rotation gives

$$T^T C T = y^T P^T C P y = y^T \Lambda y, \quad (A.8)$$

where

$$\Lambda = \text{diagonal } (\lambda_1, \lambda_2, \lambda_3). \quad (A.9)$$

Thus,

$$f(T) = \lambda_1 y_1^2 + \lambda_2 y_2^2 + \lambda_3 y_3^2, \quad (A.10)$$

$$0 < \lambda_1 \leq \lambda_2 \leq \lambda_3.$$

The minimum value of  $f(T)$  is  $\lambda_1$  for  $y = (1, 0, 0)$  or

$$T = P y = \begin{bmatrix} P_{11} \\ P_{21} \\ P_{31} \end{bmatrix}. \quad (A.11)$$

The problem is reduced to determining  $\lambda_1$  and  $P$ . The multipliers  $\lambda_i$  must satisfy the equation

$$|C - \lambda I| = 0. \quad (A.12)$$

Eqn. (A.12) is the characteristic polynomial of  $C$  and the minimum root  $\lambda_1$  can be found directly without an iteration procedure. The solution vector  $T$  can now be computed from the matrix equations  $C = \lambda I$  and  $|T| = 1$ .

From the geometry in Figure 73 and the properties of the dot and cross products we get

$$T \cdot N_i = \cos \alpha_i \quad (A.13)$$

$$|T \times S_i| = \sin \rho_i. \quad (A.14)$$

For the spherical triangle defined by the points  $TS_iN_i$  we get the relationship

$$\cos \alpha_i = \sin \rho_i \sin \epsilon_i. \quad (A.15)$$

Therefore,

$$\begin{aligned} (T \cdot N_i)^2 &= \cos^2 \alpha_i \\ &= |T \times S_i|^2 \sin^2 \epsilon_i. \end{aligned} \quad (A.16)$$

From this result it follows that by defining

$$W_i = (1/\sigma_i^2) |T \times S_i|^2 \quad (A.17)$$

the function

$$\Sigma(\sin^2 \epsilon_i / \sigma_i^2) \simeq \Sigma(\epsilon_i / \sigma_i^2)^2 \quad (A.18)$$

is minimized. The error introduced by the approximation  $\sin \epsilon_i = \epsilon_i$  is  $< 1\%$  for  $\epsilon_i = 14^\circ$ .

### The Confidence Region

The confidence ellipse calculation is based on the perturbations (variance) of the bearings to the BPE, i.e., bearing errors and target position errors are treated as differentials (see Stansfield, 1947). Linearization of the functional relationship between the BPE and observed bearings gives an approximate expression for the inverse covariance matrix of  $T$ . Therefore, the bearings to the BPE are used, not the observed bearings. Since both  $T$  and  $S_i$  lie in the bearing plane, the normal vector can be calculated from

$$N_i = (T \times S_i) / |T \times S_i| . \quad (A.19)$$

As before,  $C = N^T W N$ , with the exception that now  $C$  has the value of zero for an eigenvalue. Since  $T^T N_i = 0$ , or in matrix terms,  $NT = 0$  implying that  $CT = 0$ , the equation

$$x^T C x = k^2 \quad (A.20)$$

can be rotated by  $x = P y$  to

$$y^T \Lambda y = \lambda_2 y_2^2 + \lambda_3 y_3^2 = k^2 \quad (A.21)$$

where  $P^T C P = \Lambda = \text{diagonal } (0, \lambda_2, \lambda_3)$ .

When the site errors have been removed, the random errors are normally distributed and the errors with respect to the lines of position (i.e., the BPE) are independent. Eqn. (A.21) represents an ellipse in the  $y_2 y_3$  plane which is the plane tangent to the earth at  $T$ . If  $x$  is the deviation from  $T$ , then  $x$  is normally distributed in a plane tangent at  $T$ , and  $x^T C x$  has the chi-square distribution with 2 degrees of freedom.

Given the probability  $(x^2 \leq k^2) = P$  for

$$k^2 = -2 \ln (1-P), \quad (A.22)$$

the axes of the confidence ellipse for probability level P are given by

$$a = (Rk/\sqrt{\lambda_2}) ; b = (Rk/\sqrt{\lambda_3}) \quad (A.23)$$

where a and b are the semi-major and semi-minor axes of the ellipse in units of km and  $R = 6378$  km is the radius of the earth. The major axis lies along the eigenvector  $e_2$  corresponding to  $\lambda_2$ , and the orthographic projection of  $e_2$  onto the plane tangent to the earth at T determines the orientation of the confidence ellipse. If  $T = (t_1, t_2, t_3)$  and  $e_2 = (a_1, a_2, a_3)$  and  $\Theta$  is the bearing of the major axis, then

$$\sin\Theta = (t_1 a_2 - t_2 a_1) / \sqrt{t_1^2 + t_2^2} . \quad (A.24)$$

The ellipse represents a region of minimum area associated with a given probability that the lightning strike occurred on or within the ellipse perimeter. The values of  $k^2$  for the 90% ( $P=0.9$ ) and 50% ( $P=0.5$ ) ellipses, respectively, are 4.61 and 1.39. (See Gething, 1978 for more discussion on the confidence ellipse.)



## **APPENDIX B: LIGHTNING ANALYSIS SOFTWARE**

The lightning analysis software consists of programs to decode the hexadecimal data archived on 1600 bpi magnetic tape, convert the data into geophysical quantities, perform data quality control, remove site errors, compute the optimal flash position, and compute error statistics.

**PRECEDING PAGE BLANK NOT FILMED**

```

C      SUBROUTINE MAIN0
CCCCCCCCCCCCCCCCCCCCCCCCCCCCCCCCCCCCCCCCCCCCCCCCCCCCCCCCCCCC
C
C      LLP LIGHTNING DATA DECODER, USES THE DDAH TAPE FORMAT      C
C      CONVERTS RAW DATA TO PROPER UNITS , REMOVES SITE          C
C      ERRORS FOR THE MSFC NETWORK, CALLS FPIX FOR OPTIMAL        C
C      LOCATION ESTIMATES WHEN 2 OR MORE DFS DETECT THE          C
C      FLASH, CALLS NETFIX FOR TWO BEARING CUT SOLN              C
C                                                                C
CCCCCCCCCCCCCCCCCCCCCCCCCCCCCCCCCCCCCCCCCCCCCCCCCCCCCCCCCCCC

      IMPLICIT DOUBLE PRECISION(A-H,O-Z)
      DIMENSION IDATA(128)
      CHARACTER GDATE*8
      CHARACTER*1 CR,LF,AT
      CHARACTER*1 ICHAR1(512), ICHAR2(46), ITMP(46)
      CHARACTER*2 NBUF(256)
      EQUIVALENCE (IBUF, ICHAR1), (ITMP(1), ICHAR2), (NBUF, IBUF)
      EQUIVALENCE (IBUF, IBUF1)
      COMMON/BUFS/IBUF1(128), IBUF2(128)
      COMMON/COM1/IBFLAG, NREC, INCHK, IN(5), IN2(5)
      COMMON/SOLN/SNKA, SSGNL, TLAT, TLOD, RADIUS, AREA, TSOLN,
      *IYDSN, IYR, MON, NDAY, NRS, NBR, IRES, NEVT, SMA, SMI, ORIEN
      COMMON/DFSTUF/DFE1(128), NS1(128), DFR10(128), NS10(128),
      *DFR15(128), NS15(128), SQ1(128), SQ10(128), SQ15(128)
      COMMON/SUMRY/KTWOER, NTHRS(4), NBADF, NBDF2, NDUP(4), NOVR(4),
      *NDFHT(4), KDVG
      COMMON/KOUNTR/KNT1, KNT2, KNT3, KNT4, KNTHH, MTKNT, IDFTST, ISECOD
      COMMON/ECNST/TMX, RSML1, RSML2, RBIG, SBIG, BINSIZ
      DATA CR, LF, AT /ZOD, Z25, Z7C/
      DATA KL1, KL2, ISTAT, MMNUM /26, 46, 0, 8000/
      CALL DATEG(GDATE)
      CALL TIME(ETIME)
      IHTIM=INT(ETIME/360000)
      AHTIM=FLOAT(ETIME)/360000.
      AMTIM=(AHTIM-IHTIM)*60.
      INTIM=INT(AMTIM)
      ASTIM=60.*(AMTIM-INTIM)
      STIM=FLOAT((IHTIM*100 +INTIM)*100) +ASTIM
      WRITE(6,3) GDATE, STIM
3      FORMAT(1H1/20X, 'LLP QUALITY CONTROL ANALYSIS'//20X, '( ', A8, 2X,
      *F10.2, ' ' )//)
C
C      THESE VARIABLES ARE USED AS CONSTRAINTS IN ERSTAT FOR SITE ERRORS
IF NOT WANTING SITE ERRORS, SET IDFTST=0, AND ISECOD=2

      IDFTST=0
      TMX=20.
      RSML1=30.
      RSML2=50.
      RBIG=200.
      SBIG=5.
      BINSIZ=6.
C
C      SITE ERROR CODES: 0=NONE, 1=SITERC, 2=SITER2, 3=SITERR
      ISECOD=2
      IOUNIT=10
C
      DO 56 L=1, 128
      DFE1(L)=0.
      NS1(L)=0
      DFR10(L)=0.
      NS10(L)=0
      DFR15(L)=0.
      NS15(L)=0.
      SQ1(L)=0.
      SQ10(L)=0.
      SQ15(L)=0.
56      CONTINUE
      DO 66 L=1, 5
      IN2(L)=0
66      IN(L)=0
C
C..  INITIALIZE COUNTERS
C
      KNT1=0
      KNT2=0
      KNT3=0
      KNT4=0
      NBADF=0
      NEVT=0
      KDVG=0
      KTWOER=0
      MTKNT=0

```

ORIGINAL PAGE IS  
OF POOR QUALITY

```

DO 68 L=1,4
C   NQC(L)=0
   NDFHT(L)=0
   NTHRS(L)=0
68  CONTINUE
   IBFLAG=0
   LEN=512
   INCHK=0
5   IF(ISTAT.EQ.1) CALL ERSUM
C   DO 5 IJK=1,MMNUM
C   WRITE(6,72) IJK
C72  FORMAT(1X/20X,'RECORD NO.= ',I6/)
C   IF(ISTAT.EQ.1) CALL ERSUM
   CALL GETREC(LEN,ISTAT)
   NSIZ=0
   NEXT=1
   DO 10 I=1,LEN
C   IDATA(I)=IBUF(I)
C   IPT=2*I
   IPT=I
   NSIZ=I-NEXT+1
C   WRITE(6,11) I,NSIZ,NEXT,ICHAR1(I),ICHAR1(I)
11  FORMAT(1X,'I,NSIZ,NEXT,ICHAR1..',3I4,A2,2X,Z2)
   IF(ICHAR1(I).EQ.LF.AND.NSIZ.EQ.KL1.AND.IBFLAG.EQ.0) THEN
   CALL DFDATA(ICHAR1,IPT,IMES)
   NEXT=I+1
   IF(IMES.EQ.1) GOTO 10
C   ELSE IF(ICHAR1(NEXT).EQ.AT.AND.NSIZ.EQ.KL2) THEN
C   CALL PADATA(ICHAR1,IPT)

C   NEXT=I+1
   ENDIF
   IF(ICHAR1(I).EQ.LF.AND.NSIZ.NE.KL1.AND.IBFLAG.EQ.0) THEN
C   WRITE(6,49) I,NSIZ,NEXT,ICHAR1(I),ICHAR1(I)
49  FORMAT(1X,'...I,NSIZ,NEXT,ICHAR1..',3I3,A2,2X,Z2)
   NEXT=I+1
   GO TO 10
   ENDIF

C   SORTING AND SAVING DATA FROM NEXT BUFFER TO COMPLETE
C   A PARTIAL STRING
C   IF(IBFLAG.NE.0) THEN
   IBFLAG=IBFLAG+1
C   ISAVPT=2*IBFLAG
   ISAVPT=IBFLAG
   ICHAR2(IBFLAG)=ICHAR1(I)
C   WRITE(6,400) I,IPT,NSIZ,IBFLAG,ICHAR2(IBFLAG),ICHAR2(IBFLAG)
400  FORMAT(1X,'** I,IPT,NSIZ,IB,ICHAR2()',4I4,A2,2X,Z2)
   ENDIF
   IF(ICHAR2(IBFLAG).EQ.LF.AND.IBFLAG.EQ.KL1) THEN
   CALL DFDATA(ICHAR2,ISAVPT,IMES)
   NEXT=I+1
   IF(IMES.EQ.1) GOTO 10
   IBFLAG=0
   ELSE IF(IBFLAG.EQ.KL2) THEN
C   ELSE IF(ICHAR2(IBFLAG).EQ.AT.AND.IBFLAG.EQ.KL2) THEN
C   CALL PADATA(ICHAR2,ISAVPT)
   NEXT=I+1
   IBFLAG=0
   ENDIF
10  CONTINUE

C   SAVE THE LAST DF OR PA PARTIAL DATA BLOCK FROM BUFFER I
C   TO COMPLETE THE CHARACTER STRING WHICH CONTINUES IN THE
C   NEXT BUFFER
C   IF(ICHAR1(LEN).NE.LF) THEN
   K=1
   DO 50 J=NEXT,LEN
   IF(K.GT.KL2) THEN
   WRITE(6,900)
900  FORMAT(//1X,'NO LINE FEED AT END OF RECORD')
   GOTO 5
   ENDIF
   ITMP(K)=ICHAR1(J)
50  K=K+1
C   WRITE(6,500) NEXT,LEN,IBFLAG,K,ITMP(1),ITMP(K-1)
500  FORMAT(1X,'!! NEXT,LEN,IB,K,ITMPK,ITMPNXT',4I4,2A2)
   IBFLAG=LEN-NEXT+1
C   ISAVPT=2*IBFLAG
   ISAVPT=IBFLAG
   ENDIF

```

ORIGINAL PAGE IS  
OF POOR QUALITY

```

C5  CONTINUE
    GOTO 5
C   CALL ERSUM
C   STOP
    END
SUBROUTINE GETREC(LEN,ISTAT)
CCCCCCCCCCCCCCCCCCCCCCCCCCCCCCCCCCCCCCCCCCCCCCCCCCCCCCCCCCCC
C
C   RETRIEVES A 512 BYTE (CHARACTER) RECORD FROM DISK
C   AND RETURNS TO MAINO
C
CCCCCCCCCCCCCCCCCCCCCCCCCCCCCCCCCCCCCCCCCCCCCCCCCCCCCCCCCCCC
CC
    IMPLICIT DOUBLE PRECISION(A-H,O-Z)
    EQUIVALENCE (IBUF,IBUF1)
    COMMON/BUFS/IBUF1(128),IBUF2(128)
    CHARACTER*20 DFFIL
    INTEGER BFLN
    BFLN=128
    NREC=0
    IBFLAG=0
    READ(9,2,END=400) (IBUF1(IO),IO=1,128)
2   FORMAT(128A4)
    NEXT=1
    LAST=LEN
C   WRITE(6,300) (IBUF1(IO),IO=1,128)
300  FORMAT(1X,32A4)
    GOTO 500
400  ISTAT=1
500  RETURN
    END
SUBROUTINE DFDATA(LINE,IPT)
CCCCCCCCCCCCCCCCCCCCCCCCCCCCCCCCCCCCCCCCCCCCCCCCCCCCCCCCCCCC
C
C   UNPACKS AND DECODES RAW DF DATA(DDAH FORMAT) FROM TAPE
C
CCCCCCCCCCCCCCCCCCCCCCCCCCCCCCCCCCCCCCCCCCCCCCCCCCCCCCCCCCCC
C
    IMPLICIT DOUBLE PRECISION(A-H,O-Z)
C   LINE CONTAINS RAW DF DATA STRING W/ CRLF
C   TMP CONTAINS SUBSTRINGS FOR SWAPPING MSB/ LSB
    CHARACTER*1 LINE(512)
    CHARACTER TMP*4
    CHARACTER*1 OUTBUF(24)
    CHARACTER*24 IOBUF
    CHARACTER*1 IAPOL
    COMMON/BUFS/IBUF1(128),IBUF2(128)
    COMMON/COM1/IBFLAG,NREC,INCHK,IN(5),IN2(5)
    COMMON/DFSTUF/DFE1(128),NS1(128),DFR10(128),NS10(128),
*DFR15(128),NS15(128),SQ1(128),SQ10(128),SQ15(128)
    COMMON/SOLN/SNKA,SSGNL,TLAT,TLOH,RADIUS,AREA,TSOLN,
*IYDSN,YR,MON,NDAY,NRS,NBR,IRES,NEVT,SMA,SMI,ORIEN
    COMMON/SUMRY/KTWOER,NTHRS(4),NBADF,NBDF2,NDUP(4),NOVR(4),
*NDFHT(4),KDVG
    COMMON/KOUNTR/KNT1,KNT2,KNT3,KNT4,KNTHH,MTKNT,IDFTST,ISECOD
    COMMON/ECNST/TMX,RSML1,RSML2,RBIG,SBIG,BINSIZ
    INTEGER IODF(24),DF1TST
    INTEGER HX80
    INTEGER*4 JD,JDAY,IYEAR
    EQUIVALENCE (IBUF,IBUF1)
    EQUIVALENCE (OUTBUF,IOBUF),(NCNT,NBR),(IERR,IRES)
    DIMENSION IRS(4),IHH(4),IMM(4),ISS(4),IMS(4),ATMP(4),IYYDDD(4)
    DIMENSION POL(4),CBRG2(4),AZM(4),AMP(4),TM(4),CBRG1(4),AZM2(4)
    DIMENSION ITRS(4),TAMP(4),B(4),IA(2),AB(2)
    DIMENSION DLATI(4),DLONGI(4)
    DATA DLATI/34.649167,35.399167,35.83750,34.716667/
    DATA DLONGI/86.669167,86.076944,87.443889,87.881667/
    DATA IST,MNODF/26,4/
    DATA HX80/Z80/
    DTR=0.01745329
    EMISS1=-999.99
    EBAD1=-888.88
    ERAD1=6371.
    ISTART=IPT-IST+1
    IEND=IPT
C   WRITE(6,200) ISTART,IPT,(LINE(IS),IS=ISTART,IEND)
200  FORMAT(1X,'ISTART,IPT',2I4,2X,26A4)
    II=1
    J=ISTART

```

ORIGINAL PAGE IS  
OF POOR QUALITY

```

C
C .. WRITE DF STRING INTO OUTBUF FOR INTERNAL I/O, SWAPPING MSB,LSB
C
  OUTBUF(1)=LINE(J)
  OUTBUF(2)=LINE(J+1)
  OUTBUF(3)=LINE(J+4)
  OUTBUF(4)=LINE(J+5)
  OUTBUF(5)=LINE(J+2)
  OUTBUF(6)=LINE(J+3)
  OUTBUF(7)=LINE(J+8)
  OUTBUF(8)=LINE(J+9)
  OUTBUF(9)=LINE(J+6)
  OUTBUF(10)=LINE(J+7)
  OUTBUF(11)=LINE(J+12)
  OUTBUF(12)=LINE(J+13)
  OUTBUF(13)=LINE(J+10)
  OUTBUF(14)=LINE(J+11)
  OUTBUF(15)=LINE(J+14)
  OUTBUF(16)=LINE(J+15)
  OUTBUF(17)=LINE(J+18)
  OUTBUF(18)=LINE(J+19)
  OUTBUF(19)=LINE(J+16)
  OUTBUF(20)=LINE(J+17)
  OUTBUF(21)=LINE(J+22)
  OUTBUF(22)=LINE(J+23)
  OUTBUF(23)=LINE(J+20)
  OUTBUF(24)=LINE(J+21)

C
C.. CHECK FOR ILLEGAL CHARACTERS IN DF DATA STRING
C
  IMES=0
  DO 30 KC=1,24
    IF(OUTBUF(KC).LT.'A'.OR.OUTBUF(KC).GT.'9') THEN
      WRITE(6,455) OUTBUF
      FORMAT(5X,' BAD CHARACTER IN DF STRING = ',24A1)
455
C    WRITE(6,230) (IBUF1(IO),IO=1,128)
C230  FORMAT(1X,32A4)
      IMES=1
      RETURN
    ENDIF
  30  CONTINUE
  READ(UNIT=IOBUF,FMT=191) IO1,IO2,IO3,IO4,IO5,IO6,IO7,IO8
191  FORMAT(Z2,Z4,Z4,Z4,Z4,Z2,Z2,Z2)
C    WRITE(6,193) IO1,IO2,IO3,IO4,IO5,IO6,IO7,IO8
C
C.. GET DF IDENTITY, IDF=IO1+1
C
  IDF=IO1+1
  IF(IDF.LT.1.OR.IDF.GT.MNODF) THEN
    IQCKEY=-1
    WRITE(6,553) OUTBUF
553  FORMAT(5X,' ILLEGAL DF ID NUMBER IN STRING = ',24A1)
    RETURN
  ENDIF

C
C.. COUNT SUM OF EACH DF DETECTIONS
C
  IF(IDF.LE.MNODF) NDFHT(IDF)=NDFHT(IDF)+1

C
C.. GET FLASH POLARITY  HEX80 ADDED TO BYTE 12 ON TAPE IF POSITIVE
C
  POL(IDF)=-1.0
  IF(IO7.GE.HX80) POL(IDF)=1.0

C
C.. GET AMPLITUDE, 1500 IS OVERANGE VALUE (DF SIGNAL SATURATION)
C
  AMP(IDF)=POL(IDF)* (MOD(IO7,HX80)*256. +FLOAT( IO8))/10.
  IF(ABS(AMP(IDF)).GE.1500.) THEN
    NOVR(IDF)=NOVR(IDF)+1

C
C    WRITE(6,143) IDF,AMP(IDF)
C143  FORMAT(1X,'DF OVERRANGE',I4,F8.2)
    RETURN
  ENDIF
  IF(ABS(AMP(IDF)).LT.10.) THEN
    NTHRS(IDF) = NTHRS(IDF)+1
    RETURN
  ENDIF

C
C.. GET MINUTE OF THE DAY AND CONVERT TO HHMM FORMAT
C
  IHH(IDF)=INT(IO2/60)
  IMM(IDF)=IO2-60*IHH(IDF)

```

ORIGINAL PAGE IS  
OF POOR QUALITY

```

C
C.. GET MILLISECONDS OF THE MINUTE
C
    ISS(IDF)=INT(IO3/1000)
    IMS(IDF)=IO3-1000*ISS(IDF)
C
C.. GET TIME OF DAY HHMMSS FORMAT
C
    TM(IDF)=FLOAT(((IHH(IDF)*100)+IMM(IDF))*100+ISS(IDF))
    **FLOAT(IMS(IDF))/1000.D00
C
C.. GET THE YEAR
C
    JDAY=IO4+1
    NYEAR=JDAY/365
    LPYEAR=NYEAR/4
    JD=LPYEAR+365*NYEAR
    IF(JDAY-JD) 350,300,400
300    JDAY=365
    KYEAR=LPYEAR*4
    IF(KYEAR.EQ.NYEAR) JDAY=366
    NYEAR=NYEAR-1
    GOTO 450
350    NYEAR=NYEAR-1
    LPYEAR=NYEAR/4
    JD=LPYEAR+365*NYEAR
    JDAY=JDAY-JD
    IF(JDAY.EQ.0) GOTO 300
    GOTO 450
400    JDAY=JDAY-JD
450    JDAY=JDAY-1
C
C.. GET YYDDU FORMAT FROM NYEAR AND JDAY
C
    IYYDDD(IDF)=NYEAR*1000+JDAY
C
C.. GET THE EQUIVALENT MONTH, DAY, AND YEAR
C
C
C.. GET NUMBER RETURN STROKES
C
    IRS(IDF)=IO5
C
C.. GET UNCORRECTED DF AZIMUTH TO FLASH
C
    AZM(IDF)=(FLOAT(IO6)/65536.)*360.
C
193    FORMAT(1X,'IODF ',8I8)
C
C.. CHECK DF DATA FOR UNACCEPTABLE VALUES
C
    IQCKEY=0
    IF(IDF.LT.1.OR.IDF.GT.MNODF)THEN
        IQCKEY=-1
        WRITE(6,55) OUTBUF
55    FORMAT(5X,' BAD CHARACTER IN DF STRING = ',24A1)
        RETURN
    ENDIF
    IF(IHH(IDF).LT.0.OR.IHH(IDF).GT.24) IQCKEY=-1
    IF(IMM(IDF).LT.0.OR.IMM(IDF).GT.60) IQCKEY=-1
    IF(ISS(IDF).LT.0.OR.ISS(IDF).GT.60) IQCKEY=-1
    IF(IMS(IDF).LT.0.OR.IMS(IDF).GT.1000) IQCKEY=-1
    IF(IYYDDD(IDF).LT.83000.OR.IYYDDD(IDF).GT.90000) IQCKEY=-1
    IF(IRS(IDF).LT.0.OR.IRS(IDF).GT.14) IQCKEY=-1
    IF(AZM(IDF).LT.0..OR.AZM(IDF).GT.360.) IQCKEY=-1
C
C.. IF DATA UNACCEPTABLE DO NOT CONTINUE WITH STRING PROCESSING
C
    IF(IQCKEY.EQ.-1)THEN
        NQC(IDF)=NQC(IDF)+1
        WRITE(6,196) IQCKEY,IDF,IHH(IDF),IMM(IDF),ISS(IDF),IMS(IDF),
*    TM(IDF),IYYDDD(IDF),IRS(IDF),AZM(IDF),POL(IDF),AMP(IDF)
196    FORMAT(1X,'$196 DF DATA ',I2,' DF= ',I2,2X,3I2,I3,4X,F10.3,
*    I6,I4,F10.4,F6.1,F8.2/)
        WRITE(6,230) (IBUFI(IO),IO=1,128)
230    FORMAT(1X,32A4)
C
        STOP
        RETURN
    ENDIF

```

ORIGINAL PAGE IS  
OF POOR QUALITY

```

C
C.. GET A CORRECTED BEARING ANGLE FOR THIS DF
C
      IF(AZM(IDF).EQ.0..AND.IDFTST.EQ.IDF)THEN
        WRITE(6,188) IDF,AZM(IDF),TM(IDF),AMP(IDF)
188      FORMAT(1X,'ZERO DEGR. ',I2,3F12.3)
        CBRG1(IDF)=0.0
        GOTO 285
      ENDIF
C      CBRG1(IDF)=AZM(IDF)+SITERC(IDF,AZM(IDF))
C      CBRG1(IDF)=AZM(IDF)+SITERR(IDF,AZM(IDF))
C      CBRG1(IDF)=AZM(IDF)+SITER2(IDF,AZM(IDF))
C      CBRG1(IDF)=AZM(IDF)
C.. CHECK THAT CORRECTED ANGLE NON NEGATIVE, ADD 360 FOR PROPER ONE
C
      IF(CBRG1(IDF).LT.0.) THEN
        WRITE(6,211) CBRG1(IDF),IDF,AZM(IDF)
C211      FORMAT(1X,'ANGLE LESS THAN 0..',F12.3,I4,F12.3/)
        CBRG1(IDF)=CBRG1(IDF)+360.
      ENDIF
C      IF(TM(IDF).GT.225300..AND.TM(IDF).LT.225500.)THEN
C      WRITE(6,199) TM(IDF),IDF,AZM(IDF),CBRG1(IDF)
C199      FORMAT(1X,' DF, BEARINGS ',F12.3,2X,I2,2F10.4)
C      ENDIF
      GOTO 285
271      CONTINUE
299      FORMAT(1X, 'NO CORRECTION YET AVAILABLE FOR DF1')
C
C.. CHECK FOR NUMBER OF DFS IN TIME COINCIDENCE
C
285      CALL TIMECO(IDF,TM(IDF),ICNT1,ICC,IYYDDD)
C
C.. FIND NUMBER OF DFS IN COINCIDENCE, IF #DFS=2 CALL NETFIX
C.. IF # DFS IS 2 OR MORE USE OPTIMIZER FPIX. IF FPIX FAILS
C.. TO GET A GOOD SOLN, THEN GET BEST CUT FROM NETFIX BASED
C.. ON MIN. SEMIMAJOR AXIS OF THE ERROR ELLIPSE.
C
      IF(IN(5).NE.1) GOTO 275
      IERR=0
C
C.. IF ICNT1 IS GREATER THAN 4, ONE OR MORE DFS SAW MORE THAN ONE
C   EVENT WITHIN THE TIME COINCIDENCE WINDOW
C
      IF(ICNT1.GT.4)THEN
        WRITE(6,707) ICNT1,TM(IDF)
707      *      FORMAT(1X,'DF SAW MORE THAN ONE FLASH WITHIN TIME WINDOW..',
          *      I4,F12.3)
        ICNT1=4
      ENDIF
      NCNT=ICNT1
      ISUM=0
C      DO 711 IK=1,NCNT
      DO 711 IK=1,MNODF
        IF(IN(IK).EQ.1)THEN
          IN2(IK)=IK
          ISUM=ISUM+1
          AZM2(IK)=AZM(IK)
          CBRG2(IK)=ATMP(IK)
        ENDIF
711      CONTINUE
C
C.. CHECK TO SEE IF NUMBER OF DFS IN SOLN EQUALS COUNTER NCNT
C
      IF(ISUM.NE.NCNT)THEN
        WRITE(6,7277) TM(IDF),ISUM,NCNT,IN,IN2
7277      *      FORMAT(/1X,'TIME CORR ERROR AT ',F12.3,12(I2,1X))
        GOTO 901
      ENDIF
C      IF(TM(IDF).GT.185500..AND.NDAY.EQ.14) STOP
C
C.. USE THIS FOR COMPUTING DF SITE ERRORS
C
      IF(IDFTST.EQ.0) GOTO 75
      IF(IN2(IDFTST).EQ.0) GOTO 901
C      WRITE(6,2112) IN,IN2,CBRG2
C2112      FORMAT(1X,'2112 IN,IN2,CBRG2 ',10I2,4F10.4)
      DO 717 I=1,MNODF
        IF(IN2(I).EQ.IDFTST.AND.NCNT.GE.3)THEN
          IN2(I)=0
          TAZ1=CBRG2(IDFTST)
          NCNT=NCNT-1
          ICNT1=NCNT
        ENDIF

```

ORIGINAL PAGE IS  
OF POOR QUALITY

```

717      CONTINUE
          IF (NCNT.EQ.2.AND.IN2(1).EQ.IDFTST) GOTO 901
          IF (NCNT.EQ.2.AND.IN2(2).EQ.IDFTST) GOTO 901
C
75      DO 712 KI=1,MNODF-1
          IF (IN2(KI).EQ.0.AND.IN2(KI+1).NE.0) THEN
              IN2(KI)=IN2(KI+1)
              AZM2(KI)=AZM2(KI+1)
              CBRG2(KI)=CBRG2(KI+1)
              IN2(KI+1)=0
C          IF (TM(IDF).GT.185200..AND.TM(IDF).LT.185500.) THEN
C              WRITE(6,76) KI,NCNT,IN,IN2,AZM2,CBRG2
76          FORMAT(1X,'DEBUG KI',12(I2,1X),8(F7.3,1X))
C          ENDIF
          ENDIF
712      CONTINUE
C          IF (TM(IDF).GT.201815..AND.TM(IDF).LT.201818.) THEN
C              WRITE(6,76) KI,NCNT,IN,IN2,AZM2,CBRG2
C          ENDIF
C
C..  MAKE A SECOND PASS THROUGH ABOVE SORTING LOOP IF DFS NOT
C..  LISTED CONSECUTIVELY
C
          IF (IN2(1).EQ.0.OR.IN2(2).EQ.0) GOTO 75
          IF (NEVT.GE.80) STOP
C
          IF (ICNT1.GE.2) CALL FFIX(IN2,CBRG2,TM)
          IF (ICNT1.GE.2) THEN
C811      CALL FFIX(IN2,CBRG2,TM)
C          WRITE(6,848) TSOLN,IERR,TLAT,TLON,SMA,SMI,ORIEN,IN2,CBRG2,TM
848      FORMAT(/2X,'FFIX RETURN ',F12.3,I2,5F12.3/1X,5(I2,2X),
          * 4(F12.4,1X),4(F12.3,1X))
C          IF (IERR.EQ.-1) GOTO 901
          IF (IERR.NE.1.OR.ICNT1.EQ.2) THEN
C              WRITE(6,841) TM(4),IERR
C              NBADF=NBADF+1
C              IF (IERR.EQ.0.OR.ICNT1.EQ.2) THEN
C                  IF (ICNT1.GE.2) THEN
C..  THIS FORCES BEST 2 DF FIX (BEST = MIN(SMA))
C
                  IBDCHK=0
                  TSTOR3=999.
                  SMA=999.
                  ICNT1=2
                  NCNT=ICNT1
                  DO 745 I=1,MNODF-1
                      DO 754 J=2,MNODF
                          IF (I.GE.J) GOTO 754
                          IA(1)=IN2(I)
                          IA(2)=IN2(J)
                          IF (IA(1).EQ.0.OR.IA(2).EQ.0) GOTO 754
                          AB(1)=CBRG2(I)
                          AB(2)=CBRG2(J)
                          CALL FFIX(IA,AB,TM)
C          WRITE(6,872) IER,TSOLN,TLAT,TLON,SMA,IA,AB
C872      FORMAT(1X,'LN 872 CHK SOL',2X,I2,4F12.3,2X,2I2,2F8.2)
                          IF (IERR.EQ.1.AND.SMA.LE.TSTOR3) THEN
C
C..  CHECK FOR DIVERGENT ANGLES- SOLN GOES AROUND THE WORLD
C
                          XTL= TLAT*DTR
                          XTLO=TLON*DTR
                          DO 790 K=1,2
                              XSL=DLATI(IA(K))*DTR
                              XSLO=DLONGI(IA(K))*DTR
                              CALL AZRN(XSL,XSLO,XTL,XTLO,AP1,RP1)
                              ABM1=AB(K)-5.
                              ABP1=AB(K)+5.
                              RP=RP1*ERAD1
                              AZP=AP1/DTR
                              IF (AZP.GE.ABP1.OR.AZP.LT.ABM1) THEN
                                  WRITE(6,7979) TSOLN,TLAT,TLON,RP,
                                      *  AZP,IA,AB,SMA
C7979      FORMAT(1X,'DVGA',4X,5F12.3,2X,
                                      *  2I2,3F8.2)
                                  IF (NEVT.GE.80) STOP
                                  KDVG=KDVG+1
C
                                  GOTO 754
                              ENDIF
                          ENDIF
790      CONTINUE

```

ORIGINAL PAGE IS  
OF POOR QUALITY

```

TSTOR1=TLAT
TSTOR2=TLON
TSTOR3=SMA
TSTOR4=SMI
TSTOR5=ORIEN
TSTOR6=AREA
TSTOR7=RADIUS
IDT1=IA(1)
IDT2=IA(2)
TBR1=AB(1)
TBR2=AB(2)
IBDCHK=1
ENDIF
754 CONTINUE
745 CONTINUE
      TLAT=TSTOR1
      TLON=TSTOR2
      SMA=TSTOR3
      SMI=TSTOR4
      ORIEN=TSTOR5
      AREA=TSTOR6
      RADIUS=TSTOR7
      IN2(1)=IDT1
      IN2(2)=IDT2
      CBRG2(1)=TBR1
      CBRG2(2)=TBR2
      DO 775 KP=3,4
        IN2(KP)=0
        CBRG2(KP)=0
775 CONTINUE
C      ENDIF
C      WRITE(6,870) TSOLN,TLAT,TLON,SMA,IN2,CBRG2
870 FORMAT(1X,'LN 870 CHK SOL',4F12.3,2X,5I2,4F8.2)
      IF(IBDCHK.NE.1) THEN
        NBADF=NBADF+1
        GOTO 1801
        GOTO 901
      ENDIF
841 ENDIF
C      FORMAT(1X,'... NO FIX FROM FFIX AT',F12.3,' ERROR=',I3)
C      IF(IN(1).EQ.0) GOTO 901
      XTLO=TLAT*DTR
      XTLO=TLON*DTR
      IF(IDFTST.EQ.0) GOTO 1028
      GOTO 1015
C    ENDIF
C
C      IF(ICNT1.LT.4) GOTO 901 (USE THIS IF ONLY ALL 4 USED)
C
C.. SET UP FOR 2 DF FIX
C
C      IF(ICNT1.EQ.3.AND.IN(1).EQ.1.OR.ICNT1.EQ.2.AND.IN(1).EQ.0) THEN
        IF(ICNT1.EQ.2) THEN
C          WRITE(6,510) ICNT1,NCNT,IN,IN2,CBRG2,ATMP
          DO 715 K1=1,4
            IF(ATMP(K1).EQ.0.) THEN
              GOTO 715
            ENDIF
            IF(IN(K1).EQ.1.AND.IN2(1).NE.0) THEN
              IN2(2)=K1
              CBRG2(2)=ATMP(K1)
            ENDIF
            IF(IN(K1).EQ.1.AND.IN2(1).EQ.0) THEN
              IN2(1)=K1
              CBRG2(1)=ATMP(K1)
            ENDIF
715 CONTINUE
          ENDIF
          FORMAT(1X,'DFDATA..ICNT1,NCNT,IN,IN2,CBRG2,ATMP ',12I4/1X,8F12.4)
510 IF(ICNT1.EQ.2.AND.IN(1).EQ.1) GOTO 890
          NCNT=2
C          IF(IERR.EQ.0) GOTO 811
          IF(IERR.EQ.-1) GOTO 901
          IF(IERR.EQ.0) THEN
C            WRITE(6,1101) NCNT,ICNT1,NBR
1101 FORMAT(1X,'HERE WE ARE.....',3I4)
            CALL NETFIX(IN2,CBRG2,TH)
            IF(IERR.EQ.-1) GOTO 901
514 IF(IERR.NE.1) THEN
C          WRITE(6,841) TH(4),IERR
C          CALL NETFIX(IN2(1),CBRG2(1),IN2(2),CBRG2(2),TLAT,TLON)
C1801 TLON=-1.*TLON

```

ORIGINAL PAGE IS  
OF POOR QUALITY

```

        WRITE(6,2099) TSOLN,IN2(1),CBRG2(1),IN2(2),CBRG2(2),
*TLAT,TLON
2099      FORMAT(1X,'2 DF FIX',F12.3,2X,I2,F12.3,2X,I2,3F12.3)
        ENDIF
C        IF(IN(1).EQ.0) GOTO 901
1801      XTL=TLAT*DTR
        XTLO=TLON*DTR
        IF(IDFTST.GT.0) GOTO 1015
        ENDIF
        IF(IDFTST.EQ.0) GOTO 1028
C
C.. CONVERT SOLN TO RADIANS FOR AZRN TO GET DF1 SITE ERRORS
C      IF DF1 NOT IN SOLN THEN SKIP THIS
C
        XTL=TLAT*DTR
        XTLO=TLON*DTR*(-1.0)
1015      XSL=DLATI(IDFTST)*DTR
        XSLO=DLONGI(IDFTST)*DTR
        CALL AZRN(XSL,XSLO,XTL,XTLO,AZ1,R1)
C
C.. CONVERT FROM RADIANS BACK TO KM, EARTH RADIUS=6370 KM
C
        WRITE(6,912) AZ1,R1
912      FORMAT(1X,'AZRN SENDS DFDATA AZ1,R1 ',2F10.6)
        AZDEG=AZ1/DTR
        RKM=R1*ERAD1
C.. GET DF 1 BEARING ERROR
C SKIP THIS PART IF NOT NEEDING BEARING ERROR
C
C      GOTO 623
        IF(ATMP(IDFTST).EQ.0.00) GOTO 901
C      WRITE(6,3111) TSOLN,IN2,RKM,AZDEG,DIFDEG,CBRG2
3111      FORMAT(/1X,'DIFDEG BEFORE TAZ CHECK ',F12.3,2X,5I2,7F10.4)
C      TAZ1=ATMP(1)
        TAZ2=AZDEG
C      WRITE(6,3112) TAZ1,TAZ2,DIFDEG,XSL,XSLO,XTL,XTLO
        IF(ABS(TAZ2-TAZ1).GT.300.) THEN
            IF(TAZ2.GT.TAZ1) TAZ1=TAZ1+360.
            IF(TAZ2.LT.TAZ1) TAZ2=TAZ2+360.
        ENDIF
        DIFDEG=TAZ2-TAZ1
C      WRITE(6,3112) TAZ1,TAZ2,DIFDEG,XSL,XSLO,XTL,XTLO
3112      FORMAT(1X,'AFTER TAZ CHECK ',7F10.4)
C      IF(NEVT.GE.50) STOP
C
C.. BEFORE ACCEPTING THIS SOLN, CHECK FOR LARGE ERROR RADIUS AND
C      LAT/LON SOLN WHICH ARE REASONABLE
C
C
623      IF(SMA.GE.100.) GOTO 625
        IF(TLAT.GE.42..OR.TLAT.LT.30.) GOTO 625
        IF(TLON.GE.94..OR.TLON.LT.78.) GOTO 625
625      GOTO 635
C625      WRITE(6,680) TSOLN,TLAT,TLON,SMA
680      FORMAT(1X,'DISTANT OR BAD SOLN..REJECT IT AT ',F12.3,2X,
*2F12.6,' SEMI-MAJOR AXIS=',F8.2/)
C
C.. CHECK FOR A BAD SOLN USING 2 BEARINGS AND GIVING SAME
C      SOLN AS PREVIOUS SOLN. THIS IS DUE TO NARROW CUT-ANGLE
C      NBDF2 IS NO. OF WRONG SOLNS FROM FFIX, CUT SOLN BETTER
C
635      IF(ABS(DIFDEG).GT.TMX) THEN
        NBDF2=NBDF2+1
        GOTO 901
        ENDIF
        IF(TLAT.EQ.PLAT.AND.TLON.EQ.PLON) THEN
            KTWOER=KTWOER+1
C      WRITE(6,1777) TLAT,PLAT,TLON,PLON
C1777      FORMAT(1X,'TLAT,PLAT,TLON,PLON=',4F12.6)
            GOTO 901
        ENDIF
C
C.. SORT DF ANGLE ERROR AS A FCN OF ANGLE IN ERSTAT
C
C      CALL ERSTAT(AZDEG,RKM,DIFDEG)
        CALL ERSTAT(TAZ1,RKM,DIFDEG,CBRG2)
C
C.. ESTIMATE THE PEAK CURRENT FOR THIS FLASH WITH FCN FKA
C
1028      SKA= FKA(TAMP)
        SNKA=SKA
C
C.. FIND THE LARGEST NUMBER OF STROKES IN A FLASH
C

```

ORIGINAL PAGE IS  
OF POOR QUALITY

```

      NRS=0
      DO 1411 I=1,NCNT
1411    IF(ITRS(IN2(I)).GT.NRS) NRS=ITRS(IN2(I))
      C
      C    NCNT=0
      C
      C.. GET THE EQUIVALENT MONTH, DAY, AND YEAR FOR A FLASH
      C
      CALL YDDMY(IYDSN,NDAY,MON,IYR)
      C
      C.. SET NO RADIUS FROM SOLN TO EMISS1=-999.99 IN SOLN SET
      C
      IF(RADIUS.EQ.0.)THEN
        AREA=EMISS1
        SMA=EMISS1
        SMI=EMISS1
        RADIUS=EMISS1
        ORIEN=EMISS1
      ENDIF
      IF(RADIUS.GE.200.)THEN
        AREA=EBAD1
        SMA=EBAD1
        SMI=EBAD1
        RADIUS=EBAD1
        ORIEN=EBAD1
      ENDIF
      C
      C.. COUNT NUMBER OF 2 DF AND 3 DF SOLNS
      C
      IF(ICNT1.EQ.2) KNT2=KNT2+1
      IF(ICNT1.EQ.3) KNT3=KNT3+1
      IF(ICNT1.EQ.4) KNT4=KNT4+1
      IF(ICNT1.EQ.1) KNT1=KNT1+1
      C
      C.. CHECK FOR TIME >24 HOURS, DUE TO DAY CHANGE, NEED TO SUBTRACT 24
      C
      IF(TSOLN.GE.240000.) TSOLN=TSOLN-240000.
      C.. CORRECT FOR LEAP YEAR, NDAY=NDAY+1 (LLP DAY OF CENTURY COUNT IS
      C.. INCORRECTLY COMPUTING THIS.
      C
      IF(IYR.EQ.88) NDAY=NDAY+1
      C
      C
      C    WRITE(6,915) TSOLN,IYR,MON,NDAY,AZDEG,RKM,ATMP(1),DIFDEG,
      C    *TLAT,TLON,NRS,SSGNL,SNKA,RADIUS,SMA,SMI,AREA
      C915  FORMAT(1X,' SOLN AT',F12.3,5X,3I2,2X,4F12.6,'= DF 1 ERROR'/
      C    *2F12.6,I4,6F12.2)
      C    WRITE(6,918) IN2,CBRG2
      C918  FORMAT(1X,'IN2,CBRG2=',5I2,4(F6.2,2X))
      C
      C.. WRITE SOLN TO DISK FILE ON EADS (UNIT 10)
      C
      NEVT=NEVT+1
      WRITE(10,3015) NEVT,TSOLN,IYR,MON,NDAY,TLAT,TLON,SNKA,SSGNL,NRS
      3015  FORMAT(I6,2X,F12.3,1X,3I2,2F12.6,2F10.2,2X,I2)
      WRITE(10,4015) IN2,CBRG2,SMA,SMI,ORIEN,RADIUS,AREA
      4015  FORMAT(5I2,4(F6.2,1X),5(F10.2,1X))
      C
      C
      C    IF(NDAY.EQ.14.AND.TSOLN.GT.201815..AND.TSOLN.LT.201818.)THEN
      C    WRITE(6,230) (IBUFI(IO),IO=1,128)
      C    WRITE(6,915) TSOLN,IYR,MON,NDAY,AZDEG,RKM,ATMP(1),DIFDEG,
      C    *TLAT,TLON,NRS,SSGNL,SNKA,RADIUS,SMA,SMI,AREA
      C915  FORMAT(1X,' SOLN AT',F12.3,5X,3I2,2X,4F12.6,'= DF 1 ERROR'/
      C    *2F12.6,I4,6F12.2)
      C    WRITE(6,3015) NEVT,TSOLN,IYR,MON,NDAY,TLAT,TLON,SNKA,SSGNL,NRS
      C    WRITE(6,4015) IN2,CBRG2,SMA,SMI,ORIEN,RADIUS,AREA
      C    IF(TSOLN.GE.201818.) STOP
      C    ENDIF
      C.. WRITE HOURLY SOLN SUMMARY
      C
      IF(NEVT.EQ.1)THEN
        LSTHH=IHH(IDF)
        WRITE(6,2017)
      2017  FORMAT(20X,'EVT',4X,'TIME',5X,'YYMMDD',6X,'LAT',10X,'LON',
      *    8X,'KAMPS',5X,'VOLTS',2X,'RS',4X,'RADIUS',4X,'SMAJ',4X,
      *    'SMIN',3X,'AREA')
      *    WRITE(6,3017) NEVT,TSOLN,IYR,MON,NDAY,TLAT,TLON,SNKA,SSGNL,
      *    NRS,RADIUS,SMA,SMI,AREA
      3017  FORMAT(/1X,'1ST SOLN (TAPE)=' ,I4,2X,F12.3,1X,3I2,2F12.6,2X,
      *    2F10.2,I2,4F10.2/)
      *    ENDIF
      IF(IHH(IDF).EQ.LSTHH) KNTHH=KNTHH+1
      IF(IHH(IDF).NE.LSTHH)THEN

```

ORIGINAL PAGE IS  
OF POOR QUALITY

```

        LSTH1=IHH(IDF)
        IF(LSTH1.LT.0) LSTHH=0
        WRITE(6,3020) LSTHH,KNTHH,IYR,MON,NDAY,NEVT
3020    *   FORMAT(/1X,'HOURLY SUMMARY BEGINNING AT ',I2,' UT IS ',I6,4X,
        'DATE=',3I2,' TOTAL EVENT COUNT SO FAR=',I6,' ::::::::::: '/')
        LSTHH=IHH(IDF)
        KNTHH=0
    ENDIF
C
C
C890    WRITE(6,899)
890    CONTINUE
899    FORMAT(1X,' SOLN REQUIRES DF1 FOR 2 DF FIX')
C
C.. CLEAR POINTERS
C
901    NCNT=0
        ICNT1=0
        LSTDF=IDF
        PREVB=CBRG1(IDF)
        PREVA=AMP(IDF)
        PREVR=IRS(IDF)
C    IF(LSTDF.NE.1) AZM(1)=0.
        AZDEG=0.
        RKM=0.
        DIFDEG=0.
        PLAT=TLAT
        PLON=TLON
        TLAT=0.
        TLO=0.
        RADIUS=0.

        AREA=0.
        SMA=0.
        SMI=0.
        ORIEN=0.
        DO 340 INF=1,5
            IN2(INF)=0
340    IN(INF)=0
            XTL=-1.
            XTLO=-1.
            ICC=0
            DO 345 INF=1,4
                B(INF)=0.
                AMP(INF)=0.
                IRS(INF)=0
                CBRG2(INF)=0.
345    CBRG1(INF)=0.
                CBRG1(IDF)=PREVB
                AMP(IDF)=PREVA
                IRS(IDF)=PREVR
275    DO 2275 INF=1,4
                ATMP(INF)=CBRG1(INF)
                TAMP(INF)=AMP(INF)
                ITRS(INF)=IRS(INF)
2275 CONTINUE
        RETURN
        END
        SUBROUTINE TIMECO(IDN,TMN,ICNT1,ICC,IYYDDD)
CCCCCCCCCCCCCCCCCCCCCCCCCCCCCCCCCCCCCCCCCCCCCCCCCCCCCCCCCCCC
C
C    TIMECO CHECKS FOR TIME COINCIDENCE BETWEEN DFS TO SEE    C
C    HOW MANY DF FIXES SHOULD BE USED IN COMPUTING A SOLN    C
C                                                                C
CCCCCCCCCCCCCCCCCCCCCCCCCCCCCCCCCCCCCCCCCCCCCCCCCCCCCCCCCCCC
C
        IMPLICIT DOUBLE PRECISION(A-H,O-Z)
        COMMON/COM1/IBFLAG,NREC,INCHK,IN(5),IN2(5)
        COMMON/SOLN/SNKA,SSGNL,TLAT,TLON,RADIUS,AREA,TSOLN,
        *IYDSN,IYR,MON,NDAY,NRS,NBR,IRES,NEVT,SMA,SMI,ORIEN
        COMMON/SUMRY/KTWOER,NTHRS(4),NBADF,NBDF2,NDUP(4),NOVR(4),
        *NDFHT(4),KDVG
        COMMON/KOUNTR/KNT1,KNT2,KNT3,KNT4,KNTHH,MTKNT,IDFTST,ISECOD
        DOUBLE PRECISION LTIM
        DIMENSION IYYDDD(4)
        TCO=0.016
        TCP=0.008
C
C.. FIRST TIME THROUGH HERE ONLY
C    ICNT1 IS NUMBER OF DFS IN TIME COINCIDENCE
C

```

ORIGINAL PAGE IS  
OF POOR QUALITY

```

      IF(INCHK.EQ.1) GOTO 15
      IF(IN(IDN).EQ.0) THEN
        ICC=0
        IN(IDN)=1
        INCHK=1
        FTIM=TMN
        LTIM=FTIM
        CTIM=FTIM+TCO
        CLOCK=FTIM+TCO
        LIDF=IDN
        ICNT=1
        GOTO 20
      ENDIF
C
C..      SUBSEQUENT PASSES GO THRU HERE
C        CHECK FOR CHANGE OF DAY AFTER MIDNIGHT
C
15      IF(IYYDDD(IDN).GT.IYYDDD(LIDF)) THEN
        IF((TMN+240000.).GT.CLOCK) ITMN=1
        IF(ITMN.EQ.1) THEN
          TMN=TMN+240000.
          WRITE(6,202) TMN,LTIM
202      FORMAT(1X,'DAY-TIME CHANGE  CUR TIME=',F12.3,2X,'LAST=',
        *      F12.3)
        ENDIF
      ENDIF
C
C..      SOLN EXISTS WITHIN THE TIME CORRELATION WINDOW
C
      IF(TMN.GT.CLOCK) THEN
        IF(ICNT.GE.2) THEN
          IN(5)=1
          ICNT1=ICNT
          TSOLN=FTIM
          IYDSN=IYYDDD(LIDF)
        ENDIF
        GOTO 30
      ENDIF
C
C..      CURRENT TIME STILL WITHIN CORRELATION WINDOW
C
      IF(TMN.LE.CLOCK) THEN
        IF(TMN.GT.CTIM) THEN
          IF(ICNT.EQ.1) GOTO 30
C
C..      CHECK FOR DUPLICATE DF IN TIME WINDOW
C
        IF(IN(IDN).EQ.1) THEN
35          IN(5)=1
          ICNT1=ICNT
          TSOLN=FTIM
          IYDSN=IYYDDD(LIDF)
          GOTO 30
        ENDIF
      ENDIF
C
C..      DO NOT ALLOW TIME TO DECREASE FROM EVENT I TO EVENT I+1
C
      IF(TMN.LT.LTIM) THEN
        DO 40 I=1,4
          IN(I)=0
40        CONTINUE
        WRITE(6,300) TMN,IDN,LTIM,LIDF
C300      FORMAT(5X,'CURRENT TIME ',F12.3,' FOR DF',I2,' LESS THAN',
C        *' LAST TIME OF ',F12.3,' FOR DF',I2)
C      MTKNT IS NUMBER OF OCCURRENCES OF CURRENT TIME LESS THAN PREVIOUS
C
        MTKNT=MTKNT+1
        GOTO 30
      ENDIF
C
C..      LOOK FOR MULTIPLE SOLNS WITHIN TIME WINDOW
C
      IF(TMN.LE.CTIM.AND.ICNT.GE.2.AND.IN(IDN).EQ.1) GOTO 35
      IF(TMN.LE.CTIM.AND.ICNT.EQ.1.AND.IDN.EQ.LIDF) GOTO 30
C
      ICNT=ICNT+1
      IN(IDN)=1
C
C..      RECOVER THE PREVIOUS DF AND PUT IN SOLN SPACE
C
      IF(ITMP.EQ.1) THEN
        ITMP=0

```

```

        IN(LIDF)=1
      ENDIF
      LTIM=TMN
      LIDF=IDN
      GOTO 20
    ENDIF
  C
  C.. RESET THE POINTERS AND TIME VARIABLES
  C
30    ITMP=1
      FTIM=TMN
      LTIM=FTIM
      CTIM=FTIM+TCP
      CLOCK=FTIM+TCO
      LIDF=IDN
      ICNT=1
C20   IF (CLOCK.GT.201815..AND.CLOCK.LT.201818.) THEN
  C     WRITE(6,23) ICNT1,IDN,IN,ICNT,LIDF,LTIM,FTIM,CLOCK,CTIM
C23   FORMAT(1X,'ICNT1,IDN,IN,ICNT,LIDF ',9I6/1X,'LTIM,FTIM,CLOCK,
  C     CTIM FOR S23',4F12.3)
  C   ENDIF
  C   RETURN
20   RETURN
END
      SUBROUTINE ERSTAT(OBSAZ,RKM,DIFDEG,CBRG2)
CCCCCCCCCCCCCCCCCCCCCCCCCCCCCCCCCCCCCCCCCCCCCCCCCCCCCCCCCCCC
  C   SUBROUTINE ERSTAT SORTS DF ANGLE ERROR AS A FUNCTION OF
  C   ANGLE FOR ALL FIXES, AND IN BINS WITH ERROR ELLIPS LESS
  C   THAN 10 KM AND FLASHES WITHIN 400 KM OF DF.
  C
  CCCCCCCCCCCCCCCCCCCCCCCCCCCCCCCCCCCCCCCCCCCCCCCCCCCCCCCCCCCCC
  C   IMPLICIT DOUBLE PRECISION(A-H,O-Z)
      COMMON/COM1/IBFLAG,NREC,INCHK,IN(5),IN2(5)
      COMMON/SOLN/SNKA,SSGNL,TLAT,TLON,RADIUS,AREA,TSOLN,
      *IYDSN,IYR,MON,NDAY,NRS,NBR,IRES,NEVT,SMA,SMI,ORIEN
      COMMON/DFSTUF/DFE1(128),NS1(128),DFR10(128),NS10(128),
      ADFR15(128),NS15(128),SQ1(128),SQ10(128),SQ15(128)
      COMMON/SUMRY/KTWOER,NTHRS(4),NBAF,NBDF2,NDUP(4),NOVR(4),
      *NDFHT(4),KDVG
      COMMON/KOUNT/KNT1,KNT2,KNT3,KNT4,KNTHH,MTKNT,IDFTST,ISECOD
      COMMON/ECNST/TMX,RSML1,RSML2,RBIG,SBIG,BINSIZ
      DIMENSION AZM(129),ANWAZM(61),CBRG2(4)
      DATA AZM/0.,2.,5.,8.,11.,14.,16.,19.,22.,25.,28.,30.,33.,
      *36.,39.,42.,45.,47.,50.,53.,56.,59.,61.,64.,67.,70.,73.,
      *75.,78.,81.,84.,87.,90.,92.,95.,98.,101.,104.,106.,109.,
      *112.,115.,118.,120.,123.,126.,129.,132.,135.,137.,140.,
      *143.,146.,149.,151.,154.,157.,160.,163.,165.,168.,171.,
      *174.,177.,180.,182.,185.,188.,191.,194.,196.,199.,202.,205.,
      *208.,210.,213.,216.,219.,222.,225.,227.,230.,233.,236.,239.,
      *241.,244.,247.,250.,253.,255.,258.,261.,264.,267.,270.,272.,
      *275.,278.,281.,284.,286.,289.,292.,295.,298.,300.,303.,306.,
      *309.,312.,315.,317.,320.,323.,326.,329.,331.,334.,337.,340.,
      *343.,345.,348.,351.,354.,357.,360./
      DATA ANWAZM/0.,6.,12.,18.,24.,30.,36.,42.,48.,54.,60.,
      *66.,72.,78.,84.,90.,96.,102.,108.,114.,120.,126.,132.,138.,
      *144.,150.,156.,162.,168.,174.,180.,186.,192.,198.,204.,210.,
      *216.,222.,228.,234.,240.,246.,252.,258.,264.,270.,276.,282.,
      *288.,294.,300.,306.,312.,318.,324.,330.,336.,342.,348.,354.,
      *360./
  C   LI2=128
  C   LI2=60
  C   LIM1=LI2-1
      DO 15 II=1,LI2
  C     IF(OBSAZ.GE.AZM(II).AND.OBSAZ.LT.AZM(II+1)) THEN
      IF(OBSAZ.GE.ANWAZM(II).AND.OBSAZ.LT.ANWAZM(II+1)) THEN
        DFE1(II)=DFE1(II)+DIFDEG
        SQ1(II)=SQ1(II)+DIFDEG**2
        NS1(II)=NS1(II)+1
        IF (ABS(DIFDEG).LE.TMX) THEN
          IF (SMA.GT.0..AND.SMA.LE.SBIG.AND.RKM.GE.RSML1.AND.
          *RKM.LT.RBIG) THEN
            DFR10(II)=DFR10(II)+DIFDEG
            SQ10(II)=SQ10(II)+DIFDEG**2
            NS10(II)=NS10(II)+1
          ENDIF
          IF (SMA.GT.0..AND.SMA.LE.SBIG.AND.RKM.GE.RSML2.AND.
          *RKM.LT.RBIG) THEN
            DFR15(II)=DFR15(II)+DIFDEG
            SQ15(II)=SQ15(II)+DIFDEG**2
            NS15(II)=NS15(II)+1
          ENDIF
        ENDIF
      ENDIF

```

ORIGINAL PAGE IS  
OF POOR QUALITY

```

C      IF(II.EQ.14)THEN
C      WRITE(6,40) II,OBSAZ,DIFDEG,ANWAZM(II),DFE1(II),NS1(II),SMA,
C      *   DFR10(II),NS10(II),DFR15(II),NS15(II),SQ1(II),SQ10(II),
C      *   SQ15(II)
40      *   FORMAT(1X,'ERR STATS',I4,4F8.2,I4,2F8.2,I4,F8.2,I4,3(F8.2,
C      *   2X))
C      WRITE(6,44) TSOLN,TLAT,TLON,IN,IN2,CBRG2
44      *   FORMAT(1X,'SOLN ',F12.3,2F10.4,10I2,4F10.4)
C      ENDIF
C
C      ENDIF
15      CONTINUE
C
C      RETURN
C      END
C      SUBROUTINE ERSUM
CCCCCCCCCCCCCCCCCCCCCCCCCCCCCCCCCCCCCCCCCCCCCCCCCCCCCCCCCCCC
C      C
C      SUMMARIZES AND PRINTS THE DF ERROR STATISTICS
C      C
CCCCCCCCCCCCCCCCCCCCCCCCCCCCCCCCCCCCCCCCCCCCCCCCCCCCCCCCCCCC
C
C      IMPLICIT DOUBLE PRECISION(A-H,O-Z)
C      CHARACTER GDATE*8
C      COMMON/SOLN/SNKA,SSGNL,TLAT,TLON,RADIUS,AREA,TSOLN,
C      *IYDSN,IYR,MON,NDAY,NRS,NBR,IRES,NEVT,SMA,SMI,ORIEN
C      COMMON/DFSTUF/DFE1(128),NS1(128),DFR10(128),NS10(128),
C      ADFR15(128),NS15(128),SQ1(128),SQ10(128),SQ15(128)
C      COMMON/SUMRY/KTWOER,NTHRS(4),NBADF,NBDF2,NDUP(4),NOVR(4),
C      *NDFHT(4),KDVG
C      COMMON/KOUNTR/KNT1,KNT2,KNT3,KNT4,KNTHH,MTKNT,IDFTST,ISECOD
C      COMMON/ECNST/TMX,RSML1,RSML2,RBIG,SBIG,BINSIZ
C      EQUIVALENCE (NCNT,NBR)
C      DIMENSION AZM(129),ANWAZM(61)
C      DATA AMES,NT1,NT10,NT15/-999.99,0,0,0/
C      DATA AZM/0.,2.,5.,8.,11.,14.,16.,19.,22.,25.,28.,30.,33.,
C      *36.,39.,42.,45.,47.,50.,53.,56.,59.,61.,64.,67.,70.,73.,
C      *75.,78.,81.,84.,87.,90.,92.,95.,98.,101.,104.,106.,109.,
C      *112.,115.,118.,120.,123.,126.,129.,132.,135.,137.,140.,
C      *143.,146.,149.,151.,154.,157.,160.,163.,165.,168.,171.,
C      *174.,177.,180.,182.,185.,188.,191.,194.,196.,199.,202.,205.,
C      *208.,210.,213.,216.,219.,222.,225.,227.,230.,233.,236.,239.,
C      *241.,244.,247.,250.,253.,255.,258.,261.,264.,267.,270.,272.,
C      *275.,278.,281.,284.,286.,289.,292.,295.,298.,300.,303.,306.,
C      *309.,312.,315.,317.,320.,323.,326.,329.,331.,334.,337.,340.,
C      *343.,345.,348.,351.,354.,357.,360./
C      DATA ANWAZM/0.,6.,12.,18.,24.,30.,36.,42.,48.,54.,60.,
C      *66.,72.,78.,84.,90.,96.,102.,108.,114.,120.,126.,132.,138.,
C      *144.,150.,156.,162.,168.,174.,180.,186.,192.,198.,204.,210.,
C      *216.,222.,228.,234.,240.,246.,252.,258.,264.,270.,276.,282.,
C      *288.,294.,300.,306.,312.,318.,324.,330.,336.,342.,348.,354.,
C      *360./
C      LI3=128
C      LI3=60
C      WRITE(6,3000) NEVT,TSOLN,IYR,MON,NDAY,TLAT,TLON,SNKA,SSGNL,
C      *   NRS,RADIUS,AREA
3000      *   FORMAT(/1X,'LAST SOLN ON TAPE=',I6,2X,F12.3,1X,3I2,2F12.6,2X,
C      *   2F10.2,I2,2F8.2/)
C      WRITE(6,510) TSOLN,KNTHH,IYR,MON,NDAY
510      *   FORMAT(/1X,'FINAL HOURLY SUMMARY ON TAPE ENDING AT ',F12.3,
C      *   *' IS',I6,4X,'DATE=',3I2/)
C      WRITE(6,190) IDFTST,TMX,RSML1,RSML2,RBIG,SBIG,BINSIZ
190      *   FORMAT(1H1/1X,'ERROR SUMMARY FOR DF',I2//4X,' CONSTRAINTS:',
C      *   *5X,'MIN. ANGLE DEV.=' ,F4.1,' RANGES=' ,3F6.1,' MIN. SMA=' ,F6.1,
C      *   *' BEARING ANGLE BIN=' ,F4.1/)
C
C      IF IDFTST=0 THEN NOT WANTING SITE ERRORS, SKIP TO SUMMARY
C
C      IF(IDFTST.EQ.0) GOTO 600
C
C      WRITE(6,210)
210      *   FORMAT(/4X,'I',4X,'AZM',4X,'N',5X,
C      *   *'AV1',6X,'VAR',8X,'SD',6X,'N',6X,'AV10',6X,'VAR10',6X,'SD10',6X,
C      *   *'N',6X,'AV15',5X,'VAR15',6X,'SD15'/)
C      DO 15 IK=1,LI3
C      IF(NS1(IK).LE.1)THEN
C      X1=DFE1(IK)
C      V1=AMES
C      SD1=AMES
C      GOTO 300
C      ENDIF
C      AS1=FLOAT(NS1(IK))
C      ASM1=AS1-1.
C      X1=DFE1(IK)/AS1

```

ORIGINAL PAGE IS  
OF POOR QUALITY

```

      V1=(SQ1(IK) - DFE1(IK)**2/AS1)/ASM1
      SD1=SQRT(V1)
300      IF(NS10(IK).LE.1)THEN
            X10=DFR10(IK)
            V10=AMES
            SD10=AMES
            GOTO 400
      ENDIF
      AS10=FLOAT(NS10(IK))
      ASM10=AS10-1.
      X10=DFR10(IK)/AS10
      V10=(SQ10(IK) - DFR10(IK)**2/AS10)/ASM10
      SD10=SQRT(V10)
400      IF(NS15(IK).LE.1)THEN
            X15=DFR15(IK)
            V15=AMES
            SD15=AMES
            GOTO 500
      ENDIF
      AS15=FLOAT(NS15(IK))
      ASM15=AS15-1.
      X15=DFR15(IK)/AS15
      V15=(SQ15(IK) - DFR15(IK)**2/AS15)/ASM15
      SD15=SQRT(V15)

C
C..  WRITE SITE ERROR INFO TO DISK FILE AND TO PRINTER
C
      LUIN=10+IDFTST
500      WRITE(LUIN,110) IK,ANWAZM(IK),NS10(IK),X10,SD10
110      FORMAT(I4,1X,F5.1,I5,2F10.2)
      WRITE(6,100) IK,ANWAZM(IK),NS1(IK),X1,V1,SD1,NS10(IK),X10,
*          V10,SD10,NS15(IK),X15,V15,SD15
100      FORMAT(1X,I4,2X,F5.1,I5,3F10.2,I5,3F10.2,I5,3F10.2)
      NT1=NT1+NS1(IK)
      NT10=NT10+NS10(IK)
      NT15=NT15+NS15(IK)
15      CONTINUE
600      WRITE(6,601) NT1,NT10,NT15
601      FORMAT(1X,128(' '))//1X,'TOTAL NO. OF INPUTS',4X,'N1=',I6,4X,
*          'N10=',I6,4X,'N15=',I6)
      WRITE(6,611) KNT1,KNT2,KNT3,KNT4,KTWOER,NBADF,NBDF2,
*          NDFHT,NTHRS,NDUP,MTKNT,NOVR,KDVG
611      FORMAT(/2X,'NO. OF 1,2,3, OR 4 DF SOLNS=',4(I6,2X)/
*          2X,'NO. OF BAD REPEAT SOLNS=',I5,/
*          2X,'NO. OF NO-FIXES (NO SOLN) FROM FPIX=',I6,/
*          2X,'NO. OF BAD DF AZMS, ANGLE DEVIATION FROM SOLN TOO BIG=',I6,/
*          2X,'TOTAL NO. OF DF HITS=',4(I6,2X)/
*          2X,'NO. OF DF HITS BELOW MIN. AMPLITUDE OF 10=',4I6,/
*          2X,'NO. OF DF DUPLICATE HITS WITHIN TIME CORR. WINDOW=',4I6,/
*          2X,'NO. OF OCCURRENCES WITH LATEST TIME LESS THAN PREVIOUS=',I6/
*          2X,'NO. OF DIVERGENT DF ANGLE PAIRS=',I6/)
      CALL DATEG(GDATE)
      CALL TIME(ETIME)
      IHTIM=INT(ETIME/360000)
      AHTIM=FLOAT(ETIME)/360000.
      AMTIM=(AHTIM-IHTIM)*60.
      IMTIM=INT(AMTIM)
      ASTIM=60.*(AMTIM-IMTIM)
      STIM=FLOAT((IHTIM*100 +IMTIM)*100) +ASTIM
      WRITE(6,3) GDATE,STIM,IDFTST
3      FORMAT(/20X,'END LLP QUALITY CONTROL ANALYSIS'/20X,'(',A8,2X,
*          *F10.2,')',10X,'DF TEST=',I2)
      STOP
      END
      FUNCTION FKA(TAMP)
CCCCCCCCCCCCCCCCCCCCCCCCCCCCCCCCCCCCCCCCCCCCCCCCCCCCCCCCCCCC
C
C  FUNCTION FKA RECEIVES THE AMPLITUDES (AMP) OF THE DF'S
C  AND USES THE GREATEST SIGNAL STRENGTH (BMAX) TO COMPUTE
C  A RANGE NORMALIZED SIGNAL STRENGTH = DIST*BMAX, WHERE
C  DIST IS THE DISTANCE BETWEEN THE DF AND THE SOLN POINT.
C  THIS PRODUCT IS DIVIDED BY 298, A CALIBRATION FACTOR
C  BASED ON THE LLP ANTENNA AND LIN ET AL'S TRANSMISSION
C  LINE MODEL OF THE RETURN STROKE, RETURNS PEAK CURRENT
C  ESTIMATE FOR DISCHARGE
C
CCCCCCCCCCCCCCCCCCCCCCCCCCCCCCCCCCCCCCCCCCCCCCCCCCCCCCCCCCCC
      IMPLICIT DOUBLE PRECISION (A-H,O-Z)
      COMMON/COM1/IBFLAG,NREC,INCHK,IN(5),IN2(5)
      COMMON/SOLN/SNKA,SSGNL,TLAT,TLON,RADIUS,AREA,TSOLN,
*          IYDSN,IYR,MON,NDAY,NRS,NBR,IRES,NEVT,SMA,SMI,ORIEN
      COMMON/DFSTUF/DFE1(128),NS1(128),DFR10(128),NS10(128),
      ADFR15(128),NS15(128),SQ1(128),SQ10(128),SQ15(128)

```

ORIGINAL PAGE IS  
OF POOR QUALITY

```

COMMON/SUMRY/KTWOER,NTHRS(4),NBADF,NBDF2,NDUP(4),NOVR(4),
*NDFHT(4),KDVG
COMMON/KOUNTR/KNT1,KNT2,KNT3,KNT4,KNTHH,MTKNT,IDFTST,ISECOD
EQUIVALENCE (NCNT,NBR)
DIMENSION TAMP(4)
DIMENSION ALATI(4),ALONGI(4)
DATA ALATI/34.649167,35.399167,35.83750,34.716667/
DATA ALONGI/86.669167,86.076944,87.443889,87.881667/
DATA DTR,ERAD2,NST/0.01745329,6371.,4/
ISPOL=0
BMAX=0.
C
C.. FIND ID AND AMP OF LARGEST SIGNAL STRENGTH
C
DO 20 I=1,NCNT
    IF(TAMP(IN2(I)).GT.0.) ISPOL=ISPOL+1
    IF(ABS(TAMP(IN2(I))).GT.BMAX) THEN
        BMAX=ABS(TAMP(IN2(I)))
        KDF=IN2(I)
    ENDIF
20 CONTINUE
    IF(KDF.EQ.0) THEN
        WRITE(6,50) TSOLN,KDF,IN2,AZ2,R2,BMAX,SPOL,FKA,NCNT,TLAT,TLO,
        *RADIUS,TAMP
        FKA=-9999.
        RETURN
    ENDIF
C
C.. FIND POLARITY OF MAX AMPLITUDE (POSITIVE IFF ALL DFS POSITIVE)
C
    SPOL=-1.
    IF(ISPOL.EQ.NCNT) SPOL=1.
    RMAX2= BMAX*SPOL
    SSGNL=RMAX2
C
C.. FIND RANGE NORMALIZED DISTANCE
C
    SLAT = ALATI(KDF)*DTR
    SLONG = ALONGI(KDF)*DTR
    XTL2= TLAT*DTR
    XTLO2= TLO*DTR
    CALL AZRN(SLAT,SLONG,XTL2,XTLO2,AZ2,R2)
C
    FKA = R2*ERAD2*RMAX2/298.
C
    WRITE(6,50) TSOLN,KDF,IN2,AZ2,R2,BMAX,SPOL,FKA,NCNT,TLAT,TLO,
    *RADIUS,TAMP
50 FORMAT(/1X,'KA SOLN.. ',F12.3,1X,6I4,5F12.4/1X,' NCNT',I2,7F10.4)
    RETURN
    END
    FUNCTION SITERR(IDF,BRG)
CCCCCCCCCCCCCCCCCCCCCCCCCCCCCCCCCCCCCCCCCCCCCCCCCCCCCCCCCCCC
C
C FUNCTION SITERR RECEIVES A DIRECTION FINDER ID AND C
C AN UNCORRECTED BEARING HAVING A KNOWN SITE ERROR WHICH C
C CAN BE FOUND BY A LINEAR INTERPOLATION PROCEDURE APPLIED C
C TO A LOOK-UP TABLE FOR THAT DF C
C C
CCCCCCCCCCCCCCCCCCCCCCCCCCCCCCCCCCCCCCCCCCCCCCCCCCCCCCCCCCCC
C
COMMON/DFSTUF/DFE1(128),NS1(128),DFR10(128),NS10(128),
*DFR15(128),NS15(128),SQ1(128),SQ10(128),SQ15(128)
COMMON/KOUNTR/KNT1,KNT2,KNT3,KNT4,KNTHH,MTKNT,IDFTST,ISECOD
DIMENSION DF1(60),DF2(60),DF3(60),DF4(60),AZM(61)
DIMENSION DFA(128),DFB(128),DFC(128),DFD(128),AZM1(129)
DATA DF1/-2.47,-1.89,-1.65,-0.13,-1.02,-2.69,-3.57,
*-3.45,-4.00,-2.78,-7.0 ,0.83,1.08,0.89,
*2.14,2.69,3.4,4.09,4.90,5.58,5.39,5.38,5.59,5.89,6.03,6.72,
*6.51,6.44,6.86,7.14,7.04,6.56,6.29,6.21,-4.2,5.13,
*4.61,4.85,5.05,3.50,3.46,2.67,2.72,1.68,-1.2,-1.21,-1.20,
*-0.6,-0.42,-0.3,-0.4,-.87,-1.35,-1.3,-1.65,-4.18,
*-4.5,-3.99,-4.29,-3.53/
DATA DF2/-2.1,-1.4,-1.6,-1.6,-1.1,-0.2,0.01,-.15,-.21,
*-.46,-.74,-.61,.96,0.2,-1.7,-3.8,-5.5,-6.1,-6.6,-7.2,
*-5.6,-5.0,-6.8,-9.9,-12.2,-14.0,-14.8,-13.5,-11.6,-9.9,
*-8.0,-6.5,-4.6,-3.2,-0.8,-3.9,2.8,2.50,1.8,1.,-6.4,1.5,
*2.50,3.9,5.4,6.8,3.00,-2.1,-3.2,-2.8,-3.7,-6.6,-9.70,-10.7,
*-8.5,-6.1,-5.3,-3.8,-2.8,-2.3/

```

```

DATA DF3/-1.5,-1.2,-2.0,-2.0,-0.6,-1.7,-1.4,-1.3,-1.2,
*-1.2,-1.1,-0.9,-0.3,.1,0.3,0.50,-.30,-1.9,-0.8,0.4,
*-0.2,-1.5,-2.4,-3.3,-4.3,-5.2,-6.1,-7.0,-8.0,-8.9,-9.8,
*-8.9,-8.0,-7.1,-6.2,-5.3,-4.4,-5.5,-2.0,-1.5,-1.0,-0.46,
*0.05,0.6,1.1,1.6,2.1,2.6,3.1,3.1,2.9,2.1,0.2,-.7,-0.8,
*-2.7,-2.8,-1.5,-1.3,-1.4/
DATA DF4/-4,-.7,-.6,.24,.67,1.9,2.0,2.0,2.2,2.3,2.2,
*1.8,5.2,4.2,4.1,4.7,5.1,5.2,5.6,6.4,6.4,5.9,5.0,4.7,4.4,4.1,
*3.7,3.2,3.0,2.7,1.9,1.0,.22,.64,1.3,2.5,2.6,2.3,1.9,1.3,
*.68,.56,.62,.15,.07,-.2,.07,.05,.10,-.2,-.6,-.3,-.1,.5,1.3,
*1.7,1.2,.1,-0.01,-.3/
DATA DFA/-3.7,-2.3,-1.5,-2.0,-.9,.5,.9,.4,-.7,-1.3,
*-1.4,-1.9,-1.8,-3.6,-4.4,-5.5,-4.6,-3.6,-4.2,-2.8,
*-4.2,-2.7,-.2,-1.7,-1.1,1.4,-2.2,1.0,.5,.9,
*.1,2.,.8,0.0,.4,1.5,1.5,3.3,1.7,3.2,
*2.7,1.8,2.9,2.5,2.8,3.0,3.3,4.2,5.3,4.8,
*4.9,3.9,4.3,3.5,4.5,4.4,5.1,6.0,6.4,6.8,
*7.9,8.9,8.9,9.4,6.1,6.0,5.3,5.6,4.7,4.8,
*3.8,3.4,4.3,3.9,4.1,4.6,5.6,5.3,5.6,6.1,
*4.7,4.3,5.8,6.0,3.6,3.6,3.7,2.0,2.8,-3.4,
*-2.0,-1.5,.5,-4.0,.4,-3.7,-2.2,-3.8,-1.2,-4.4,
*-3.0,-2.6,-4.2,-1.7,-5.2,-4.9,-4.5,-7.1,-11.1,-5.4,
*-7.2,-5.8,-2.8,1.2,1.5,-2.4,-1.3,-1.5,-3.8,-2.5,
*-5.4,-.2,-2.0,-.8,-1.2,-.8,-.4,1.5/
DATA DFB/-2.3,-2.3,-1.6,-1.3,-1.5,-1.6,-1.7,-1.7,-1.5,
*-1.2,-0.8,-0.5,-0.3,-0.1,0.,0.,-0.1,-0.2,-0.2,-0.3,
*-0.4,-0.6,-0.7,-0.8,-0.7,-0.4,0.1,0.7,1.0,0.5,-0.6,-1.5,
*-2.3,-3.3,-4.5,-5.3,-5.7,-6.0,-6.2,-6.5,-6.9,-7.2,-7.0,
*-6.5,-5.8,-5.2,-5.0,-5.3,-6.2,-7.7,-9.4,-10.8,-11.9,-12.9,
*-13.8,-14.4,-14.7,-14.9,-14.7,-13.9,-12.8,-11.9,-11.1,
*-10.2,-9.2,-8.3,-7.5,-6.8,-5.9,-5.0,-4.3,-3.5,-2.4,-1.2,
*0.,1.,1.9,2.5,2.8,2.8,2.6,2.3,1.9,1.5,1.1,0.9,0.8,1.,
*1.4,1.7,2.2,3.3,3.3,3.7,4.3,5.1,6.1,6.8,6.1,3.9,1.1,-1.2,
*-2.8,-3.3,-3.1,-2.9,-2.7,-2.8,-3.4,-4.6,-6.1,-7.6,-9.1,
*-10.2,-10.7,-10.3,-9.0,-7.3,-6.3,-5.8,-5.4,-5.,-4.6,-4.1,
*-3.5,-3.,-2.3,-2.3/
DATA DFC/-1.4,-1.4,-1.6,-1.3,-1.1,-1.6,-2.4,-2.3,-1.4,
*-0.7,-0.6,-1.2,-1.7,-1.6,-1.4,-1.3,-1.3,-1.2,-1.1,
*-1.2,-1.2,-1.1,-1.0,-.9,-.8,-.7,-.4,-.1,.1,.2,.3,.4,.5,
*.5,0.,-.9,-1.7,-1.9,-1.2,-.1,.4,-.4,-.1,-.9,-1.6,-2.1,
*-2.5,-2.7,-2.9,-2.9,-2.8,-2.8,-2.8,-2.9,-3.1,-3.4,
*-3.7,-4.,-4.1,-4.2,-4.3,-4.4,-4.5,-4.5,-4.5,-4.5,-4.5,
*-4.5,-4.1,-3.6,-3.5,-4.1,-4.5,-4.4,-4.,-3.4,-2.7,-2.1,
*-1.7,-1.4,-1.1,-1.1,-1.2,-1.3,-1.4,-1.5,-1.3,-.9,-1.,
*-1.5,-1.9,-2.1,-2.,-1.7,-1.4,-1.1,-.6,.3,1.4,1.8,1.4,
*1.,1.3,2.6,3.8,3.9,3.2,2.6,2.2,1.6,.6,-.2,-.6,-.8,-.8,
*-1.3,-2.4,-3.1,-2.9,-2.5,-2.3,-1.8,-1.2,-1.2,-1.4,-1.4/
DATA DFD/-3,-.3,-.6,-.7,-.7,-.7,-.4,.1,.5,.6,.9,1.4,
*1.8,2.,2.,2.,2.1,2.2,2.3,2.3,2.3,2.2,2.1,1.9,1.6,1.7,
*2.6,3.6,4.1,4.1,4.1,4.3,4.6,4.9,5.1,5.2,5.2,5.3,5.5,5.9,
*6.3,6.5,6.6,6.5,6.3,6.,5.6,5.2,4.9,4.7,4.6,4.5,4.3,4.2,4.,
*3.8,3.6,3.5,3.3,3.1,3.,2.9,2.7,2.5,2.1,1.7,1.2,.7,.3,.2,.5,
*.9,1.2,1.6,2.1,2.4,2.6,2.6,2.5,2.4,2.2,2.,1.7,1.4,1.1,.8,.5,
*.5,.7,.8,.7,.4,2.,1.,1.,-1.,-2.,-1.0,.2,1.0,-.1,-1,-.2,
*-.3,-.4,-.6,-.6,-.4,0.,1.,1.,.4,.8,1.2,1.5,1.7,1.6,1.3,.9,
*.5,.2,.2,.1,-.3,-.3/
DATA AZH/0.,6.,12.,18.,24.,30.,36.,42.,48.,54.,60.,66.,72.,
*78.,84.,90.,96.,102.,108.,114.,120.,126.,132.,138.,144.,150.,
*156.,162.,168.,174.,180.,186.,192.,198.,204.,210.,216.,222.,
*228.,234.,240.,246.,252.,258.,264.,270.,276.,282.,288.,
*294.,300.,306.,312.,318.,324.,330.,336.,342.,348.,354.,360./
DATA AZM1/0.,2.,5.,8.,11.,14.,16.,19.,22.,25.,28.,30.,33.,
*36.,39.,42.,45.,47.,50.,53.,56.,59.,61.,64.,67.,70.,73.,
*75.,78.,81.,84.,87.,90.,92.,95.,98.,101.,104.,106.,109.,
*112.,115.,118.,120.,123.,126.,129.,132.,135.,137.,140.,
*143.,146.,149.,151.,154.,157.,160.,163.,165.,168.,171.,
*174.,177.,180.,182.,185.,188.,191.,194.,196.,199.,202.,205.,
*208.,210.,213.,216.,219.,222.,225.,227.,230.,233.,236.,239.,
*241.,244.,247.,250.,253.,255.,258.,261.,264.,267.,270.,272.,
*275.,278.,281.,284.,286.,289.,292.,295.,298.,300.,303.,306.,
*309.,312.,315.,317.,320.,323.,326.,329.,331.,334.,337.,340.,
*343.,345.,348.,351.,354.,357.,360./
DTR=0.01745329
C LI=128
LI=60
LI1=LI-1
IF (ISECOD.EQ.3) THEN
WRITE(6,32)
32 FORMAT(1H1/1X,'SITE ERROR TABLE'/)
DO 5 I=1,LI
WRITE(6,2) I,AZH(I),DF1(I),DF2(I),DF3(I),DF4(I)
2 FORMAT(1X, I4,5F10.2)
5 CONTINUE

```

```

ISECOD=-1
WRITE(6,33)
FORMAT(1H1)
33  ENDIF
NDF=4
DO 10 I=1,LI
  IF(BRG.GE.AZM(I).AND.BRG.LT.AZM(I+1)) THEN
C
    IF(IDF.EQ.1) THEN
      ER1=DF1(I)
      ER2=DF1(I+1)
      AZ1=AZM(I)
      AZ2=AZM(I+1)
    ELSE IF(IDF.EQ.2) THEN
      ER1=DF2(I)
      ER2=DF2(I+1)
      AZ1=AZM(I)
      AZ2=AZM(I+1)
    ELSE IF(IDF.EQ.3) THEN
      ER1=DF3(I)
      ER2=DF3(I+1)
      AZ1=AZM(I)
      AZ2=AZM(I+1)
    ELSE IF(IDF.EQ.4) THEN
      ER1=DF4(I)
      ER2=DF4(I+1)
      AZ1=AZM(I)
      AZ2=AZM(I+1)
    ENDIF
  ENDIF
10  CONTINUE
C
C..  PERFORM INTERPOLATION
C
  SLOPE=(ER2-ER1)/(AZ2-AZ1)
  SITERR=ER2-SLOPE*(AZ2-BRG)
  IF(IDF.GT.0) GOTO 909
C
C..  TEMPORARY CORRECTION TO DFS3 AND 1
C
  IF(IDF.EQ.3) THEN
    SITERR=-3.5+.6*SIN(2.*BRG*DTR)-5.1*COS(2.*BRG*DTR)
  ENDIF
  IF(IDF.EQ.IDFTST) SITERR=0.
  IF(IDF.EQ.1) SITERR=0.
  WRITE(6,25) IDF,BRG,SITERR
  FORMAT(1X,I2,2X,2(F6.2,2X))
25  DO 120 I=1,LI
    WRITE(6,35) I,DF2(I),DF3(I),DF4(I),AZM(I)
    FORMAT(1X,I4,4(F6.2,2X))
35  CONTINUE
C120 WRITE(6,399)
399  FORMAT(1X,'GOING BACK TO DFDATA')
909  RETURN
END
FUNCTION SITERC(IDF,BRG)
CCCCCCCCCCCCCCCCCCCCCCCCCCCCCCCCCCCCCCCCCCCCCCCCCCCCCCCCCCCC
C
C  FUNCTION SITERC IS A MOD TO SITERR USING CONSTRAINT
C  POINTS FROM VISUAL AND RADR CONFIRMATION OF CELL
C  LOCATION. USES A LINEAR INTERPOLATION PROCEDURE APPLIED
C  TO A LOOK-UP TABLE FOR THAT DF
C
CCCCCCCCCCCCCCCCCCCCCCCCCCCCCCCCCCCCCCCCCCCCCCCCCCCCCCCCCCCC
C
COMMON/SOLN/SNKA,SSGNL,TLAT,TLON,RADIUS,AREA,TSOLN,
*LYDSN,IYR,MON,NDAY,NRS,NBR,IRES,NEVT,SMA,SMI,ORIEN
COMMON/DFSTUF/DFE1(128),NS1(128),DFR10(128),NS10(128),
*DFR15(128),NS15(128),SQ1(128),SQ10(128),SQ15(128)
COMMON/KOUNTR/KNT1,KNT2,KNT3,KNT4,KNTHH,MTKNT,IDFTST,ISECOD
DIMENSION DF1(60),DF2(60),DF3(60),DF4(60),AZM(61)
DATA DF1/4.0,4.0,1.65,-0.13,-2.0,-5.0,2.0,
*4.0,-4.00,-5.0,-5.5,0.83,1.08,0.89,
*2.14,2.69,3.4,4.09,4.90,5.58,5.39,5.38,5.59,5.89,6.03,6.72,
*6.51,6.44,6.86,7.14,7.04,6.56,6.29,6.21,-4.2,5.13,
*4.61,4.85,5.05,-1.0,-1.0,2.67,2.72,1.68,-1.2,-1.21,-1.20,
*-0.6,-0.42,-3.0,-5.0,-.87,-1.35,-1.3,-1.2,-.5,
*0.5,0.5,0.5,2./
DATA DF2/-2.1,-1.4,-1.6,-1.6,-1.1,-0.2,0.01,-.15,-.21,
*-.46,-.74,-.61,-1.,-1.5,-1.7,-3.8,-5.5,-6.1,-6.6,-7.2,
*-5.6,-5.0,-6.8,-9.9,-12.2,-14.0,-14.8,-13.5,-11.6,-9.9,

```

00147223  
00147323  
00147423  
00147523  
00147723  
00147823  
00148023



```

C      IF (IDF.EQ.2) THEN
C      IF (BRG.GE.230..AND.BRG.LE.250.) THEN
C          SITERC=SITERC-6.
C      ENDIF
C  ENDIF
C      IF (IDF.EQ.1) THEN
C      IF (BRG.GE.330..AND.BRG.LE.340.) THEN
C          SITERC=SITERC+3.
C      ENDIF
C  ENDIF
C      IF (IDF.EQ.4) THEN
C      IF (BRG.GE.65..AND.BRG.LE.75.) THEN
C          SITERC=SITERC+1.5
C      ENDIF
C  ENDIF
C      IF (IDF.EQ.3) THEN
C          SITERR=-3.5+.6*SIN(2.*BRG*DTR)-5.1*COS(2.*BRG*DTR)
C      ENDIF
C      WRITE(6,25) IDF,BRG,SITERR
C      FORMAT(1X,I2,2X,2(F6.2,2X))
25  DO 120 I=1,LI
C      WRITE(6,35) I,DF2(I),DF3(I),DF4(I),AZM(I)
C      FORMAT(1X,I4,4(F6.2,2X))
35  CONTINUE
C120  WRITE(6,399)
C      399  FORMAT(1X,'GOING BACK TO DFDATA')
919  RETURN
C      END
C      FUNCTION SITER2(IDF,BRG)
CCCCCCCCCCCCCCCCCCCCCCCCCCCCCCCCCCCCCCCCCCCCCCCCCCCCCCCCCCCC
C      FUNCTION SITER2 RECEIVES A DIRECTION FINDER ID AND
C      AN UNCORRECTED BEARING HAVING A KNOWN SITE ERROR WHICH
C      CAN BE FOUND BY FITTING A POLYNOMIAL OF DEGREE 6.
C      CCCCCCCCCCCCCCCCCCCCCCCCCCCCCCCCCCCCCCCCCCCCCCCCCCCCCCCCCCCCC
C      COMMON/DFSTUF/DFE1(128),NS1(128),DFR10(128),NS10(128),
*DFR15(128),NS15(128),SQ1(128),SQ10(128),SQ15(128)
COMMON/KOUNTR/KNT1,KNT2,KNT3,KNT4,KNTHH,MTKNT,IDFTST,ISECD
DIMENSION DFA(60),DFB(60),DFC(60),DFD(60),AZM(61)
DIMENSION AO(4),AD1(12),AD2(12),AD3(12),AD4(12)
DATA AO/1.63,-3.33,-1.47,1.94/
DATA AD1/0.8788,-4.9730,-0.4359,0.2113,-0.2401,0.2218,
*0.4777,0.0991,0.8518,0.1006,0.4715,0.4008/
DATA AD2/-2.1636,1.6295,4.9684,-2.5906,-0.0242,1.3654,
*0.7188,0.7636,-1.6591,0.7491,0.2532,-0.1620/
DATA AD3/-0.3506,1.2770,-0.3550,-1.5981,-0.0535,-0.1957,
*0.4947,-0.1734,0.5484,0.4748,-0.2303,0.3460/
DATA AD4/2.0684,-1.2777,-0.6224,-0.6550,-0.3275,0.4715,
*0.0013,-0.5282,0.0014,-0.2151,-0.3507,-0.3409/
DATA DFA/-2.47,-1.89,-1.65,-0.13,-1.02,-2.69,-3.57,
*-3.45,-4.00,-2.78,-7.0,0.83,1.08,0.89,
*2.14,2.69,5.3,4.09,4.90,5.58,5.39,5.38,5.59,5.89,6.03,6.72,
*6.51,6.44,6.86,7.14,7.04,6.56,6.29,6.21,-4.2,5.13,
*4.61,4.85,5.05,3.50,3.46,2.67,2.72,1.68,2.0,-1.21,-1.20,
*-0.6,-0.42,-0.3,-0.4,-.87,-1.35,-1.3,-1.65,-4.18,
*-1.3,-3.99,-4.29,-3.53/
DATA DFB/-2.1,-1.4,-1.6,-1.6,-1.1,-0.2,0.01,-.15,-.21,
*-.46,-.74,-.61,.96,0.2,-1.7,-3.8,-5.5,-6.1,-6.6,-7.2,
*-5.6,-5.0,-6.8,-9.9,-12.2,-14.0,-14.8,-13.5,-11.6,-9.9,
*-8.0,-6.5,-4.6,-3.2,-0.8,-3.9,2.8,2.50,1.8,1.,-6.4,1.5,
*2.50,3.9,5.4,6.8,3.00,-2.1,-3.2,-2.8,-3.7,-6.6,-9.70,-10.7,
*-8.5,-6.1,-5.3,-3.8,-2.8,-2.3/
DATA DFC/-1.5,-1.2,-2.0,-2.0,-0.6,-1.7,-1.4,-1.3,-1.2,
*-1.2,-1.1,-0.9,-0.3,.1,0.3,0.50,-.30,-1.9,-0.8,0.4,
*-0.2,-1.5,-2.4,-3.3,-4.3,-5.2,-6.1,-7.0,-8.0,-8.9,-9.8,
*-8.9,-8.0,-7.1,-6.2,-5.3,-4.4,-5.5,-2.0,-1.5,-1.0,-0.46,
*0.05,0.6,1.1,1.6,2.1,2.6,3.1,3.1,2.9,2.1,0.2,-.7,-0.8,
*-2.7,-2.8,-1.5,-1.3,-1.4/
DATA DFD/-.4,-.7,-.6,.24,.67,1.9,2.0,2.0,2.2,2.3,2.2,
*1.8,5.2,4.2,4.1,4.7,5.1,5.2,5.6,6.4,6.4,5.9,5.0,4.7,4.4,4.1,
*3.7,3.2,3.0,2.7,1.9,1.0,.22,.64,1.3,2.5,2.6,2.3,1.9,1.3,
*.68,.56,.62,.15,.07,-.2,.07,.05,5.0,-.2,-.6,-.3,.1,.5,1.3,
*1.7,1.2,.1,-0.01,-.3/
DATA AZM/0.,6.,12.,18.,24.,30.,36.,42.,48.,54.,60.,66.,72.,
*78.,84.,90.,96.,102.,108.,114.,120.,126.,132.,138.,144.,150.,
*156.,162.,168.,174.,180.,186.,192.,198.,204.,210.,216.,222.,
*228.,234.,240.,246.,252.,258.,264.,270.,276.,282.,288.,
*294.,300.,306.,312.,318.,324.,330.,336.,342.,348.,354.,360./
DTR=0.01745329
LI=12
LI1=LI-1

```

```

      IF (ISECOD.EQ.2) THEN
        WRITE(6,32)
32      FORMAT(1H1/1X,'SITE ERROR POLYNOMIAL'/)
        WRITE(6,3) (AO(I),I=1,4)
3      FORMAT(1X,'AO=',4F10.4/)
        DO 5 I=1,12
          WRITE(6,2) I,AD1(I),AD2(I),AD3(I),AD4(I)
2          FORMAT(1X,I4,4F10.4)
5          CONTINUE
          ISECOD=-1
          WRITE(6,33)
33      FORMAT(1H1)
        ENDIF
        NDF=4
C
C.. CORRECTED BEARING ANGLE  Y=A0+A1SINX+A2COSX+...+A11SIN6X+A12COS6X
C
      STERM=0.
      CTERM=0.
      DO 20 J=1,6
        TJ=DTR*FLOAT(J)
        ITJ=(J-1)*2+1
        ICJ=(J-1)*2+2
        IF (IDF.EQ.1) THEN
          STERM=AD1(ITJ)*SIN(TJ*BRG)+STERM
          CTERM=AD1(ICJ)*COS(TJ*BRG)+CTERM
        ENDIF
        IF (IDF.EQ.2) THEN
          STERM=AD2(ITJ)*SIN(TJ*BRG)+STERM
          CTERM=AD2(ICJ)*COS(TJ*BRG)+CTERM
        ENDIF
        IF (IDF.EQ.3) THEN
          STERM=AD3(ITJ)*SIN(TJ*BRG)+STERM
          CTERM=AD3(ICJ)*COS(TJ*BRG)+CTERM
        ENDIF
        IF (IDF.EQ.4) THEN
          STERM=AD4(ITJ)*SIN(TJ*BRG)+STERM
          CTERM=AD4(ICJ)*COS(TJ*BRG)+CTERM
        ENDIF
20      CONTINUE
        SITER2=A0(IDF)+STERM+CTERM
C
        IF (IDF.EQ.IDFTST) SITER2=0.
C      WRITE(6,25) IDF,BRG,SITER2
25      FORMAT(1X,I2,2X,2(F6.2,2X))
C      DO 120 I=1,LI
C      WRITE(6,35) I,DF2(I),DF3(I),DF4(I),AZM(I)
35      FORMAT(1X,I4,4(F6.2,2X))
C120    CONTINUE
C      WRITE(6,399)
399    FORMAT(1X,'GOING BACK TO DFDATA')
909    RETURN
      END
      FUNCTION STDEVB(IDF,BRG)
CCCCCCCCCCCCCCCCCCCCCCCCCCCCCCCCCCCCCCCCCCCCCCCCCCCCCCCCCCCC
C
C  FUNCTION STDEVB RECEIVES A DIRECTION FINDER ID AND
C  AN BEARING ANGLE HAVING A KNOWN SITE ERROR WHICH
C  IS USED TO COMPUTE THE POLYNOMIAL FORM OF THE BEARING
C  STANDARD DEVIATION AS A FCN. OF ANGLE FOR USE IN FFI
C
C
CCCCCCCCCCCCCCCCCCCCCCCCCCCCCCCCCCCCCCCCCCCCCCCCCCCCCCCCCCCC
C
      COMMON/DFSTUF/DFE1(128),NS1(128),DFR10(128),NS10(128),
      *DFR15(128),NS15(128),SQ1(128),SQ10(128),SQ15(128)
      COMMON/KOUNTR/KNT1,KNT2,KNT3,KNT4,KNTHH,MTKNT,IDFTST,ISECOD
      DIMENSION SDA(60),SDB(60),SDC(60),SDD(60),AZM(61)
      DIMENSION BD0(4),BD1(12),BD2(12),BD3(12),BD4(12)
      DATA BD0/1.63,-3.33,-1.47,1.94/
      DATA BD1/0.8788,-4.9730,-0.4359,0.2113,-0.2401,0.2218,
      *0.4777,0.0991,0.8518,0.1006,0.4715,0.4008/
      DATA BD2/-2.1636,1.6295,4.9684,-2.5906,-0.0242,1.3654,
      *0.7188,0.7636,-1.6591,0.7491,0.2532,-0.1620/
      DATA BD3/-0.3506,1.2770,-0.3550,-1.5981,-0.0535,-0.1957,
      *0.4947,-0.1734,0.5484,0.4748,-0.2303,0.3460/
      DATA BD4/2.0684,-1.2777,-0.6224,-0.6550,-0.3275,0.4715,
      *0.0013,-0.5282,0.0014,-0.2151,-0.3507,-0.3409/
      DATA SDA/-2.47,-1.89,-1.65,-0.13,-1.02,-2.69,-3.57,
      *-3.45,-4.00,-2.78,-7.0,0.83,1.08,0.89,
      *2.14,2.69,5.3,4.09,4.90,5.58,5.39,5.38,5.59,5.89,6.03,6.72,
      *6.51,6.44,6.86,7.14,7.04,6.56,6.29,6.21,-4.2,5.13,
      *4.61,4.85,5.05,3.50,3.46,2.67,2.72,1.68,2.0,-1.21,-1.20,
      *-0.6,-0.42,-0.3,-0.4,-.87,-1.35,-1.3,-1.65,-4.18,
      *-1.3,-3.99,-4.29,-3.53/

```

```

DATA SDB/-2.1,-1.4,-1.6,-1.6,-1.1,-0.2,0.01,-.15,-.21,
*-46,-.74,-.61,.96,0.2,-1.7,-3.8,-5.5,-6.1,-6.6,-7.2,
*-5.6,-5.0,-6.8,-9.9,-12.2,-14.0,-14.8,-13.5,-11.6,-9.9,
*-8.0,-6.5,-4.6,-3.2,-0.8,-3.9,2.8,2.50,1.8,1.,-6.4,1.5,
*2.50,3.9,5.4,6.8,3.00,-2.1,-3.2,-2.8,-3.7,-6.6,-9.70,-10.7,
*-8.5,-6.1,-5.3,-3.8,-2.8,-2.3/
DATA SDC/-1.5,-1.2,-2.0,-2.0,-0.6,-1.7,-1.4,-1.3,-1.2,
*-1.2,-1.1,-0.9,-0.3,.1,0.3,0.50,-.30,-1.9,-0.8,0.4,
*-0.2,-1.5,-2.4,-3.3,-4.3,-5.2,-6.1,-7.0,-8.0,-8.9,-9.8,
*-8.9,-8.0,-7.1,-6.2,-5.3,-4.4,-5.5,-2.0,-1.5,-1.0,-0.46,
*0.05,0.6,1.1,1.6,2.1,2.6,3.1,3.1,2.9,2.1,0.2,-.7,-0.8,
*-2.7,-2.8,-1.5,-1.3,-1.4/
DATA SDD/-4,-.7,-.6,.24,.67,1.9,2.0,2.0,2.2,2.3,2.2,
*1.8,5.2,4.2,4.1,4.7,5.1,5.2,5.6,6.4,6.4,5.9,5.0,4.7,4.4,4.1,
*3.7,3.2,3.0,2.7,1.9,1.0,.22,.64,1.3,2.5,2.6,2.3,1.9,1.3,
*.68,.56,.62,.15,.07,-.2,.07,.05,5.0,-.2,-.6,-.3,.1,5,1.3,
*1.7,1.2,.1,-0.01,-.3/
DATA AZM/0.,6.,12.,18.,24.,30.,36.,42.,48.,54.,60.,66.,72.,
*78.,84.,90.,96.,102.,108.,114.,120.,126.,132.,138.,144.,150.,
*156.,162.,168.,174.,180.,186.,192.,198.,204.,210.,216.,222.,
*228.,234.,240.,246.,252.,258.,264.,270.,276.,282.,288.,
*294.,300.,306.,312.,318.,324.,330.,336.,342.,348.,354.,360./
DTR=0.01745329
LI=12
LI1=LI-1
IF (ISECOD.EQ.2) THEN
32   WRITE(6,32)
      FORMAT(1H1/1X,'SITE ERROR ST. DEV. POLYNOMIAL'/)
      WRITE(6,3) (B0(I),I=1,4)
3    FORMAT(1X,'B0=' ,4F10.4/)
      DO 5 I=1,12
      WRITE(6,2) I,BD1(I),BD2(I),BD3(I),BD4(I)
2    FORMAT(1X, I4,4F10.4)
5    CONTINUE
      ISECOD=-1
      WRITE(6,33)
33   FORMAT(1H1)
      ENDIF
      NDF=4
C
C.. CORRECTED BEARING ANGLE  Y=A0+A1SINX+A2COSX+...+A11SIN6X+A12COS6X
C
      STERM=0.
      CTERM=0.
      DO 20 J=1,6
        TJ=DTR*FLOAT(J)
        ITJ=(J-1)*2+1
        ICJ=(J-1)*2+2
        IF (IDF.EQ.1) THEN
          STERM=BD1(ITJ)*SIN(TJ*BRG)+STERM
          CTERM=BD1(ICJ)*COS(TJ*BRG)+CTERM
        ENDIF
        IF (IDF.EQ.2) THEN
          STERM=BD2(ITJ)*SIN(TJ*BRG)+STERM
          CTERM=BD2(ICJ)*COS(TJ*BRG)+CTERM
        ENDIF
        IF (IDF.EQ.3) THEN
          STERM=BD3(ITJ)*SIN(TJ*BRG)+STERM
          CTERM=BD3(ICJ)*COS(TJ*BRG)+CTERM
        ENDIF
        IF (IDF.EQ.4) THEN
          STERM=BD4(ITJ)*SIN(TJ*BRG)+STERM
          CTERM=BD4(ICJ)*COS(TJ*BRG)+CTERM
        ENDIF
20    CONTINUE
      STDEVB=B0(IDF)+STERM+CTERM
C    WRITE(6,25) IDF,BRG,STDEVB
25    FORMAT(1X,I2,2X,2(F6.2,2X))
C    DO 120 I=1,LI
C    WRITE(6,35) I,DF2(I),DF3(I),DF4(I),AZM(I)
35    FORMAT(1X,I4,4(F6.2,2X))
C120  CONTINUE
909   RETURN
      END
      SUBROUTINE FFIX(BRGID,TEMPBR,TM)
CCCCCCCCCCCCCCCCCCCCCCCCCCCCCCCCCCCCCCCCCCCCCCCCCCCCCCCCCCCC
CC   THIS PROGRAM IS A VECTOR APPROACH TO DF FIXING
CC   MODIFIED AT MSFC TO COMPUTE OPTIMAL LLP SOLNS FROM DF DATA
CC   AFTER SITE ERRORS REMOVED FROM DATA (SJG/01-05-86)
C CCCCCCCCCCCCCCCCCCCCCCCCCCCCCCCCCCCCCCCCCCCCCCCCCCCCCCCCCCCC
C
      IMPLICIT DOUBLE PRECISION(A-H,O-Z)
      DIMENSION TEMPBR(4),LOD(4),LOS(4),LOM(4),LAD(4),LAM(4),LAS(4)

```

```

DIMENSION BRGSV(50)
DIMENSION ISUB(50), IUSE(50)
CHARACTER*1 N,S,E,W,NORS,EORW
INTEGER KNAME(50), BRGID(4)
DIMENSION SIGX(4), TM(4)
DOUBLE PRECISION NXSX, NXSY, NXSZ
INTEGER SEQ1, SEQ2

DOUBLE PRECISION INVAR
INTEGER SAVE
DIMENSION SINT(32)
EQUIVALENCE (SINT(1), STAZ(1)), (NCNT, NBR), (IERR, IRES)
DIMENSION XHISQ(30)
COMMON K, NST, WBRF, INVAR(50), COST(50),
1 SING(50), COSG(50), STAX(50), STAY(50), STAZ(50), ISTA(50),
2 BRNX(50), BRNY(50), BRNZ(50), IL(50), SAVE(50), SWT(50),
3 NXSX(50), NXSY(50), NXSZ(50),
4 CHISQ(30), DTR, WT(50), TX, TY, TZ, E1, E2, E3,
5 C11, C22, C33, C13, C12, C23
COMMON/SOLN/SNKA, SSGNL, TLAT, TLO, RADIUS, AREA, TSOLN,
* IYDSN, IYR, MON, NDAY, NRS, NBR, IRES, NEVT, SMA, SMI, ORIEN
COMMON/KOUNTR/KNT1, KNT2, KNT3, KNT4, KNTHH, MTKNT, IDFTST, ISECOD
DATA N,S,E,W/'N','S','E','W'/
DATA KNAME/1,2,3,4,46*0/
DATA LOD/86,86,87,87/,
* LOM/40,04,26,52/,
* LOS/09,37,38,54/,
* LAD/34,35,35,34/,
* LAM/38,23,50,43/,
* LAS/57,57,15,00/
C ***** USING 20 PER CENT TABLES *****
DATA XHISQ/1.642,3.219,4.642,5.989,7.289,8.558,9.803,11.030,
B12.242,13.442,14.631,15.812,16.985,18.151,19.311,20.465,21.615,
C22.760,23.900,25.038,26.171,27.301,28.429,29.553,30.675,31.795,
D32.912,34.027,35.139,36.250/
C
IF(NBR.EQ.0) GOTO 869
IF(NBR.EQ.2) THEN
IF(BRGID(1).EQ.0.OR.BRGID(2).EQ.0) THEN
WRITE(6,1191) NBR, BRGID, TEMPBR, TM(1), TM(2)
1191 FORMAT(1X, 'NULL BRGID FOR NBR =', 5I3, 4F12.6, 2X, 2(F12.3, 2X))
GOTO 871
ENDIF
ENDIF
DTR = .01745329
TX=0.
TY=0.
TZ=0.
E1=0.
E2=0.
E3=0.
C11=0.
C22=0.
C33=0.
C13=0.
C12=0.
C23=0.
WBRF=0.
IFLSH=0
DO 101 II=1,30
101 CHISQ(II) = XHISQ(II)
C NST IS THE NUMBER OF STATIONS IN THE TABLE
C READ (5,1) NST
C 1 FORMAT(I3)
NST=4
DO 20 I=1,NST
C READ THE INDIVIDUAL STATION PARAMETERS
C READ(5,2) KNAME(I), LAD, LAM, LAS, LOD, LOM, LOS, SIGX(I)
2 FORMAT(A2, 6I4, 1X, F5.1)
SLAT = LAD(I) + (LAM(I) + LAS(I) / 60.) / 60.
SLONG = LOD(I) + (LOM(I) + LOS(I) / 60.) / 60.
SLAT = SLAT * DTR
C
C LONGITUDE INTERNAL TO THE PROGRAM IS NEGATIVE FOR WEST AND
C POSITIVE FOR EAST. DATA SUBMITTED AND PRINTED USES THE OPOSITE
C CONVENTIONS
C
SLONG = -SLONG * DTR
COSG(I) = DCOS(SLONG)
SING(I) = DSIN(SLONG)
COST(I) = DCOS(SLAT)
C COMPUTE THE STATION VECTOR(STAX, STAY, STAZ)
STAZ(I) = DSIN(SLAT)
STAX(I) = COST(I) * COSG(I)
STAY(I) = COST(I) * SING(I)

```

ORIGINAL PAGE IS  
OF POOR QUALITY

```

C      WRITE(6,324) STAX(I),STAY(I),STAZ(I)
C324  FORMAT(1X,3(F12.4,1X))
C
C      #####CALCULATE INVERSE STATION VARIANCE HERE
C
C..  SIGX IS THE STANDARD DEVIATION IN DEGREES OF BEARINGS FROM THIS
C      'DF ID#'=I. IT HAS LITTLE OR NO IMPACT ON THE SOLN, BUT THE
C      CONFIDENCE RADII ARE DIRECTLY PROPORTIONAL TO THE VALUE OF
C      SIGX. IN ADDITION, SOME DISTANT SOLNS MAY NOT BE COMPUTED
C      WHEN SIGX IS LARGE (SAY 1 DEG WITH SOLN 500 KM FROM DF).
C      SIGX(I)=1.5
C      WRITE(6,3) KNAME(I),LAD(I),LAM(I),LAS(I)
C      * ,LOD(I),LOM(I),LOS(I),SIGX(I)
C      3 FORMAT(1X,I2,6I6,F5.2)
C      20 CONTINUE
108    FORMAT(A3)
      INDSK=10
900    CONTINUE
      DO 301 IX=1,50
      IUSE(IX)=0
301    ISUB(IX)=0
C
C..  NBR IS THE NUMBER OF BEARINGS IN THIS FLASH
C
      IFLSH=IFLSH+1
      DO 40 J=1,NBR
C      READ(9,235) BRGID,TEMPBR(J)
235    FORMAT(1X,I11,1X,F6.2)
C      WRITE(6,241) BRGID,TEMPBR(J)
C241    FORMAT(1X,1A1,1X,F10.4)
      DO 38 I=1,NST
C      WRITE(6,646) BRGID,KNAME(I)
646    FORMAT(1X,2(I2,1X))
      IF(BRGID(J).EQ.KNAME(I)) GO TO 39
38    CONTINUE
C
C      STATION NOT IN TABLE SPACE
C
      IF(BRGID(J).NE.KNAME(I)) THEN
869      WRITE(6,873) NBR,BRGID,TM(BRGID(J))
873      FORMAT('STATION NOT IN TABLE SPACE; NBR= ',I2,', ID= ',I4,
      * 2X,F12.3)
871      IRES=-1
      GO TO 975
      ENDIF
39    ISTA(J)=I
      INVAR(J)=1/(DTR*SIGX(I))**2
      BRG=TEMPBR(J)*DTR
      BRGSV(J)=TEMPBR(I)
      CBRG = DCOS(BRG)
      SBRG = DSIN(BRG)
C
C      BEARING PLANE NORMAL VECTOR
C
C      COMPUTE THE BEARING VECTOR AS THE CROSS PRODUCT OF THE BEARING
C      PLANE NORMALS AND THE SITE VECTORS
C
      BRNX(J) = CBRG *SING(I)-SBRG *SINT(I)*COSG(I)
      BRNY(J) = -CBRG *COSG(I)-SBRG *SINT(I)*SING(I)
      BRNZ(J) = SBRG *COST(I)
C
      NXSX(J) = BRNY(J)*STAZ(I)-BRNZ(J)*STAY(I)
      NXSY(J) = BRNZ(J)*STAX(I)-BRNX(J)*STAZ(I)
      NXSZ(J) = BRNX(J)*STAY(I)-BRNY(J)*STAX(I)
40    CONTINUE
C
C
C      USE EXHAUSTIVE REJECTION FOR 10 OR LESS BEARINGS
C      USE SEQUENTIAL REJECTION FOR MORE THAN 10 BEARINGS
C      IF (NBR .LE.10) GO TO 50
      CALL SEQ
      GO TO 60
50    K = NBR
      CALL EXH
60    IF (IRES .NE. 1) GO TO 800
C      NREJ IS THE NUMBER OF REJECTED BEARINGS
C      K IS THE NUMBER OF BEARINGS USED IN THE FIX
      NREJ = NBR -K
C      WRITE(6,699) TLAT,TLON
699    FORMAT (' LAT=',F10.6,' LON=',F10.6)
      TLON=-TLON
      NORS=N
      EORW=E

```

ORIGINAL PAGE IS  
OF POOR QUALITY

```

C      WRITE(6,12) LTD,LTM,LTS,NORS,LND,LNM,LNS,EORW,SMA,SMI,ORIEN,AREA,
C      1 RADIUS
12     FORMAT(/,15X,'FIX',37X,'S-MAJ AXIS S-MIN AXIS ORIEN ELLIPSE
1AREA',/15X,'BPE',3I4,A1,2X,3I4,A1,8X,2(F6.1,5X),F5.1,4X,F8.1,
2/15X,'EQUIVALENT CIRCULAR RADIUS=',F6.1)
      DO 309 IX=1,K
309    IUSE(ISTA(IL(IX)))=IUSE(ISTA(IL(IX)))+1
C      WRITE(6,307)
307    FORMAT(4(/,15X,'BEARING UTILIZATION',//,15X,'PDDG',3X,'#SUBMITTE
1D',4X,'#USED',4X,'#REJECTED')
      DO 303 IX=1,50
      IF(ISUB(IX).EQ.0) GO TO 303
      NUSE=ISUB(IX)-IUSE(IX)
C      WRITE(6,302) KNAME(IX),ISUB(IX),IUSE(IX),NUSE
302    FORMAT(/,15X,I5,6X,I5,5X,I5,7X,I5)
303    CONTINUE
      NUSE=K+NREJ
C      WRITE(6,319) NUSE,K,NREJ
319    FORMAT(/,15X,'TOTAL',6X,I5,5X,I5,7X,I5)
      GO TO 950
800    IRES = 0
C      WRITE(6,14) IRES,IFLSH
14     FORMAT(1X,I1,I4,8X,'NO FIX' )
950    CONTINUE
C      GO TO 900
975    CONTINUE
      RETURN
      END
      SUBROUTINE EXH
CCCCCCCCCCCCCCCCCCCCCCCCCCCCCCCCCCCCCCCCCCCCCCCCCCCCCCCC
C
C      SETS UP FOR BEST POINT ESTIMATE
C
C      CCCCCCCCCCCCCCCCCCCCCCCCCCCCCCCCCCCCCCCCCCCCCCCCCCCC
C
      IMPLICIT DOUBLE PRECISION(A-H,O-Z)
      DOUBLE PRECISION NX SX,NX SY,NX SZ
      DOUBLE PRECISION INVAR
      INTEGER SAVE
      DIMENSION KLIM(10)
      COMMON K,NST,WBRF,INVAR(50),COST(50),
1 SING(50),COSG(50),STAX(50),STAY(50),STAZ(50),ISTA(50),
2 BRNX(50),BRNY(50),BRNZ(50),IL(50),SAVE(50),SWT(50),
3 NX SX(50),NX SY(50),NX SZ(50),
4 CHISQ(30),DTR,WT(50),TX,TY,TZ,E1,E2,E3,
5 C11,C22,C33,C13,C12,C23
      COMMON/SOLN/SNKA,SSGNL,TLAT,TLON,RADIUS,AREA,TSOLN,
* IYDSN,IYR,MON,NDAY,NRS,NBR,IRES,NEVT,SMA,SMI,ORIEN
      COMMON/KOUNTR/KNT1,KNT2,KNT3,KNT4,KNTHH,MTKNT,IDFTST,ISECOD
      EQUIVALENCE (NCNT,NBR),(IERR,IRES)
      DATA KLIM/3,3,3,3,3,3,4,4,5,5/
      DO 330 IP=1,4
C      WRITE(6,31) STAX(IP),STAY(IP),STAZ(IP)
31     FORMAT(1X,3(F12.4,1X),' IN EXH')
330    CONTINUE
10     CONTINUE
      DO 15 I = 1,K

```

ORIGINAL PAGE IS  
OF POOR QUALITY

```

10 CONTINUE
   DO 15 I = 1,K

      IL(I) = I
15 CONTINUE
   REJ = 1000.
C
C   IS STATION UNIQUE?
C
20 IS = ISTA(IL(1))
   DO 21 I = 2,K
      IF (IS .NE. ISTA(IL(I))) GO TO 25
21 CONTINUE
   GO TO 40
C
C   SET INITIAL WEIGHTS AND CALL BPE
C
25 CONTINUE
   DO 26 I=1,K
      WT(IL(I))=INVAR(IL(I))
26 CONTINUE
   CALL BPE(2)
C
C   IS BEARING SET BETTER THAN PREVIOUS BEST?
C
800 CONTINUE
   IF (WBRF .GE. REJ) GO TO 40
C
C   SAVE THIS CASE
C
   DO 30 I=1,K
      SAVE(I) = IL(I)
      SWT(IL(I))=WT(IL(I))
30 CONTINUE
   REJ = WBRF
C
C.. THIS FORCES FFIIX TO GET SOLN IN ONE PASS IF THERE
C.. ARE THREE OR LESS BEARINGS IN THE FIX.
C
   IF (K.LE.2) GOTO 60
C
C   FIND NEXT COMBINATION
C
40 I=K
41 CONTINUE
   IF (IL(I) .LT. NBR -K+I) GO TO 45
   IF (I .LE. 1) GO TO 50
   I = I - 1
   GO TO 41
45 J = I
46 IL(I) = IL(J)+1
   IF (I .GE. K) GO TO 20
   J = I
   I = I+1
   GO TO 46
C
C   ALL COMBINATIONS COMPLETE
C
50 WBRF = REJ
   IF (WBRF .LT. CHISQ(K-2)) GO TO 60
C
C   TRY SMALLER K
C
   IF (K .LE. KLIM(NBR)) GO TO 90
   K = K-1
   GO TO 10
C
C   OUTPUT RESULTS
C
60 CONTINUE
   DO 61 I=1,K
      IL(I) = SAVE(I)
      WT(IL(I))=SWT(IL(I))
61 CONTINUE
   CALL BPE(1)
   IRES=1
   CALL CONFID
   GO TO 999
90 IRES = 2
999 RETURN
   END
   SUBROUTINE SEQ
C

```

ORIGINAL PAGE IS  
OF POOR QUALITY

```

      IMPLICIT DOUBLE PRECISION(A-H,O-Z)
      DOUBLE PRECISION NXSX,NXSY,NXSZ
      DOUBLE PRECISION INVAR
      INTEGER SAVE
      COMMON K,NST,WBRF,INVAR(50),COST(50),
1 SING(50),COSG(50),STAX(50),STAY(50),STAZ(50),ISTA(50),
2 BRNX(50),BRNY(50),BRNZ(50),IL(50),SAVE(50),SWT(50),
3 NXSX(50),NXSY(50),NXSZ(50),
4 CHISQ(30),DFR,WT(50),TX,TY,TZ,E1,E2,E3,
5 C11,C22,C33,C13,C12,C23
      COMMON/SOLN/SNKA,SSGNL,TLAT,TLON,RADIUS,AREA,TSOLN,
* IYDSN,IYR,MON,NDAY,NRS,NBR,IRES,NEVT,SMA,SMI,ORIEN
      COMMON/KOUNTR/KNT1,KNT2,KNT3,KNT4,KNTHH,MTKNT,IDFTST,ISECOD
      EQUIVALENCE (NCNT,NBR),(IERR,IRES)
      K = NBR
      DO 15 I=1,K
      IL(I) = I
15 CONTINUE
      DO 20 I=1,K
      WT(I) = INVAR(I)
20 CONTINUE
21 CONTINUE
      CALL BPE(2)
C
C      TEST RESULTS
C
      M = K-2
      IF (K .GE. 33) GO TO 25
      IF (WBRF .LT. CHISQ(M)) GO TO 50
      GO TO 26
25 RM=M
      XCHI = DSQRT(2.0*WBRF)-DSQRT(2.0*RM-1.)
      IF (XCHI .LT. 0.842) GO TO 50
26 CONTINUE
C
C      NOT ACCEPTABLE - FIND BEARING TO REMOVE
C      IF (K .LE. (NBR+1)/2.) GO TO 900
      EMAX = 0.
      DO 30 I=1,K
      IB = IL(I)
C      FIND THE BEARING HAVING THE LARGEST WEIGHTED ERROR TO THE
C      CURRENT BPE( X )
      X = WT(IB)*(BRNX(IB)*TX+BRNY(IB)*TY+BRNZ(IB)*TZ)**2
      IF(0.LT.TX*NXSX(IB)+TY*NXSY(IB)+TZ*NXSZ(IB)) GO TO 60
      X=2*WT(IB)-X
60 CONTINUE
      IF (X .LE. EMAX) GO TO 30
      EMAX = X
C      SAVE THE INDEX OF THE BEARING TO BE REJECTED
      IS = I
C      WRITE(6,515) IS
515 FORMAT(1X,'REJECTED BEARING ID=',I4)
30 CONTINUE
      K = K-1
C      DELETE THE REJECTED BEARING FROM THE LIST
      DO 35 I=IS,K
      IL(I) = IL(I+1)
35 CONTINUE
C
C      IS STATION UNIQUE
C
      I1 = ISTA(IL(1))
      DO 40 I =2,K
      IF (ISTA(IL(I)) .NE.I1) GO TO 21
40 CONTINUE
C
C      NO FIX
C
900 IRES = 2
      GO TO 999
50 CONTINUE
      CALL BPE(1)
      IRES=1
      CALL CONFID
999 RETURN
      END
      SUBROUTINE BPE(ITER)
C
      IMPLICIT DOUBLE PRECISION(A-H,O-Z)
      DOUBLE PRECISION NXSX,NXSY,NXSZ
      DOUBLE PRECISION INVAR
      INTEGER SAVE

```

ORIGINAL PAGE IS  
OF POOR QUALITY

```

COMMON K,NST,WBRF,INVAR(50),COST(50),
1 SING(50),COSG(50),STAX(50),STAY(50),STAZ(50),ISTA(50),
2 BRNX(50),BRNY(50),BRNZ(50),IL(50),SAVE(50),SWT(50),
3 NXSX(50),NXSY(50),NXSZ(50),
4 CHISQ(30),DTR,WT(50),TX,TY,TZ,E1,E2,E3,
5 C11,C22,C33,C13,C12,C23
COMMON/SOLN/SNKA,SSGNL,TLAT,TLON,RADIUS,AREA,TSOLN,
* IYDSN,IYR,MON,NDAY,NRS,NBR,IRES,NEVT,SMA,SMI,ORIEN
COMMON/KOUNTR/KNT1,KNT2,KNT3,KNT4,KNTHH,MTKNT,IDFTST,ISECOD
EQUIVALENCE (NCNT,NBR), (IERR,IRES)
DATA RFN/1.0/
DO 100 KK=1,ITER
C11= 0.
C22= 0.
C33= 0.
C12= 0.
C13= 0.
C23= 0.
DO 6 I=1,K
J = IL(I)
C BUILD THE C MATRIX AS THE PRODUCT OF THE 3 BY N MATRIX OF THE
C WEIGHTED BEARING PLANE NORMAL VECTORS (BRNX,BRNY,BRNZ) AND
C ITS TRANSPOSE
C11=C11+WT(J)*BRNX(J)**2
C22=C22+WT(J)*BRNY(J)**2
C33=C33+WT(J)*BRNZ(J)**2
C12=C12+WT(J)*BRNX(J)*BRNY(J)
C13=C13+WT(J)*BRNX(J)*BRNZ(J)
C23=C23+WT(J)*BRNY(J)*BRNZ(J)
6 CONTINUE
CALL EIGEN(C11,C22,C33,C12,C13,C23,E1,E2,E3,TX,TY,TZ)
C WRITE(6,509) C11,C22,C33
509 FORMAT(1X,'C11,C22,C33= ',3(2X,F16.4))
C WRITE(6,509) C12,C13,C23
C WRITE(6,512) TX,TY,TZ,E1
512 FORMAT(1X,'X,Y,Z= ',4(2X,F12.7))
C WRITE(6,513) E1
C513 FORMAT(' E= ',F12.7)
C
C NEED ANTIPODE?
C
C ICT = 0
DO 10 I=1,K
J = IL(I)
IF (0 .LE. TX*NXSX(J)+TY*NXSY(J)+TZ*NXSZ(J)) ICT = ICT+1
10 CONTINUE
C IF ICT IS K ALL BEARINGS ARE FORWARD
C IF ICT IS 0 ALL BEARINGS ARE BACKWARD
IF (K .LE. 2*ICT) GO TO 11
TX = -TX
TY = -TY
TZ = -TZ
11 CONTINUE
DO 20 I= 1,K
J = IL(I)
L = ISTA(J)
C TDOTS IS THE COSINE OF THE DISTANCE OF THE BPE TO THE SITE
TDOTS = TX*STAX(L)+TY*STAY(L)+TZ*STAZ(L)
IF (TDOTS .GT. .99999) TDOTS = .99999
IF (TDOTS .LT. -.99999) TDOTS = -.99999
C
C INSERT RANGE WEIGHTING FUNCTION HERE
C NOTE RFN=1.0 GIVES BEST (SMALLEST) ERROR ELLIPSE FOR LLP
C THE COMPLICATED RFN RELATION ACCOUNTS FOR INCREASED VARIANCE
C IN THE BEARINGS DUE TO SKY WAVE EFFECTS WHEN SOLN CLOSE TO
C THE STATIONS (HIGH INCIDENCE ANGLE TO IONOSPHERE)- THIS IS
C AN IMPORTANT CONSIDERATION IN HF DIRECTION FINDING, NOT HERE.
C
C RGE = 34.44*DACOS(TDOTS)
C WRITE(6,222) RGE,TDOTS
C222 FORMAT(1X,'RGE AND TDOTS ARE ',2F12.3)
C IF (RGE .LT. 10.) GO TO 137
C IF (RGE .LT. 1.) GO TO 137
C RFN = .285714+RGE*.0714256
C GO TO 138
C 137 RFN = 3.-RGE*(.402-RGE*.0204)
C
C MODIFY THE WEIGHTS BY THE RANGE TO THE CURRENT BPE
C SEE STANSFIELD(1947) FOR WEIGHT
C
138 WT(J) = INVAR(J)/(RFN**2*(1.-TDOTS**2))
20 CONTINUE
100 CONTINUE

```

```

      WBRF = E1
      IF (K .EQ. ICT) RETURN
      IF (0 .EQ. ICT) RETURN
      WBRF = 2*K
      RETURN
      END
      SUBROUTINE EIGEN(D11,D22,D33,D12,D13,D23,E1,E2,E3,TX,TY,TZ)
      CCCCCCCCCCCCCCCCCCCCCCCCCCCCCCCCCCCCCCCCCCCCCCCCCCCCCCCCCCCCCC
      C
      C   THIS SUBROUTINE COMPUTES THE SMALLEST EIGENVALUE OF THE MATRIX C C
      C   THE EIGEN SUBROUTINE USES NEWTON ITERATION C C
      C C C
      CCCCCCCCCCCCCCCCCCCCCCCCCCCCCCCCCCCCCCCCCCCCCCCCCCCCCCCCCCCCCC
      C
      IMPLICIT DOUBLE PRECISION(A-H,O-Z)
      C11 = D11
      C22 = D22
      C33 = D33
      C12 = D12
      C13 = D13
      C23 = D23
      B = C11+C22+C33
      C = C11*(C22+C33)+C22*C33-(C12**2+C23**2+C13**2)
      A=C12/C11
      D=C11*(C22-C12*A)*(C33-C13*C13/C11-((C23-C13*A)**2)
      1 / (C22-C12*A))
      IF(D.GT.0) GO TO 13
      E1=0
      RETURN
13  CONTINUE
      X=0
      DO 10 I=1,10
      FX=X**3-B*X**2+C*X-D
      FP=3*X**2-2*B*X+C
      XN=X-FX/FP
      IF(XN.EQ.0) GO TO 12
      IF(ABS((XN-X)/XN).LT..0001) GO TO 12
      X=XN
10  CONTINUE
      C
      WRITE(6,107)
107  FORMAT(' 10 ITERATIONS INSUFFICIENT TO CONVERGE')
12  E1=XN
      CALL ETECT(E1,D11,D22,D33,D12,D13,D23,TX,TY,TZ)
      RETURN
      END
      SUBROUTINE ETECT(E1,C11,C22,C33,C12,C13,C23,TX,TY,TZ)
      CCCCCCCCCCCCCCCCCCCCCCCCCCCCCCCCCCCCCCCCCCCCCCCCCCCCCCCCCCCCCC
      C
      C   THIS SUBROUTINE COMPUTES THE EIGENVECTOR ASSOCIATED WITH THE C
      C   EIGEN VALUE E1 C
      C C C
      CCCCCCCCCCCCCCCCCCCCCCCCCCCCCCCCCCCCCCCCCCCCCCCCCCCCCCCCCCCCCC
      C
      IMPLICIT DOUBLE PRECISION(A-H,O-Z)
      D1 = (C11-E1)*(C22-E1)-C12**2
      IF (ABS(D1) .LE. .0001) GO TO 10
      X = C13*(E1-C22)+C12*C23
      Y = (E1-C11)*C23+C13*C12
      Z = D1
      GO TO 50
10  D2 = (C11-E1)*(C33-E1)-C13**2
      IF (ABS(D2) .LE. .0001) GO TO 20
      X = (E1-C33)*C12+C13*C23
      Y = D2
      Z = (E1-C11)*C23+C13*C12
      GO TO 50
20  X = (C22-E1)*(C33-E1)-C23**2
      Y = (E1-C33)*C12+C23*C13
      Z = (E1-C22)*C13+C23*C12
50  TEMP = DSQRT(X**2+Y**2+Z**2)
      TX = X/TEMP
      TY = Y/TEMP
      TZ = Z/TEMP
      RETURN
      END
      SUBROUTINE CONFID
      CCCCCCCCCCCCCCCCCCCCCCCCCCCCCCCCCCCCCCCCCCCCCCCCCCCCCCCCCCCCCC
      C
      C   COMPUTES THE CONFIDENCE ELLIPSE FOR GIVEN DF ANGLE ERROR C
      C   WHERE THE ANGLE STANDARD DEVIATION IS IN DEGREES C
      C   RETURNS ERROR RADIUS AND AREA FOR THIS ELLIPSE. C
      C C C
      CCCCCCCCCCCCCCCCCCCCCCCCCCCCCCCCCCCCCCCCCCCCCCCCCCCCCCCCCCCCCC
      C

```

ORIGINAL PAGE IS  
OF POOR QUALITY

```

      IMPLICIT DOUBLE PRECISION(A-H,O-Z)
      DOUBLE PRECISION NX SX,NXSY,NXSZ
      DOUBLE PRECISION INVAR
      INTEGER SAVE

C
      COMMON K,NST,WBRF,INVAR(50),COST(50),
1 SING(50),COSG(50),STAX(50),STAY(50),STAZ(50),ISTA(50),
2 BRNX(50),BRNY(50),BRNZ(50),IL(50),SAVE(50),SWT(50),
3 NX SX(50),NXSY(50),NXSZ(50),
4 CHISQ(30),DTR,WT(50),TX,TY,TZ,E1,E2,E3,
5 C11,C22,C33,C13,C12,C23
      COMMON/SOLN/SNKA,SSGNL,TLAT,TLOH,RADIUS,AREA,TSOLN,
*YDSN,IYR,MON,NDAY,NRS,NBR,IRES,NEVT,SMA,SMI,ORIEN
      COMMON/KOUNTR/KNT1,KNT2,KNT3,KNT4,KNTHH,MTKNT,IDFTST,ISECOD
C      FACT = EARTH RADIUS * DSQRT(-2 LN (1-P))
C      FACT IS IN UNITS OF NAUT. MI.; FOR P=.5, FACT=4055
C      FACT= 7391 FOR P=0.9
      DATA FACT /4055./
      MISS=10000.

C
      TLAT = DASIN(TZ)/DTR
      IF (ABS(TX).LE. 1.E-6) GO TO 10
      TLOH = ATAN (TY/TX)/DTR
      IF (TX .LE. 0.) TLOH = TLOH + 180.
      IF (TLOH .GT. 180.) TLOH = TLOH - 360.
      GO TO 15
10      TLOH = 90.
      IF (TY .LE. 0.) TLOH = -90.
15      CONTINUE
      C11 = 0.
      C22 = 0.
      C33 = 0.
      C12 = 0.
      C13 = 0.
      C23 = 0.
      DO 30 I=1,K
      J = ISTA(IL(I))
C      COMPUTE THE BEARING PLANE NORMAL VECTORS(BX,BY,BZ) TO THE BPE
      BX = STAY(J)*TZ-STAZ(J)*TY
      BY = STAZ(J)*TX-STAX(J)*TZ
      BZ = STAX(J)*TY-STAY(J)*TX
C      WRITE(6,222) COF,BX,BY,BZ,J,STAX(J),STAY(J),STAZ(J),TX,TY,TZ
C222      FORMAT(/1X,'COF ETC ',4F8.4,I2,2X,6(F8.4,2X))
      BSQAR=BX**2+BY**2+BZ**2
      IF(BSQAR.EQ.0.)THEN
        IRES=0
        GOTO 250
      ENDIF
      COF = WT(IL(I))/BSQAR
C      COMPUTE THE WEIGHTED C MATRIX
      C11 = C11+COF*BX**2
      C22 = C22+COF*BY**2
      C33 = C33+COF*BZ**2
      C12 = C12+COF*BX*BY
      C13 = C13 + COF*BX*BZ
      C23 = C23 + COF*BY*BZ
30      CONTINUE
      B = (C11+C22+C33)/2.
      C = C11*(C22+C33)+C22*C33-(C12**2+C13**2+C23**2)
      D = DSQRT(B**2-C)
      E2 = B-D
      E3 = B+D
C      COMPUTE THE CONFIDENCE REGION PARAMETERS
      SMA = FACT/DSQRT(E2)
      SMI = FACT/DSQRT(E3)
      CALL EVECT(E2,C11,C22,C33,C12,C13,C23,X,Y,Z)
      IF ((X*TY-Y*TX) .GT. 0.) Z = -Z
      TEMP = Z/DSQRT(1.-TZ**2)
      IF (1. .GE. ABS(TEMP)) GO TO 20
      ORIEN = 0.
      GO TO 22
20      CONTINUE
      ORIEN = DACOS(TEMP)/DTR
22      CONTINUE
      AREA = 3.14159*SMA*SMI
C      CIRCULAR REGION APPROXIMATION (NOT OUTPUT IN THIS VERSION)
      RATIO=(SMI/SMA)
      RADIUS=SMA*(.29294*(RATIO**2)-.063163*RATIO+.76996)
250      RETURN
      END

```

```

      SUBROUTINE NETFIX(I1,AZ1,I2,AZ2,XTL,XTLO)
      CCCCCCCCCCCCCCCCCCCCCCCCCCCCCCCCCCCCCCCCCCCCCCCCCCCCCC
      CC      THIS PROGRAM COMPUTES A TWO STATION FIX      CC
      CC      INPUT:  XSL1  =LAT OF STATION 1 (DEGREES)    CC
      CC                XSLO1 =LON OF STATION 1 (DEGREES)  CC
      CC                AZ1   =OBSERVED BEARING (DEGREES)   CC
      CC                XSL2  =LAT OF STATION 2 (DEGREES)   CC
      CC                XSLO2 =LON OF STATION 2 (DEGREES)   CC
      CC                AZ2   =OBSERVED BEARING (DEGREES)   CC
      CC      OUTPUT: XTL   =LAT OF TARGET (DEGREES)        CC
      CC                XTLO  =LON OF TARGET (DEGREES)       CC
      CC      MODIFIED FOR USE ON EADS                      CC
      CC      JAN 1987                                      CC
      CCCCCCCCCCCCCCCCCCCCCCCCCCCCCCCCCCCCCCCCCCCCCCCCCCCCCC
      C
      IMPLICIT DOUBLE PRECISION(A-H,O-Z)
      DOUBLE PRECISION LAD(4),LAM(4),LAS(4),LOD(4),LOM(4),LOS(4)
      DATA LAD/34.,35.,35.,34./
      A      ,LAM/38.,23.,50.,43./
      B      ,LAS/57.,57.,15.,00./
      C      ,LOD/86.,86.,87.,87./
      D      ,LOM/40.,04.,26.,52./
      E      ,LOS/09.,37.,38.,54./
      XSL1=LAD(I1)+(LAM(I1)+(LAS(I1)/60.))/60.
      XSLO1=LOD(I1)+(LOM(I1)+(LOS(I1)/60.))/60.
      XSL2=LAD(I2)+(LAM(I2)+(LAS(I2)/60.))/60.
      XSLO2=LOD(I2)+(LOM(I2)+(LOS(I2)/60.))/60.
      C      WRITE(6,901) XSL1,XSLO1,AZ1,XSL2,XSLO2,AZ2
      C901  FORMAT(1X,'NETFIX...XSL1,XSLO1,AZ1,XSL2,XSLO2,AZ2 ',6(F10.4,1X))
      PI=3.14159265359
      RAD=57.2957795131
      XSL1=XSL1/RAD
      XSLO1=XSLO1/RAD
      XSL2=XSL2/RAD
      XSLO2=XSLO2/RAD
      C
      C      COMPUTE RANGE (RADIAN) BETWEEN SITES
      C
      5      AZ1=AZ1/RAD
      AZ2=AZ2/RAD
      WRITE(6,19) XSL1,XSLO1,XSL2,XSLO2,AZ12,RN
      19      FORMAT(1X,'BEFORE AZRN ',6F12.4)
      CALL AZRN(XSL1,XSLO1,XSL2,XSLO2,AZ12,RN)
      CALL AZRN(XSL2,XSLO2,XSL1,XSLO1,AZ21,RN)
      C
      C      COMPUTE INCLUDED ANGLES
      C
      ANG1=DABS(AZ12-AZ1)
      IF(ANG1.GT.PI) ANG1=2.*PI-ANG1
      ANG2=DABS(AZ21-AZ2)
      IF(ANG2.GT.PI) ANG2=2.*PI-ANG2
      C
      C      COMPUTE 1/2 SUM AND DIFFERENCE ANGLES
      C
      SUM=0.5*(ANG2+ANG1)
      DIFF=0.5*(ANG2-ANG1)
      C
      C      SET UP FOR NAPIER ANALOGY SOLUTION
      C
      SINS=DSIN(SUM)
      SIND=DSIN(DIFF)
      COSS=DCOS(SUM)
      COSD=DCOS(DIFF)
      TANR=DTAN(0.5*RN)
      C
      C      COMPUTE LENGTH OF SIDE OPPOSITE STATION 2
      C
      ALN=DATAN(TANR*SIND/SINS)+DATAN(TANR*COSD/COSS)
      C
      C      COMPUTE LOCATION OF TARGET
      C
      CALL LOCLO(XSL1,XSLO1,ALN,AZ1,XTL,XTLO)
      XTL=XTL*RAD
      XTLO=XTLO*RAD
      C      WRITE(6,46) XTL,XTLO
      46      FORMAT(1X,'NETFIX...XTL,XTLO ',F12.7,2X,F12.7)
      RETURN
      END

```

ORIGINAL PAGE IS  
OF POOR QUALITY

```

      SUBROUTINE LOCLO(XLA,XLOT,RT,AT,XLATD,XLOTD)
      CCCCCCCCCCCCCCCCCCCCCCCCCCCCCCCCCCCCCCCCCCCCCCCCCCCCCCCCCC
      CC LOCLO COMPUTES THE LATITUDE AND CC
      CC LONGITUDE OF A POINT GIVEN: CC
      CC XLA =LAT OF REFERENCE PT(RAD) CC
      CC XLO =LONG OF REF PT(RAD) CC
      CC RT =GCB FROM REF PT TO TARGET CC
      CC AT =OBSERVED AZIMUTH (RAD) CC
      CC OUTPUT: XLATD =LAT OF PT IN QUESTION (RAD) CC
      CC XLOTD =LON OF PT IN QUESTION (RAD) CC
      CCCCCCCCCCCCCCCCCCCCCCCCCCCCCCCCCCCCCCCCCCCCCCCCCCCCCCCCCC
      C
      IMPLICIT DOUBLE PRECISION(A-H,O-Z)
      PI=3.1415926535
      XAT=AT
      XLO=-XLOT
      IF(AT.GT.PI) XAT=DABS(2.*PI-AT)
      XLARL=(PI/2.)-XLA
      XLATL=DACOS(DCOS(XLARL)*DCOS(RT)+DSIN(XLARL)*DSIN(RT)*DCOS(XAT))
      IF(XLATL.LT.0.) XLATL=PI+XLATL
      XLATD=(PI/2.)-XLATL
      BETA1=ATAN2((DSIN(0.5*(RT-XLARL))*DCOS(.5*XAT)),(DSIN(.5*
      C (RT+XLARL))*DSIN(.5*XAT)))
      BETA2=ATAN2((DCOS(.5*(RT-XLARL))*DCOS(.5*XAT)),(DCOS(.5*
      C (RT+XLARL))*DSIN(.5*XAT)))
      GAM=BETA1+BETA2
      IF(GAM.LT.0.0) GAM=(2.*PI)+GAM
      XLOTD=XLO+GAM
      IF(AT.GE.PI) XLOTD=XLO-GAM
      IF(XLOTD.LT.-PI) XLOTD=(2.*PI)-XLOTD
      IF(XLOTD.GT.PI) XLOTD=XLOTD-(2.*PI)
      ABVAL=DABS(XLOTD)+DABS(XLO)
      IF(((XLOTD*XLO).LT.0.).AND.(ABVAL.GT.PI)) XLOTD=2.*PI-XLOTD
      IF(XLOTD.GT.2.*PI) XLOTD=2.*PI-XLOTD
      RETURN
      END
      SUBROUTINE AZRN(XSL,XSLO,XTL,XTLO,AZ,R)
      CCCCCCCCCCCCCCCCCCCCCCCCCCCCCCCCCCCCCCCCCCCCCCCCCCCCCCCCCC
      CC THIS ROUTINE COMPUTES THE RANGE AND AZIMUTH CC
      CC FROM ONE GEOGRAPHICAL COORDINATE TO ANOTHER CC
      CC INPUT: XSL =LAT OF POINT S (RADIAN) CC
      CC XSLO =LON OF POINT S (RADIAN) CC
      CC XTL =LAT OF POINT T (RADIAN) CC
      CC XTLO =LON OF POINT T (RADIAN) CC
      CC OUTPUT: R =RANGE (RADIAN) CC
      CC AZ =AZIMUTH (RADIAN) CC
      CCCCCCCCCCCCCCCCCCCCCCCCCCCCCCCCCCCCCCCCCCCCCCCCCCCCCCCCCC
      C
      IMPLICIT DOUBLE PRECISION(A-H,O-Z)
      C INITIALIZE EAST WEST FLAG
      C
      C WRITE(6,33) XSL,XSLO,XTL,XTLO,AZ,R
      33 FORMAT(1X,'AZRN INPUT.. ',6F12.6)
      IEAWE=0
      PI=3.1415926535
      C
      C A : POLAR ANGLE OF SITE AND TARGET
      C
      A=DABS(XSLO-XTLO)
      C
      C BRANCH IF A IS GREATER THAN PI RADIAN
      IF(A.LE.PI) GO TO 10
      A=2.*PI-A
      IEAWE=1
      C
      C DS = DISTANCE (RAD) FROM SITE TO NORTH POLE
      C
      10 DS=PI/2.-XSL
      C
      C DT=DISTANCE (RAD) FROM TARGET TO NORTH POLE
      C
      DT=PI/2.-XTL
      C
      C AZ1 = .5*(AZ-B)
      C

```

```

      AZ1=ATAN2(DCOS(.5*A)*DSIN(.5*(DT-DS)),DSIN(.5*A)*DSIN(.5*(DT+DS)))
C
C  AZ2 = .5*(AZ+B)
      AZ2=ATAN2(DCOS(.5*A)*DCOS(.5*(DT-DS)),DSIN(.5*A)*DCOS(.5*(DT+DS)))
      AZ=AZ1+AZ2
C
C  USE LAW OF COSINES FOR SIDES
C
      R=DACOS(DCOS(DS)*DCOS(DT)+DSIN(DS)*DSIN(DT)*DCOS(A))
C
C  DISTANCE CANNOT BE NEGATIVE
C
      IF(R.LT.0.) R=-R
C
C  DETERMINE WHICH WAY TARGET IS FROM SITE
C
      IF((IEAWE.EQ.1).AND.(XSLO.LT.XTLO)) AZ=2.*PI-AZ
      IF((IEAWE.EQ.0).AND.(XTLO.LT.XSLO)) AZ=2.*PI-AZ
C
C  AZ CANNOT BE GT 2*PI OR LT 0.
C
      IF(AZ.GE.2.*PI) AZ=AZ-2.*PI
      IF(AZ.LT.0.) AZ=-AZ
C
C  CONVERT RADIANS TO KM
C
      AZ=2.*PI-AZ
      RETURN
      END
      SUBROUTINE YDDMY(SYD,DAY,MON,YR)
CCCCCCCCCCCCCCCCCCCCCCCCCCCCCCCCCCCCCCCCCCCCCCCCCCCCCCCCCCCC
C
C          CONVERT YYDDD (SYD) DAY,MONTH,YEAR
C  CONVERT   YYDDD TO DAY, MONTH, YEAR (VALID FROM 1901 TO 1999)
C  DAY = (I) OUTPUT DAY
C  MON = (I) OUTPUT MONTH
C  YR = (I) OUTPUT YEAR
C
CCCCCCCCCCCCCCCCCCCCCCCCCCCCCCCCCCCCCCCCCCCCCCCCCCCCCCCCCCCC
C
      IMPLICIT INTEGER (A-Z)
      DIMENSION DN(12,2)
      DATA DN/31,59,90,120,151,181,212,243,273,304,334,365,
      *      31,60,91,121,152,182,213,244,274,305,335,366/
C
C
      YY=INT(SYD/1000)
      DDD=MOD(SYD,1000)
      ILY=1
      IF (MOD(YY,4).EQ.0) ILY=2
      DO 20 ID=1,12
      IF (DDD.LE.DN(ID,ILY)) GOTO 21
20  CONTINUE
21  MON=ID
      DAY=DDD
      IF (MON.GT.1) DAY=DDD-DN(MON-1,ILY)
      YR=YY
C  WRITE(6,100) SYD,MON,DAY,YR
100 FORMAT(1X,'YYDDD',4I6)
      RETURN
      END

```

ORIGINAL PAGE IS  
OF POOR QUALITY

## APPENDIX C: CLUSTER ANALYSIS SOFTWARE

The cluster analysis software consists of programs to read the lightning data from a disk file, convert the lightning locations from spherical earth coordinates to rectangular coordinates within a user defined region from a user defined reference point, compute an extrapolation vector, compute seed points for input to the K-means algorithm, and write the results to an output file.

```

CCCCCCCCCCCCCCCCCCCCCCCCCCCCCCCCCCCCCCCCCCCCCCCCCCCCCCCCCCCC
CC CLUSTERING ALGORITHM FOR LTG DATA AND FCSTS OF Y/N AHEAD CC
CC GRID. READ FROM STAT2A WITH X,Y DATA, NOT LDATA CC
CCCCCCCCCCCCCCCCCCCCCCCCCCCCCCCCCCCCCCCCCCCCCCCCCCCCCCCCCCCC
C
  IMPLICIT DOUBLE PRECISION (A-H,O-Z)
  COMMON/SOLN/NEVT,TSOLN,IYR,MON,NDAY,TLAT,TLON,SNKA,SSGNL,NRS,
  * SMA,SMI,ORIEN,RADIUS,AREA
  COMMON/SETGRD/NROW,NCOL,IMIDPT,IRADII,INCR,X,Y,AZ
  COMMON/CM1/LGRID(50,50,40),LNUM(100,100),SGRID(100,100),
  * SNUM(100,100),AGRID(100,100),ANUM(100,100),A(8000,2)
  INTEGER SNUM,ANUM
  INTEGER IFRQ,IPRINT,IWT,KK,LDCM,LDSWT,LDX,MAXIT,JCOL,NOBS,NV,NVAR
  DIMENSION IN2(5),CBRG2(4),XBAR(40),YBAR(40)
  PARAMETER (IFRQ=0,IPRINT=0,IWT=0,KK=6,MAXIT=10,JCOL=2,
  * NOBS=62,NV=2,NVAR=2,LDCM=KK,LDSWT=KK,LDX=NOBS)
  INTEGER IC(NOBS),IND(NVAR),NOB1,NV1
  REAL CM(KK,NVAR),NC(KK),SWT(KK,NVAR),WSS(KK),SMTRIX(NOBS,NV)
  CHARACTER ILABEL(NOBS),ICHR(26)
  EXTERNAL KMEAN,WRIRN,WRRRN
  DATA ICHR/'A','B','C','D','E','F','G','H','I','J','K','L','M',
  * 'N','O','P','Q','R','S','T','U','V','W','X','Y','Z'/
  DATA IND/1,2/
  DATA CM(1,1),CM(1,2),CM(2,1),CM(2,2)/10.,60.,0.,0./
  DATA CM(3,1),CM(3,2),CM(4,1),CM(4,2)/20.,0.,-20.,-10./
  DATA CM(5,1),CM(5,2),CM(6,1),CM(6,2)/-70.,-20.,-50.,-30./
  DATA FL2LAT,FL2LON,DTR/0.604817,1.515038,0.017453/
  DATA CP2LAT,CP2LON/0.608223,1.515513/
  DATA BNALAT,BNALON/0.632682,1.510932/
  DATA CP4LAT,CP4LON/0.606008,1.515445/
  DATA ATIME,BTIME,BTIME2/223000.,223500.,223443./
  DATA ALAT,BLAT,ALON,BLON/34.0,36.5,86.0,90./
C
C.. ADD SYSTEM MOTION VECTOR HERE
C.. DT=0 GIVES OBSERVED DATA IF DX,DY USED THEN
C.. DT WILL BE 5-MIN TRANSLATION OF DATA AND CLUSTERS, DX,DY ARE
C.. SYSTEM DISPLACEMENT VECTORS FOR 5-MIN INTERVAL FOR EACH DT
C.. DT=2 IS 10 MIN ETC...
C
  ISTOP=1
  TINCR=5000.
  KZ=1
  DT=0.
  DX=4.45*DT
  DY=-7.95*DT
  DO 5 LC=1,KK
    CM(LC,1)=CM(LC,1)+DX
    CM(LC,2)=CM(LC,2)+DY
  5 CONTINUE
  XB=0.
  YB=0.
  IDAY=15
  KNUMB=0
  IRADII=200
  INCR=5
  NROW=(IRADII*2)/INCR
  NCOL=NROW
  IMIDPT=NROW/2
C *** READ IN NEXT RECORD FROM DISK FILE STAT2A_.
C
10 READ(10,5000) NNUMB,TSOLN,TLAT,TLON,X,Y
C CHECK FOR DAY OF INTEREST
C
  IF(NDAY.NE.IDAY) GOTO 10
  IF(TSOLN.GE.ATIME.AND.TSOLN.LT.BTIME.AND.NDAY.EQ.IDAY) THEN
  IF(TSOLN.GE.BTIME2) GOTO 37
  IF(TSOLN.LT.ATIME) GOTO 10
    WRITE(6,5000) NNUMB,TSOLN,TLAT,TLON,X,Y
    FORMAT(I6,2X,5(F12.5,1X))
  5000 IF(TSOLN.GE.BTIME) GOTO 37
  IF(TLAT.GE.ALAT.AND.TLAT.LT.BLAT.AND.TLON.GE.ALON.AND.TLON.
  * LT.BLON) THEN
C
C.. CALL AZRN IF NEED CONVERSION OF LAT/LON TO (X,Y) FROM REF. POINT
C
  CALL AZRN(FL2LAT,FL2LON,TARLT,TARLO,AZ,R)
  IF(R.LE.IRADII) THEN
C
C.. IF FORECASTING SYSTEM MOVEMENT, ADD TO X,Y BY DX,DY
C
  X=SIN(AZ)*R+DX
  Y=COS(AZ)*R+DY
  X=SIN(AZ)*R

```

```

C      Y=COS(AZ)*R
C      IF(Y.LE.100) GOTO 10
      X=X+DX
      Y=Y+DY
      SMTRIX(KNUMB+1,1)=X
      SMTRIX(KNUMB+1,2)=Y
      XB=XB+X
      YB=YB+Y
      KNUMB=KNUMB+1
      GOTO 10
60      CONTINUE
      WRITE(6,2211) NOBS,NVAR,LDX,IFRQ,IWT,(IND(J),J=1,NVAR),
*      KK,MAXIT
2211      FORMAT(1H1,1X,'NOBS ETC...',9I8/)
C
C.. ASSEMBLE 5 MIN GRIDS
C
37      DO 40 I=1,KNUMB
      JL=20+INT(SMTRIX(I,1)/10.)
      IL=20+INT(SMTRIX(I,2)/10.)
      LGRID(IL,JL,KZ)=LGRID(IL,JL,KZ)+1
      WRITE(6,2882) I,KNUMB,IL,JL,KZ
      WRITE(6,2883) (SMTRIX(I,JJ),JJ=1,2),LGRID(IL,JL,KZ)
2882      FORMAT(1X,'I,KNUMB,IL,JL,KZ,SMTRIX,LGRID',5(I4,2X))
2883      FORMAT(1X,2F8.2,2X,I6)
40      CONTINUE
C
C.. FIND MEAN X,Y OF DATA SET FOR SYSTEM MOTION VECTOR
C
      XBAR(KZ)=XB/KNUMB
      YBAR(KZ)=YB/KNUMB
      WRITE(6,2900) ATIME,BTIME,KNUMB,KZ,XBAR(KZ),YBAR(KZ),DX,DY,DT
      DO 80 IJ=1,40
      C      JI=40-IJ+1
      C      WRITE(6,2902) IJ,(LGRID(IJ,JJ,KZ),JJ=1,40)
      C      WRITE(6,2902) JI,(LGRID(JI,JL),JL=1,40)
80      CONTINUE
      WRITE(6,2904) (I,I=1,40)
2904      FORMAT(3X,40(1X,I2))
C      IF(ISTOP.EQ.1) STOP
2900      FORMAT(1H1/1X,'INTERVAL= ',F10.2,2X,F10.2,' KNUMB= ',I6,
*      ' KZ= ',I2,' XBAR SYSTEM= ',F8.2,' YBAR SYSTEM= ',F8.2/
*      ' DX= ',F8.2,' DY= ',F8.2,' DT= ',F8.2/)
2902      FORMAT(1X,I2,40(1X,I2))
      WRITE(6,1299) NOBS,XBAR(KZ),YBAR(KZ),DT,DX,DY,ATIME,BTIME
1299      FORMAT(1X,'NOBS FOR SYSTEM= ',I4,2X,'XBAR= ',F10.2,2X,'YBAR= ',
*      F10.2/2X,'DT = ',F8.2,2X,'DX= ',F8.2,2X,'DY= ',F8.2/2X,'INTERVAL= ',
*      F12.3,2X,F12.3/1H1/)
C
      DO 2213 JK=1,KK
      WRITE(6,2215) JK,(CM(JK,JJ),JJ=1,2)
2215      FORMAT(1X,'SEED ',I4/1X,2(F10.2,2X))
2213      CONTINUE
C      IF(NOBS.NE.-1) STOP
C
      CALL KMEAN(NOBS,JCOL,NVAR,SMTRIX,LDX,IFRQ,IWT,IND,KK,MAXIT,
*      CM,LDCM,SWT,LDSWT,IC,NC,WSS)
      CALL WRRRN('CM',KK,NVAR,CM,LDCM,0)
      CALL WRRRN('SWT',KK,NVAR,SWT,LDSWT,0)
      CALL WRIRN('IC',1,NOBS,IC,1,0)
      CALL WRIRN('NC',1,KK,NC,1,0)
      CALL WRRRN('WSS',1,KK,WSS,1,0)
      DO 2230 I=1,NOBS
      ILABEL(I)=ICHR(IC(I))
C      WRITE(6,2244) I,IC(I),ICHR(IC(I)),ILABEL(I)
C2244      FORMAT(2X,I4,2X,' IC= ',I4,A1,2X,A1)
2230      CONTINUE
      WRITE(6,6000)
6000      FORMAT(1H1/6X,'I',6X,'X',10X,'Y',6X,'CLUSTER'//)
      DO 4000 I=1,NOBS
      WRITE(6,4005) I,(SMTRIX(I,J),J=1,NV),IC(I),ILABEL(I)
      WRITE(11,4005) I,(SMTRIX(I,J),J=1,NV),IC(I),ILABEL(I)
4005      FORMAT(1X,I6,2X,2F10.2,2X,I4,2X,A1)
4000      CONTINUE
      KZ=KZ+1
      XB=0.
      YB=0.
      ATIME=ATIME+TINCR
      BTIME=BTIME+TINCR
      STOP
993      STOP
      END

```

```

CC PROGRAM AZRN
CCCCCCCCCCCCCCCCCCCCCCCCCCCCCCCCCCCCCCCCCCCCCCCCCCCC
CC THIS ROUTINE COMPUTES THE RANGE AND AZIMUTH CC
CC FROM ONE GEOGRAPHICAL COORDINATE TO ANOTHER CC
CC CC
CC INPUT: XSL =LAT OF POINT S (DEGREES) CC
CC XSLO =LON OF POINT S (DEGREES) CC
CC XTL =LAT OF POINT T (DEGREES) CC
CC XTLO =LON OF POINT T (DEGREES) CC
CC CC
CC OUTPUT: R =RANGE (KM) CC
CC AZ =AZIMUTH (RADIAN) CC
CC CC
CCCCCCCCCCCCCCCCCCCCCCCCCCCCCCCCCCCCCCCCCCCCCCCCCCCC
C
SUBROUTINE AZRN(XSL,XSLO,XTL,XTLO,AZ,R)
IMPLICIT DOUBLE PRECISION(A-H,O-Z)
CC
C INITIALIZE EAST WEST FLAG
C
IEAWE=0
PI=3.1415926535
C
C A : POLAR ANGLE OF SITE AND TARGET
C
A=DABS(XSLO-XTLO)
C
C BRANCH IF A IS GREATER THAN PI RADIAN
IF(A.LE.PI) GO TO 10
A=2.*PI-A
IEAWE=1
C
C DS = DISTANCE (RAD) FROM SITE TO NORTH POLE
C
10 DS=PI/2.-XSL
C
C DT=DISTANCE (RAD) FROM TARGET TO NORTH POLE
C
DT=PI/2.-XTL
C
C AZ1 = .5*(AZ-B)
C
AZ1=ATAN2(DCOS(.5*A)*DSIN(.5*(DT-DS)),DSIN(.5*A)*DSIN(.5*(DT+DS)))
C
C AZ2 = .5*(AZ+B)
C
AZ2=ATAN2(DCOS(.5*A)*DCOS(.5*(DT-DS)),DSIN(.5*A)*DCOS(.5*(DT+DS)))
AZ=AZ1+AZ2
C
C USE LAW OF COSINES FOR SIDES
C
R=DACOS(DCOS(DS)*DCOS(DT)+DSIN(DS)*DSIN(DT)*DCOS(A))
C
C DISTANCE CANNOT BE NEGATIVE
C
IF(R.LT.0.) R=-R
C
C DETERMINE WHICH WAY TARGET IS FROM SITE
C
IF((IEAWE.EQ.1).AND.(XSLO.LT.XTLO)) AZ=2.*PI-AZ
IF((IEAWE.EQ.0).AND.(XTLO.LT.XSLO)) AZ=2.*PI-AZ
C
C AZ CANNOT BE GT 2*PI OR LT 0.
C
IF(AZ.GE.2.*PI) AZ=AZ-2.*PI
IF(AZ.LT.0.) AZ=-AZ
C
C CONVERT RADIAN TO KM
C
AZ=2.*PI-AZ
R=R*6370.
RETURN
END

```

```

CCCCCCCCCCCCCCCCCCCCCCCCCCCCCCCCCCCCCCCCCCCCCCCCCCCCCCCCCCCC
CC  SEED ALGORITHM FOR LTG DATA AND FCSTS OF Y/N AHEAD          CC
CC  Program GRID21                                              CC
CCCCCCCCCCCCCCCCCCCCCCCCCCCCCCCCCCCCCCCCCCCCCCCCCCCCCCCCCCCC
C
  IMPLICIT DOUBLE PRECISION (A-H,O-Z)
  COMMON/SOLN/NEVT,TSOLN,IYR,MON,NDAY,TLAT,TLON,SNKA,SSGNL,NRS,
  * SMA,SMI,ORIEN,RADIUS,AREA
  COMMON/SETGRD/NROW,NCOL,IMIDPT,IRADII,INCR,X,Y,AZ
  COMMON/CM1/LGRID(50,50,40),LNUM(100,100),SGRID(100,100),
  * SNUM(100,100),AGRID(100,100),ANUM(100,100),A(8000,2)
  INTEGER SNUM,ANUM
  INTEGER IFRQ,IPRINT,IWT,KK,LDCM,LDSWT,LDX,MAXIT,JCOL,NOBS,NV,NVAR
  DIMENSION IN2(5),CBRG2(4),XBAR(40),YBAR(40),LSEED(40,40,40)
  INTEGER IC(8000),IND(2),NOB1,NV1
  REAL CM(80,2),NC(80),SWT(80,2),WSS(80),SMTRIX(8000,2)
  EQUIVALENCE (LDCM,KK),(LDSWT,KK),(LDX,NOBS)
  EXTERNAL KMEAN,WRIRN,WRRRN
  DATA IND/1,2/
  DATA IFRQ,IPRINT,IWT,MAXIT,JCOL,NV,NVAR/0,0,0,10,2,2,2/
C  DATA CM(1,1),CM(1,2),CM(2,1),CM(2,2)/-152.2,-49.3,-118.8,-27.2/
C  DATA CM(3,1),CM(3,2),CM(4,1),CM(4,2)/-89.0,-5.3,-49.9,-20.1/
C  DATA CM(5,1),CM(5,2),CM(6,1),CM(6,2)/-72.2,15.1,-54.3,53.8/
C  DATA CM(7,1),CM(7,2),CM(8,1),CM(8,2)/-23.2,119.5,29.5,129.0/
  DATA FL2LAT,FL2LON,DTR/0.604817,1.515038,0.017453/
  DATA CP2LAT,CP2LON/0.608223,1.515513/
  DATA BNALAT,BNALON/0.632682,1.510932/
  DATA CP4LAT,CP4LON/0.606008,1.515445/
  DATA ATIME,BTIME,BTIME2/214500.,215000.,223443./
  DATA ALAT,BLAT,ALON,BLON/34.0,36.5,86.0,90./
C
C.. ADD SYSTEM MOTION VECTOR HERE
C.. DT=0 GIVES OBSERVED DATA IF DX,DY USED THEN
C.. DT WILL BE 5-MIN TRANSLATION OF DATA AND CLUSTERS, DX,DY ARE
C.. SYSTEM DISPLACEMENT VECTORS FOR 5-MIN INTERVAL FOR EACH DT
C.. DT=2 IS 10 MIN ETC...
C
  ISTOP=1
  TINCR=5000.
  KZ=1
  DT=0.
  DX=4.45*DT
  DY=-7.95*DT
  WRITE(6,2233) ATIME,BTIME,DT,DX,DY
2233 FORMAT(1H1,1X,'TIME INTERVAL PROCESSED =',2F10.2,' DT,DX,DY=',
  *3F8.2/)
  DO 5 LC=1,KK
    CM(LC,1)=CM(LC,1)+DX
    CM(LC,2)=CM(LC,2)+DY
  5  CONTINUE
  XB=0.
  YB=0.
  IDAY=15
  KNUMB=0
  IRADII=200
  INCR=5

  NROW=(IRADII*2)/INCR
  NCOL=NROW
  IMIDPT=NROW/2
C *** READ IN NEXT RECORD FROM DISK FILE STAT2A_.
C
10  READ(10,5000,END=993) NNUMB,TSOLN,TLAT,TLON,X,Y
  IF(TSOLN.GE.BTIME2) GOTO 37
  IF(TSOLN.LT.ATIME) GOTO 10
C  WRITE(6,5000) NNUMB,TSOLN,TLAT,TLON,X,Y
5000 FORMAT(16,2X,5(F12.5,1X))
  IF(TSOLN.GE.BTIME) GOTO 37
  X=X+DX
  Y=Y+DY
  SMTRIX(KNUMB+1,1)=X
  SMTRIX(KNUMB+1,2)=Y
  XB=XB+X
  YB=YB+Y
  KNUMB=KNUMB+1
  GOTO 10
60  CONTINUE
37  NOBS=KNUMB
  WRITE(6,2211) NOBS,NVAR,LDX,IFRQ,IWT,(IND(J),J=1,NVAR),
  * KK,MAXIT
2211 FORMAT(1H1,1X,'NOBS ETC...',9I8/)

```

```

C
C.. ASSEMBLE 5 MIN GRIDS
C
  DO 40 I=1,KNUMB
    JL=20+INT(SMTRIX(I,1)/10.)
    IL=20-INT(SMTRIX(I,2)/10.)
    LGRID(IL,JL,KZ)=LGRID(IL,JL,KZ)+1
    LSEED(IL,JL,KZ)=LGRID(IL,JL,KZ)
40  CONTINUE
C
C.. FIND SET OF SEEDS FROM DENSITY GRID
C
  DO 90 IL=2,39
  DO 90 JL=2,39
    N1=LSEED(IL-1,JL-1,KZ)
    N2=LSEED(IL-1,JL,KZ)
    N3=LSEED(IL-1,JL+1,KZ)
    N4=LSEED(IL,JL-1,KZ)
    N5=LSEED(IL,JL,KZ)
    N6=LSEED(IL,JL+1,KZ)
    N7=LSEED(IL+1,JL-1,KZ)
    N8=LSEED(IL+1,JL,KZ)
    N9=LSEED(IL+1,JL+1,KZ)
    M1=LGRID(IL-1,JL-1,KZ)
    M2=LGRID(IL-1,JL,KZ)
    M3=LGRID(IL-1,JL+1,KZ)
    M4=LGRID(IL,JL-1,KZ)
    M5=N5
    M6=LGRID(IL,JL+1,KZ)
    M7=LGRID(IL+1,JL-1,KZ)
    M8=LGRID(IL+1,JL,KZ)
    M9=LGRID(IL+1,JL+1,KZ)
    IF(N5.LE.N1.OR.N5.LE.N2.OR.N5.LE.N3.OR.N5.LE.N4.OR.N5.LE.N6.
*   OR.N5.LE.N7.OR.N5.LE.N8.OR.N5.LE.N9) LSEED(IL,JL,KZ)=0
    IF(M5.LT.M1.OR.M5.LT.M2.OR.M5.LT.M3.OR.M5.LT.M4.OR.M5.LT.M6)
*   LSEED(IL,JL,KZ)=0
90  CONTINUE
    WRITE(6,190) ATIME,BTIME
190  FORMAT(1H1/1X,'TIME INTERVAL',2F10.2/2X,'FIRST GUESS FOR SEEDS'/)
    DO 95 IJ=1,40
      WRITE(6,2902) IJ,(LSEED(IJ,JJ,KZ),JJ=1,40)
95  CONTINUE
      WRITE(6,2904) (I,I=1,40)
C
C.. CONVERT GRID POINT INDEXES INTO X,Y POINTS FOR SEEDING CLUSTERS
C
  KK=0
  DO 110 I=1,40
  DO 110 J=1,40
    IF(LSEED(I,J,KZ).GT.0) THEN
      K1=KK+1
      CM(K1,1)=FLOAT(J-20)*10.+DX
      CM(K1,2)=FLOAT(20-I)*10.+DY
      WRITE(6,2220) I,J,KZ,K1,LSEED(I,J,KZ),(CM(KK+1,JJ),JJ=1,2)
2220  FORMAT(1X,'I,J,KZ,K1 ',4I4,' VALUE=',I4,' SEED(X,Y)=' ,2F8.2)
      KK=KK+1
    ENDIF
110  CONTINUE
C
C.. FIND MEAN X,Y OF DATA SET FOR SYSTEM MOTION VECTOR
C
  XBAR(KZ)=XB/KNUMB
  YBAR(KZ)=YB/KNUMB
  WRITE(6,2900) ATIME,BTIME,KNUMB,KZ,XBAR(KZ),YBAR(KZ),DX,DY,DT
2900  FORMAT(1H1/1X,'INTERVAL= ',F10.2,2X,F10.2,' KNUMB= ',I6,
*   ' KZ=',I2,' (XBAR,YBAR) SYSTEM=(',F6.1,',',F6.1,',')'/
*   ' DX=',F8.2,' DY=',F8.2,' DT=',F8.2/)
C
  DO 80 IJ=1,40
  JI=40-IJ+1
  WRITE(6,2902) IJ,(LGRID(IJ,JJ,KZ),JJ=1,40)
2902  FORMAT(1X,I2,40(1X,I2))
80  CONTINUE
  WRITE(6,2904) (I,I=1,40)
2904  FORMAT(3X,40(1X,I2))
  WRITE(6,1299) NOBS, KK, XBAR(KZ), YBAR(KZ), DT, DX, DY, ATIME, BTIME
1299  FORMAT(1X, 'NOBS, SEEDS=',2I4,2X,'XBAR= ',F10.2,2X,'YBAR= ',
*   F10.2,2X,'DT =',F8.2,2X,'DX= ',F8.2,2X,'DY= ',F8.2,2X,'INTERVAL',
*   F12.3,2X,F12.3/)
  IF(ISTOP.EQ.1) STOP 993
993  STOP
  END

```

ORIGINAL PAGE IS  
OF POOR QUALITY

## BIBLIOGRAPHY

- Abraham, B., and J. Ledolter, 1983. Statistical Methods for Forecasting. New York: John Wiley & Sons.
- Anderberg, M. R., 1973. Cluster Analysis for Applications. New York: Academic Press, Inc.
- Austin, G. L., and A. Bellon, 1974. The use of digital weather records for short-term precipitation forecasting. Q. J. R. Meteor. Soc., 100, 658-664.
- Barclay, P. A., and K. E. Wilk, 1970. Severe thunderstorm radar echo motion and related weather events hazardous to aviation operations. Tech. Memo. ERLTM-NSSL 46, 63pp., Environ. Sci. Serv. Admin., Boulder, Colo.
- Bard, Y., 1974. Nonlinear Parameter Estimation. New York: Academic Press, Inc.
- Bent, R. B., and W. A. Lyons, 1984. Theoretical evaluations and initial operating experiences of LPATS (Lightning Positioning and Tracking System) to monitor lightning ground strikes using a time-of-arrival (TOA) technique, Preprints, VII Int. Conf. on Atmospheric Electricity, Albany, NY, Am. Meteor. Soc., Boston, 317-324.
- Bjerkaas, C. L., and D. E. Forsyth, 1980. An automated real-time storm analysis and tracking program (WEATRK). Air Force Geophysics Laboratory Tech. Rep.
- Blackmer, R. H., Jr., and R. O. Duda, 1972. Application of pattern recognition techniques to digitized radar data. Proc. 15th Radar Meteor. Conf., Am. Meteor. Soc., Boston, 138-143.  
80-0316.
- Box, G. E. P., and G. M. Jenkins, 1976. Time Series Analysis: Forecasting and Control, 2nd ed., San Francisco: Holden-Day.
- Boyce, W. E., and R. C. DiPrima, 1977. Elementary Differential Equations and Boundary Value Problems, 3rd ed. New York: John Wiley & Sons, Inc.
- Brasunas, J. C., 1984. A comparison of storm tracking and extrapolation algorithms. FAA Rep. DOT-FAA-PM 84-1. (Available from National Technical Information Service, U. S. Dept. of Commerce, Springfield, VA 22161)
- Browning, K. A., C. G. Collier, P. R. Larke, P. Menmuir, G. A. Monk, and R. G. Owens, 1982. On the forecasting of frontal rain using a weather radar network, Mon. Wea. Rev., 110, 534-552.
- Browning, K. A., and C. G. Collier, 1989. Nowcasting of precipitation systems. Rev. Geophysics, 27, 345-370.

- Buechler, D. E., S. J. Goodman, and M. E. Weber, 1988. Cloud-to-ground lightning activity in microburst-producing storms. Preprints, 15th Conf. on Severe Local Storms, Baltimore, MD, Am. Meteor. Soc., 496-500.
- \_\_\_\_\_, and \_\_\_\_\_, 1990. Echo size and asymmetry: Impact on NEXRAD storm identification. J. Appl. Meteor., 29, in press.
- Byers, H. R., and R. R. Braham, Jr., 1949. The Thunderstorm. U. S. Govt. Printing Office, Washington, DC.
- Cherna, E. V., and E. J. Stansbury, 1986. Sferics rate in relation to thunderstorm dimensions. J. Geophys. Res., 91, 8701-8707.
- Christian, H. J., R. J. Blakeslee, and S. J. Goodman, 1989. The detection of lightning from geostationary orbit. J. Geophys. Res., 94, 13329-13337.
- Crane, R. K., 1979. Automatic cell detection and tracking. IEEE Trans. on Geoscience Electronics, GE-17, 250-262.
- Dodge, J., J. Arnold, G. Wilson, J. Evans, and T. Fujita, 1986. The Cooperative Huntsville Meteorological Experiment (COHMEX). Bull. Amer. Meteor. Soc., 67, 417-419.
- Donaldson, R. J., Jr., R. M. Dyer, and M. J. Kraus, 1975. An objective evaluator of techniques for predicting severe weather events. Preprints, 9th Conf. Severe Local Storms, Norman, OK, Amer. Meteor. Soc., Boston, 321-326.
- Doswell, C. A., 1986. "Short-range forecasting." In Mesoscale Meteorology and Forecasting, ed. Peter S. Ray, American Meteorological Society, Boston, MA, 689-719.
- Draper, N. R., and H. Smith, 1981. Applied Regression Analysis, 2nd ed. New York: John Wiley & Sons.
- Elvander, R. C., 1976. An evaluation of the relative performance of three weather radar echo forecasting techniques. Preprints, 17th Radar. Meteor. Conf., Seattle, Wash., Am. Meteor. Soc., Boston, 526-532.
- Engholm, C. D., E. R. Williams, and R. M. Dole, 1990. Meteorological and electrical conditions associated with positive cloud-to-ground lightning. Mon. Wea. Rev., 118, 470-487.
- Feteris, P.J., 1952. Detailed observations of thunderstorms. Weather, 7, 35-39.
- Fischer, B., and E. P. Krider, 1982. On-line lightning maps lead crews to trouble, Electr. World, 196, 111-114.
- Fritsch, J. M., R. J. Kane, and C. R. Chelius, 1986. The contribution of mesoscale convective weather systems to the warm-season precipitation in the U. S. J. Clim. Appl. Meteor., 25, 1333-1345.
- Gething, P.J.D., 1978. Radio Direction Finding and the Resolution of Multicomponent Wave-fields. England: Peter Peregrinus Ltd..

- Goodman, S. J., and D. R. MacGorman, 1986. Cloud-to-ground lightning activity in mesoscale convective complexes. Mon. Wea. Rev., 114, 2320-2328.
- \_\_\_\_\_, D.E. Buechler, and P. J. Meyer, 1988a. Convective tendency images derived from a combination of lightning and satellite data. Wea. Forecasting., 3, 173-188.
- \_\_\_\_\_, \_\_\_\_\_, P. D. Wright, and W. D. Rust, 1988b. Lightning and precipitation history of a microburst-producing storm. Geophys. Res. Lett., 15, 1185-1188.
- \_\_\_\_\_, H. J. Christian, and W. D. Rust, 1988c. Optical pulse characteristics of intracloud and cloud-to-ground lightning observed from above clouds. J. Appl. Meteor., 27, 1369-1381.
- Greene, D. R., and R. A. Clark, 1972. Vertically integrated liquid water - a new analysis tool. Mon. Wea. Rev., 100, 548-552.
- Haberman, R., 1977. Mathematical Models in Mechanical Vibrations, Population Dynamics, and Traffic Flow. Englewood Cliffs, N. J.: Prentice-Hall, Inc.
- Hald, A., 1952. Statistical Theory With Engineering Applications. New York: John Wiley & Sons, Inc.
- Hartigan, J. A., 1975. Clustering Algorithms. New York: John Wiley & Sons, Inc.
- \_\_\_\_\_, and M. A. Wong, 1979. Algorithm AS 136: A K-Means Clustering Algorithm. Appl. Statistics, 28, 100-108.
- Hatakeyama, H., 1958. The distribution of the sudden change of electric field on the earth's surface due to lightning discharge. Recent Advances in Atmospheric Electricity, L.G. Smith, Ed., Pergamon Press, 289-298.
- Helsdon, J. H., and R. D. Farley, 1987. A numerical modeling study of a Montana thunderstorm, 2, Model results versus observations involving electrical aspects. J. Geophys. Res., 92, 5661-5675.
- Hiscox, W.L., E.P. Krider, A.E. Pifer, and M.A. Uman, 1984. A systematic method for identifying and correcting "site errors" in a network of magnetic direction finders. Preprints, 1984 Int. Aerospace and Ground Conf. on Lightning and Static Electricity, 26-28 June, Orlando, FL.
- Horner, F., 1954. The accuracy of the location sources of atmospherics by radio direction finding. Proc. IEE, 101, 383-390.
- Jayaratne, E. R., C. P. R. Saunders, and J. Hallett, 1983. Laboratory studies of the charging of soft-hail during ice crystal interactions. Q. J. R. Meteor. Soc., 106, 609-630.
- Jones, D. M. A., 1956. Rainfall drop size distribution and radar reflectivity. Res. Rep. No. 6, Urbana Meteor. Lab., Illinois State Water Survey, 20pp.
- Kirkpatrick, S., C.D. Gelatt, and M.P. Vecchi, 1983. Optimization by simulated annealing. Science, 220, 671-680.

- Krehbiel, P. R., 1986. The electrical structure of thunderstorms. The Earth's Electrical Environment, National Academy Press, 90-113.
- Krider, E.P., R.C. Noggle, and M.A. Uman, 1976. A gated, wideband magnetic direction finder for lightning return strokes. J. Appl. Meteor., 15, 301-306.
- \_\_\_\_\_, A.E. Pifer, and D.L. Vance, 1980. Lightning direction finding systems for forest fire detection. Bull. Am. Meteor. Soc., 61, 980-986.
- \_\_\_\_\_, 1988. Spatial distribution of lightning strikes to ground during small thunderstorms in Florida. Preprints, 1988 Int. Aerospace and Ground Conf. on Lightning and Static Elec., 19-22 Apr., Oklahoma City, OK, 318-323.
- Lenth, R.V., 1981. On finding the source of a signal. Technometrics, 23, 149-154.
- Leone, D. A., R. M. Endlich, J. Petriceks, R. T. H. Collis, and J. R. Porter, 1989. Meteorological considerations used in planning the NEXRAD network. Bull. Am. Meteor. Soc., 70, 4-13.
- Lewis, J., 1989. Real time lightning data and its application in forecasting convective activity, Preprints, 12th AMS Conf. on Weather Analysis and Forecasting, Oct. 2-6, 1989, Monterey, CA, Am. Meteor. Soc., Boston, MA, 97-102.
- Ligda, M. G. H., 1956. The radar observation of lightning. J. Atmos. Terr. Physics, 9, 329-346.
- Lightning, Location, and Protection, Inc., 1988. 280 Series APA Advanced Position Analyzer User's Guide. UOM-010.0/280, Lightning, Location, and Protection, Inc., Tucson, AZ 85706.
- Livingston, J. M., and E. P. Krider, 1978. Electric fields produced by Florida thunderstorms. J. Geophys. Res., 83, 385-401.
- Lovejoy, S., 1982. Area-perimeter relation for rain and cloud areas. Science, 216, 185-187.
- Mach, D.M., D.R. MacGorman and W.D. Rust, 1986. Site errors and lightning detection efficiency in a magnetic direction finder for lightning return strokes. J. Atmos. Oceanic Technol., 3, 67-74.
- Marshall, J. S., and W. M. Palmer, 1948. The distribution of raindrops with size. J. Meteor., 5, 165-166.
- Marquardt, D. W., 1963. An algorithm for least-squares estimation of non-linear parameters. J. Soc. Indust. Appl. Math., 11, 431-441.
- May, R. M., 1974. Biological populations with nonoverlapping generations: Stable points, stable cycles, and chaos. Science, 186, 645-647.
- \_\_\_\_\_, 1976. Simple mathematical models with very complicated dynamics. Nature, 261, 459-467.
- McAnelly, R. L., and W. R. Cotton, 1986. Meso- $\beta$ -scale characteristics of an episode of meso- $\alpha$ -scale convective complexes. Mon. Wea. Rev., 114, 1740-1770.

- MSI Services, Inc., 1986. The status of national programs for lightning detection systems, Prepared for: Office of the Federal Coordinator for Meteorological Services and Supporting Research. (Available from MSI Services, Inc., 600 Maryland Ave., S. W., Washington, DC, 20024.)
- Myers, R. H., 1986. Classical and Modern Regression With Applications. Boston: Duxbury Press.
- Neter, J., W. Wasserman, and M. H. Kutner, 1983. Applied Linear Regression Models. Homewood, IL: Richard D. Irwin, Inc.
- Newton, C. W., and J. C. Fankhauser, 1964. On the movements of convective storms with emphasis on size discrimination in relation to water budget requirements. J. Appl. Meteor., **3**, 651-658.
- \_\_\_\_\_, and \_\_\_\_\_, 1975. Movement and propagation of multi-cellular convective storms. Pure Appl. Geophys., **113**, 747-764.
- NEXRAD, 1985. Next generation weather radar (NEXRAD) algorithm report. NEXRAD Joint System Program Office, Washington, DC.
- Orville, R. E., Jr., 1987. An analytical solution to obtain the optimum source location using multiple direction finders on a spherical surface. J. Geophys. Res., **92**, D9, 10,877-10,886.
- Orville, R. E., R. W. Henderson, and L. F. Bosart, 1988. Bipole patterns revealed by lightning locations in mesoscale storm systems. Geophys. Res. Lett., **15**, 129-132.
- Peckham, D. W., M. A. Uman, and C. E. Wilcox, Jr., 1984. Lightning phenomenology in the Tampa Bay area. J. Geophys. Res., **89**, 11789-11805.
- Piepgrass, M. V., E. P. Krider, and C. B. Moore, 1982. Lightning and surface rainfall during Florida thunderstorms. J. Geophys. Res., **87**, 11193-11201.
- Richards, F. J., 1959. A flexible growth function for empirical use. J. of Exper. Botany, **10**, 290-300.
- Rinehart, R. E., and E. T. Garvey, 1978. Three-dimensional storm motion detection by conventional weather radar. Nature, **273**, 287.
- Roberts, W. F., W. R. Moninger, B. deLorenzis, E. Ellison, J. Flueck, J. C. McLeod, C. Lusk, P. D. Lampru, R. Shaw, T. R. Stewart, J. Weaver, K. C. Young, and S. Zubrick, 1990. Shootout 89: A comparative evaluation of AI systems for convective storm forecasting. Preprints, 6th International Conf. on Interactive Info. Proc. Sys. for Meteorology, Oceanography, and Hydrology, 5-9 February, Anaheim, CA, Am. Meteor. Soc., Boston, MA, 167-172.
- Romesburg, H. C., 1984. Cluster Analysis for Researchers. Belmont, CA: Lifetime Learning Publications.
- Rosenfeld, D., 1987. Objective method for analysis and tracking of convective cells as seen by radar. J. Atmos. Oceanic Technol., **4**, 422-434.

- Ross, W., and F. Horner, 1952. The siting of direction finding stations. Radio Res., Spec. Rept. 22, 38 pp.
- Rust, W. D., 1986. Positive cloud-to-ground lightning. The Earth's Electrical Environment, National Academy Press, 41-45.
- \_\_\_\_\_, 1989. Utilization of a mobile laboratory for storm electricity measurements. J. Geophys. Res., 94, 13313-13318.
- Rutledge, S.A., and D.R. MacGorman, 1988. Cloud-to-ground lightning activity in the 10-11 June 1985 mesoscale convective system observed during the Oklahoma-Kansas PRE-STORM project. Mon. Wea. Rev., 116, 1393-1408.
- SAS Institute Inc., 1985. SAS User's Guide: Statistics, Cary, North Carolina: SAS Institute Inc.
- Seliga, T. A., K. Aydin, and H. Direskeneli. Disdrometer measurements during an intense rainfall event in Central Illinois: Implications for differential reflectivity radar observations. J. of Clim. and Appl. Meteor., 25, 835-846.
- Shackford, C. E., 1960. Radar indications of a precipitation-lightning relationship in New England thunderstorms. J. Meteor., 17, 15-17.
- Shutte, T. E. Pislser and S. Israelsson, 1987. A new method for the measurement of the site errors of a lightning direction-finder: Description and first results. J. Atmos. Oceanic. Technol., 4, 305-311.
- Sokal, R. R., and P. H. A. Sneath, 1963. Principles of Numeric Taxonomy. San Francisco: W. H. Freeman & Co.
- Stansfield, R.G., 1947. Statistical theory of D.F. fixing. J. IEE, 94, 762-770.
- Szu, H., and R. Hartley, 1987a. Fast simulated annealing. Physics Lett. A., 122, No. 3,4, 157-162.
- \_\_\_\_\_, and \_\_\_\_\_, 1987b. Nonconvex optimization by fast simulated annealing. Proc. IEEE, 75, 1538-1540.
- Wangsness, D.L., 1973. A new method of position estimation using bearing measurements. IEEE Trans. Aero. and Elec. Sys., AES-9, 959-960.
- Watson, A.I., R.E. Lopez, R.L. Holle, and R.J. Daugherty, 1987. The relationship of lightning to surface convergence at Kennedy Space Center: A preliminary study. Wea. Forecasting, 2, 140-157.
- Weisman, M. L., and J. B. Klemp, 1982. The dependence of numerically simulated convective storms on vertical wind shear and buoyancy. Mon. Wea. Rev., 110, 504-520.
- Williams, E. J., 1959. Regression Analysis. New York: John Wiley & Sons, Inc.
- Williams, E. R., 1985. Large-scale charge separation in thunderclouds. J. Geophys. Res., 90, 6013-6025.

- Wilson, J., and R. Carbone, 1984. Nowcasting with Doppler radar: the forecaster-computer relationship, Proc., Nowcasting-II Symposium, Norrkoping, Sweden, 3-7 Sept., ESA SP-208, 177-186.
- Workman, E. J., and S. E. Reynolds, 1949. Electrical activity as related to thunderstorm cell growth. Bull. Amer. Meteor. Soc., 30, 142-144.
- Zawadzki, I., E. Torlaschi, and R. Sauvageau, 1981. The relationship between mesoscale thermodynamic variables and convective precipitation. J. Atmos. Sci., 38, 1535-1540.
- Ziegler, C. L., P. S. Ray, and D. R. MacGorman, 1986. Relations of kinematics, microphysics, and electrification in an isolated mountain thunderstorm. J. Atmos. Sci., 43, 2098-2114.
- Zipser, E. J., 1983. Nowcasting and very short-range forecasting. In The National STORM Program: Scientific and Technological Bases and Major Objectives, Univ. Corp. for Atmos. Res., Boulder, CO, 6-1 to 6-30.
- Zittel, W. D., 1976. Evaluation of a remote weather radar display. Vol. II-Computer applications for storm tracking and warning. FAA Rep. FAA-RD-75-60, II. (Available from National Technical Information Service, U. S. Dept. of Commerce, Springfield, VA 22161.)

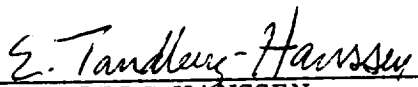


APPROVAL

PREDICTING THUNDERSTORM EVOLUTION  
USING GROUND-BASED LIGHTNING DETECTION NETWORKS

By Steven J. Goodman

The information in this report has been reviewed for technical content. Review of any information concerning Department of Defense or nuclear energy activities or programs has been made by the MSFC Security Classification Officer. This report, in its entirety, has been determined to be unclassified.

  
\_\_\_\_\_  
E. TANDBERG-HANSEN  
Director  
Space Science Laboratory





